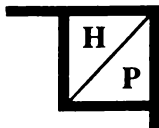


HADRONIC PRESS MONOGRAPHS IN THEORETICAL PHYSICS

Ampere-Neumann Electrodynamics of Metals

Peter Graneau
Massachusetts Institute of Technology

Second Edition



HADRONIC PRESS, INC.

35246 US 19 North # 115, Palm Harbor, FL 34684, USA

Copyright © 1994 by Peter Graneau

All rights reserved.

*No part of this book may be reproduced, stored in a retrieval system
or transmitted in any form or by any means
without the written permission
of the copyright owner.*

**U. S. Library of Congress
Cataloging in Publication Data:**

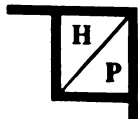
Graneau, Peter

*Ampere-Neumann Electrodynamics
of Metals*

**with Bibliography
and Index**

Additional data supplied on request

ISBN 0-911767-75-4



HADRONIC PRESS, INC.

35246 US 19 North # 115, Palm Harbor, FL 34684, USA

To my wife Brigitte,

and in memory of my staunch friend

Ted Calnan

ABOUT THE BOOK

More than 160 years have elapsed since Oersted discovered electromagnetism. The dominant theory of the first eighty years was the electrodynamics developed by Ampere, Neumann, and Weber. It presided over the invention of generators, motors, transformers, transmission lines, and electromagnets. Flourishing mainly in the schools of France and Germany, the key memoirs were not translated into English. Contemporary scientists and engineers are largely ignorant of the old electrodynamics and frequently confuse it with later ideas. This knowledge gap, it is hoped, will be filled by the first chapter of this book. It is essentially an abbreviated text of 19th century electromagnetism.

The second chapter contains the body of experimental evidence for longitudinal forces in metallic conductors. These forces comply with Ampere's force law and exist in addition to the transverse forces predicted by both Ampere's and Lorentz's force laws. Recent discoveries of electromagnetic jet propulsion, wire fragmentation by current pulses, and the correct recoil action in railguns are fully discussed. An ingenious electrodynamic impulse pendulum, invented at the University of Athens, is described. It proves that electric current in a metallic conductor is not associated with "equivalent electromagnetic mass in the field" which could be invoked for momentum conservation and the seat of reaction forces.

Every opportunity has been taken to stress that the Ampere-Neumann electrodynamics is an empirical theory devised for metallic conductors. It certainly does not apply to convecting charges in vacuum or dielectric fluids which are the arena of experimental particle

physics. It is only in metals, presumably through the presence of lattice ions, that Ampere forces and the Neumann induction phenomena make themselves felt.

There is mention in the second chapter of the range of technological applications of these unfamiliar Ampere forces. The practical applications comprise exploding wires, multi-arc generators for current limiting fuses and switching operations, liquid metal jets and pumps, the railgun dynamics, forces in electromagnets, and explosions in liquid plasma conductors.

The theoretical evolution of the Newtonian electrodynamics for metals, subsequent to Ampere, Neumann, and Weber, is covered in the third chapter. It will come as a surprise just how great a contribution Maxwell made to this topic. Perhaps the most important aspect of this chapter is the outline of computer-aided macroscopic current element analysis for force and inductance calculations. In the past calculations of this nature have been bedevilled by integration singularities which are easily removed by the use of finite-size current elements and filaments.

A major new addition to the Ampere-Neumann electrodynamics is the proposed pivoted atomic current element discussed in the last chapter of the book. It arose from consideration of the magnetic energy stored between pairs of metallic current elements and the angle-dependence of this energy. The virtual work concept then requires that the elements should not only be subject to mutual forces, but also to mutual torques. Two different kinds of torque have been revealed. One of them should be able to turn the pivoted element about the lattice site and thereby furnish a microscopic mechanism of generating e.m.f.'s. Quite unexpectedly, the same mechanism also offered a new explanation of diamagnetism in metals. Near the end of the last chapter, an experiment is proposed which should be capable of testing the validity of the pivoted current element model.

CONTENTS

Preface	viii
Preface to Second Edition	x

CHAPTER 1

Evolution of Electrodynamics

Beginning of electromagnetism	1
Ampere's force law	7
Neumann's electrodynamic potential	23
Neumann's law of induction	38
Grassmann's force law	45
Weber's force law and electrodynamic potential	55
Retarded potentials and the electromagnetic field	72
Matter—bound versus free energy	80
The electron	84
Convection currents in vacuum	92

CHAPTER 2

Longitudinal Ampere Forces

Ampere tension	95
Nasilowski's discovery of wire fragmentation	105
Pappas' electrodynamic impluse pendulum	116
Railgun recoil	130
Ampere's hairpin experiment	133
Neumann's demonstration of longitudinal forces	138
One of Hering's longitudinal force experiments	144
Cleveland's experiment	149

Ampere tension in dipole magnets	155
Liquid metal conductors	165
Electrodynamic explosions in liquids	168
Do longitudinal Ampere forces exist in gaseous arcs and plasmas?	177

CHAPTER 3

Theoretical Developments

Finite current element analysis	179
Reaction forces from the selfinductance gradient	204
Inductance calculations	214
Relationship between self and mutual inductance	214
Inductance of single-filament circuits	221
Inductance of straight conductors and cables	233
Transient and alternating currents in linear conductors	241
The induction of eddy currents	259

CHAPTER 4

Atomic Current Elements

Current elements of Ampere, Weber, and Lorentz	261
Mutual torques between Amperian current elements	265
Generalization of Neumann's law of induction	269
Diamagnetism and the Meissner effect	275
Unification notwithstanding	290
References	298
Index	305

PREFACE

It is widely thought that science always progresses in a forward direction and we never have to retrace our steps to see if somewhere we took a wrong turn. The experiments described in this book tell a different story. They suggest we should go back nearly one hundred years and examine again Lorentz's hypothesis of the metallic current element being nothing more than an electron in motion. This hypothesis has worked well for electrons traveling in vacuum and also explained many—but not all—observations with currents in metallic conductors. It will be uncomfortable for teachers and textbook writers to have to think in terms of two electromagnetic theories resting, as they do, on totally different philosophical bases. Yet experiment is unforgiving, and new advances in our understanding of nature demand robust honesty. In this respect, the nicely rounded and pedagogically unified treatment of a subject often signals stagnation.

Modern physics appears to be dominated by belief for which there exists no experimental proof nor disproof. Instances are the flight of free energy, commonly called radiation, the probabilistic interpretation of quantum mechanics, and the universal validity of cer-

tain space—time geometries. Strict adherence to belief has concentrated research in narrow areas and there produced remarkable results. However, reckoned on the time scale of centuries, it was the breaking of physics dogma which produced the greatest advances. No more dramatic example of this will be found in the history of science than the surplanting of cartesian aether whirlpools by Newton's forces of gravitational attraction.

The Ampere—Neumann electrodynamics belongs to the family of newtonian theories which have distinguished themselves by their ready application to practice. The old electrodynamics returns in a new guise at a time when ever larger current pulses are being forced through metallic conductors for a variety of purposes, from the containment of plasma fusion to hurling objects into space with electromagnetic accelerators. It is hoped this book will be of help in the emerging field of pulse power technology.

In this research I have been ably assisted by my son Neal who, at the age of fourteen, gently led me to computers. He had a major hand in developing the macroscopic current element analysis. During the last six years, he was involved with the building and running of all crucial experiments. Now that he is about to venture forth on his own, I wish him that measure of luck without which no research can succeed.

I am indebted to Linda—Jo Ruscak for letting her computer run weeks on end to hammer out the convergence figures on page 198.

Peter Graneau
Concord, Massachusetts
September, 1985

PREFACE TO SECOND EDITION

The continued demand for this book is gratifying. It does not imply that the majority of physicists are abandoning relativistic field theories, but rather that the Ampere-Neumann electrodynamics is slowly and securely gaining ground. Its principal support comes from experimentalists and engineers. Textbooks on electromagnetism will not be revised in the present century and it may take most of the twenty-first century to implement their inevitable adjustment to experimental facts. In his biography, Planck wrote:

"New scientific truth does not triumph by convincing its opponents and making them see the light but rather because its opponents eventually die, and a new generation grows up that is familiar with it."

Some high school students and undergraduates have already repeated simple Ampere force experiments with little more than car batteries and pocket money.

Since the publication of the first edition, much of the debate has revolved around the far-action versus field-contact-action controversy. It became clear that electric motors are not driven by energy impact and recoil forces, as required by the Poynting energy-momentum vector. The forces in common motors must therefore arise from simultaneous far-actions. Virtual photons of the quantum electrodynamics are also helpless in overcoming the field energy discrepancy first revealed by the impulse pendulum experiment. These issues are more fully discussed in a new book co-authored with my son Neal of Oxford University *"Newton versus Einstein: How Matter Interacts with Matter"* (Carlton Press, New York, 1993).

Apart from making typographical corrections, two errors have been eliminated in this new edition. I am indebted to Andre K. T. Assis for explaining to me very clearly that Ampere forces can be integrated without singularities. While drafting this book I was misled by the fact that specific Ampere forces ($\Delta F/i^2$) will diverge as the current element becomes infinitely small. But infinitely small current elements are not allowed by the atomicity of matter.

The second error concerns the sign of the mutual alpha and epsilon torques between a pair of current elements. These torques represent a major extension of the Ampere-Neumann electrodynamics. Without them energy conservation would be jeopardized. Much remains to be discovered in this intriguing new area. There exist indications that the two torques may interact with each other and cancel certain alpha-torque effects. Figure 88 is new because of the sign correction. A more comprehensive treatment of the torque analysis awaits further developments.

Only in the last year has it become obvious that Newton's third law enforces a sharp distinction between the usual Newtonian mechanics and relativistic mechanics (statics). Publications now in the press deal with this conflict. The reader is warned that the doubling of hoop tension, discussed on pages 160-164, may not be true because it arose from a confused analysis in which no line was drawn between the two mechanics.

Scientifically and technologically, most important discoveries have been made, or come to light, in the past eight years with regard to electric arc explosions, the cause of thunder and capillary (non-thermonuclear) fusion. Only the Ampere-Neumann electrodynamics has been able to explain these phenomena. There is little doubt left that Ampere's force law also applies to dense arc plasma. A further book is in the course of preparation to deal with this subject.

Peter Graneau
Concord, Massachusetts
July, 1993

CHAPTER 1

EVOLUTION OF ELECTRODYNAMICS

BEGINNINGS OF ELECTROMAGNETISM

Electricity and magnetism are words of Greek origin. For two thousand years it was believed that the attraction of iron by the lodestone and the attraction of many kinds of matter by electrified amber had something in common. At least since the Middle Ages man had known that lightning striking iron could imbue this metal with magnetism. By the same token, the fire from heaven was capable of changing the polarity of a compass needle. Dibner [1] reports that in 1802 Romagnosi, a lawyer and physicist at the University of Parma, Italy, reversed the polarity of a compass by passing a galvanic current through it. This experiment came close to the discovery of electromagnetism, universally attributed to the Danish scientist Hans Christian Oersted, eighteen years later.

The professor of natural philosophy in Copenhagen determined the direction in which a compass needle would turn when a straight wire carrying an electric current was brought near to the compass without touching it. One might ask why this particular experiment was singled out as the beginning of electromagnetism?

Oersted felt so certain of the enthusiastic reception of his discovery that he had a paper printed for the occasion and sent to all scientists and journals of note at his time. The paper was dated July 21, 1820. It explained how magnetic flux encircled the current, but Oersted called flux 'electric conflict'. Here finally was the missing link between elec-

tricity and magnetism.

It has to be remembered Oersted's explanation of the magnetic influence came at a time when effluvia, the aether, and cartesian vortices were on the wane because of the success of Newton's and Coulomb's action-at-a-distance laws which avoided any reference to what was happening in the space between the interacting bodies. Newton's own words serve best to describe the then prevailing philosophy of mathematical thinkers. In the preface to the first edition of the 'Principia' he said:

"Then from these forces, by other propositions which are also mathematical, I deduce the motions of the planets, the comets, the moon, and the sea. I wish we could derive the rest of the phenomena of Nature by the same kind of reasoning from mechanical principles, for I am induced by many reasons to suspect that they may all depend upon certain forces by which the particles of bodies, by some causes hitherto unknown, are either mutually impelled towards one another, and cohere in regular figures, or are repelled and recede from one another. These forces being unknown, philosophers have hitherto attempted the search of Nature in vain; but I hope the principles here laid down will afford some light either to this or some truer method of philosophy."

These words apply equally to the Ampere-Neumann electrodynamics which followed on the heels of Oersted's experiment.

Neither Ampere nor F.E. Neumann took heed of the magnetic circles around electric currents. They wrote down the laws of force and potential in accordance with the action-at-a-distance model of newtonian gravitation. Newton was more precise and spoke of mutual (simultaneous) interaction so as not to create the impression of something travelling at finite or infinite speed between the interacting partic-

les. In 1820, as today, there lived many scientists who disliked action-at-a-distance and in their hearts had adhered to the aristotelian principle of contact-action. Oersted must have known they were in the majority and would welcome an electromagnetic theory in terms of an active field. Forty years later Maxwell placed the electromagnetic field on mathematical foundations. Within a few decades of this last event the world of physics had shed all remote action concepts.

Oersted's announcement [2] triggered a frenzy of activity in Paris which at the time was the science capital of the world. It caused the French Academy to stage a demonstration of the Copenhagen experiment in front of its members. As Hammond [3] recounts the occasion, Ampere went straight home after the lecture to begin working on his electrodynamics, missing the discussion at the Academy which he would normally have enjoyed. This was September 11, 1820. Precisely one week later Ampere read a paper before the Academy and reported that parallel wires carrying electric currents attract or repel each other, depending on whether the two currents flow in the same or opposite directions. This was as great a step forward in electromagnetism as Oersted had taken. Ampere followed up with weekly presentations to the members of the Academy of the progress he was making in his experimental investigation of the interaction of electric currents. Within a few months he had laid the foundations of a new science which he himself called electrodynamics.

Like Ampere, Jean-Baptiste Biot was also a professor in Paris. He was an expert in the measurement of the strength of the earth's magnetic field. The frequency of oscillation of a compass needle had been found to be a measure of the field strength. Biot had accompanied Gay-Lussac in the first balloon flight in order to determine if the earth's magnetic field varied with height above ground level. Biot was another French scientist who was present at the Academy meeting of September 11 and, like Ampere, he too rushed back to his

laboratory. With his assistant Felix Savart he set up a galvanic current in a long vertical wire and, with due compensation for the terrestrial field, the two proceeded to survey the magnetic field strength around the wire with their well established method of the oscillating compass needle. Figure 1(a) illustrates the nature of the Biot-Savart result. The force H which would be exerted on unit magnetic pole was found

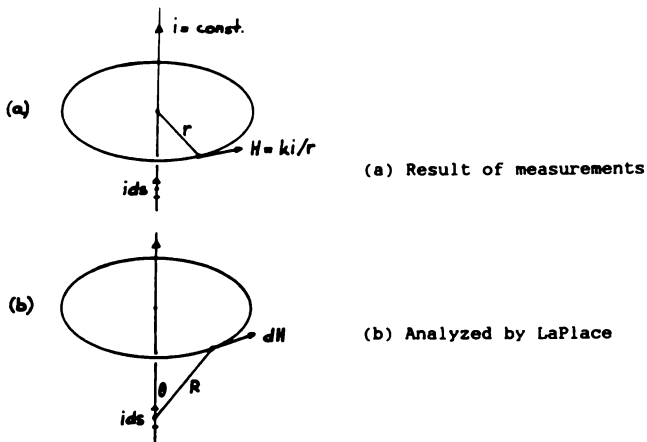


Fig.1 Biot-Savart law

to be inversely proportional to the shortest distance r to the wire. These investigators had no means of measuring the strength of the current i , as the galvanometer was still to be invented by Ampere. It is not clear, therefore, if the proportionality of H to i was taken for granted or established by a later series of measurements. At any rate, the Biot-Savart experiments led to the following wellknown formula for straight conductors

$$H = k i / r$$

(1.1)

where k is a dimensional constant.

Biot and Savart spoke of their findings to the French Academy on October 30, 1820. They were obviously competing with Ampere in the unravelling of further electromagnetic mysteries. What today is understood to be the Biot-Savart law is not equation (1.1), but the differential of it with respect to the current element $i.ds$, as shown in fig.1(b). The law may be written

$$dH = (k/R^2)i.ds \sin\theta \quad (1.2)$$

where k is again a dimensional constant. According to Biot and Ampere, (1.2) was derived from (1.1) by La Place, who never claimed credit for it. An excellent account of these happenings has been written by Tricker [4, 5].

The Biot-Savart law introduces the concept of the 'current-element' which has become the 'particle' of the Ampere-Neumann electrodynamics. Without subdividing the wire into short length-elements it would have been impossible to compute the magnetic field strength at a point due to a closed circuit. Ampere employed the same current element in a different way. Before going on to Ampere's work, a little has to be said about the status of electrostatics at the beginning of the nineteenth century.

Whittaker in his famous "History of the theories of aether and electricity" [6] maintains:

"By Franklin's law of the conservation of electric charge, and Priestley's law of attraction between charged bodies, electricity was raised to the position of an exact science."

Benjamin Franklin working in isolation in America propounded the one-fluid theory of electricity which may be

taken as the natural precursor of our present electronic theory of solids. He also came to the conclusion that certain substances, which we now describe as dielectrics, are impenetrable to electric effluvia. Therefore the two electrodes of a Leyden jar had to communicate by action-at-a-distance. Through his friend Priestley in England, Franklin's work was published in Europe. Particularly his experiments of drawing lightning out of thunderclouds received much attention. During the 1750's the German physicist Aepinus took up Franklin's ideas and with them illuminated the phenomenon of electrostatic induction.

In 1766 Franklin wrote to Priestley asking him to repeat an experiment with cork balls in an electrically charged metal container. Franklin had found to his surprise that the cork balls did not respond to the charge. Subsequently Priestley established that the electric field strength, as it would be called today, is zero inside an electrically charged and closed metallic vessel. He clearly recognized the analogy to gravitation and concluded [6]:

"May we not infer from this experiment that the attraction of electricity is subject to the same laws with that of gravitation, and is therefore according to the square of the distances; since it is easily demonstrated that were the earth in the form of a shell, a body in the inside of it would not be attracted to one side more than another?"

However the inverse-square-law of the interaction of electric charges did not become common property of the scientific community of the eighteenth century until Coulomb proved it directly in 1785 by measurements with a torsion balance. Coulomb's law may be written

$$F = k q_1 q_2 / r^2 \quad (1.3)$$

The charges q_1 and q_2 are separated by the distance r between their centers and k is a dimensional constant. If the charges are both positive or both negative, the force F is positive and this represents repulsion. For charges of unlike sign the force is negative which stands for attraction.

AMPERE'S FORCE LAW

In the tradition of the great French mathematicians who developed the science of mechanics from Newton's laws, Ampere set out to cast electromagnetism in a newtonian frame.

For this he required an appropriate fundamental law of 'particle' interaction. He suspected this would turn out to be an inverse-square-law akin to those of Newton and Coulomb which, to use his own words in English translation [4], ".... opened a new highway into the sciences which have natural phenomena as their object of study".

However difficult it may appear today, the question of what constitutes the elementary particle of electrodynamics apparently posed no problem to Ampere, Biot and Savart.

They concurrently plunged for the 'current-element'. It is not certain who may have thought of the concept first.

Ampere clearly recognized that, unlike the elementary particles of gravitation and electrostatics which were characterized by a simple scalar magnitude (of mass or charge), the current element would in addition to the magnitude of current strength have to possess length and direction.

On the basis of his first electrodynamic experiments, showing the attraction and repulsion of straight and parallel current carrying wires, Ampere expected the law of mechanical force between two current elements to be of the general form

$$\Delta F_{m,n} = - i_m i_n (dm \cdot dn / r_{m,n}^2) f(\alpha, \beta, \epsilon) \quad (1.4)$$

The delta is meant to indicate that we are dealing with an elemental force which cannot be measured because current elements of wire circuits are not available in isolation.

The forces which we do measure in the laboratory are sums of many elemental forces. In (1.4) the elements carry currents of strength i_m and i_n , and their lengths are dm and dn . The distance between the center points of the elements is $r_{m,n}$ and the angles of the function f are shown in fig.3.

If the angle function $f(\alpha, \beta, \epsilon)$ is positive, $\Delta F_{m,n}$ is negative and this sign stands for attraction between the elements. Ampere actually proposed the opposite sign convention, but his was subsequently dropped in order to coordinate (1.4) with Coulomb's law (1.3). Both the current strengths and element lengths were taken to be positive scalar quantities while the directional properties of the elements were incorporated in the angle function f .

With respect to the proportionality of the elemental force to the lengths and currents of the two elements Ampere said [4]:

"First of all, it is evident that the mutual action of two elements of electric current is proportional to their lengths; for assuming them to be divided into infinitesimal equal parts along their length, all attractions and repulsions of these parts can be regarded as directed along one and the same straight line, so that they necessarily add up. This action must also be proportional to the intensities of the two currents."

In his early papers on electrodynamics Ampere also assumed the proportionality of the elemental force to the inverse square of the distance of separation, because he

believed all fundamental forces of nature obeyed this law. Later he proved the validity of this early assumption with the three-circle experiment of fig.2. For the sake of clarity the figure does not show the current leads to the three parallel and coaxial current circles arranged in vertical planes. All three circles were connected in series to ensure equal current intensities in all of them. Ampere's method of compensating for the effect of the earth's magnetic field has also been omitted in fig.2. The radii and distances

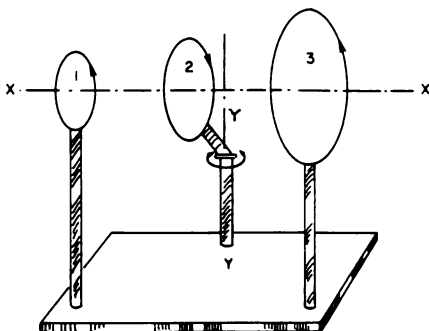


Fig.2 Ampere's three-circle experiment

between the three current circles were chosen such that the geometrical relationship of circle 1 to circle 2 was similar to the relationship of circle 2 to circle 3. In other words, the only difference between the 1-2 and 2-3 combinations was a linear scale factor. Circles 1 and 3 were fixed to the laboratory frame, while circle 2 was held coaxial with the other two but with its insulator arm free to rotate about the vertical line YY. The purpose of this experiment was to show that, if the currents in 1 and 3 encircle the common axis XX in the same direction, circle 2 will remain stationary, it being either attracted

or repelled equally strongly by the two adjacent circles. When the current in circle 2 flows in the direction shown in fig. 2, the forces would be attractive.

This experiment proves that the reciprocal electrodynamic forces between two current loops are independent of the linear scale factor and therefore independent of the size of the electrodynamic system of conductors. The same must be true for all elemental forces into which the total force may be divided. Hence the geometrical factor $dm \cdot dn / r^2$ of equation (1.4) must be a dimensionless number, a condition which can only be fulfilled by the inverse square law. In addition to the proof provided by the three-circle experiment, the knowledge that geometrically similar small and large conductor arrangements are subject to the same mechanical forces, for the same currents, is a valuable result in its own right.

Not surprisingly, Ampere's most challenging task proved to be the determination of the angle function $f(\alpha, \beta, \epsilon)$. A recurrent difficulty for those who have tried to understand Ampere's force law, and others who have used it for engineering calculations, has been the visualization of the three angles, particularly when the two elements do not lie in the same plane. Figure 3 attempts to make this visualization as easy as is possible. M and N are the center points of two unequal current elements. The distance between M and N, that is $r_{m,n}$, must be treated as a vector. The polarity of this vector is arbitrary. It may be chosen to point from M to N, or from N to M. The current elements must also be treated as vectors and have to point in the direction of current flow. The angle through which the element $i \cdot dm$ has to be turned about M to make it point in the same direction as $r_{m,n}$ is α . Similarly, the angle through which the element $i \cdot dn$ has to be turned about N to point in the same direction as $r_{m,n}$ is β . Since both these angles ultimately appear in cosines, and since $\cos \alpha = \cos(360^\circ - \alpha)$, it does not

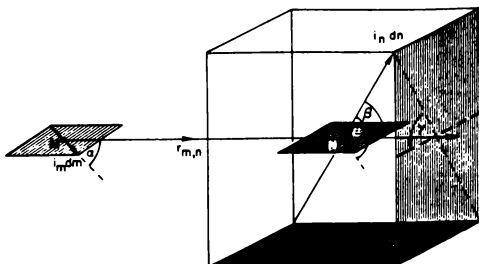


Fig.3 Angles in Ampere's force formula

matter in which direction the element vectors are turned to make them coincide with the distance vector. Each element and the distance vector lie in a separate plane. These two planes intersect in the distance vector. Of the two complimentary angles between the planes, γ is that angle through which one plane would have to be turned in order to make the components of the current elements which are perpendicular to the distance vector point in the same direction.

An important angle in Ampere's formula is ϵ . It stands for the angle of inclination of the two current elements toward each other. It may best be visualized by transferring one of the elements parallel to itself along MN until its center coincides with the center of the other element. In fig.3 the dm element has been transferred from M to N and ϵ is the angle through which the transferred element has to be turned about N to make it point in the same direction as dn . Since ϵ also appears in a cosine, its direction is as arbitrary as that of α and β .

To see how Ampere determined $f(\lambda, \ell, \epsilon)$ we resolve the two current elements of fig.3 into their cartesian components shown in fig.4. The elements $i_m dm$ and $i_n dn$ are then represented as vectors m and n , pivoted at the centers of the elements. The resolved components of the two current elements along the x , y , and z axes are given by

$$\begin{aligned} m(x) &= i_m dm \cos \alpha ; & m(y) &= i_m dm \sin \alpha ; \\ n(x) &= i_n dn \cos \beta ; & n(y) &= i_n dn \sin^2 \beta \cos \gamma ; \\ n(z) &= i_n dn \sin \beta \sin \gamma ; \end{aligned} \quad (1.5)$$

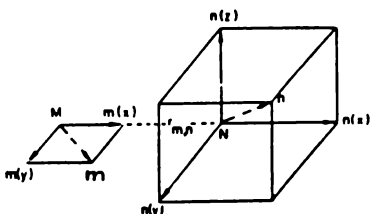


Fig.4 Resolved-component vector representation of the two general current elements of fig.3

Now each component of m interacts with each component of n , resulting in a total of six contributions to the elemental force between two current elements. Four of them are zero according to a theorem first mentioned by Ampere. Generations of physicists have been uncertain how this theorem follows from Ampere's experiments or how it could be deduced from his postulates. We will refer to it as Ampere's Rule, leaving the question open of it being a theorem or an assumption. Ampere writes about it as follows [4]:

"An infinitely small portion of current exerts no action on another infinitesimal portion of a current which is situated in a plane which passes through the midpoint and which is perpendicular to its direction. In fact, the two halves of the first element produce equal actions on the second, the one attractive and the other repellent, because the current tends to approach the common perpendicular in one of those halves and to move away from it in the other. These two equal forces form an angle which tends to two right angles according as the element tends to zero. Their resultant is therefore infinitesimal in relation to these forces and in consequence it can be neglected in the calculations."

In compliance with Ampere's Rule, the four vanishing force contributions of the element components drawn in fig.4 are

$$\Delta F_{m(x),n(y)} = \Delta F_{m(x),n(z)} = \Delta F_{m(y),n(x)} = \Delta F_{m(y),n(z)} = 0 \quad (1.6)$$

A corollary of Ampere's Rule is that the mechanical interaction of two current elements arises from two sets of parallel element components, one of them being the set which lies along the line connecting the two elements, and the other is the set which is perpendicular to that line. Ampere then assumed that the two non-vanishing force contributions may be expressed by

$$\Delta F_{m(y),n(y)} = - m(y).n(y)/r_{m,n}^2 \quad (1.7)$$

$$\Delta F_{m(x),n(x)} = - k m(x).n(x)/r_{m,n}^2 \quad (1.8)$$

where k is a numerical constant and the element components are defined by equation (1.5). At this stage (1.4) may

be expressed as

$$\Delta F_{m,n} = -i_m i_n (dm \cdot dn / r_{m,n}^2) (\sin \alpha \sin \beta \cos \gamma + k \cos \alpha \cos \beta) \quad (1.9)$$

Ampere then introduced the trigonometrical equation

$$\cos \epsilon = \cos \alpha \cos \beta + \sin \alpha \sin \beta \cos \gamma \quad (1.10)$$

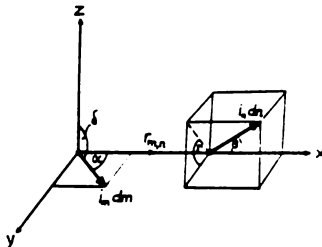


Fig.5 Angles for determining the direction cosines of of two general current elements

For proof of (1.10) he referred to a spherical triangle. This relationship may also be derived with the help of fig.5 from the direction cosines of the two general current elements. It is known that the cosine of the angle of inclination between two vectors is equal to the sum of the three products of corresponding direction cosines of the two vectors. With regard to fig.5, the direction cosines along the x, y, and z axes of the dm-element are

$$\cos \alpha ; \cos[(\pi/2) - \alpha] = \sin \alpha ; \cos \delta = \cos(\pi/2) = 0;$$

and those of the dn-element are

$$\cos \beta ; \cos[(\pi/2) - \beta] \cos \gamma = \sin \beta \cos \gamma ;$$

$$\cos[(\pi/2)-\beta] \cos[(\pi/2)-\gamma] = \sin\beta \sin\gamma.$$

Hence

$$\cos\epsilon = \cos\alpha \cos\beta + \sin\alpha \sin\beta \cos\gamma + 0 \times \sin\beta \sin\gamma$$

which confirms equation (1.10).

With (1.10) the force formula (1.9) may be transformed to

$$\Delta F_{m,n} = -i_m i_n (dm \cdot dn / r_{m,n}^2) [\cos\epsilon + (k-1) \cos\alpha \cos\beta] \quad (1.11)$$

After this step Ampere converts the cosines to partial differentials of $r_{m,n}$ with respect to small displacements of the centers of the elements, M and N, along the lines of action of the elements. These partial differentials are further defined by fig.6. In the limit as the displacements of M and N tend to zero, and writing r for the distance between the elements, we find that

$$\cos\alpha = \partial r / \partial m ; \quad \cos\beta = -\partial r / \partial n ; \quad (1.12)$$

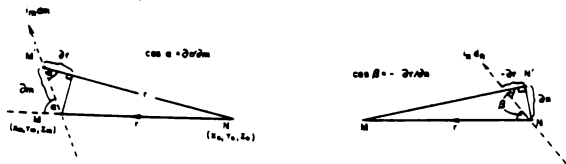


Fig.6 Partial differentials of the distance vector with respect to displacements of current elements

Furthermore, if M and N have the coordinates x_m, y_m, z_m , and x_n, y_n, z_n , we have

$$r^2 = (x_m - x_n)^2 + (y_m - y_n)^2 + (z_m - z_n)^2 \quad (1.13)$$

Differentiating (1.13) with respect to m results in

$$r(\partial r / \partial m) = (x_m - x_n)(\partial x_m / \partial m) + (y_m - y_n)(\partial y_m / \partial m) + (z_m - z_n)(\partial z_m / \partial m) \quad (1.14)$$

and a second differentiation with respect to n gives

$$\begin{aligned} r(\partial^2 r / \partial m \partial n) + (\partial r / \partial m)(\partial r / \partial n) = \\ = -(\partial x_m / \partial m)(\partial x_n / \partial n) - (\partial y_m / \partial m)(\partial y_n / \partial n) - (\partial z_m / \partial m)(\partial z_n / \partial n) \end{aligned} \quad (1.15)$$

But the right-hand side of (1.15) contains the negative products of the direction cosines of the two current elements. Therefore

$$\cos \epsilon = -r(\partial^2 r / \partial m \partial n) - (\partial r / \partial m)(\partial r / \partial n) \quad (1.16)$$

Substituting (1.12) and (1.16) into the force equation (1.11) transforms the latter to

$$\Delta F_{m,n} = i_m i_n (dm \cdot dn / r^2) [r(\partial^2 r / \partial m \partial n) + k(\partial r / \partial m)(\partial r / \partial n)] \quad (1.17)$$

This may also be written

$$\begin{aligned} \Delta F_{m,n} &= i_m i_n (dm \cdot dn / r^2) (1/r^{k-1})(\partial / \partial n) [r^k (\partial r / \partial m)] \\ &= i_m i_n r^{-(k-1)} (\partial / \partial n) [r^k (\partial r / \partial m)] dm \cdot dn. \end{aligned} \quad (1.18)$$

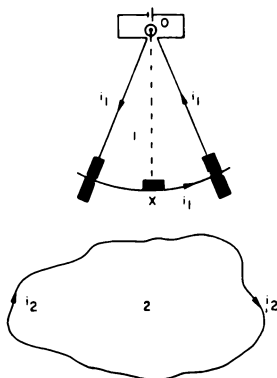


Fig.7 Ampere's wire-arc experiment

Ampere then invokes the result of another of his null-experiments to determine the value of k . The experiment to which he refers is sketched in fig.7. To distinguish it from the other null-experiments it will be called the wire-arc experiment. It proves the mechanical force on a circular arc section of a current carrying circuit 1, due to current in a separate closed circuit 2 of any shape and disposition, to be entirely perpendicular to the arc. As shown in fig.7, Ampere floated the arc section on two mercury troughs and left it free to rotate the insulator arm OX about the pivot O. During the experiment the arc remained stationary as circuit 2 was brought up to it and moved around. From this it could be concluded that the tangential force on the wire-arc portion was zero.

Take (1.18) and substitute for $\partial r / \partial m$ from (1.12).

$$\Delta F_{m,n} = i_m i_n dm r^{-(k+1)} \left(\frac{\partial}{\partial n} \right) (r^k \cos \alpha) dn \quad (1.19)$$

That component of the mutual force which acts tangentially on the dm -element is obtained by multiplying (1.19) with

$\cos \alpha$. If it is to agree with experiment, this tangential force, when integrated over all dn -elements in circuit 2, must come to zero. Hence we may write

$$\int_2 \Delta F_{m,n} \cos \alpha = i_m i_n \int_2 r^{-(2k+1)} r^k \cos \alpha (\partial/\partial n) (r^k \cos \alpha) dn = 0. \quad (1.20)$$

For integration by parts according to $\int u dv = uv - \int v du$ we let

$$u = r^{-(2k+1)}; \quad \partial u / \partial n = -(2k+1) r^{-2(k+1)} \partial r / \partial n$$

$$v = \frac{1}{2} r^{2k} \cos^2 \alpha; \quad dv = r^k \cos \alpha (\partial/\partial n) (r^k \cos \alpha) dn$$

Therefore

$$\int_2 \Delta F_{m,n} \cos \alpha = \frac{1}{2} i_m i_n \left[\left(\cos^2 \alpha / r \right) \right]_n^n + (2k+1) \int_2 (\cos^2 \alpha / r^2) dr \quad (1.21)$$

The limits n and n' of the first term are actually adjacent infinitely short elements on circuit 2 and therefore the first term of (1.21) vanishes. However, as Ampere pointed out, many closed circuits can be imagined for which the integral in the second term of (1.21) will not vanish. Hence we are left with

$$k = -1/2 \quad (1.22)$$

as the only possibility of reducing (1.20) to zero, whatever the shape or disposition of circuit 2. As can be seen from (1.7) and (1.8), k determines the difference in the mutual interaction of equal parallel current elements between (a) elements lying along the line connecting their centers, and (b) elements set perpendicular to that line. With (1.22) substituted into (1.8) it is evident that two elements of unit strength and separated by unit distance repel each

other half as strongly, when lying along the line connecting their centers, than they would attract each other when arranged transverse to this line.

With equations (1.11) and (1.22) Ampere wrote his force law as follows

$$\Delta F_{m,n} = -i_m i_n (dm \cdot dn / r_{m,n}^2) [\cos \epsilon - (3/2) \cos \alpha \cos \beta] \quad (1.23)$$

It was Ampere who first clarified the difference between what we now call voltage and current. His force law proved that the square of current must have the same dimension as mechanical force. With this fact he defined an electrodynamic unit of current which was smaller than today's electromagnetic unit of current measured in absolute ampere. To obtain electromagnetic units of current, the electrodynamic measures have to be multiplied by $\sqrt{2}$. With this change of units we obtain Ampere's force law in the modern form

$$\Delta F_{m,n} = -i_m i_n (dm \cdot dn / r_{m,n}^2) (2 \cos \epsilon - 3 \cos \alpha \cos \beta) \quad (1.24)$$

This gives the elemental force in dyn provided the currents i_m and i_n are inserted in absolute-ampere.

A most important aspect of Ampere's theory is that the individual current element does not interact with itself. There is little or no discussion of this point in Ampere's papers because he took it for granted that in any newtonian model every elemental force must be the result of the mutual interaction of two elements of matter.

Ampere considered current elements to be infinitely divisible. This was in harmony with the ideas of the 1820's when electricity was still considered to be a subtile fluid or continuum. In any case without the differential and integral calculus Ampere would have been unable to calculate forces. This is an example illustrating how the availability

of mathematical tools shapes contemporary physics. If the Ampere electrodynamics is to gain a place in modern physics it has to be related to electrons and ions which impose a lower limit on the size of current elements. This clashes with the differential calculus but may become manageable with computers.

An often voiced contemporary criticism of current elements is that they are a fictitious concept and produce discontinuities at straight line junctions. This fact was also of concern to Ampere. He went to great length to demonstrate to his own satisfaction that a smooth wire curve could be adequately represented with his discontinuous elements. One of his null-experiments was specifically designed to prove this argument. The essential features of the experiment are shown in fig.8. It will be referred to as the

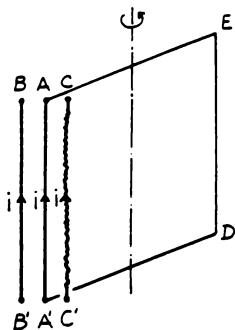


Fig.8 Ampere's bent-wire experiment

bent-wire experiment. AA'DE is a rectangular current loop in a vertical plane and suspended so that it is free to rotate about its vertical center line. As before, for the sake of clarity, Ampere's additional circuit to offset the effect of the terrestrial magnetic field is not shown in fig.8.

BB' is a straight wire parallel to AA' and placed close to it. CC' is the bent wire arranged with its axis parallel to and at the same level as BB' and AA'. Ampere fitted the bent wire into a narrow slot of a wooden post and described it as being twisted over its entire length in the plane perpendicular to BCC'B' and such that the wire at no point departed more than a very short distance from the midpoint of the slot. The experiment proved that if the wires BB' and CC' carried currents in the same direction and were equidistant from AA', as indicated in fig.8. no turning moment was exerted on the loop AA'DE. Hence, depending on the sign of the current in AA', the bent wire CC' exerted the same force of attraction or repulsion on the center wire as did the straight wire BB'.

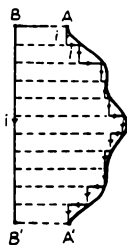


Fig.9 Equivalence of bent and straight wire sections

Based on this experimental result Ampere argued a curved wire section, as for example AA' in fig.9, was equivalent to the straight section BB' provided B coincided with A and B' with A'. For an explanation he offered the vectorial cancellation of the transverse subelements shown by broken lines in fig.9, and the vectorial addition of longitudinal subelements. Ampere believed the equivalence to hold also when AA' was a three-dimensional curve, although the bent-wire experiment was only a two-dimensional test.

For the few years during which Ampere concerned himself

with electrodynamics the published record shows little discussion of the current distribution over the wire cross-section and to what extent this may be compatible with a line representation of the current element. At his time most experiments were carried out with a relatively small number of galvanic cells and the conductors were thin wires. The three-dimensional representation of the current stream was not a pressing issue. Ampere's theory can be adapted to conductors of large cross-section by subdividing them into thin wire-like filaments. This will be undertaken in later chapters.

Energy conservation was introduced after Ampere's death. Electrodynamic forces are capable of doing work and they must therefore be associated with a store of energy. It was left to Ampere's followers and opponents to illucidate this issue which, to a large extent, has been responsible for giving the electromagnetic field preference over Ampere's matter-bound interaction model.

Equation (1.24) is an empirical law which is not known to have failed during the more than 160 years of its existence, so long as it is applied only to metallic conductors. The method by which Ampere deduced his law from experiments is of academic interest, but it has no bearing on the validity of the law. Like the scaffolding used to erect a building, the method of deducing an empirical law may be discarded as soon as the law has been found.

NEUMANN'S ELECTRODYNAMIC POTENTIAL

Twenty years elapsed between the conclusion of Ampere's study of electrodynamics and F.E. Neumann's first memoir, in 1845, on the theory of electromagnetic induction. This was Franz Neumann, the father of Carl Neumann. The latter also became one of the famous electricians of the nineteenth century. Much had happened in these twenty years. Faraday discovered electromagnetic induction in 1831. There was a general awakening to the atomicity of electricity.

By theoretical reasoning Neumann [8, 9] arrived at the concept of the electrodynamic potential. With the notation used for Ampere's theory, this may be expressed as

$$P_{m,n} = \pm \frac{1}{2} i_m i_n \iint_{mn} (\cos \epsilon / r_{m,n}) dm \cdot dn \quad (1.25)$$

This is the mutual potential of two closed circuits, m and n , carrying currents i_m and i_n . The double integration involves each pair of current elements twice, but Ampere's electrodynamics assumes them to interact only once. Neumann takes account of this by the factor of $\frac{1}{2}$. This has to be born in mind when summing the potential contributions of finite elements by computer when time may be saved by computing each interaction only once. Neumann felt uncertain about the sign of the electrodynamic potential until, with the help of 'virtual work', he had been able to derive Ampere's force law from the potential.

Neumann is best remembered by his mutual inductance formula

$$M_{m,n} = \pm \iint_{mn} (\cos \epsilon / r_{m,n}) dm \cdot dn \quad (1.26)$$

which arises directly from the electrodynamic potential. The sign of mutual inductance is also determined by virtual

work considerations. In the last equation the factor of $\frac{1}{2}$ has been quietly dropped, but it applies just as much to (1.26) as it does to (1.25). Many precise inductance calculations are based on Neumann's mutual inductance formula. Maxwell incorporated it into field theory and in the process changed its meaning to magnetic flux linkage per unit current.

Comparing the electrodynamic potential (1.25) with Ampere's force law (1.24), it will be seen that the dimension of the potential is force times distance, or energy. Any change in the current intensities or the relative position of the current elements which increases the potential requires work to be done on the two circuits, while energy is being stored in them or by them. Conversely, if the potential is reduced, stored energy will be transformed to mechanical work or Joule heat or both.

While Neumann speaks of work, free energy divorced from matter was not considered in his mathematical analysis.

In the Ampere-Neumann electrodynamics P appears to be potential energy, for the framework of this theory lacks a mechanism by which the slow lateral displacement of a constant current could involve the transfer of kinetic energy. Though both Ampere and Neumann used the term 'current', neither of them ascribed to it momentum, as Maxwell would do later.

Neumann changed his mind about the sign which should be given to the electrodynamic potential. In his first paper [8] he defined it as follows:

"The potential of two closed currents of unity intensity, relative to each other, is the sum of the products of the elements of one current with the elements of the other, each product of two elements being multiplied with the cosine of the angle of their inclination and divided by their distance."

Following this definition he used (1.25) with the positive sign. In the second paper [9] presented two years later in 1847, he repeated the definition but inserted "the negative half-sum" for "the sum". From then onward he used (1.25) with the negative sign.

In potential theory there have always existed difficulties in agreeing on a universal sign convention. Kellogg [10] points out that the most popular rule is to assign negative potential energy to elements of like sign which attract each other, and positive potential energy to elements of like sign which repel each other. Gravitating particles are an example of the former class and electrical charges are an example of the latter. If elements have signs attached to them they are scalar quantities, and current elements are not of this nature. They have definite directions and therefore are vectors. Hence it would seem the potential energy of current elements and circuits made up of these elements may sometimes be positive and sometimes negative. What could be meant by negative potential energy? We cannot conceive of less than no energy. Hence positive and negative potential energy must be two kinds of energy, like positive and negative charge are two kinds of electricity. One kind of potential energy would be associated with forces of attraction and the other with repulsion. However, unlike charge, the two could not be neutralized by putting them together.

Let us now examine the particular case of two very long, parallel, straight wires m and n , as sketched in fig.10. In case (a) of that figure they carry currents in the same direction. From experience we know the wires will then attract each other. Following common practice in potential theory we should say they are associated with negative potential energy. Now assume an externally applied force F_x tends to increase the distance of separation x and brings about the displacement ∂x by moving n to n' . This external force

has to do work and expend an amount of energy equal to $F_x \partial x$. At first it may be thought that this energy is being added to the stored potential energy. However, this cannot be so because the magnitude of the electrodynamic potential of (1.25) decreases as a result of the lengthening of the distances between pairs of contributing current elements. Not only does the mechanical source which sustains the external force supply energy, but the potential energy store also gives up energy. What absorbs these two streams of energy? As the currents are assumed to remain constant, no additional Joule heat will be dissipated. As we will show later, according to Neumann's theory all this energy flows to the two electrical sources which maintain the currents. Some of the Joule heat normally furnished by these sources will, during the transition of one conductor from n to n' , be supplied by the potential energy store and the mechanical energy source.

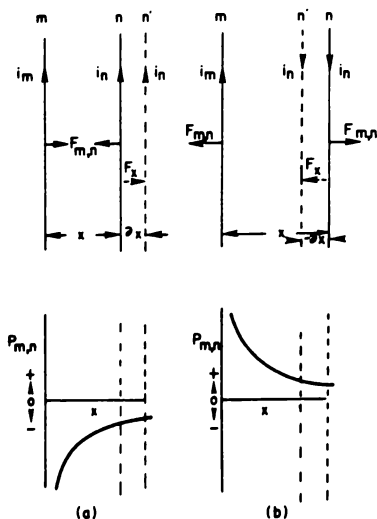


Fig.10 Electrodynamic potential energy of straight and parallel currents

In the case of fig.10(b), where the currents flow in opposite directions and the conductors repel each other, the displacement ∂x from n to n' again requires the supply of energy by the mechanical source sustaining the external force, but now the magnitude of the stored energy increases because of the shortening of element distances. This opens the possibility of all the energy provided by the mechanical source being stored as potential energy, and the electrical sources maintaining the currents are either not involved in the transaction or they exchange energy with each other.

Neumann related the reciprocal force of repulsion or attraction between two circuits m and n to the mutual potential of the circuits by

$$(F_{m,n})_x = -\partial P_{m,n} / \partial x \quad (1.27)$$

where x denotes a particular direction in which the virtual displacement ∂x takes place. At the same time he chose the negative sign for the potential of (1.25). The cosine of ϵ then decides whether, in any particular circuit arrangement, the mutual potential energy turns out to be positive or negative.

When applying Neumann's sign convention to the two conductor arrangements of fig.10 it is found, first of all, that

$$\text{for fig.10(a):} \quad \cos \epsilon = +1 \quad (1.28)$$

$$\text{for fig.10(b):} \quad \cos \epsilon = -1 \quad (1.29)$$

Therefore

$$\text{for fig.10(a):} \quad P_{m,n} = -i_m i_n \iint_{mn} (1/r_{m,n}) dm \cdot dn \quad (1.30)$$

$$\text{for fig.10(b):} \quad P_{m,n} = +i_m i_n \iint_{mn} (1/r_{m,n}) dm \cdot dn \quad (1.31)$$

In this way attraction becomes associated with negative potential energy and repulsion with positive energy. Taking the gradient of the potential energy with respect to x we find

$$\text{for fig.10(a): } \partial P_{m,n}/\partial x = +i_m i_n \iint_{mn} (1/r_{m,n}^2) (\partial r/\partial x) dm \cdot dn \quad (1.32)$$

$$\text{for fig.10(b): } \partial P_{m,n}/\partial x = -i_m i_n \iint_{mn} (1/r_{m,n}^2) (\partial r/\partial x) dm \cdot dn \quad (1.33)$$

So we arrive at the interaction force in the specific direction x given by

$$(F_{m,n})_x = -\partial P_{m,n}/\partial x = \pm i_m i_n \iint_{mn} (1/r_{m,n}^2) (\partial r/\partial x) dm \cdot dn \quad (1.34)$$

In the case of fig.10(a) the force defined by this last equation is negative, signifying attraction, in agreement with experience. Similarly, for fig. 10(b), the force becomes positive or repulsion. Hence Neumann's sign convention gives the correct direction of the forces in the specific example of fig.10. He extended this proof to the general case of two circuits of any shape. The potential function ultimately adopted by Neumann therefore was

$$P_{m,n} = -i_m i_n \iint_{mn} (\cos \epsilon / r_{m,n}) dm \cdot dn \quad (1.35)$$

which at times has been multiplied by $\frac{1}{4}$ to allow for a double summation of element interactions. Equation (1.35) will henceforth be used in preference to (1.25).

Neumann did not set out to derive the electrodynamic potential. He discovered it while developing a theory of electromagnetic induction based on Ampere's force law. It means (1.35) must be compatible with (1.24). This can be shown in the following way. The x -component of the ampe-

rian force on a current element $i_m dm$ due to a closed current circuit n may be written

$$\int_n (\Delta F_{m,n})_x dn = -i_m dm i_n \int_n (\cos \theta_{r,x} / r^2) (2 \cos \epsilon - 3 \cos \alpha \cos \beta) dn \quad (1.36)$$

where $\theta_{r,x}$ is the angle between the distance vector $r_{m,n} - r$ and the positive x -direction. It should also be noted that $\cos \theta_{r,x} = (\partial r / \partial x)$.

Now we consider the integral

$$\int_n (1/r^2) \cos \alpha \cos \theta_{n,x} dn = \int_n (1/r^2) (\partial r / \partial n) (dx_n / dn) dn \quad (1.37)$$

where $(dx_n / dn) = \cos \theta_{n,x}$ is the cosine of the angle between $i_n dn$ and the positive x -direction. But (1.37) may also be written

$$\begin{aligned} & - \int_n (dx_n / dn) (\partial / \partial n) (1/r) dn \\ & = \int_n (\partial / \partial n) [(x_m - x_n) (\partial / \partial n) (1/r)] - (x_m - x_n) (\partial^2 / \partial n \partial n) (1/r) dn \end{aligned} \quad (1.38)$$

Being a closed integral, the first term of (1.38) vanishes on integration because all quantities involved have the same value at both limits. Therefore

$$\int_n (1/r^2) \cos \alpha \cos \theta_{n,x} dn = - \int_n (x_m - x_n) (\partial^2 / \partial n \partial n) (1/r) dn \quad (1.39)$$

$$(\partial / \partial n) (1/r) = -(1/r^2) (\partial r / \partial n)$$

$$(\partial^2 / \partial n \partial n) (1/r) = (2/r^3) (\partial r / \partial n) (\partial r / \partial n) - (1/r^2) (\partial^2 r / \partial n \partial n)$$

But from (1.12)

$$(\partial r / \partial m)(\partial r / \partial n) = -\cos \alpha \cos \beta \quad (1.41)$$

and from (1.16)

$$-\cos \epsilon = r(\partial^2 r / \partial m \partial n) + (\partial r / \partial m)(\partial r / \partial n)$$

so that

$$(\partial^2 r / \partial m \partial n) = -[(\cos \epsilon) / r] + (1/r) \cos \alpha \cos \beta \quad (1.42)$$

Substitute (1.41) and (1.42) into (1.40).

$$\begin{aligned} (\partial^2 / \partial m \partial n)(1/r) &= (2/r^3)(-\cos \alpha \cos \beta) + [(\cos \epsilon) / r^3] - (1/r^3) \cos \alpha \cos \beta \\ &= (1/r^3)(\cos \epsilon - 3 \cos \alpha \cos \beta) \end{aligned} \quad (1.43)$$

Substitute (1.43) into (1.39).

$$\begin{aligned} \int_n (1/r^2) \cos \alpha \cos \theta_{n,x} dn &= \\ &= - \int (\cos \theta_{r,x} / r^2) (\cos \epsilon - 3 \cos \alpha \cos \beta) dn \end{aligned} \quad (1.44)$$

By combining (1.36) with (1.44) it can be shown that

$$\int_n (\Delta F_{m,n})_x dn = i_m dm \int_n (1/r^2) (\cos \epsilon \cos \theta_{r,x} - \cos \alpha \cos \theta_{n,x}) dn \quad (1.45)$$

To evaluate the integral in (1.45) we follow Neumann's original method [8] and resolve each current element with respect to x , y , and z , as indicated in fig.11. A total of nine interactions have then to be taken into account between the six components. Their contributions to (1.44) are listed in table 1. We note that

$$(\partial r / \partial x_m) = -(\partial r / \partial x_n); \quad (\partial r / \partial y_m) = -(\partial r / \partial y_n); \quad (\partial r / \partial z_m) = -(\partial r / \partial z_n)$$

This and table 1 enables us to write (1.45) as follows

$$\begin{aligned} \int_n (\Delta F_{m,n})_x \, dn &= \\ &= i_m i_n \int_n \{ [(\partial r / \partial x_m) - (\partial r / \partial x_n)] (dx_m dx_n / r^2) + (\partial r / \partial y_m) (dy_m dx_n / r^2) \\ &\quad - (\partial r / \partial x_n) (dy_m dy_n / r^2) + (\partial r / \partial z_m) (dz_m dx_n / r^2) - (\partial r / \partial x_n) (dz_m dz_n / r^2) \} \\ &= i_m i_n \int_n \{ -[(\partial / \partial x_m)(1/r) dx_m + (\partial / \partial y_m)(1/r) dy_m + (\partial / \partial z_m)(1/r) dz_m] dx \\ &\quad + (dx_m dx_n + dy_m dy_n + dz_m dz_n) (\partial / \partial x_n)(1/r) \} \end{aligned} \quad (1.46)$$

On integrating the first term around the complete circuit n this will disappear because it represents the differential of $(1/r)$ which has the same value at both limits. Therefore the x -component of the force acting on i_m is

$$\int_n (\Delta F_{m,n})_x \, dn = i_m i_n \int_n (dx_m dx_n + dy_m dy_n + dz_m dz_n) (\partial / \partial x_n)(1/r) \quad (1.47)$$

With direction cosines it can be seen that the first bracketed factor of (1.47) is equal to $dn \cos \epsilon$. The total force of attraction or repulsion between the entire circuits m and n , resolved with respect to the x -direction, is then given by

$$\begin{aligned} (F_{m,n})_x &= \int_m \int_n (\Delta F_{m,n})_x \, dm \, dn = i_m i_n (\partial / \partial x) \int_m \int_n (\cos \epsilon / r) \, dm \, dn \\ &= -\partial P_{m,n} / \partial x. \end{aligned} \quad (1.48)$$

Equation (1.48) proves the amperian forces on current elements to be consistent with Neumann's electrodynamic poten-

tial (1.35) and the potential gradient defined by (1.27).

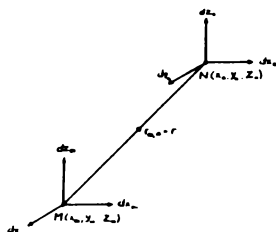


Fig.11 Resolution of current elements $i_m dm$ at M and $i_n dn$ at N

Table 1. Contributions to (1.44) of the current element components shown in fig.11

Inter- action	$\cos \alpha$	$\cos \theta_{n,x}$	$\cos \epsilon$	$\cos \theta_{r,x}$	$\cos \alpha \cos \theta_{n,x}$ $-\cos \epsilon \cos \theta_{r,x}$
$dx_m dx_n$	$\partial r / \partial x_m$	1	1	$\partial r / \partial x_n$	$\partial r / \partial x_m - \partial r / \partial x_n$
$dx_m dy_n$		0	0		0
$dx_m dz_n$		0	0		0
$dy_m dx_n$	$\partial r / \partial y_m$	1	0		$\partial r / \partial y_m$
$dy_m dy_n$		0	1	$\partial r / \partial x_n$	$-\partial r / \partial x_n$
$dy_m dz_n$		0	0		0
$dz_m dx_n$	$\partial r / \partial z_m$	1	0		$\partial r / \partial z_m$
$dz_m dy_n$		0	0		0
$dz_m dz_n$		0	1	$\partial r / \partial x_n$	$-\partial r / \partial x_n$

Since any straight line connected to the two circuits m and n may be chosen as the x -axis, the three axes can be interchanged and the cartesian components of the mutual force are therefore

$$\left\{ \begin{matrix} F_{m,n} \end{matrix} \right\}_x = -\partial P_{m,n} / \partial x; \quad \left\{ \begin{matrix} F_{m,n} \end{matrix} \right\}_y = -\partial P_{m,n} / \partial y; \quad \left\{ \begin{matrix} F_{m,n} \end{matrix} \right\}_z = -\partial P_{m,n} / \partial z \quad (1.49)$$

According to (1.48) the mutual force between two closed circuits is made up of contributions which take the form

$$\begin{aligned} (\Delta F_{m,n}) &= i_m i_n \, dm \cdot dn \cos \epsilon \, (\partial / \partial x) (1/r_{m,n}) \\ &= -i_m i_n (dm \cdot dn / r_{m,n}^2) \cos \epsilon \, (\partial r_{m,n} / \partial x) \end{aligned}$$

and when the x-direction coincides with $r_{m,n}$ this simplifies to

$$\Delta F_{m,n} = -i_m i_n (dm \cdot dn / r_{m,n}^2) \cos \epsilon \quad (1.50)$$

Equation (1.50) may be called Neumann's force law for current elements. Its use must be restricted to computing the reciprocal reaction force between two closed metallic circuits.

This law will not reveal balanced internal stress producing forces in either circuit. The interaction of current elements of the same circuit can generate tension and compression which are accurately predicted by Ampere's force law (1.23). Neither Ampere nor Neumann studied the distribution of ponderomotive forces around a single isolated circuit. Difficulties with diverging integrals probably prevented them from undertaking this task.

A long forgotten aspect of Neumann's theory is the derivation of turning moments, or mechanical torques, from the electrodynamic potential. Consider two rigid, closed circuits m and n carrying currents i_m and i_n , respectively. If circuit n is fixed to the laboratory frame, circuit m will exert torques $\{T_{m,n}\}_x$, $\{T_{m,n}\}_y$, and $\{T_{m,n}\}_z$ about arbitrarily chosen cartesian coordinates x , y , and z . Alternatively, if m is fixed, n will exert torques of the same magnitudes but in opposite directions about the coordinate axes.

To show the relationship between torque and electrodynamic potential we examine $(T_{m,n})_z$ exerted by circuit m about the z -axis, with ψ_z being the angular displacement. Following Neumann's method and with the aid of fig.12 it will be seen that

$$(T_{m,n})_z = \int_m [x_m \int_n (\Delta F_{m,n})_y dn - y_m \int_n (\Delta F_{m,n})_x dn] dm \quad (1.51)$$

But from (1.46)

$$\int_n (\Delta F_{m,n})_x dn = -i_m i_n \int_n [(\partial/\partial m)(1/r) dx_n - (\partial/\partial x_m)(1/r) \cos \epsilon dn] \quad (1.52)$$

$$\int_n (\Delta F_{m,n})_y dn = -i_m i_n \int_n [(\partial/\partial m)(1/r) dy_n - (\partial/\partial y_m)(1/r) \cos \epsilon dn] \quad (1.53)$$

Substitution of (1.52) and (1.53) into (1.51) and rearranging the terms gives

$$\begin{aligned} (T_{m,n})_z &= i_m i_n \iint_{mn} \cos \epsilon [x_m (\partial/\partial y_n)(1/r) - y_m (\partial/\partial x_n)(1/r)] dm \cdot dn \\ &\quad - i_m i_n \iint_{mn} \{ [x_m (\partial y_n / \partial n) - y_m (\partial x_n / \partial n)] (\partial/\partial m)(1/r) \} dm \cdot dn \end{aligned} \quad (1.54)$$

Integrating the second term of (1.54) by parts gives

$$\begin{aligned} &-i_m i_n \left[\int_n (1/r) \{ x_m (\partial y_n / \partial n) - y_m (\partial x_n / \partial n) \} \right]_{r_2}^{r_1} \\ &\quad - i_m i_n \iint_{mn} (1/r) \{ (\partial x_m / \partial m) (\partial y_n / \partial n) - (\partial y_m / \partial m) (\partial x_n / \partial n) \} dm \cdot dn \end{aligned} \quad (1.55)$$

The first term of (1.55) has the same value at both limits of r and therefore vanishes, so that (1.54) may be written

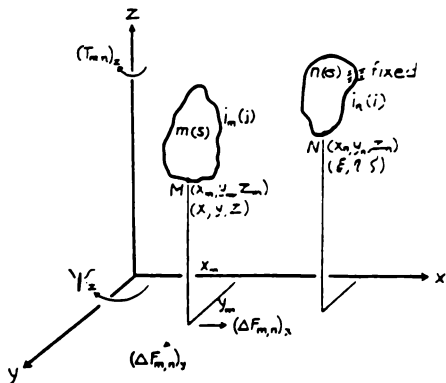


Fig.12 Torque from electrodynamic potential

$$\begin{aligned}
 (T_{m,n})_z &= i_m i_n \iint \cos \varepsilon [x_m (\partial / \partial y_m) (1/r) - y_m (\partial / \partial x_m) (1/r)] dm \cdot dn \\
 &\quad + i_m i_n \iint (1/r) [(\partial x_m / \partial m) (\partial y_n / \partial n) - (\partial y_m / \partial m) (\partial x_n / \partial n)] dm \cdot dn
 \end{aligned}
 \quad (1.56)$$

As ψ_z is the angular displacement about the z-axis it follows that

$$\begin{aligned}
 (\partial / \partial \psi_z) (1/r) &= (\partial / \partial x_m) (1/r) (\partial x_m / \partial \psi_z) + (\partial / \partial y_m) (1/r) (\partial y_m / \partial \psi_z) \\
 &\quad + (\partial / \partial z_m) (1/r) (\partial z_m / \partial \psi_z)
 \end{aligned}
 \quad (1.57)$$

$$\cos \varepsilon = (\partial x_n / \partial n) (\partial x_m / \partial m) + (\partial y_n / \partial n) (\partial y_m / \partial m) + (\partial z_n / \partial n) (\partial z_m / \partial m)
 \quad (1.58)$$

$$\begin{aligned}
(\partial/\partial\psi_z)(\cos\epsilon) &= (\partial x_n/\partial n)(\partial/\partial m)(\partial x_m/\partial\psi_z) \\
&+ (\partial y_n/\partial n)(\partial/\partial m)(\partial y_m/\partial\psi_z) + (\partial z_n/\partial n)(\partial/\partial m)(\partial z_m/\partial\psi_z)
\end{aligned} \quad (1.59)$$

$$(\partial x_m/\partial\psi_z) = -y_m; \quad (\partial y_m/\partial\psi_z) = x_m; \quad (\partial z_m/\partial\psi_z) = 0 \quad (1.60)$$

Substituting (1.60) into (1.57)

$$(\partial/\partial\psi_z)(1/r) = x_m(\partial/\partial y_m)(1/r) - y_m(\partial/\partial x_m)(1/r) \quad (1.61)$$

and (1.60) into (1.59)

$$(\partial/\partial\psi_z)(\cos\epsilon) = (\partial y_n/\partial n)(\partial x_m/\partial m) - (\partial x_n/\partial n)(\partial y_m/\partial m) \quad (1.62)$$

The angular gradient of the electrodynamic potential is

$$\begin{aligned}
i_m i_n (\partial/\partial\psi_z) \iint_{mn} (\cos\epsilon/r) dm dn &= i_m i_n \iint_{mn} [\cos\epsilon (\partial/\partial\psi_z)(1/r) \\
&+ (1/r)(\partial/\partial\psi_z)(\cos\epsilon)] dm dn
\end{aligned} \quad (1.63)$$

With (1.57) to (1.62) the angular gradient of the electrodynamic potential may be expressed by

$$\begin{aligned}
i_m i_n (\partial/\partial\psi_z) \iint_{mn} (\cos\epsilon/r) dm dn &= \\
&= i_m i_n \iint_{mn} [\cos\epsilon \{x_m (\partial/\partial y_m)(1/r) - y_m (\partial/\partial x_m)(1/r)\}] dm dn \\
&+ i_m i_n \iint_{mn} (1/r) [(\partial y_n/\partial n)(\partial x_m/\partial m) - (\partial x_n/\partial n)(\partial y_m/\partial m)] dm dn
\end{aligned} \quad (1.64)$$

A comparison of (1.64) with (1.56) shows that

$$(T_{m,n})_z = i_m i_n (\partial/\partial\psi_z) \iint_{mn} (\cos\epsilon/r) dm dn \quad (1.65)$$

or with (1.35)

$$(T_{m,n})_z = -(\partial P_{m,n}/\partial\psi_z) \quad (1.66)$$

Similarly

$$(T_{m,n})_x = -(\partial P_{m,n} / \partial \psi_x); \quad (T_{m,n})_y = -(\partial P_{m,n} / \partial \psi_y) \quad (1.67)$$

This completes Neumann's proof that the mutual torque of two rigid current-carrying circuits, with respect to any arbitrary axis, is the negative angular gradient of the electrodynamic potential.

Neumann's electrodynamic potential is a quantity which in field theory is called stored magnetic energy. The potential given by equation (1.35) refers only to the mutually stored energy between the two circuits. The total stored magnetic energy would contain additional contributions from the interaction of current element pairs residing in the same circuit. This self-potential and the resulting reaction forces between parts of an isolated circuit were not considered by Neumann. He was probably stumped by the same integration singularities which are still baffling us today. It will later be shown how this difficulty can be overcome with computer aided finite current element analysis.

In Neumann's theory the magnetic energy of metallic circuits is associated with the forces of attraction and repulsion of current elements. These elements consist of the substance of the conductor material. The energy never becomes detached from the matter elements. In contrast to this matter theory, modern relativistic electromagnetism assumes that the energy is stored in the field or vacuum. Some of it resides in the vacuum space that is actually being occupied by the conductor. For the magnetic field energy to change in magnitude it has to move in and out of the conductor material. This poses philosophical questions which are absent in the Ampere-Neumann electrodynamics.

One of them would be: by what mechanism can magnetic field energy be recalled to the conductor from near and far zones of space?

Neumann's virtual work method of deriving mutual ponderomotive forces and torques from the change in stored magnetic energy has survived to this day. Formulas (1.48) and (1.65) are often preferred to calculations involving the Lorentz force. The double integral in these two equations will be recognized as the mutual inductance between the two circuits. This may be determined by a measurement with conveniently small ac currents which avoids involved computations.

It has become common practice to calculate the reaction forces between two parts of the same circuit also with equation (1.48), but the mutual inductance between two circuits is then replaced by the selfinductance of the isolated circuit. This procedure gives correct answers. It cannot be traced back to Neumann. Whilst the Lorentz force gives the same result as (1.48) for two circuits, it disagrees with Ampere's force law, and therefore (1.48), on the tension in an isolated circuit. Hence the use of (1.48) with a selfinductance gradient constitutes a calculation with Ampere's law and not with that of Lorentz. This fact is rarely appreciated by engineers using the virtual work concept for force calculations.

NEUMANN'S LAWS OF INDUCTION

As mentioned before, Neumann discovered the electrodynamic potential while working on his theory of electromagnetic induction. He started by setting up an elemental equation of induction due to the relative motion of two current elements. For this purpose he assumed that the electromotive force, e.m.f., induced in one of the elements depends on the current intensity in the other and also on the amperian force exerted between the elements which would arise if

the element experiencing the induction would simultaneously carry unit current. In this connection Neumann described the force as an action, instead of an interaction, to emphasize that induction can also occur when no current flows in one of the elements and therefore no mechanical force exists between the two.

Neumann's elemental law of induction due to relative motion may, in the notation employed in previous sections, be expressed as

$$\Delta e_n = -v_x (\Delta F_{m,n} / i_n) \cos \theta_{r,x} \quad (1.68)$$

where Δe_n is the induced e.m.f. in the conductor element dn shown in fig.13. The element dn is taken to move with velocity v_x along an arbitrary x -direction fixed relative to the position M of the inducing element $i_m dm$. $\Delta F_{m,n}$ is Ampere's mechanical force given by (1.24). Although Neumann assumed $i_n = 1$, (1.68) will hold for any value of this current. The angle $\theta_{r,x}$ lies between the distance vector $r_{m,n}$ and the positive x -direction. The negative sign arises from Lenz's law which Neumann quotes as follows [8]:

"If a metallic conductor moves relative to, and in the vicinity of, a galvanic current or magnet, the current induced in the conductor will flow in such a direction that, were the conductor at rest, it would be set in motion in the opposite direction, it being understood that the line of relative motion is fixed."

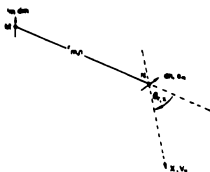


Fig.13 Diagram for equation (1.68)

Neumann treated the proportionality of the induced e.m.f. to the relative velocity and to the inducing current i_m as an experimentally established fact following from Faraday's and later work. The elemental (differential) law of induction (1.68) accords with the Newton-Ampere philosophy of simultaneous matter interaction at a distance and Δe_n should at all times be proportional to v_x , irrespective of any relative acceleration. However, Neumann felt a little uncertain on this point and on a number of occasions he refers to the 'stationary state' in which changes in current intensity and relative position of the elements progress at a rate which is slow compared with the 'Fortpflanzungsgeschwindigkeit' (velocity of travel) of electricity. As an example of non-stationary phenomena he quotes discharge currents from capacitors. In order to allow for delays between the cause of induction and its effect, Neumann makes a certain dimensional constant a function of time but does not proceed with the analysis of non-stationary phenomena. This constant was dropped in later years and Neumann's law of induction has ever since been assumed to be a law of simultaneous matter interaction.

Neumann noticed the induced e.m.f. to be related to the rate of change of the electrodynamic potential. This can be seen from (1.68), for

$$v_x \cos \theta_{r,x} = dr/dt \quad (1.69)$$

If we assume with (1.35) that the mutual potential of two closed currents is the sum of the elemental potential contributions $\Delta P_{m,n}$ from all current element pairs, with one element in either circuit, (1.68) may be given the form

$$i_n \Delta e_n = (d/dt)(\Delta P_{m,n}) \quad (1.70)$$

The left side of this equation represents power or energy flow to element dn and the right side gives the rate of

change of mutually stored potential energy of the two elements.

Neumann went to great length to show that a similar relationship applies to two complete circuits m and n . This can simply be written

$$i_n e_n = dp_{m,n}/dt \quad (1.71)$$

Substituting for the electrodynamic potential from (1.35), the total e.m.f. induced in the circuit n becomes

$$e_n = -(d/dt) \iint_{mn} (i_m \cos \epsilon / r_{m,n}) dm. dn \quad (1.72)$$

or

$$e_n = -(d/dt)(i_m M_{m,n}) \quad (1.73)$$

where $M_{m,n}$ is the mutual inductance of the two circuits also given by (1.26). The step from (1.72) to (1.73) may be taken as the definition of Neumann's mutual inductance in terms of matter interactions rather than magnetic flux linkage. Modern textbooks on electromagnetism call equation (1.73) Faraday's law. Without wishing to take away anything from the important experimental achievements of Faraday, it would be historically correct and fairer to F.E. Neumann to describe equation (1.73) as Neumann's law of induction.

When computing mutual inductances with Neumann's formula it is necessary to assign directions of current flow to the two closed circuits, as only this will make the angle ϵ unique for every element pair. When the directions of current flow are not known when the mutual inductance is being computed, it is customary to choose directions which will make $M_{m,n}$ positive. Reversing the direction of current flow in one of the circuits will not change the magnitude of the mutual inductance but reverse its sign.

Provided the conductor elements belong to two closed circuits it follows from (1.72) that the elemental e.m.f. may be expressed as

$$\Delta e_{/dn} = -(d/dt)[(i_{dm} \cos \varepsilon)/r_{m,n}] \quad (1.74)$$

The quantity inside the square brackets turns out to be the magnetic vector potential of the current element i_{dm} at point N, the center of the conductor element dn. Neumann wrote his papers before vector analysis was invented and he did not mention the magnetic vector potential. Denoting the vector potential by \underline{A} , Neumann's law of induction may be stated as

$$\Delta \underline{e}/dn = -(d/dt)\Delta \underline{A}_{m,n} \quad (1.75)$$

where the vector potential is given by

$$\Delta \underline{A}_{m,n} = i_{dm}/r_{m,n}; \quad \Delta \underline{A}_{n,m} = i_{dn}/r_{m,n} \quad (1.76)$$

Comparing equation (1.75) with (1.70) reveals just how closely the magnetic vector potential is related to the electrodynamic potential. If it is permissible to associate an individual current element with magnetic vector potential then it should be equally permissible to associate it with electrodynamic potential.

The vector potential is not a reciprocal interaction parameter because it involves only one current element. Therefore

$$\Delta \underline{A}_{m,n} \neq \Delta \underline{A}_{n,m} \quad (1.77)$$

As a consequence of (1.35), the electrodynamic potential of a pair of current elements belonging to separate closed circuits is

$$\Delta P_{m,n} = i_m i_n (\cos \epsilon / r_{m,n}) dm \cdot dn \quad (1.78)$$

and with (1.76) this is equal to the scalar products

$$\Delta P_{m,n} = i_m \underline{dm} \cdot \underline{A}_{n,m} = i_n \underline{dn} \cdot \underline{A}_{m,n} \quad (1.79)$$

Closed conduction currents may induce e.m.f's in open-circuited conductor sections. This problem was examined by Neumann. Consider a conductor n consisting of just a single element dn . In order to obtain the action (force) of the closed current i_m on dn , this single element must be assumed to carry unit current ($i_n = 1$ ab-amp). From (1.70) and (1.71) it follows that

$$i_n \Delta e_n = (d/dt) [-i_n dn i_m \int (\cos \epsilon / r_{m,n}) dm]$$

or

$$\Delta e_n = -dn (d/dt) i_m \int (\cos \epsilon / r_{m,n}) dm \quad (1.80)$$

An angle function which first occurred in equation (1.4) has the general form

$$f(\alpha, \beta, \epsilon) = 2 \cos \epsilon - 3 \cos \alpha \cos \beta \quad (1.81)$$

But Ampere's wire-arc experiment proved that, when one of the circuits is closed, we may set

$$3 \cos \alpha \cos \beta = \cos \epsilon \quad (1.82)$$

and then

$$f(\alpha, \beta, \epsilon) = \cos \epsilon \quad (1.83)$$

It is this restricted angle function which is being used in (1.80).

If the conductor n comprises more than one element and

extends from n_1 to n_2 , the e.m.f. induced in this length of conductor is

$$e_n = (d/dt) \left[i_m \int_{n_1}^{n_2} (\cos \epsilon / r_{m,n}) dm \cdot dn \right] \quad (1.84)$$

Neumann's theory of electromagnetic induction pertaining to metallic conductors survives in modern field theory. The words around the formulas have changed. Where Neumann spoke of interacting conductor elements and complete circuits we now talk of magnetic flux linkage. The e.m.f. per unit length has become the electric field intensity, and so on. The flux linkage idea breaks down when one of the circuits is unclosed. However, Neumann's method can deal with the e.m.f. in an unclosed conductor, as has been shown with equation (1.84).

Since the electrodynamic potential was derived from Ampere's force law, and since this potential also furnishes the law of induction preserved in field theory, one might expect Maxwell's equations to contain Ampere's force law. This is not the case. Maxwell [14] himself was aware of the fact that field theory is apparently not based on a unique force law. He strongly endorsed Ampere's law but thought the Grassmann formula would do equally well. This latter formula will be discussed in the next section. It has become the magnetic component of the Lorentz force acting between two moving charges and thereby has been thought to supersede Ampere's force law.

Classical physics was built on the pillars of three empirical laws, those of Newton, Coulomb and Ampere. Modern physics seems to rest on three floating platforms: the field, relativity and quantized free energy. Newton's refusal to let hypotheses prevail ushered in the first two centuries of quantitative science and brought us the spiritual shackles of determinism. Modern physics has broken out of this confinement and set the human spirit free and roaming once

more, as it was in the days of the alchemist and aether whirlpools. The first step toward the new physics was taken by Maxwell when he gave us a theory that was not based on an empirical force law.

GRASSMANN'S FORCE LAW

Ampere and Neumann concerned themselves not only with the interaction of linear currents in metallic conductors but also with the mechanical and electromotive forces between magnets and mixed systems containing magnets and current circuits. Ampere's concept of the magnetic molecule has proved to have lasting value and Neumann showed the equivalence of a current carrying circuit and a magnetic shell bounded by the circuit. However, the present book does not deal with the behavior of magnetic materials and concerns itself solely with the interaction of electric currents in non-magnetic metals. In this restricted sense electrodynamics is the science of metallic current elements.

The force law for two current elements which has been used almost to the exclusion of all others during the past eighty years was first proposed by Grassmann [11] in 1845, the same year Neumann published his theory of induction. Grassmann's is an unsymmetrical law and therefore has to be stated by two equations. One is for the force on element dm , to be written ΔF_m , and the other for the force ΔF_n acting on element dn . In vector form, but otherwise with the previously employed notation, these two equations may be written

$$\Delta \underline{F}_m = (i_m i_n / r_{m,n}^2) \underline{dm} \times (\underline{dn} \times \underline{a}_{r,m}) \quad (1.85)$$

$$\Delta \underline{F}_n = (i_m i_n / r_{m,n}^2) \underline{dn} \times (\underline{dm} \times \underline{a}_{r,n})$$

where the direction of the unit distance vectors $\underline{a}_{r,m}$ and

$\underline{a}_{r,n}$ is along the line connecting the elements and pointing toward the element at which the force is being determined.

To see the connection with the Ampere-Neumann electrodynamics it is best to resolve the triple vector products in (1.85) according to

$$\underline{A} \times (\underline{B} \times \underline{C}) = \underline{B}(\underline{A} \cdot \underline{C}) - \underline{C}(\underline{A} \cdot \underline{B}) \quad (1.86)$$

Applying (1.86) to (1.85) results in

$$\begin{aligned} \Delta \underline{F}_m &= \underline{dn}(1/r_{m,n}^2) \underline{i}_m \underline{i}_n \underline{dm} \cos \alpha_m - \underline{a}_{r,m}(1/r_{m,n}^2) \underline{i}_m \underline{i}_n \underline{dm} \cdot \underline{dn} \cos c \\ \Delta \underline{F}_n &= \underline{dm}(1/r_{m,n}^2) \underline{i}_m \underline{i}_n \underline{dn} \cos \alpha_n - \underline{a}_{r,n}(1/r_{m,n}^2) \underline{i}_m \underline{i}_n \underline{dm} \cdot \underline{dn} \cos c \end{aligned} \quad (1.87)$$

The angles α_m and α_n must not be confused with α and β in Ampere's force law (1.24), but c is the same in both laws.

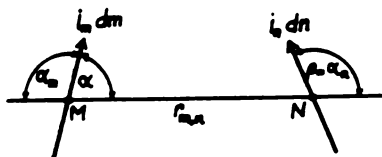


Fig.14 Angle convention for Ampere's and Grassmann's force laws (1.24) and (1.87)

Figure 14 further elucidates the angle convention of the two elemental force laws.

According to (1.85) a pair of current elements do not attract or repel each other, but each experiences a force perpendicular to itself which has its cause in the existence of the other. Furthermore, this force lies in the plane containing the element in question and the line connecting both elements. Grassmann also points out that, as a result

of Ampere's Rule (see page 13), the interaction of two current elements can always be reduced to a two-dimensional problem. With respect to fig.14 this means if we wish to determine the force on element dm we need only consider that component of the other element which lies in the plane of dm and the line connecting the two elements. In compliance with Ampere's Rule the component of the other element which is perpendicular to this plane produces no force on the element dm . Therefore the interacting components of two current elements and the Grassmann forces all lie in the same plane.

The abandonment of mutual attraction and repulsion between matter elements of electric conductors, and the violation of Newton's third law of motion which this entailed, signalled the end of classical physics. The Grassmann and Lorentz force laws required a new mechanics which was to become that of special relativity. Even if the Michelson and Morly experiment had never been carried out, the theory of special relativity would have been an inevitable consequence of the Grassmann and Lorentz electrodynamics. This aspect will be further discussed in connection with measurements of field-energy momentum conservation.

In the expanded form of Grassmann's force law, (1.87), there appears a newtonian term of repulsion or attraction which is exactly equal to Neumann's force term (1.50) for a closed circuit. The remaining term of the Grassmann formula is a force in the direction of the other current element. This term violates Newton's third law. It will be called the relativistic term of the Grassmann or Lorentz force. Whittaker [6] and a number of other authors have shown that when the Grassmann force on, say, dm is summed for a closed current circuit n , all the relativistic contributions add up to zero and only the force contributions made by the newtonian term survive. Precisely the same result would have been obtained with Ampere's force law. Hence if in

the Grassmann (or Lorentz) electrodynamics forces are being calculated due to closed metallic circuits we automatically, and in most instances unknowingly, slip back into the Ampere-Neumann electrodynamics. This is the explanation why the field theory of electric machines and devices has no problems with Newton's third law and special relativity appears to be irrelevant. This state of affairs is often wrongly attributed to the small magnitude of relative velocities. Special relativity produces large effects at the lowest relative velocities, but with closed circuits these effects integrate to zero and thereby seem to vanish.

The magnitude of the perpendicular force acting on, say, dn Grassmann gave as

$$\Delta F_n = i_m i_n (dm \cdot dn / r_{m,n}^2) \sin \theta \quad (1.88)$$

where θ is the angle of the Biot-Savart law (1.2), but with the ds -element replaced by the dm -element. Figure 15 depicts the connection between the Grassmann and Biot-Savart laws.

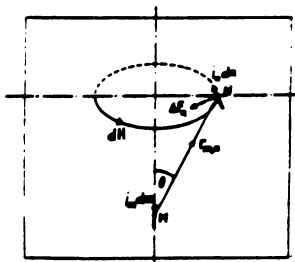


Fig.15 Derivation of Grassmann's force from the Biot-Savart law

The Biot-Savart law gives the magnetic field strength dH at N due to the dm current element. Therefore

$$\Delta F_n = i_n \underline{dn} \times \underline{dH} \quad (1.89)$$

This last equation clearly reveals that the Grassmann force is actually the magnetic component of the Lorentz force of modern field theory.

It is rather surprising to find Grassmann enunciating his law twenty years before Maxwell wrote his field equations and only Faraday spoke of magnetic flux. Grassmann was a mathematics teacher at a German high school. He was working in isolation of Neumann, the first professor of theoretical physics at the University of Koenigsberg, East Prussia. Grassmann's great achievement as a mathematician was the introduction of the vector calculus. There is some suspicion that he proposed his new electrodynamics [11] mainly in order to have a good application of vectors. He certainly achieved this with equation (1.85). The Lorentz force expression did not appear until the 1890's, fifty years after Grassmann published his electrodynamics. Lorentz was led to (1.89) by his theory of electrons [29].

On Grassmann's own authority, his analysis was prompted by two objections to Ampere's force law (1.24). The action of the forces along the straight line connecting the current elements Grassmann considered to be an arbitrary assumption. He could see no reason why these elements should behave like gravitating or charged particles which were scalar quantities while current elements had direction and were vectors.

As far as his second objection to Ampere's law is concerned he said [4]:

"The complicated form of this formula arouses suspicion, and the suspicion is heightened when an attempt is made to apply it. If, for example, the simplest case is considered, in which the circuit elements are parallel, so that $\epsilon = 0$ and $\alpha = \beta$, the Ampere expres-

sion becomes

$$(i_m i_n dm \cdot dn / r_{m,n}^2) (2 - 3 \cos^2 \alpha),$$

from which it appears that, when $\cos^2 \alpha$ is equal to $2/3$ or, which comes to the same thing, $\cos 2\alpha$ is equal to $1/3$, that is if the position of the mid-point of the attracted element lies on the surface of a cone whose apex is at the attracting element, and whose apex angle is $\arccos(1/3)$, there is no interaction; while for smaller angles there is repulsion, and for larger ones attraction. This is such an unlikely result, that the principle from which it is derived must come under the gravest suspicion and with it the supposition that the force in question must show an analogy with all other forces. It must be concluded that there is little reason to apply this analogy to our present field. Since in the case of all other forces it is originally point elements, without any definite direction, which interact with each other, so that the mutual interaction must 'a priori' be regarded as necessarily operating along the line connecting them, it is hard to see any justification for transferring this analogy to an entirely foreign field in which the elements are arranged in definite directions. The formula itself, which in no way resembles that for gravitational attraction, also indicates that there is no real analogy."

The force reversal which takes place when a current element, held parallel to itself, describes a circle around another element is plotted on fig.16. The mutual Ampere force varies from one arbitrary unit of repulsion at $\alpha=0$ or 180° to two units of attraction at $\alpha=90^\circ$ or 270° . In each quadrant there exists an angular position for which the force is zero and changes from attraction to repulsion, or vice versa. Grassmann did not like this unusual variation

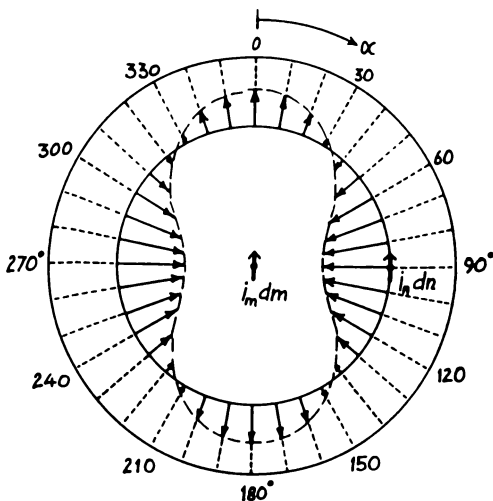


Fig.16 Polar diagram of the Ampere force between two parallel current elements of constant distance of separation

of the elemental force with angular position, but was unable to provide an argument which proved Ampere's force law to be wrong.

Lorentz established that Grassmann's formula was an empirical law for electric charges moving in vacuum, the current elements then being products of charges and their velocities. In 1845 Grassmann had no experimental results to support his force law. Instead he used mathematical and verbal arguments. His mathematical treatment is difficult to understand as he was still groping for an easy method of handling vectors.

The verbal logic which Grassmann put forward is interesting and worth summarizing. He had recognized that an infinitely long current behaves like a closed current loop in its interaction with other currents. That is to say, the force which an infinitely long current, closed through infinity, will exert on an element of another current is always perpendicular to the latter element, as proved by Ampere's wire-arc experiment. Grassmann then extended this principle to an angle-current (Winkelstrom). This is meant to be an infinitely long current forming the two arms of an angle, the current coming from infinity in one straight conductor arm and returning to infinity in another. Subsequently he assumed the force on any current element lying in the plane of an angle-current to be perpendicular to the element whatever its position or orientation in that plane. As

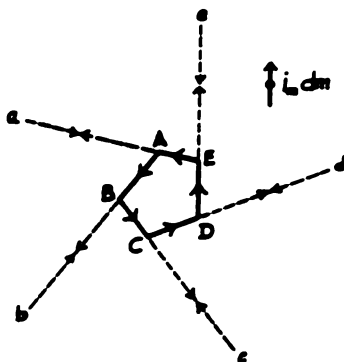


Fig.17 Grassmann's angle-current representation of a closed circuit

Ampere had done. Grassmann then assumed the wire to consist of a very large number of short and straight elements. Each element could be thought of as lying right at and to one side of the apex of an angle-current. This idea is further explained by fig.17 which deals with a simple arrange-

ment in which the closed circuit ABCDE consists merely of five elements. Now the element AB is part of the angle-current aAb and the element BC of the angle-current bCc , and so on. It will be appreciated that each of the infinite rays a , b , c , d , and e carry outgoing and incoming currents of the same magnitude superimposed on each other and therefore carry no current at all. With this mental picture established, Grassmann considered the force exerted on an external current element and in particular the interactions of this external current element with any of the elements of a closed circuit such as ABCDE of fig.17. He was convinced each of the latter elements would, independently of the others, generate a perpendicular force on the external element, because each of the elements of ABCDE was also part of a separate angle-current. Each angle-current of ABCDE could lie in a different plane. So the total force on the external element had to be the vector sum of the perpendicular force contributions of the individual elements of ABCDE. This appears to have been the basis on which Grassmann justified the directions of his elemental interaction forces. It is remarkable that Lorentz, using field theory, came up with the same directions. Grassmann's law conflicts with Newton's third law according to which every force on a particle of matter must be accompanied by an equal and opposite force on another particle of matter. The Grassmann forces were unequal and not opposite in direction. Grassmann did not discuss this issue.

Had Grassmann known Neumann's force law (1.50), he might have recognized that the angle-current argument should also apply to (1.50). As this latter equation did not agree with Grassmann's formula, the chances were that at least one of them was wrong.

Grassmann accepted Ampere's proof of the inverse square of distance relationship and the proportionality of the force to the current intensities and element lengths. The

sing of (1.88) stems from the Biot-Savart law, but Grassmann arrived at it without having to mention the two Frenchmen. The agreement between Grassmann's equation (1.88) and the expansion of the triple vector product (1.87) may be shown with fig.18. In this diagram $i_n dn$ is the resolved component of the general element at N in the plane of $i_m dm$ and $r_{m,n}$.

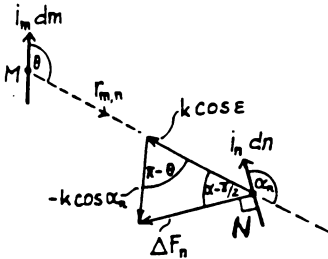


Fig.18 To prove the equality of (1.87) and (1.88)

Furthermore if

$$k = i_m i_n (dm \cdot dn / r_{m,n}^2)$$

then $k \cos \epsilon$ is the newtonian vector of (1.87) and $-k \cos \alpha_n$ the relativistic vector of the same equation. Applying the rule of sines to the force triangle of fig.18 gives

$$\Delta F_n / \sin(180^\circ - \epsilon) = -k \cos \alpha_n / \sin(\alpha_n - 90^\circ)$$

Therefore

$$\Delta F_n = k \cdot \sin \epsilon$$

which proves the magnitude equality of (1.87) and (1.88).

Grassmann's new electrodynamics had little impact on his contemporaries. It would now be completely forgotten but for the fact that it fitted in well with the 20th century field, relativity, and electron theories. Although it was based on many of Ampere's ideas and experiments, Grassmann's law did not contribute to the Ampere-Neumann electrodynamics. Historically, it was the beginning of a relativistic electrodynamics.

WEBER'S FORCE LAW AND ELECTRODYNAMIC POTENTIAL

Finding mathematical laws capable of quantifying Faraday's discovery, in 1831, of electromagnetic induction proved to take much longer than Ampere's deduction of a force law. No less than fourteen years elapsed before Neumann in Koenigsberg revealed his law of induction in 1845. Other physicists were studying this problem at the same time.

Among them were Fechner [12] and Weber [13] in Leipzig. Neumann had derived his theory of electromagnetic induction without hypothesis as to the nature of the electric fluid or fluids. He did, however, have to invent a new force, which he called the electromotive force, to distinguish it from the ponderomotive force which moved the metallic conductor. The Leipzig school employed the same two kinds of forces but let the electromotive force act on charged particles that possessed mass. Electrolysis had clearly revealed the existence of charged particles in an electric current, yet Fechner and Weber did not know of the rigid connection of positive ions to the metal lattice. That not all electrodynamic forces in a metal are ponderomotive forces must certainly have something to do with the bonds that exist between positive and negative charges, and the bonds between the charges and the solid body. By the end of the twentieth century, this whole subject has still not been satisfactorily resolved.

In its mathematical consequences, Weber's work added little to that of Coulomb, Ampere, and Neumann. It was based on the same simultaneous action-at-a-distance principle and involved relative velocities that were invariant under galilean transformations. However, Weber was the first to take notice of the atomicity of electricity and formulated a model of the metallic current element in terms of charged particles. Because of the mobility Weber assigned to positive ions in the solid metal conductor, his current element model proved unacceptable. The task of finding a microscopic model of the metallic current element which can account for the latest experimental findings has still to be accomplished, at the time of writing this book. Weber's theory will be reviewed in order to illustrate pitfalls which must be avoided on the way to a satisfactory, microscopic model of the metallic current element.

At the instigation of Fechner, Weber searched for a force expression which was mathematically equivalent to Ampere's law but defined the mechanical force between two current elements in terms of the static and dynamic, simultaneous interactions of positively and negatively charged mass particles streaming in opposite directions, past each other, through and along current elements. As this law had to include the interaction of charges at rest relative to each other, it was an attempt to unify electrostatics and electrodynamics while at the same time acknowledging the atomicity of electricity. As a result of this remarkable undertaking Weber proposed the following laws for the force $\Delta F_{e,e'}$ between two electrical charges e and e' , and the mutual potential $\Delta P_{e,e'}$ associated with this force.

$$\Delta F_{e,e'} = (e \cdot e' / r^2) [1 - (1/2c^2)(dr/dt)^2 + (r/c^2)(d^2r/dt^2)] \quad (1.90)$$

$$\Delta P_{e,e'} = (e \cdot e' / r) [1 - (1/2c^2)(dr/dt)^2] \quad (1.91)$$

where r is the distance between the charges, t the time,

and c a dimensional constant. So far the Ampere-Neumann electrodynamics has been formulated in fundamental electromagnetic units (e.m.u.). In contrast to this the Weber equations are given in fundamental electrostatic units (e.s.u.) because they contain Coulomb's law. According to the e.s.u. system the product of two electrostatic units of charge divided by the distance (in centimeter) squared gives the force in dyn. Therefore the factor outside the main bracket of (1.90) has the dimension of a force. The terms inside the bracket have to be dimensionless numbers. This means c must have the dimension of a velocity. Weber went on to show that if (1.90) was to be in agreement with Ampere's force law (1.24) when each current element consists of a single electric charge travelling with constant velocity with respect to the metallic conductor element containing it, and furthermore if this law was also to agree with the results of Ampere's experimental measurements, the constant c had to have the value of 3×10^{10} cm/s. This constant later became known as the velocity of light and it seems to emerge always when the laws of electrostatics are combined with those of electrodynamics.

Weber attributed no particular importance to c . Today it appears truly astonishing that the velocity of light should have revealed itself in a simultaneous action-at-a-distance theory such as Weber's. Although the charges to which (1.90) relates move relative to each other and r is a function of time, the force of repulsion or attraction between the charges changes simultaneously with r . The formula does not allow for an energy propagation delay which could be linked with the velocity of light.

Weber [13] proved in detail how (1.90) can be transformed to (1.24). His proof involves a relatively long mathematical process and teaches little. Of course Weber did not guess the form of (1.90) and subsequently prove it to be compatible with (1.24). How he derived his formula from Ampere's work is very instructive and worth repeating. It has to be re-

alized that Weber published his force law in 1846, the year between the two Neumann memoirs [8, 9], and he was obviously not aware of Neumann's researches on inductions to which he referred extensively in later years. Weber begun his analysis as follows:

"To lay down a guideline for this study, which is based on experience, we consider three specific facts resting partly on direct observation and partly on the indirect measurements underlying Ampere's fundamental law.

(1) The first fact is that two current elements lying on the same straight line either repel or attract each other, depending on whether their currents flow in the same or opposite directions.

(2) The second fact is that two parallel current elements perpendicular to the line joining them either attract or repel each other, depending on whether their currents flow in the same or opposite directions.

(3) The third fact is that a current element, which lies on a straight line with a wire element, induces similarly directed or opposed current, depending on whether its own current intensity decreases or increases.

These three facts are not direct results of experiments, because the action of an element on another cannot be observed, but they accurately correspond to observed phenomena to the extent that they almost have the same validity. The first two facts are already incorporated in Ampere's basic formula of electrodynamics and the third has been added by Faraday's discovery (of induction)."

Figure 19 depicts Weber's model of two interacting current elements. Each element need only contain one positive and one negative charge. The two charges in each element move toward each other, along the line of the element, with velocity v relative to the metal. They are allowed to pass each other without appreciable deviation from straight line motion because, as Weber explained, we are not dealing with the actual happenings in the conductor but only with an action-at-a-distance theory in which the charges are treated as if they could pass each other on a line. The current intensity of the element is taken to be $e.v$, where e is the positive one of the two charges.

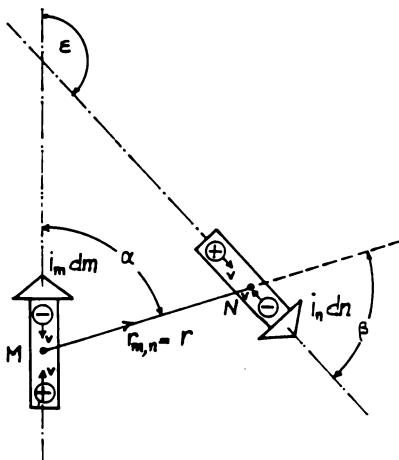


Fig.19 Weber's model of two current elements

Four Coulomb-type interactions have to be considered, two of which are repulsions of like charges and the remaining

two are attractions of unlike charges. All four sets of forces act along r , the line connecting the center points M and N of the two elements. All that was known about these forces at Weber's time was their strengths as given by Coulomb's law (1.3) for the case where they are at rest with respect to each other. Weber deemed it probable that relative motion between the charges would modify the actions, and Coulomb's law would give the limiting value of the forces when the relative velocities tended to zero. He considered it to be his task to determine the departure from Coulomb's law as a function of the relative motion between the charges.

Of the three facts on which Weber claimed he had built his theory, (1) and (2) referred to ponderomotive forces on the conductor metal, but (3) involved an electromotive force on charge. He convinced himself that the total force experienced by the metal of the current element was the vector sum of all the electric forces exerted on the charges within it by charges located elsewhere. If charges cannot penetrate the surface of a conductor, there is some reason to believe that a transverse force on a charge will be directly transmitted to the metal. However this mechanism of force transmission becomes quite dubious when electromotive forces act along current elements to generate Faraday's induced currents. With regard to these latter forces Weber seemed to argue that, since they are only of a transient nature and their magnitude is related to the ratio of the mass of the moving charges to the much greater mass of the stationary metal, they may be ignored in computations, although their mechanical effect does exist.

The lack of a credible mechanism of force transmission from the moving charges to the body of the metal is the weakest point of Weber's electrodynamics. This is particularly true for the longitudinal Ampere forces which should generate tension in wire conductors.

From Coulomb's law alone, the force between the elements

at M and N of fig.19 should be zero because the static attractions and repulsions cancel each other, the positions of the charges being assumed to be the points M and N. However Weber's facts (1) and (2) required the existence of finite forces, and he argued these forces must be due to relative velocities and be quantitatively related to these velocities.

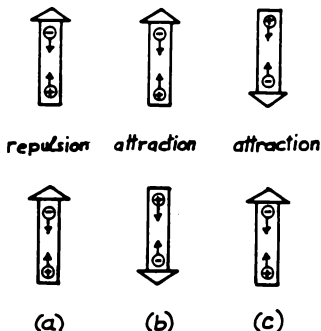


Fig.20 Current elements on the same straight line

Weber then analyzed the element and charge arrangements illustrated in fig.20 which correspond to his fact (1). When the two collinear current elements point in the same direction, as in (a), they repel each other. From this fact he deduced a rule which will be coupled with his name. Weber's Rule is:

"Whatever their sign, charges moving in the same direction along a straight line produce more mechanical force between the associated conductor elements than charges moving in opposite directions along the line."

It will be seen that this rule also applies to the element pairs of fig.20(b) and (c) which point away from, or toward, each other.

The relative velocity of two charges separated by the distance r is dr/dt . This differential coefficient is positive when the charges move apart and negative when they come together. In order to make the inter-particle force, which was caused by relative motion, the same for approaching and receding motion, Weber assumed it to be proportional to the square of the velocity and thereby freed it of the sign of dr/dt .

Let e and e' be the positive particles in the two current elements and u and u' the associated velocities with respect to some rest frame. Furthermore, let the direction of current flow in an element be defined by the motion of the positive charge with respect to the conductor metal. The negative particles in the two elements will be denoted by $-e$ and $-e'$ and their velocities with respect to the rest-frame by $-u$ and $-u'$. In the element arrangement of fig.20(a) we then encounter the four relative velocities

$$\text{for } +e \text{ and } +e': \quad dr/dt = +u - u';$$

$$\text{for } -e \text{ and } -e': \quad dr/dt = -u + u';$$

$$\text{for } +e \text{ and } -e': \quad dr/dt = +u + u';$$

$$\text{for } -e \text{ and } +e': \quad dr/dt = -u - u'.$$

Hence for equal polarity particles

$$(dr/dt)^2 = (u - u')^2 \tag{1.92}$$

and for unequal polarity particles

$$(dr/dt)^2 = (u + u')^2 \tag{1.93}$$

According to Weber's Rule of the stronger velocity-dependent interaction of charges moving in the same direction, (1.92) and (1.93) can only be interpreted as reductions of the electrostatic force. From this follows the intermediate

result for each of the four interactions between two current elements of

$$(e.e'/r^2)[1 - a^2(dr/dt)^2]$$

where a^2 is a dimensional constant and e and e' may be positive or negative. The four sets of forces are

$$\begin{aligned} \text{between } +e \text{ and } +e': & +(e.e'/r^2)[1-a^2(u-u')^2] \\ \text{between } -e \text{ and } -e': & +(e.e'/r^2)[1-a^2(u-u')^2] \\ \text{between } +e \text{ and } -e': & -(e.e'/r^2)[1-a^2(u+u')^2] \\ \text{between } -e \text{ and } +e': & -(e.e'/r^2)[1-a^2(u+u')^2] \end{aligned}$$

Therefore the total forces of repulsion and attraction between the two current elements are given by

$$\begin{aligned} \text{repulsion:} & +2(e.e'/r^2)[1-a^2(u-u')^2] \\ \text{attraction:} & -2(e.e'/r^2)[1-a^2(u+u')^2] \end{aligned}$$

These forces differ in magnitude and sign and their resultant is

$$\Delta F_{e,e'} = +8(e.e'/r^2)a^2u.u' \quad (1.94)$$

In the arrangement of fig.20(a) $+e.u$ and $+e'.u'$ are the element currents i_m and i_n and therefore this last expression agrees with Ampere's force law in so far as the mutual mechanical force between the elements is proportional to the two current intensities, inversely proportional to the square of the distance of separation, and is a repulsion as indicated by the positive sign. For the other two arrangements of fig.20, one of the velocities is reversed which results in a negative interaction force signifying attraction.

Weber found expression (1.94) inadequate to explain

his fact (2), as the elements then lie perpendicular to r and $dr/dt=0$ for all charge combinations. To account for the strong interaction between parallel current elements arranged perpendicular to the line joining them, it was necessary to bring in the relative acceleration d^2r/dt^2 . With the acceleration term the inter-particle force took the form

$$\Delta F_{e,e'} = (e \cdot e' / r^2) [1 - a^2 (dr/dt)^2 + b (d^2r/dt^2)] \quad (1.95)$$

In order to comply with Weber's fact (2) the dimensional constant b had to be positive.

To make the acceleration term compatible with Ampere's force law Weber distinguished the distance between two interacting charges, that is r , from the distance R between the interacting current elements. With respect to fact (2) R is constant while r varies with time. In the case of two positive charges e and e' , travelling with velocities u and u' with respect to a common rest frame, the relationship between r and R is

$$r^2 = R^2 + (u - u')^2 t^2 \quad (1.96)$$

Neither u nor u' are varying with time. Therefore

$$dr/dt = (u - u')^2 t / r \quad (1.97)$$

$$d^2r/dt^2 = [(u - u')^2 / r] [1 - (t/r)] \quad (1.98)$$

Hence in the particular circumstances of Weber's fact (2), which implies $dr/dt=0$, the following interactions are obtained from (1.95), (1.97), and (1.98)

$$\text{between } +e \text{ and } +e': \quad + (e \cdot e' / r^2) [1 + (b/r)(u - u')^2]$$

$$\text{between } -e \text{ and } -e': \quad + (e \cdot e' / r^2) [1 + (b/r)(u - u')^2]$$

$$\text{between } +e \text{ and } -e': \quad - (e \cdot e' / r^2) [1 + (b/r)(u + u')^2]$$

between $-e$ and $+e'$: $-(e.e'/r^2)[1+(b/r)(u+u')^2]$

The force between the two current elements is the sum of these four components and it comes to

$$\Delta F_{e,e'} = -8(e.e'/r^2)(b/r)u.u' \quad (1.99)$$

The negative sign of (1.99) indicates attraction when both currents $e.u$ and $e'.u'$ flow in the same direction, which agrees with Weber's fact (2). When one of the currents is reversed the attraction changes to repulsion. The strength of the force is seen to be proportional to the product of the currents, as required by Ampere's law. However, in this particular case, the force is not inversely proportional to the square of the distance of separation but to the cube of that distance.

Weber's facts (1) and (2) also define the relationship between the dimensional constants a and b of (1.95). The forces for these particular situations are given by (1.94) and (1.99). In the latter situation Ampere's law (1.24) gives a force that is twice as large as in the former situation. Hence

$$b/r = 2a^2 \quad (1.100)$$

With (1.100) Weber's formula (1.95) may be written

$$\Delta F_{e,e'} = (e.e'/r^2)[1-a^2(dr/dt)^2+2a^2r(d^2r/dt^2)] \quad (1.101)$$

To relate (1.101) to Weber's law (1.90) and Ampere's law (1.24), while in the process clarifying the meaning of the dimensional constant a , we rely on Maxwell's analysis [14] which is easier to understand than Weber's.

The first step is to replace the angle function in Ampere's law by the differential coefficients of $r_{m,n}-r$ with

respect to the current element lengths dm and dn . It follows from (1.16) and (1.41) that

$$f(\alpha, \beta, \varepsilon) = 2\cos\varepsilon - 3\cos\alpha \cos\beta + (\partial r/\partial m)(\partial r/\partial n) - 2r(\partial^2 r/\partial m \partial n)$$

Ampere's law then becomes

$$\Delta F_{m,n} = -i_m i_n (dm \cdot dn / r^2) [(\partial r/\partial m)(\partial r/\partial n) - 2r(\partial^2 r/\partial m \partial n)] \quad (1.102)$$

Now

$$dr/dt = (\partial r/\partial m)(dm/dt) + (\partial r/\partial n)(dn/dt) = u(\partial r/\partial m) + u'(\partial r/\partial n) \quad (1.103)$$

$$(dr/dt)^2 = u^2(\partial r/\partial m)^2 + 2u \cdot u'(\partial r/\partial m)(\partial r/\partial n) + u'^2(\partial r/\partial n)^2 \quad (1.104)$$

$$d^2 r/dt^2 = u^2(\partial^2 r/\partial m^2) + 2u \cdot u'(\partial^2 r/\partial m \partial n) + u'^2(\partial^2 r/\partial n^2) \quad (1.105)$$

If the object is to express $\Delta F_{m,n}$ in terms of relative velocities and accelerations between charges in two elements, it will be seen from (1.104) and (1.105) that only terms involving the product $u \cdot u'$ can be responsible for the differential coefficients in (1.102). Therefore terms involving u^2 and u'^2 must vanish for physical reasons. From this Maxwell drew the conclusion that in Weber's theory the electric current cannot be taken as being charge transfer in only one direction, but must be the combination of two opposite streams in each current element, so that the combined effect of the terms involving u^2 and u'^2 may be zero.

Suppose the element dm contains only two electric particles carrying charges $e_{m,1}$ and $e_{m,2}$ travelling with velocities $u_{m,1}$ and $u_{m,2}$ with respect to the wires. Similarly, let element dn contain two charges $e_{n,1}$ and $e_{n,2}$ travelling with velocities $u_{n,1}$ and $u_{n,2}$ with respect to the metal

of dn . Then there arise four sets of interactions between

$$e_{m,1} \text{ and } e_{n,1}: e_{m,1}e_{n,1}(u_{m,1}-u_{n,1})^2 - e_{m,1}e_{n,1}(u_{m,1}^2 - 2u_{m,1}u_{n,1} + u_{n,1}^2)$$

$$e_{m,1} \text{ and } e_{n,2}: e_{m,1}e_{n,2}(u_{m,1}-u_{n,2})^2 - e_{m,1}e_{n,2}(u_{m,1}^2 - 2u_{m,1}u_{n,2} + u_{n,2}^2)$$

$$e_{m,2} \text{ and } e_{n,1}: e_{m,2}e_{n,1}(u_{m,2}-u_{n,1})^2 - e_{m,2}e_{n,1}(u_{m,2}^2 - 2u_{m,2}u_{n,1} + u_{n,1}^2)$$

$$e_{m,2} \text{ and } e_{n,2}: e_{m,2}e_{n,2}(u_{m,2}-u_{n,2})^2 - e_{m,2}e_{n,2}(u_{m,2}^2 - 2u_{m,2}u_{n,2} + u_{n,2}^2)$$

Of the above twelve terms, each consists of the product of two charges and the square of a velocity or the product of two velocities. Collecting the terms in u_m^2 , u_n^2 , and $u_m u_n$, it follows that

$$\begin{aligned} \{e_m e_n u_m^2 - u_{m,1}^2(e_{m,1}e_{n,1} + e_{m,1}e_{n,2}) + u_{m,2}^2(e_{m,2}e_{n,1} + e_{m,2}e_{n,2}) \\ - (u_{m,1}^2 e_{m,1} + u_{m,2}^2 e_{m,2})(e_{n,1} + e_{n,2}) \end{aligned} \quad (1.106)$$

Similarly

$$\{e_m e_n u_n^2 - (u_{n,1}^2 e_{n,1} + u_{n,2}^2 e_{n,2})(e_{m,1} + e_{m,2}) \quad (1.107)$$

$$\{e_m e_n u_m u_n - (u_{m,1}e_{m,1} + u_{m,2}e_{m,2})(u_{n,1}e_{n,1} + u_{n,2}e_{n,2}) \quad (1.108)$$

(1.106) and (1.107) contain terms with squares of velocity which must be zero if Weber's force law is to agree with Ampere's. Therefore in the case of (1.106) we must have

$$\text{either } (u_{m,1}^2 e_{m,1} + u_{m,2}^2 e_{m,2}) = 0; \text{ or } (e_{n,1} + e_{n,2}) = 0 \quad (1.109)$$

According to Fechner's original hypothesis, on which Weber based his theory, the flow of positive charge in the positive direction of the wire is exactly equal to the flow of negative charge in the negative direction. This means both conditions of (1.109) are fulfilled by Fechner's hypothesis. However it is possible to deliberately charge a conductor such that $e_{n,1} + e_{n,2} \neq 0$, and if the force law is to hold for

conductors which are not electrically neutral, we must have

$$u_{m,1}^2 e_{m,1} + u_{m,2}^2 e_{m,2} = 0$$

Maxwell then continues to say:

"Whatever hypothesis we adopt, there can be no doubt that the total transfer of electricity, reckoned algebraically, along the first circuit (m) is represented by

$$u_{m,1} e_{m,1} + u_{m,2} e_{m,2} = c \cdot i_m dm$$

where e is the number of units of statical electricity which are transmitted in the unit electric current in the unit of time so that we may write (1.108)"

$$\sum e_m e_n u_m u_n = c^2 i_m i_n dm \cdot dn \quad (1.110)$$

The current strength having thus been defined, (1.102) can be expressed by

$$\Delta F_{m,n} = -(1/c^2 r^2) \sum e_m e_n u_m u_n [(\partial r / \partial m)(\partial r / \partial n) - 2r(\partial^2 r / \partial m \partial n)] \quad (1.111)$$

But from (1.104), and since the terms containing the square of velocities must be zero

$$u_m u_n (\partial r / \partial m)(\partial r / \partial n) = (1/2)(dr/dt)^2 \quad (1.112)$$

and from (1.105)

$$u_m u_n (\partial^2 r / \partial m \partial n) = (1/2)(d^2 r / dt^2) \quad (1.113)$$

Substituting (1.112) and (1.113) into (1.111) gives

$$\Delta F_{m,n} = \sum (e_m e_n / r^2) [(r/c^2)(d^2 r / dt^2) - (1/2c^2)(dr/dt)^2] \quad (1.114)$$

When considering the force between any two charges e and e' , rather than the force between two current elements $i_m dm$ and $i_n dn$, the electrostatic interaction has to be added to (1.114), so that

$$\Delta F_{e,e'} = (e \cdot e' / r^2) \{ (1/2c^2)(dr/dt)^2 + (r/c^2)(d^2r/dt^2) \}$$

which is Weber's force law (1.90). In this formula the force is given in dyn when e and e' are inserted in e.s.u. of charge, r in centimeters and t in seconds. Therefore c , which was introduced as the number of e.s.u. of charge per second in one absolute ampere, now appears to have the dimension of a velocity. This transformation of a number to a velocity had farreaching consequences in the further evolution of physics and now underpins the whole of radiation science. In his determination of measure ratios, Weber found the number of e.s.u. of charge in 1 ab.amp. to be

$$c = 3 \times 10^{10} \quad (1.115)$$

When given the dimension of cm/s this has become the velocity of light.

Weber collaborated with Kohlrausch in the first determination of the charge content of an electric current. At the time they published their results in 1856 [15] they did not know they were dealing with a number related to the velocity of light. Laboring under the misconception of the electric fluidum of two polarities moving simultaneously in two opposite directions, they quoted the number of 'positive' charges passing through a conductor section per second, when one absolute ampere of current is flowing, as $155,370 \times 10^6$. This determination was based on the millimeter being the unit of length. Maxwell later multiplied the Weber-Kohlrausch number by two to account for the transfer of positive and an equal number of negative charges, and then divided the product by ten to obtain a velocity in c.g.s. units of 3.1074×10^{10} cm/s. Maxwell's own measurements

gave $2.88 \cdot 10^{10}$ cm/s. These figures he then compared with measurements of the velocity of light carried out a few years earlier by Fizeau and Foucault, and ranging from 2.98 to $3.14 \cdot 10^{10}$. The good agreement led Maxwell to believe that electromagnetic disturbances are propagated with the speed of light, and that light itself was an electromagnetic phenomenon.

The first to pronounce this fact appears to have been Kirchhoff who, almost simultaneously with Weber, studied the speed with which electromagnetic signals travelled along telegraph wires. Both Kirchhoff and Weber came to the conclusion that this speed varied from one circuit to another but has c as its upper limit. Kirchhoff felt this limiting speed was actually the velocity of light.

Writing Weber's electrodynamic potential of two charged particles (1.91) as

$$\Delta P_{e,e'} = (e \cdot e' / r) - (e \cdot e' / 2rc^2)(dr/dt)^2$$

it is seen to be the difference between the electrostatic potential and a term containing the relative velocity between the charges. The velocity term cancels the first term when

$$v_r = (dr/dt) = 2c \quad (1.116)$$

The term involving the square of the relative velocity is akin to a quantity of kinetic energy given by

$$(1/2)m_e v_r^2$$

where m_e is some non-material 'electromagnetic mass' and v_r the relative velocity between the charges. Weber's potential defines the electromagnetic mass as

$$m_e = (e \cdot e' / rc^2) \quad (1.117)$$

which leads to the following mass-energy relationship

$$m_e c^2 = (e \cdot e' / r) \quad (1.118)$$

Because of the inclusion of kinetic energy in Weber's potential, the interparticle force is not simply the negative gradient of the potential, but the Lagrange-force defined by the differential operator $[-(\partial / \partial r) + (d/dt)(\partial / \partial v_r)]$, that is

$$\begin{aligned} \Delta F_{e,e'} &= [-(\partial / \partial r) + (d/dt)(\partial / \partial v_r)] \{ (e \cdot e' / r) [1 - (1/2c^2)v_r^2] \} \\ &= (e \cdot e' / r^2) [1 - (1/2c^2)(dr/dt)^2 + (r/c^2)(d^2r/dt^2)] \end{aligned} \quad (1.119)$$

which corresponds to Weber's force law (1.90). It should be noted that the electromagnetic rest-mass ($v_r=0$) in Weber's theory is zero.

As Weber's theory leads back to Ampere's force law, it must also be compatible with Neumann's law of induction.

This was proved in different ways by both Weber and Neumann. Electrical engineers have found little use for Weber's formulas because they do not refer directly to current elements and are therefore difficult to apply to metallic circuits. From the theoretical point of view, Weber's charged particle dynamics injected something analogous to kinetic energy into electromagnetism. The idea of the magnetic effect of the electric current being a kinetic phenomenon was fully elaborated by Maxwell and is an indispensable part of special relativity and our present understanding of the motion of electrons. It was with the charge kinetics that Weber clearly departed from the Ampere-Neumann electrodynamics. The electrodynamic potential of Neumann was a pure potential in the sense that all the energy to which it referred was dependent only on the position of current elements without reference to velocities. It did not require the existence of a non-material electromagnetic mass and the energy always belonged to matter.

RETARDED POTENTIALS AND THE ELECTROMAGNETIC FIELD

On the whole philosophers have preferred to explain the motion of matter by the pushing and pulling of connected neighboring bodies rather than attraction and repulsion exerted by distant objects. For a time the enormous success of Newton's theory of gravitation suppressed this inbred preference. But 150 years later, in the middle of the nineteenth century, men like Faraday, W. Thompson (Lord Kelvin), Maxwell, Riemann, Lorenz turned away from the Ampere-Neumann electrodynamics which had been cast in the newtonian mold. These scientists showed renewed interest in contact-action theories.

The new electrodynamics arose from two lines of thought. Faraday and Maxwell believed in the existence of an aether that could support mechanical stresses and strains which were set up by electric and magnetic molecules of matter embedded in the aether. According to the English school the aether was capable of imparting the stresses to other material objects by being in contact with them. Disturbances of the aether were assumed to be propagated at the velocity of light without requiring the transport of aether over long distances.

The other approach originated with L. Lorenz [17] in Denmark and Riemann [18] in Goettingen. It found a strong supporter in Carl Neumann [19], the son of Franz Neumann, and resulted in the invention of retarded potentials which were thought of as actions travelling at the constant velocity of light through empty space from one particle to another. As the potential of a charged or a current-carrying body receded into space it was assumed, sooner or later, to reach every other particle in the universe. In other words, the potential spread like a spherical wave in a fluid medium, but since it was not considered to be a disturbance of some aether, it had to be of the nature of a spherical projectile which, let us say, 'painted' the space through which it

had passed with potential of decreasing intensity. The dynamics of the aether and the ballistic potential concept strained the imagination of all who wished to create a mechanistic explanation of the world. Quite surprisingly, the two apparently unrelated mechanical models led to the same system of equations, that is Maxwell's equations, which have become the backbone of field theory.

In a period of approximately twenty years, from 1850 to 1870, the models of the electromagnetic aether and traveling potentials evolved side by side, both having been more or less completed when Maxwell published his Treatise [14] in 1873. Lorenz postulated the retarded scalar potential ϕ_P at a point P. of a charge distribution ρ throughout the volume V to be

$$\phi_P = \int_V ([\rho]/r) dV \quad (\text{e.s.u.}) \quad (1.120)$$

Apart from the retardation, this was derived directly from Coulomb's law. It represents electrostatic potential energy per unit test charge at P. The distance between P and the volume element dV is r. The square brackets in (1.120) are meant to indicate that the position of each charge must be that which it occupied at some earlier time when its potential was emitted with velocity c to arrive at P at the instant of evaluation of ϕ_P . If t is the time of evaluation, the position of each charge at time $t-(r/c)$ has to be ascertained before executing the integration of (1.120).

Lorenz applied the same hypothesis to the magnetic vector potential A at point P.

$$\underline{A}_P = \int_V ([\underline{J}]/r) dV \quad (\text{e.m.u.}) \quad (1.121)$$

J is the current density vector inside the volume element dV at a distance r from P. The magnetic vector potential represents electrodynamic potential energy per unit current

element strength at P. The square brackets in (1.121) again indicate retardation.

In order to avoid confusion between the retarded potentials of field theory and the mutual potential of charges and current-elements in the Ampere-Neumann electrodynamics, some important differences between these two concepts have to be noted. First of all, the mutual potentials have the dimension of energy and are actual measures of potential energy. The mutual potentials always involve at least two material entities or particles. The retarded potentials have the dimension of energy divided by charge or current-element strength. One can speak legitimately of the retarded potential of a single charge or current-element. The mutual potential of an isolated particle has no meaning. Equations (1.120) and (1.121) have been expressed in fundamental electrostatic and electromagnetic units to emphasize their physical contents.

Electric charges can be created or neutralized instantaneously in pairs by collision processes. The mutual potentials are thought to arise or vanish simultaneously with charge splitting or neutralization. Current element pairs are also subject to instantaneous creation and extinction together with their mutual potentials. There is no need for the mutual potentials to exist outside the charges or current-bearing matter. This is not so with retarded potentials which in their travels through space become detached from the matter that created them. The question arises: how is the retarded potential (or field) of a charge cancelled when the charge is suddenly neutralized? The only way in which we can conceive of a process of cancellation appears to be the emission of another spherical wave projectile from the eclipsing charge which strips the 'potential paint' off the space through which it passes. To distinguish this second wave from the first it must be of opposite polarity. Hence we have to have positive and negative retarded potentials which travel in the same direction with the same

velocity c . The mutual potentials of the older electrodynamics also have polarity. This decides whether the potential energy is the result of repulsion or attraction and is in no way related to the polarity of retarded potentials. Another crucial difference between the two kinds of potential is the type of relativity to which they are linked.

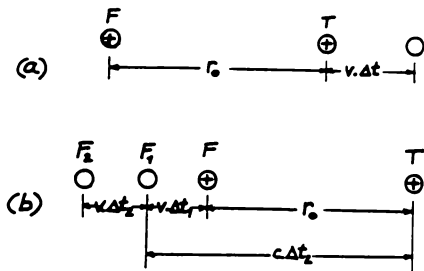


Fig. 21 Retarded potential and relative motion
 (a) field charge stationary
 (b) test charge stationary

For example, consider two positive charges as indicated in fig. 21. Let F be the charge which generates the retarded potential and T the test charge. In the Ampere-Neumann electrodynamics the mutual potential between the two charges, and hence the force between them, changes simultaneously with any alteration in the distance of separation r . It does not matter if F is considered to be the stationary and T the moving charge, or vice versa. Also, no restriction need be imposed on the positioning of observers who measure the mutual force. This is galilean relativity.

The same arguments do not apply to retarded potentials. Take the case when F is at rest and T moves away from it at velocity v . T then advances into space which already contains the painted retarded potential information which was emitted by F when it first arrived, or was generated,

at its rest position. Therefore the interaction distance between the charges is the actual distance

$$r = r_0 + v \cdot \Delta t \quad (1.122)$$

where r_0 is the original distance of separation and Δt the time for which T has been moving away from F. Now let T be at rest and F move away from it with velocity v . Then after a time interval Δt , following the commencement of the relative motion, the field charge is at F_2 but the signal of its arrival there has not yet reached T. In fact the latest position of which T has knowledge is F_1 at a distance of

$$r = r_0 + v(\Delta t - \Delta t_2) \quad (1.123)$$

$$c \cdot \Delta t_2 = r_0 + v \cdot \Delta t_1 \quad (1.124)$$

$$\Delta t_2 = (r_0/c) + (v/c)\Delta t \quad (1.125)$$

Substituting (1.125) into (1.123) gives the interaction distance as

$$r = r_0 + v \cdot \Delta t - (v/c)r_0 + (v^2/c)\Delta t_1 \quad (1.126)$$

This last equation will in general not be equal to (1.122), although it can approach it very closely when $c \gg v$. As electrical charges in vacuum can and do move with a significant fraction of the velocity of light, we see that galilean relativity does not hold for retarded potentials. Field theory using retarded potentials calls for a special relativity. This was provided by Einstein [20] in 1905.

Lorenz and Riemann were guided to retarded potentials by an analogy with the diffusion of heat and sound through material media. Accordingly, the diffusion through empty space of the scalar and vector potentials was assumed to

be governed by

$$\nabla^2 \phi - (1/c^2)(\partial^2 \phi / \partial t^2) = 0 \quad (1.127)$$

$$\nabla^2 \underline{A} - (1/c^2)(\partial^2 \underline{A} / \partial t^2) = 0 \quad (1.128)$$

Both Whittaker [6] and O'Rahilly [22] have shown how Maxwell's field equations may be derived directly from the diffusion equations (1.127) and (1.128). For vacuum the Maxwell equations may be written

$$\nabla \cdot \underline{E} = 0 = \nabla \cdot \underline{B} \quad (1.129)$$

$$\nabla \times \underline{E} = -(\partial \underline{B} / \partial t); \quad \nabla \times \underline{B} = (1/c^2)(\partial \underline{E} / \partial t) \quad (1.130)$$

where \underline{E} and \underline{B} are the electric and magnetic field vectors, respectively. Maxwell himself obtained his equations from the aether model and displacement currents. He went on to show that the field equations lead to the diffusion equations and were therefore compatible with the propagation of retarded potentials.

At this stage we might pause and ask the question: where precisely does field theory deviate from the Ampere-Neumann electrodynamics? Three fundamental points of departure come to mind.

1. Coulomb, Ampere, Neumann, and Weber attributed all electric and magnetic interactions of ponderable matter to forces residing entirely inside the material. In field theory the space between material bodies and particles has become a participating entity, by way of an aether or energy filling, or through being the bearer of abstract, mathematical projectiles.

2. In the newtonian model of electromagnetism the forces between material bodies act simultaneously. Any delay between

cause and effect must be due to the fact that we observe only relative motion--not force--and it takes time for forces to set matter in motion. In field theory the time delay between cause and effect is easily explained by the transmission-lag of potential or energy travelling across space. Only in one isolated instance, involving electromagnetic induction in metals, has the time-lag between cause and effect been revealed with the Ampere-Neumann electrodynamics.

3. We cannot mark a point in space other than by placing a particle at the point. If this particle is to be a lookout for passing electromagnetic disturbances, it must itself have electromagnetic properties, that is it must be charged. Such a particle inevitably sets up its own field and thereby makes the objective observation of other fields impossible. Hence tracking waves or energy through space will, at best, be confusing. The need for a special theory of relativity is then hardly surprising. The matter-bound Ampere-Neumann description of electromagnetic phenomena rests solely on the relative positions and motions of material elements, and therefore remains in harmony with the natural relativity of the newtonian mechanics.

At the time of his death, in 1879, Maxwell could scarcely have foreseen the relativity problem which was to attract so much attention twenty years later. Nor did he expect any conflict between his aether field and the laws of Ampere and Neumann, whom he considered to be mathematicians rather than physicists. His confidence in the agreement of the two electrodynamics with regard to experimentally verifiable facts shines through the following quotation from the Preface to the first edition of his Treatise [14]:

"For instance, Faraday, in his minds eye, saw lines of force traversing all space where the mathematicians saw centers of force attracting at a distance: Faraday saw a medium where they saw nothing but distance :

Faraday sought the seat of the phenomena in real actions going on in the medium, they were satisfied that they had found it in a power of action at a distance impressed on the electric fluids.

When I had translated what I considered to be Faraday's idea into a mathematical form, I found that in general the results of the two methods coincided, so that the same phenomena were accounted for, and the same laws of action deduced by both methods, but that Faraday's methods resembled those in which we begin with the whole and arrive at the parts by analysis, while the ordinary mathematical methods were founded on the principle of beginning with the parts and building up the whole by synthesis"

It is indeed surprising that two so different philosophies could accurately explain the same experimental facts. Nonetheless, the Ampere-Neumann electrodynamics, in its narrow scope, would by now have slipped into complete oblivion had it not been for one experimental discrepancy between the two theories. This concerned forces in metals. It arose from the introduction of the Grassmann-Lorentz force law and Einstein's special relativity, added to field theory after Maxwell's death. Grassmann's law was found indispensable for explaining the behavior of electrons in vacuum. Difficulties arise only when Grassmann's law is applied to metallic circuits. We have every reason to believe that this law correctly describes the forces acting on moving electrons and ions in empty space. Maxwell preferred Ampere's law over Grassmann's. He considered two more possible expressions for the ponderomotive force between two current elements and then summarized his findings by saying [14]:

"Of these four different assumptions that of Ampere is undoubtedly the best, since it is the only one which makes the forces on the two elements not only equal and opposite but in the straight line joining them."

Today this strikes us as an odd statement to have been made by the man who provided an alternative to the newtonian electrodynamics. Maxwell's admiration of Ampere and his work was unbounded as the following quotation from the Treatise reveals:

"The experimental investigation by which Ampere established the laws of the mechanical action between electric currents is one of the most brilliant achievements in science. The whole, theory and experiment, seems as if it had leaped, full grown and full armed, from the brain of the 'Newton of electricity'. It is perfect in form, and unassailable in accuracy, and it is summed up in a formula from which all the phenomena may be deduced, and which must always remain the cardinal formula of electrodynamics."

MATTER-BOUND VERSUS FREE ENERGY

As much as the newtonian physics is ruled by forces, so relativistic field theory is dominated by the concept of free energy. Only in the second half of the nineteenth century did it become fashionable to speak of energy; Newton and Ampere never used the word. One of the first definitions of energy was: the ability of a body to do work. Thus in the beginning energy was inseparably associated with matter. It means energy was not considered to be another fluidum pervading the body, but rather a state of affairs relating to material particles. The molecules of hot air contained energy by virtue of their fast motion. A brick at the top of the house was richer in energy than one at the bottom because of its greater distance from the center of the earth. It was found that in changing the arrangement of material bodies, energy would be transformed from the potential to

the kinetic and thermodynamic versions, or the other way around. These transformations did not necessarily involve the flight of energy from one body to another, and the total quantity of energy was always conserved.

The Ampere-force on a short section of wire has a transverse and a longitudinal component. If the force acted on the electrons, rather than the atoms, the transverse component would still be translated to a body force by the surface work function which stops the electrons from leaving the metal. However the longitudinal force component would simply accelerate electrons and thereby contribute to current flow rather than produce mechanical stress. Yet the Ampere law defines the longitudinal component as a ponderomotive force, and not an electromotive force. Therefore this force has to attach itself to the atoms and not just the electrons. It would seem unnatural if one component of the same force attached itself to electrons and the other to atoms. Logic appears to dictate that both must act on the atom. Since the atoms of the metal lattice are essentially stationary, the energy associated with Ampere forces cannot be kinetic energy. It has to be potential energy which, most likely, resides in the atoms.

Field theory paints a very different picture. Not only are we accustomed to the idea of energy leaving the metal and residing in the magnetic field, but this energy depends on the velocity of electrons. In Maxwell's view this was clearly kinetic energy. According to special relativity the kinetic energy of the moving electrons in the metal exists largely as free energy in the magnetic field. We can associate with it an electromagnetic mass which is also located in the field and gives rise to field-energy momentum. These dynamic concepts related to magnetic energy have no counterpart in the Ampere-Neumann electrodynamics.

In the old electrodynamics energy and forces were always related to pairs of particles or bodies. In a newtonian

world, the discussion of the energy of an isolated particle or body is meaningless. How can this pair-rule be made to comply with Newton's first law of motion, which involves kinetic energy and states that: "Every body continues in its state of rest, or uniform motion in a straight line, unless it is compelled to change that state by forces impressed upon it". Is the lone cannonball sailing through space far away from all other heavenly bodies not an isolated object possessing kinetic energy of $\frac{1}{2}mv^2$? To clarify this question we have to explain what is meant by the velocity v . This has to be relative to something: the earth, the sun, the fixed stars. It immediately suggests that we are not concerned with a totally isolated object. How could the definition of a relative velocity influence the meaning of inertia of Newton's first law?

Mach [23] maintained that it is not possible to remove a body from the gravitational influence of the remainder of the universe. He went on to reason that the gravitational pulls of the widely distributed, enormous amount of matter in the universe must hold the key to the inertial behaviour of objects in the solar system. This is Mach's principle. It unshackles newtonian dynamics from absolute space and lets us believe that kinetic energy is also associated with pairs of particles and therefore is, in fact, mutual energy. It is the inertia of matter which introduces the time-lags between causal forces and observed motions into the mechanics of Newton. If the interaction of terrestrial charges with charges in the remainder of the universe were able to produce "electrodynamic inertia", the explanation of time-lags in radiation theory by a simultaneous action-at-a-distance theory, like the Ampere-Neumann electrodynamics, no longer seems out of the question. Of the scientists who have seriously studied Mach's principle we might mention Einstein [25], Sciama [26], Moon and Spencer [27], Burniston Brown [28], and more recently Assis [99].

Here are Lorentz's views on the subject of free energy

as he expressed them in connection with his theory of electrons [29]:

"For this reason, the flow of energy can, in my opinion, never have quite the same meaning as a flow of material particles, which by our imagination at least, we can distinguish from each other and follow in their motion. It might even be questioned whether, in electromagnetic phenomena, the transfer of energy really takes place in the way indicated by Poynting's law, whether, for example, the heat developed in the wire of an incandescent lamp is really due to the energy which it receives from the surrounding medium, as the theorem teaches us, and not to a flow of energy along the wire itself. In fact, all depends on the hypothesis which we make concerning the internal forces in the system, and it may very well be, that a change in these hypotheses would materially alter our ideas about the path along which the energy is carried from one part of the system to another. It must be observed however that there is no longer room for any doubt, so soon as we admit that the phenomena going on in some part of the ether are entirely determined by the electric and magnetic force existing in that part. No one will deny that there is a flow of energy in a beam of light; therefore, if all depends on the electric and magnetic force, there must also be one near the surface of the wire carrying a current, because here, as well as in the beam of light, the two forces exist at the same time and are perpendicular to each other."

The word energy with its present connotation is said to have been introduced by Lord Kelvin. However, it was a lecture given by Helmholtz in 1847 [30] on the conservation of force, but actually dealing with the conservation of energy, which aroused the greatest interest. From then onward

physical theories were required to be consistent with the energy conservation principle. More than 200 years before then, Galileo already had a fair idea of energy conservation, or the impossibility of perpetual motion. At the end of the nineteenth century this same principle looked very much more important because of a measure of unity which it brought to the three distinct disciplines of mechanics, thermodynamics, and electromagnetism. Ampere was dead when Helmholtz spoke and Neumann had just published his second paper on induction. Neumann lived through the energy revolution, but he did not return to write about electromagnetism.

Being closer to the action-at-a-distance theories than we are now, Lorentz was still a trifle uncertain about the existence of free energy. He correctly pointed out, however, that once we accept electric and magnetic forces in the field we have no choice but believe also in free energy. This energy replaced the aether and became yet another continuous fluidum. What a surprise, therefore, when it was revealed that this fluidum comes in parcels, which are now known as quanta or photons. Had scientists adhered to the matter-bound energy of the Ampere-Neumann electrodynamics, they would have expected energy to be quantized in the same way matter is quantized. Quantum mechanics is a natural partner of simultaneous matter interaction theories.

THE ELECTRON

Wilhelm Weber [13] considered the electric current in a wire to be the progression of small material particles carrying either positive or negative charge. Particles of opposite charge were assumed to move in opposite directions. The current strength was defined as the total positive charge passing through a given wire cross-section in unit time. Weber's analysis did not refer to the inertial mass of the

charge carriers. His mutual potential energy of a pair of charges (1.91) contained a term which was proportional to the square of the relative velocity. This could have been interpreted as representing kinetic rather than potential energy. If the kinetic interpretation was chosen, the charge had to be associated with an electromagnetic mass given by (1.117). When this electromagnetic mass is multiplied by the square of the velocity of light it becomes equal to the electrostatic potential energy of the two charges, as shown by (1.118). This indicates that Weber's theory, although in complete quantitative agreement with the Ampere-Neumann electrodynamics, contained the seeds of modern field theory provided one believed that the magnetic force and energy were the result of the motion of charges and not the instantaneous distribution of charges.

It was Maxwell who convinced scientists of the kinetic nature of the magnetic field. The alternative view was dropped without having received serious consideration. This alternative explanation would have to start by recognizing that in a current-free metallic conductor the positive and negative charges neutralize each other by combination or chaotic motion. When a current is impressed on the conductor, some order is brought to the charge distribution without upsetting the numerical balance between positive and negative charges. The Coulomb effect of this order must then be responsible for the mechanical and electromotive forces on current elements. In such a model Neumann's electrodynamic potential (1.35) would depend on the instantaneous order of charge distribution, which represents potential energy in the true sense of the word.

The enormous success of Maxwell's electromagnetism in the hands of Hertz [33], who used it in his experiments with electromagnetic wave propagation, swept any thought of nonkinetic magnetism away. Even the atomicity of electricity had to take a backstand for some years while the con-

tinuum reigned supremely. When proposing his new electron theory, Lorentz apologized for having to return to the old concept of discrete charges. At the same time he made the electron compatible with the field, as far as this could be done. It turned out to be a rather strenuous effort and had to overcome a number of unexpected difficulties. Their resolution anticipated the special theory of relativity.

It was mainly research on cathode rays, β -radiation from radium, and the deflection of streams of electric charges in vacuum by electric and magnetic fields which placed the electron on a firm experimental basis. Its rest-mass and charge established it as the smallest charged particle and therefore the building block of electrical science. Handling the electron inside and out of matter became a great scientific and technological challenge in the present century and led to stunning achievements.

Can Weber's theory deal with the electron moving through the ionic lattice of a metal? The definition of current strength, as being the motion of positive charge with respect to the conductor, would have to be changed. This presents no difficulty. A suitable new definition would be: the negative product of the negative charge multiplied by its relative velocity with respect to the host metal. Weber's idea of both types of charge moving in opposite directions with only one counting toward the current was in any case strange. This oddity disappears as we freeze the positive ions to the lattice.

Consider two elements dm and dn of a straight conductor, as shown in fig.22(a). The electron velocity relative to the lattice is v in both elements. The magnitudes of the four charges are all equal to the electronic charge e . To comply with Weber's fact (1) (see page 58), the four relevant pair interactions of page 63, with one charge in dm and the other in dn , then become

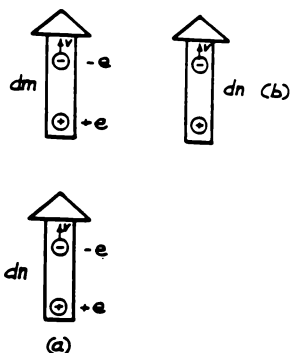


Fig.22 The electron in Weber's current element model

between +e and +e:	$+e^2/r^2$
between -e and -e:	$+e^2/r^2$
between +e and -e:	$-(e^2/r^2)(1-a^2v^2)$
between -e and +e:	$-(e^2/r^2)(1-a^2v^2)$

Summing these interactions gives the collinear repulsion force

$$\Delta F_{m,n} = 2a^2v^2e^2/r^2 \quad (1.131)$$

which corresponds to (1.94) and, with an appropriate dimensional constant a , it agrees with the Ampere force between two collinear elements. In the Weber model, the current element is given by the product of charge and its velocity. The reduction of the numerical factor in (1.94) from 8 to 2 is the result of eliminating relative motion between the positive ions and the lattice.

Using Weber's fact (2) on page 58, we can in the same way derive the force between two parallel elements arranged side by side, as shown in fig.22(b). This force will corres-

pond to (1.99) and with (1.100) comes to

$$\Delta F_{m,n} = -4a^2 v^2 e^2 / r^2 \quad (1.132)$$

Since $e.v$ represents a current element, and with the dimensional constant 'a' defined to make (1.131) agree with Ampere's law, equation (1.132) is identically the same as the Ampere force between two parallel elements which lie perpendicular to the line joining them. Hence conduction electrons streaming through the metal lattice with some average velocity, in the eyes of Weber's mathematics, generate longitudinal and transverse mechanical forces on the substance of current elements which agree with Ampere's force law and therefore also with the induction of electromotive forces according to Neumann's laws. This is quite remarkable when one considers that the Ampere-Neumann electrodynamics was formulated more than fifty years before Lorentz suggested the electron theory of metals.

Weber claimed the electrical forces exerted on the charges were passed on by the charges to the body of the metal. With today's picture of the atomic and electronic structure of metals it is easy to see that this is true for the stationary positive ions. How the conduction electrons exert steady ponderomotive forces on the lattice has remained a mystery ever since Weber formulated his theory.

It will be realized that if the positive charges are removed from Weber's current elements, the forces described by (1.131) and (1.132) become zero and all magnetic effects of the electric current would disappear. It is fair to say, therefore, the whole of the Ampere-Neumann electrodynamics depends on the interplay between positive and negative charges in metallic current elements. Either charge, but not both, may be immobile. In contrast to this, the metallic current element proposed by Lorentz is just a negative electron. Today's electromagnets have all been designed on the

assumption that the positive ions of the conductor lattice make no contribution to the magnetic effect of the current. This represents a major departure from the Weber electrodynamics.

In terms of modern field theory, the total force an electron of charge $-e$ experiences in the presence at its location of an electric field strength E and a magnetic flux density B is

$$\underline{F} = -e(\underline{E} + \underline{v} \times \underline{B}), \quad (1.133)$$

where v is the relative velocity between the electron and the observer of special relativity. This is said to hold for electrons in vacuum and conduction electrons in metals. (1.133) is known as the Lorentz equation or the Lorentz force. The first term is the Coulomb interaction of the electron with other charges which are responsible for the E -field. It is now common practice, as for example in reference [34], to derive (1.133) directly from special relativity by analyzing the interaction of two charges in relative motion with respect to each other. This is not how Lorentz found his important formula in the 1890s, before the publication of Einstein's special relativity theory [20]. Lorentz accepted (1.133) as an empirical fact of the ion dynamics in vacuum when treated in conjunction with Maxwell's field equations. This is how Lorentz expressed his way of thinking in 1909 [29] when the electron theory had reached maturity:

"However this may be, we must certainly speak of such a thing as the force acting on a charge, or on an electron, on charged matter, whichever appellation you prefer. Now, in accordance with the general principles of Maxwell's theory, we shall consider this force as caused by the state of the ether, and even, since this medium pervades the electrons, as exerted

by the ether on all internal points of these particles where there is a charge. If we divide the whole electron into elements of volume, there will be a force acting on each element and determined by the state of the ether existing within it. We shall suppose that this force is proportional to the charge of the element, so that we only want to know the force acting per unit charge. This is what we can now properly call the 'electric force'. We shall represent it by \underline{f} . The formula by which it is determined, and which is the one we still have to add to Maxwell's equations is as follows:

$$\underline{f} = \underline{d} + (1/c)(\underline{v} \times \underline{h})$$

Like our former equations, it is got by generalizing the results of electromagnetic experiments. The first term represents the force acting on an electron in an electrostatic field; indeed, in this case, the force per unit charge must be wholly determined by the dielectric displacement. On the other hand, the part of the force expressed by the second term may be derived from the law according to which an element of a wire carrying a current is acted on by a magnetic field with a force perpendicular to itself and the lines of force, an action, which in our units may be represented in vector notation by

$$\underline{F} = (s/c)(\underline{i} \times \underline{h})$$

where \underline{i} is the intensity of the current considered as a vector, and s the length of the element. According to the theory of electrons, \underline{F} is made up of all the forces with which the field \underline{h} acts on the separate electrons moving in the wire. Now, simplifying the question by the assumption of only one kind of moving electrons with equal charges e and a common velocity \underline{v} , we may write

$$s_i = Ne_{\underline{v}}$$

if N is the whole number of these particles in the element s . Hence

$$\underline{F} = (Ne/c)(\underline{v} \times \underline{h})$$

so that, dividing by Ne , we find for the force per unit charge

$$(1/c)(\underline{v} \times \underline{h})$$

As an interesting and simple application of this result, I may mention the explanation it affords of the induction current that is produced in a wire moving across the magnetic lines of force."

It is important to note Lorentz's remark about his force equation having been "got by generalizing the results of electromagnetic experiments". The derivation of equation (1.89) illustrates the part played by the Lorentz force in Grassmann's electrodynamics. Grassmann never claimed this force to be a generalization of experimental results. He simply did not like Ampere's law, as is evident from the quotation on page 49, because this law was too complicated and gave a zero force for parallel elements inclined at an angle of 35.26° to the line joining them. Neither Grassmann nor Lorentz appear to have paid much attention to, or were concerned about, the imbalance of the reaction forces on a pair of current elements, and the effect this may have on the compliance of electrodynamics with Newton's third law of motion.

Lorentz immediately recognized that, within the framework of field theory, the electron cannot be treated as a point charge. The electric field strength due to a charge obeys an inverse square law and, therefore, should be infinite

at the location of the charge. It also implies the storage of an infinite amount of energy. To Lorentz it looked an unlikely state of affairs and it still does so today, nearly a century later, with relativity and quantum theory firmly established in the armory of theoretical physics. This problem does not arise in the Ampere-Neumann electrodynamics because energy is associated with the mutual force of interaction of at least two particles, or components of particles, and never with an isolated entity of matter.

CONVECTION CURRENTS IN VACUUM

The disappearance of Ampere's force law from textbooks and the teaching of electromagnetism was primarily the result of the failure of the law to cope with the interactions of charges convecting through vacuum. Furthermore, when equating convecting electrons in vacuum to amperian current elements, Ampere's force law (1.24) no longer agrees with Weber's law (1.90), and both laws are then in conflict with the Grassmann-Lorentz force. Consider the two cases (a) and (b) illustrated in fig.23. In (a) two electrons convect

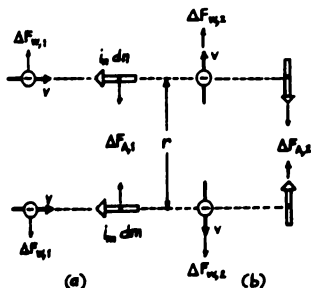


Fig.23 Weber and Ampere forces between electrons

side-by-side at the common velocity v . Their relative velocity $dr/dt=0$, and therefore the Weber force between them is simply the Coulomb repulsion

$$\Delta F_{W,1} = e_s^2/r^2 \quad (1.134)$$

where e_s is the electronic charge in electrostatic units (e.s.u.). The corresponding current elements, indicated in fig.23 by large arrows, point in the direction opposite to the electron motion, because the direction of a current is the direction in which positive charges would move. We now have to transform the current elements into products of charge and velocity. For this we have Lorentz's hypothesis

$$i_m dm = i_n dn = (e_m/c)v \quad (1.135)$$

where e_m is the electronic charge in electromagnetic units (e.m.u.). The electromagnetic and electrostatic units of charge have different dimensions and are related by

$$1 \text{ e.m.u. of charge} = c \times 1 \text{ e.s.u. of charge} \quad (1.136)$$

With this relationship between the two types of charge, the Ampere force between the two current elements (a) of fig.23 may be written

$$\Delta F_{A,1} = -2e_m^2 v^2 / r^2 c^2 \quad (1.137)$$

Hence $\Delta F_{W,1}$ and $\Delta F_{A,1}$ are opposite in direction and different in magnitude. This proves that a convecting electron of Weber's theory cannot be equated to an amperian current element. The same conclusion can be drawn from fig.23(b) which refers to a situation of two electrons moving relative to each other with velocity $2v$. According to Weber's law (1.90) these two electrons repel each other less than would two electrons at rest with respect to each other. The mutual force actually comes to

$$\Delta F_{W,2} = (e_s^2/r^2)[1-(2v^2/c^2)] \quad (1.138)$$

while the corresponding Ampere force is one of attraction and given by

$$\Delta F_{A,2} = -(e_m^2/r^2)(v/c)^2 \quad (1.139)$$

Next it might be asked whether Weber's convecting charges exert forces on each other that agree with the Lorentz equation (1.133)? In the case of fig.23(a), the Weber force is simply the first term of (1.133). Weber's law does not embrace a component corresponding to the Lorentz force $e\mathbf{v} \times \mathbf{B}$. In the Lorentz theory, or more precisely in the special theory of relativity, the $e\mathbf{v} \times \mathbf{B}$ component can be made to disappear by allowing the observer to travel with one of the electrons. In this one special way of observing the forces, there is agreement between the Weber and Lorentz equations. When the forces are measured in the laboratory rest-frame, the Lorentz force produces attraction between the electrons which subtracts from the Coulomb repulsion, but Weber's force remains the same, for the newtonian laws are independent of the positioning of observers. For the electron motion depicted in fig.23(b), the Lorentz equation reduces to Coulomb's law because $\mathbf{B}=0$ along the velocity vector, and this disagrees with Weber's force. In general, therefore, Weber's and Lorentz's electron theories are not in accord with each other so far as the electromagnetic forces acting between convecting charges in vacuum are concerned. Both Ampere's and Weber's law seem to fail under these circumstances. This is the reason why the empirical Ampere-Neumann electrodynamics has to be restricted to metallic conductors for which it was originally devised.

CHAPTER 2

LONGITUDINAL AMPERE FORCES

AMPERE TENSION

When two current elements lie on a straight line and point in the same direction, the angles of Ampere's force law (see fig.3) are $\epsilon=0$ and $\alpha=\beta=0$ or 180° . This reduces the angle function of (1.24) to -1 and the mutual force between the elements is seen to be

$$\Delta F_{m,n} = i_m i_n (dm \cdot dn / r_{m,n}^2). \quad (2.1)$$

This latter expression is always positive and therefore represents repulsion. If the two elements belong to the same rigid metallic conductor, they will create tension in the inter-atomic bonds between the elements. This will be called Ampere tension.

The tensile interaction will be greatest for two neighboring in-line elements. Let us take two cubic elements of side r , such that $dm=dn=r$; $r_{m,n}=r$. Furthermore, for the same current in both elements $i_m=i_n=i$. Then we may express the interaction by

$$\Delta F_{r,r} = i^2 \quad (\text{e.m.u.}). \quad (2.2)$$

This shows immediately that in fundamental electromagnetic units ponderomotive force has the dimension of current squared. If i_1 is the current when $r=r_1$, then the current density is $j=i_1/r_1^2$. If we keep the current density constant while r is being reduced, equ.(2.2) becomes

$$\Delta F_{r,r} = (jr^2)^2 = i_1^2 (r/r_1)^4. \quad (2.3)$$

That is, for constant current density, the force between adjacent co-linear elements reduces with the fourth power of the element side. When r tends to zero, the force tends to zero. Therefore no singularities occur in the calculation of Ampere tension when the filament diameter tends to zero. On this point the first edition of this book was in error. The author thanks Dr. Assis for the correction.

When the co-linear current elements belong to separate solid metal circuits, they do not give rise to tension in either one of the circuits, but will strain the structure that keeps the circuits in place. Hence Ampere tension reveals itself only in isolated current-carrying circuits. The order of magnitude of Ampere tension and the resulting tensile stress are indicated by the graphs of fig.24. Tension and stress depend quite strongly on the shape and size of the conductor cross-section and are greatest for

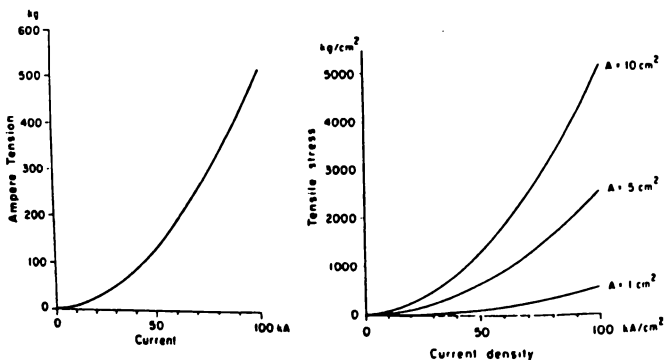


Fig.24 Order of magnitude of Ampere tension and stress

round conductors. The plot of Ampere tension versus current indicates that the effect is almost negligible below 10 kA and very large above 100 kA. In mega-ampere circuits Ampere tension is likely to be the dominant design parameter.

Most conductors used for the transmission and distribution of electricity carry less than 10 kA continuously. The largest power conductors have cross-sectional areas ranging from 50 to 100 cm² in order to keep them cool and waste as little energy as possible. Tensile stresses in the widely used copper and aluminum conductors are then less than 1 N/cm². They are negligible compared to thermally induced stresses, created by Joule heating, and other support and weight induced stresses. This explains why Ampere tension has gone unnoticed in a century of electric power distribution. Substantially larger currents may flow for brief periods of time when power circuits are accidentally short-circuited or struck by lightning. Fault currents of this nature are known to have reached 100 kA. This implies power conductors may occasionally experience tensile impulses up to 5000 N lasting for a few cycles of the power frequency. Since the Ampere tension is proportional to the square of the instantaneous current, an ac current will set up a tension corresponding to the root-mean-square amplitude pulsating unidirectionally at twice the ac frequency.

Ampere tension will play a major role in pulse-power circuits where currents in excess of 100 kA are commonplace. Current pulses of this magnitude are used in railguns and other electromagnetic accelerators, in plasma fusion experiments, in the simulation of the electromagnetic pulse (EMP) of a nuclear explosion, in laser drives of space weapons, in exploding wires and fuses, in opening switches for the discharge of inductively stored energy, in commutating interruptors of capacitor discharges, in dipole and other pulse magnets, and so on.

Most of the Ampere tension is being generated between close-neighbor current elements. It is therefore not a phenomenon occurring only in straight wires, but applies to all circuit shapes. It seems wherever an electric current flows in a metallic conductor, there will be tension induced in

the metal lattice. The question arises: can close-neighbor repulsion be cancelled by the interaction of the elements with many others in a near or remote branch of the circuit used to return the current to the power source? No categorical answer can be given at the time of writing. However, the limited evidence now available suggests the tension cannot be eliminated and, if anything, will be enhanced by the current return circuit. This conclusion has been drawn from the following analysis of a square circuit. As there are no analytical solutions available, the task had to be accomplished by finite current element analysis. The principal rules of finite current element analysis are:

1. Current elements are volume elements designed to fill the space occupied by the conductor metal.
2. Experience has shown that the length-to-width ratio of the element must be approximately one, or the calculation may diverge widely from force measurement.
3. The location of the current element is a point at its geometrical center.
4. Strings of touching elements are aligned along current streamlines. A single string of elements will be called a current filament.
5. At corners of circuits and, in fact, everywhere along a curved filament, there may have to be some overlap of adjacent elements. This is the major defect of finite current element analysis as it stands at the time of writing.

An infinitely long, straight conductor could be and has been treated as a closed circuit. Yet it would be futile to analyze it because, even with finite elements, the Ampere

formula would give infinite tension at every point along the conductor. To prove anything about Ampere tension the investigation has to concentrate on closed metallic circuits of finite size. In a straight portion of a finite circuit the elemental repulsion indicated by (2.1) should create tensile stress. In order to determine to what extent this stress is modified by the presence of the remainder of the circuit we consider the example illustrated by fig.25. A square circuit carries a steady current i and is adequately cooled to ensure constant temperature. Sides BC, CD, and AD of the circuit are firmly embedded in a dielectric structure which is rigidly anchored to the laboratory frame. AB is a free length of wire resting against a wall meant to absorb the lateral force on AB.

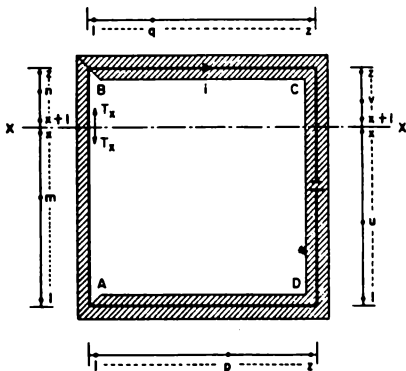


Fig.25 Square circuit with one free side

Let T_x/i^2 be the specific tension in interatomic bonds across plane X intersecting the wire AB. As further shown by fig.25, each side of the square is assumed to be divided into z equal length elements thin enough so that the conductor may be treated as a single filament.

A major contribution to T_x will come from the repulsion exerted by the general elements m in AX on the general elements n in XB. Since (2.1) is independent of the unit of length we may choose this to be

$$dm = dn = 1 \text{ unit of length} \quad (2.4)$$

With the labeling of current elements indicated on fig.25, the distance between the two general elements may be written

$$r_{m,n} = n-m \quad (2.5)$$

The specific (tension/square-of-current) tension contribution by the m - n element combinations is

$$T_1/i^2 = \sum_{m=1}^x \sum_{n=x+1}^z [1/(n-m)^2] \quad (2.6)$$

This will be a maximum when $x=z/2$.

Next we consider the interactions of current elements in AB with other elements in sides BC and AD. The interactions in question are all repulsions. This is due to the fact that the angle function $(2\cos\epsilon - 3\cos\alpha \cos\beta)$ is negative for all relevant element combinations. Now we have to make some assumption about the mechanical behavior of the unsupported wire AB. It is very thin compared to its length and it will therefore have little strength as a strut, while being quite strong in resisting tension. We therefore treat it like an ideal string, recognizing that this must involve some approximation. Interactions between BC and BX are taken up by the tensile strength of the wire and do not exert tension on the atomic bonds across plane X. The same is true for interactions between AD and AX. However the repulsion between BC and AX, as well as between AD and XB, adds to T_x . This is due to AX and XB having no column strength. Hence by resolving the latter repulsions along AB we obtain the second contribution to the specific tension across plane

x , that is

$$T_2/i^2 = \sum_{n=x+1}^z \sum_{p=1}^z (3/r_{p,n}^2) \cos^2 \alpha_n \sin \alpha_n + \sum_{m=1}^{x+1} \sum_{q=1}^z (3/r_{q,m}^2) \cos^2 \alpha_m \sin \alpha_m \quad (2.7)$$

where

$$r_{p,n}^2 = (n-0.5)^2 + (p-0.5)^2 \quad (2.8)$$

$$r_{q,m}^2 = (z-m+0.5)^2 + (q-0.5)^2 \quad (2.9)$$

$$\cos \alpha_n = (n-0.5)/r_{p,n}; \quad \sin \alpha_n = (p-0.5)/r_{p,n} \quad (2.10)$$

$$\cos \alpha_m = (z-m+0.5)/r_{q,m}; \quad \sin \alpha_m = (q-0.5)/r_{q,m} \quad (2.11)$$

The 0.5 terms arise from the fact that the position of the current element is a point halfway along its length.

The third contribution to T_x derives from interactions between AB and CD. The angle function for this side pair has everywhere $\cos \epsilon = -1$ and $-\cos \beta = \cos \alpha$. Furthermore, since α varies from 45° to 135° , $2\cos \epsilon - 3\cos \alpha \cos \beta = -2 + 3\cos^2 \alpha$. This is never positive and then, because of the negative sign of (1.24), all interactions are again repulsions.

It is convenient to split CD by the plane X with general elements u on one side and v on the other. Symmetry ensures that every elemental repulsion with an upward longitudinal component is offset by a symmetrical interaction with a corresponding downward component. Therefore actions of XC on XB do not contribute to T_x . The same is true for actions of DX on AX. However tensile forces will be produced in AB by the actions of XC on AX and by DX on XB. They give

$$T_3/i^2 = \sum_{m=1}^x \sum_{v=x+1}^z (-1/r_{m,v}^2) (-2 + 3\cos^2 \alpha_v) \cos \alpha_v + \sum_{n=x+1}^z \sum_{u=1}^x (-1/r_{n,u}^2) (-2 + 3\cos^2 \alpha_u) \cos \alpha_u \quad (2.12)$$

where

$$r_{m,v}^2 = (v-m)^2 + z^2 \quad (2.13)$$

$$r_{n,u}^2 = (n-u)^2 + z^2 \quad (2.14)$$

$$\cos \alpha_v = (v-m)/r_{m,v} \quad (2.15)$$

$$\cos \alpha_u = (n-u)/r_{n,u} \quad (2.16)$$

The total specific tension in the wire AB may then be obtained by adding (2.6), (2.7), and (2.12):

$$T_x/i^2 = T_1/i^2 + T_2/i^2 + T_3/i^2 \quad (2.17)$$

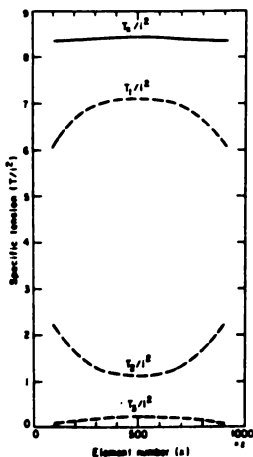


Fig.26 Specific tension in free side of square circuit

Fig.26 is a plot of the three tension components and their sum for $z=1000$. In the middle of AB the tension is seen

to be largely due to the repulsion of collinear elements. Near the ends of the side it is mostly produced by actions across the corners A and B. Side CD makes only a small contribution to the tension in AB.

It can easily be shown that the computed tension increases with z . At first sight this appears to be an unsatisfactory outcome of the Ampere electrodynamics. However this difficulty can be overcome by making reasonable assumptions about the length-to-width ratio of the current element. As a first step we calculate the most important tension contribution given by (2.6) across the midplane at $x=z/2$.

Table 1

Computer evaluation of (2.6) for z varying from 20 to 200 and $x=z/2$

z	T_1/i^2
20	3.188
30	3.593
40	3.880
50	4.103
60	4.285
70	4.369
80	4.573
90	4.691
100	4.796
110	4.891
120	4.978
130	5.058
140	5.133
150	5.202
160	5.266
170	5.327
180	5.384
190	5.438
200	5.489

Table 1 lists the results for z varying from 20 to 200. A regression analysis performed on this data revealed a

very close fit to

$$T_1/i^2 = 0.19 + \ln z \quad (2.18)$$

It can be shown that the specific tension contributions T_2/i^2 and T_3/i^2 obey similar logarithmic laws. Hence T_x/i^2 will also be a logarithmic function of z . For $z=1000$, equation (2.18) gives the specific tension of 7.098 as compared to 7.099 obtained by finite element analysis. This very good agreement gives us confidence in extrapolations of (2.18) to much larger values of z which otherwise would have to be obtained by an excessive computing expenditure.

Equation (2.18) tends to infinity with z . If the current element is assumed to be infinitely divisible, as Ampere did, his electrodynamics becomes absurd. The same is true for an electrodynamics based on the Lorentz force law. We really have no choice but to accept finite size elements. Could the lower element size limit be determined by the distance between neighboring atoms of the metal lattice? This would be of the order of 10^{-7} cm. It would amount to 10^9 current elements in AB of fig.25, if the latter side is 100 cm long. Equation (2.18) then gives a specific tension of 20.91 which is only three times the tension obtained for $z=1000$. It is not an unreasonably large number and therefore lends some support to the idea that the atomic cell is the extent of the basic current element.

It appears plausible that the reduction in current element length from macroscopic to microscopic dimensions should be accompanied by a similar reduction in the cross-sectional dimension of the element. In other words the specific tension of 20.91 probably applies to a conductor of 10^{-7} cm in diameter and 100 cm long. For conductors of larger diameter, the atomic element concept requires the consideration of a bunch of parallel filaments, each being essentially a string of atoms. How this leads to 'longitudinal force dilution' will be discussed later.

NASILOWSKI'S DISCOVERY OF WIRE FRAGMENTATION

Ampere reviewed his research in the field of electrodynamics most completely in reference [36], which has been republished as recently as 1958. There is indirect evidence for the existence of longitudinal forces in a number of his experiments. It could not have been otherwise, for his force law is merely a generalization of many experimental results obtained with circuits consisting of copper wires and liquid mercury cups and troughs. Blondel [37] in her excellent historical review "Ampere et la Creation de l'Electrodynamique" points out that on June 24, 1822, Ampere announced his formula required collinear current elements to repel each other, and that this prediction would be put to a direct test by A. de La Rive in Geneva. The experiment was performed shortly afterwards with Ampere present in de La Rive's laboratory. At the time it was considered to be an unqualified triumph of Ampere's theory. After the formulation of the Grassmann-Lorentz force law there arose much controversy about the Geneva experiment which will be fully discussed in a later section. Because of the shape of the conductor involved we will refer to the Geneva test as Ampere's hairpin experiment. Faraday repeated it in London, and Ampere wrote to him [37] in 1825 that, in some way, this experiment reveals the fundamental fact of electrodynamics.

Up to about 1960 all experimental evidence for longitudinal Ampere forces had been collected with circuits containing some liquid metal which permitted the measurement of small forces, or relative conductor motion, for easily realized, steady currents of 1000 A or less. The analysis of electrodynamic phenomena in liquid metals, normally called magneto-hydrodynamics (MHD), is more complex than the calculation of ponderomotive forces in solid conductors. The omission of MHD considerations by Ampere contributed much to the controversy surrounding his hairpin experiment.

The first experiments revealing the effect of Ampere tension without using liquid metals were performed by Nasilowski [38, 39, 40] in Warsaw. He was studying the behavior of copper wires when subjected to a sudden current pulse. The pulse amplitudes were quite small, up to approximately 2000 A, but the pulse duration was relatively long and of the order of 50 ms. Nasilowski's current pulses were generated by a rotating machine. He found that during a stepwise increase in current amplitude a point would be reached when a straight wire would fracture in the solid state at one or more places. An electric arc in air formed immediately across each fracture gap and the current continued to flow without interruption. Figure 27 shows open-shutter photographs of three wire disintegrations of 0.5 mm diameter copper wires of 56 cm length at three different voltages or current amplitudes. The smallest of the current amplitudes produced the arcs of (a) and the largest the arcs of (c).



Fig. 27 Wire fracture arcs photographed by Nasilowski

The open-shutter photography indicates by the exposed areas of light which arcs have been burning the longest. It would be surprising if all the wire fractures occurred at precisely the same time. The fracture sequence is of interest for what it may reveal about the tension producing mechanism. The photographs demonstrate, by the light areas, that the first breaks occurred at the ends of the straight wire sections. Nasilowski strung his wires horizontally between two posts. Heavier leads connected the generator with joints at the two posts. At each post there was a corner in the circuit. This is important because the Ampere tension is greatest right at a corner. The remaining early breaks are fairly widely spaced from each other. Other prominent features of the arc photographs are the increase in the number of breaks with current amplitude and the great number of arcs than can be formed without striking an overall arc. It should also be noted that the wires apparently did not move laterally although the force per unit length in that direction must have been of the same order of magnitude as the Ampere tension. It is an indication of the effectiveness of inertial positon confinement on the millisecond time scale. The waviness along the wires might possibly be the result of thermal expansion prior to wire fracture. The thermal forces are probably so strong that they cannot be inertially confined.

From the point of view of the Ampere electrodynamics one would expect straight and curved wire sections to rupture somewhere along their length before any melting can take place provided the pulse time is greater than the crack formation time. An air arc should immediately bridge the fracture gap because of the high voltage that would be induced by a sharp drop in current. The continuation of current flow ensures the continued existence of Ampere tension. Wire sections between arc gaps are mechanically decoupled from the rest of the circuit, and the tension that can develop within each inequal section depends on the length of

that section. The shortest wire fragments produced are about of the same length as the wire diameter. The sum of the voltage drops along the series-connected bridging arcs should severely limit, if not extinguish, the current. Premature current extinction has indeed been observed by many investigators of exploding wire phenomena when the current source was a capacitor bank. With the energy being stored in an inductance, the current cannot be interrupted until all the energy is discharged.

In one of his papers [39] Nasilowski shows six photographs. Two of them depict a collection of fragments of his 1 mm diameter, 1.5 m long copper wire. The diameter of the fragments looks the same as that of the original wire and the fracture faces are nearly perpendicular to the wire axis. The length of the fragments varies between 3 and 10 mm. The other four photographs are of metallurgical sections through some fragments, in the longitudinal direction, to probe the internal grain structure and visible signs of crack initiation. Baxter [41] has measured the temperature distribution along fuse wires subjected to current pulses. Except for end-effects, he found that the wire temperature rose uniformly over the wire length right up to the melting point. Nasilowski's work confirmed that melting also occurred uniformly along the wire, with the boundary between the molten and the solid phase being a cylindrical surface moving radially inward. Hence wire fragmentation could not be the result of preferential melting at some locations along the wire.

The metallurgical evidence indicated that in some of Nasilowski's experiments fracture had taken place without any change in the grain structure of the body of the wire and therefore without any prior melting. But the electric arc bridging the gap between adjacent fragments, subsequent to fracture, produced a small amount of freshly molten material which adhered to the fracture faces and was recognizable

by its dendritic structure. Nasilowski's metallurgical tests clearly indicated that the wire had parted in the solid state under the action of tension. Fig.28 shows 1 mm diameter copper wire fragments produced in Nasilowski's experiments in 1960. At the time he was not aware of Ampere's force law and could not offer a satisfactory explanation of his observations. He recognized that longitudinal forces were at work and confirmed their existence with a longitudinal force transducer. In practical terms, Nasilowski had demonstrated that wire fuses do not simply melt away, but are likely to fragment into many short pieces before melting. The connecting arcs in air then perform a current limiting function.

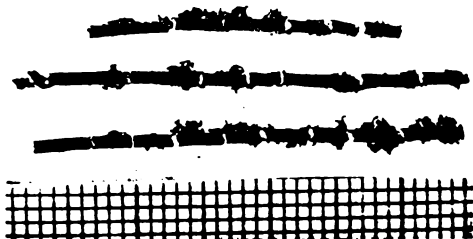
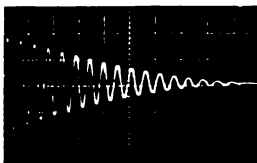


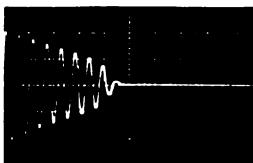
Fig.28 Copper wire fragments of Nasilowski's experiment

The author repeated Nasilowski's experiment in modified form at the Massachusetts Institute of Technology in 1982 [42, 43]. Aluminum wires of 99 percent purity and 1.2 mm diameter were subjected to current pulses of 5000 to 7000 A amplitude. The current was derived from a high-voltage capacitor bank and passed through an inductor to allow it to ring down at 2000 Hz over a period of five to ten milliseconds. When the capacitor bank was charged to 60 kV, the

discharge current would decay approximately exponentially, as shown by the oscillogram of fig.29(a), without breaking the wire. It has been estimated that the 60 kV discharge was accompanied by a wire temperature rise of several hundred degrees centigrade which must have resulted in a thermal extension of the order of one percent.



(a)



(b)

Fig.29 Discharge current oscillograms; $y=3\text{kA/cm}$, $x=1\text{ms/cm}$,
(a) at 60 kV; (b) at 68 kV

By subsequent increases of the discharge voltage in steps of 2 kV, a pulse current level was reached at which the wire broke in one or more places. The hot fragments would fall to the floor and be distorted on impact. When repeating the test with a new wire and 2 kV additional voltage, the wire would break into a greater number of pieces. At the 66 and 68 kV levels a one meter long wire would fragment into 20 - 30 pieces. Finally, at 70 kV, the test wire would show clear signs of melting which obliterated much of the tensile break evidence. The oscillogram of fig.29(b) indicates discharge current limiting and quenching due to

the many arcs across fracture gaps.

The strongest indication of Ampere tension was obtained with straight, one meter long wires mounted vertically, as shown in fig.30. The wires were held in position with cotton threads, leaving 1 cm long arc gaps in air between the wire ends and two terminations of the capacitor-inductor series circuit. When the discharge circuit was closed with a mechanical switch, the two one-centimeter arc gaps would break down, allowing the current pulse to flow through the test wire. The purpose of the arc gaps was to allow distortion-free thermal expansion and to disconnect the wire mechanically from the fixed discharge circuit.

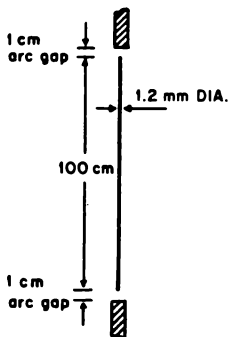


Fig.30 Suspension of wire to be fragmented

Figure 31(a) shows a collection of aluminum wire fragments produced by these experiments. Their distortions was caused by impact on the laboratory floor while they were hot. Photograph (b) clearly depicts transverse fractures which were spot-welded together again by arcing across the fracture gaps. Figure 31(c) is an optical micrograph of one fragment end, illustrating the brittle nature of the

fracture. The last photograph (d) of a fracture face was taken by scanning electron microscopy. Similar micrographs of greater magnification revealed micron-deep melting of the fracture surface, consistent with arcing across the fracture gap.

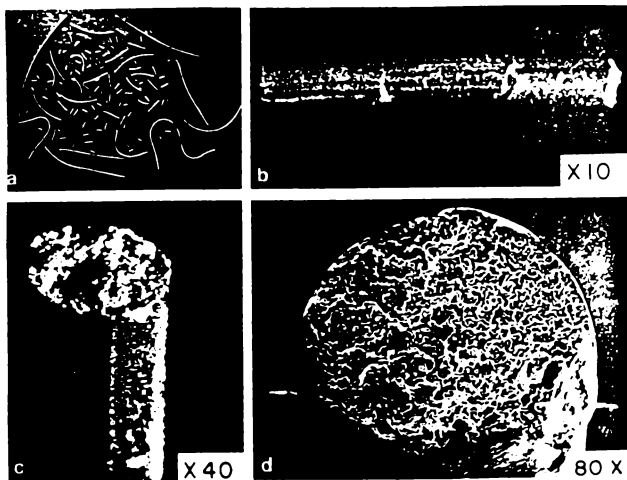


Fig.31 Fragments of a 1.2 mm diameter aluminum wire
 (a) collection of fragments from several experiments
 (b) fragments reconnected by arc spot-welding
 (c) optical micrograph of fracture face
 (d) scanning electron micrograph of fracture face

Provided the wire is treated as a bundle of filaments, the transverse pinch force may be calculated with Ampere's or the Lorentz force law. Pinch forces are potentially able to extrude soft wire. However, Northrup's analysis [44] proves that the extrusion force is less than one-tenth of the magnitude of the Ampere tension. For this reason, and even more because no significant diameter reduction (neck

formation) has been observed near the fracture faces. it seems certain that pinch-off was not the cause of wire fragmentation.

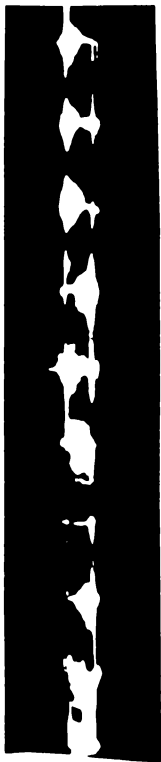
Considerable thought has been given to the possibility of the wire fractures being the result of travelling stress waves or thermal shock. The velocity of sound in the conductor metals is of the order of 5000 m/s. Hence a stress wave could travel the length of the wires used by Nasilowski and the author in 0.1 to 0.3 ms. Tensile stress magnification by multiple reflections from the wire ends or anchors is therefore not out of the question. Nasilowski employed a unidirectional current pulse. The radial pinch force was not removed from his wire until the current ceased to flow. Only after the end of the pulse could pinch force relaxation have produced travelling stress waves. But with the aid of voltage drop measurements Nasilowski proved that the wire broke well before the end of his pulse. Nasilowski's wire fragmentation evidence, therefore, cannot be explained with travelling stress waves.

A dynamic thermal shock model has been examined. Consider a straight aluminum wire of one meter length. When heated close to the melting point its length will increase approximately 1.4 cm. During the pulse period each end of the wire would be displaced 0.7 cm. If the pulse lasts for 5 ms, as in the shortest of the MIT experiments, the last centimeter on either end of the wire would attain an average velocity of 140 m/s. For a wire of 1.2 mm diameter, the mass per centimeter comes to 0.03 g, giving a kinetic energy of the last centimeter of 300 erg. Allowing for only ten percent elongation of hot aluminum before fracture, the average tensile force required to absorb the kinetic energy comes to only 3 gram-weight, which is negligible. The calculated Ampere tension of the MIT wire fragmentation experiments was of the order of 25 N.

The extent to which wire fragmentation experiments confirm the Ampere tension mechanism is quite remarkable. In Nasilowski's setup the first breaks did occur at the corners of the circuit where the tensile stress is greatest, because across the corners transverse and longitudinal forces combine to break the wire. Equations (2.6) and (2.18) claim that the Ampere tension is greatest in the middle of a straight, integral wire section, and that this maximum tension increases logarithmically with section length. Hence we may expect the early breaks in a long, straight wire to be widely separated, rather than bunched together. Nasilowski's arc photographs confirm this expectation. There should be a lower limit of fragment length below which the Ampere tension becomes too small to cause further breaks. This appears to be confirmed by figs. 28 and 31(a) and (b). The shortest fragments ever observed were only a little longer than one wire diameter. The number of fragments produced per current pulse should, for two reasons, increase with pulse amplitude. First, the Ampere tension increases with the square of pulse amplitude, and, secondly, the wire temperature rises and thereby reduces the tensile strength of the wire. Figure 27 is proof of the greater number of fragments resulting from increased pulse amplitude. The very short period of time during which Ampere tension exists should be insufficient to allow much plastic deformation and the wire fractures should have the appearance of brittle impact failures. This is confirmed by the fragment photographs of figs. 28 and 31.

The following quantitative considerations also support the Ampere tension mechanism. A 100 cm long, 1.2 mm diameter aluminum wire of the MIT experiments weighed three gram. For a peak current amplitude of 6000 A it should have experienced a maximum Ampere tension stress of 231 kg/cm^2 . This is equal to the ultimate strength of the material at around 300°C . The impact strength of the metal will be less. Therefore the first break in the wire could occur

quite early in the discharge cycle provided the fracture pieces manage to separate in the available time. The repulsion between the two wire portions is equal to the Ampere tension just before the break. If the break occurs halfway along the one-meter wire, calculations show that it should have been subject to an acceleration of 1713 times that of gravity. In 0.1 ms this would produce a wire separation of 0.08 mm which seems adequate for a clean break.



Bruce [45] recently performed an experiment at the Center for Electromagnetics Research at Northeastern University in which Ampere tension manifested itself in yet another way. He took a $\frac{1}{4}$ -inch diameter copper rod and cut it up in 50 pieces, each 2 cm long. He then reassembled the pieces in a vertical glass tube and pressed them together with a spring. When a certain current pulse was passed along the assembled copper pieces, they all separated by a small distance and arcs formed across the cuts, as shown in the open-shutter photograph of fig.32. What in the wire fragmentation experiments was Ampere tension became, in Bruce's experiment, a repulsive separation force acting between neighboring pieces of copper rod. These forces would have been far too small to fracture a $\frac{1}{4}$ -inch copper rod, but they proved sufficient to overcome the rod inertia and open gaps up to one millimeter in length.

fig. 32 Bruce's experiment

PAPPAS' ELECTRODYNAMIC IMPULSE PENDULUM

Over the years a number of researchers have performed Ampere's hairpin experiment with various modifications without very conclusive results. The problem has been that the Ampere and Lorentz laws predicted hairpin propulsion forces of nearly the same magnitude. The difference manifested itself only in the location of the forces and their reactions. The Lorentz force is supposed to pull the hairpin from the front and have its reaction in the field. The Ampere force, by contrast, should push the hairpin from the back, and have its reaction force in the metal of the remainder of the circuit. It appeared impossible to devise an experiment capable of distinguishing between those two mechanisms. The deadlock was finally broken by Pappas [46] in Athens with an ingenious pendulum experiment. To understand the Pappas experiment we have to delve a little into field theory and its relativistic ramifications.

Ever since the elastic properties of the aether were abandoned to accommodate the special theory of relativity, it was felt that another mechanism for absorbing reaction forces in the field (vacuum) was required. It is field reactions, or magnetic pressure, that counteract Lorentz forces exerted on current carrying metallic conductors. The generally accepted view, as expressed for example in reference [47], is that the rate of change of electromagnetic momentum in the field can support force which accelerates or decelerates magnetic field energy to and from the velocity of light c . The energy momentum density is related to the Poynting vector by

$$\underline{p} = (1/c^2)(\underline{E} \times \underline{H}) \quad (2.19)$$

where \underline{E} and \underline{H} are the electric and magnetic field strengths at a point. The volume integral of the rate of change of this momentum density over all space gives the vacuum reac-

tion force

$$\underline{F}_{\text{vac}} = \int (d\underline{p}/dt) dv = (1/c^2) \int (d/dt) \underline{E} \times \underline{H} dv \quad (2.20)$$

where t stands for time and v for volume. When the integral is not taken over all space, the rate of change of momentum may be smaller than indicated by equ.(2.20). It is customary to make up the difference by the surface integral of Maxwell's stress tensor over the finite volume of the momentum integral. With the integral being taken over all space, and for any instant in time, the vacuum reaction force may be written

$$\underline{F}_{\text{vac}} = (d/dt)(m_e c) \quad (2.21)$$

where m_e is the equivalent electromagnetic mass of the magnetic energy stored in the field. Since c is a constant, the vacuum force will only exist when m_e changes with time, that is when magnetic energy is radiated into the field or absorbed from the field by a conducting body. The amount of field energy U_f that must at any time be associated with the vacuum reaction force is

$$U_f = m_e c^2 \quad (2.22)$$

This is the famous mass-energy relation of special relativity.

If $\underline{F}_{\text{vac}}$ is at all times the simultaneous reaction force to the Lorentz force \underline{F}_L when the latter accelerates a metallic conductor object of real mass m from zero to the velocity u , then momentum conservation is expressed by

$$m \cdot u = \int p \cdot dv = m_e c \quad (2.23)$$

The last equation implies that Newton's third law is obeyed and the electromagnetic mass m_e has the inertia of real mass.

but no weight. The field energy which has to be radiated or absorbed by the body of the conductor, in order to comply with (2.23), is

$$U_f = m_e c^2 = m \cdot u \cdot c \quad (2.24)$$

Pappas [46] devised an experiment to check whether that much energy was actually being supplied to the field. He powered his experiment with a lead-acid battery and found that the amount of energy his battery could possibly have supplied fell far short of the requirement of equ.(2.24). The Pappas experiment involved an impulse pendulum and is a variation of Ampere's original hairpin experiment. It challenges field-energy momentum conservation only in so far as metallic conductors are concerned.

Because of its far-reaching consequences, the author repeated the Pappas experiment at MIT and made it a quantitative test. In the MIT experiment the energy available for Joule heating and conversion to kinetic and electromagnetic energy was accurately known, as it was drawn from previously charged capacitors. This was not the case in the Athens experiment, and therefore we will describe the MIT experiment fully after a brief discussion of Pappas' arrangement.

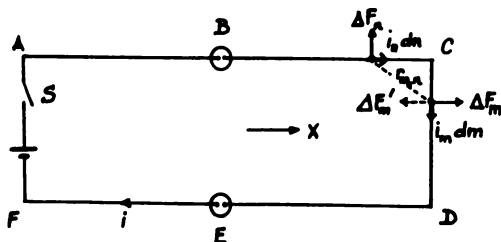


Fig.33 Pappas' impulse pendulum circuit

Figure 33 is a simplified diagram of the experimental circuit used at the University of Athens. ABCDEF is a horizontal, rectangular copper circuit and B and E are two mercury cups. The portion BCDE forms the impulse pendulum hanging from the laboratory ceiling. The remainder of the circuit is fixed to the laboratory frame and contains a battery and a switch in branch AF. When the switch is closed an instantaneous current i will flow around the copper circuit and the pendulum is observed to swing in the direction x . The swing interrupts current flow in the mercury cups.

According to field theory the force responsible for producing the pendulum motion is the Lorentz force on branch CD. This force arises from interactions of current-element pairs governed by the Grassmann formulas (1.85) in which $i.dm$ is a current element in branch CD and $i.dn$ is a current element anywhere else in the remainder of the circuit. On account of the inverse square law contained in (1.85), most of the acceleration force on the pendulum arises from the magnetic field of current elements in the legs BC and DE, that is in the manner indicated in fig.33 by ΔF_m .

In the spirit of field theory as taught today, ΔF_m and similar contributions to the pendulum acceleration force should be counteracted by a vacuum reaction force indicated by $\Delta F'_m$ on fig.33. The latter force will ensure compliance with Newton's third law and linear momentum conservation. The vacuum reaction force would either decelerate incoming energy which is then converted to Joule heat, or it could accelerate energy which is being radiated from the metal element dm . The incoming energy would be transmitted from the battery through space by the Poynting vector mechanism, while the outgoing energy radiated from dm must first reach the element somehow through the metallic conductor. Both energy streams have to be added together to arrive at the energy subtracted from the battery or other source. The vacuum reaction force acts on the space occupied by the

metal element dm . If it acted on the metal itself it would cancel the pendulum accelerations force. It will be assumed little or no energy is being reflected by dm , and no electromagnetic mass is being created in mid-space, away from the metal, which might somehow contribute to momentum conservation. As the field energy travels with the constant velocity c , all of the vacuum reaction force $\Delta F'_m$ must then arise at the location of dm . We nevertheless extend the integration in equ.(2.20) over all space to eliminate all possible Maxwell stresses.

At some finite time t after the current has been switched on, the mechanical impulse imparted to the pendulum by the Lorentz force should be equal to the mechanical momentum acquired by the pendulum. Furthermore, for momentum conservation, this mechanical momentum should be equal to the field-energy momentum change. Hence we may write

$$\begin{aligned} \int_0^t F_L dt &= m \int_0^t (du/dt) dt = c \int_0^t (dm_e/dt) dt \\ &= m \cdot u = m_e c \end{aligned} \quad (2.25)$$

where

$$F_L = \sum_m \sum_n (\Delta F_m) \quad (2.26)$$

with the summation over m extending throughout the circuit branch CD and the summation over n covering the remainder of the circuit. Since m , u , and c are known we may use (2.25) to calculate m_e , the electromagnetic mass in the field which must be furnished by the battery or other energy source. The total amount of energy that must have been subtracted from the source up to the time t is specified by (2.22). This is the minimum energy of (2.24) required by field theory to accelerate the pendulum and cover the Joule heating in the branch CD of the circuit.

The Pappas experiment permits a comparison to be made of (1) the Lorentz force impulse with the mechanical momentum acquired by the pendulum, and (2) the minimum required field energy with the energy available from the power source. Pappas concluded that, in the time available, his battery would have supplied much less energy than was required by equation (2.24), and that the Lorentz force on the circuit branch CD was therefore unlikely to be the force accelerating the pendulum. He pointed out that his experiment favors the older Ampere force law which explains the pendulum motion by newtonian repulsion between the fixed and moving parts of the circuit.

Figure 34 shows the experimental setup of the electrodynamic impulse pendulum used by the author at MIT. The 'hair-pin' was made of a copper strip 0.5 inch high and 0.05 inch thick. The strip formed two one-meter long sides and one 30 cm short side of an open rectangle. The pendulum conductor was mounted on a rigid frame (not shown in fig.34) of insulating material. The assembly weighed 0.815 kg. The pendulum was suspended from the laboratory ceiling by four 2.56 m long cotton threads. The horizontal displacement of the pendulum was measured with the cardboard slide C resting lightly on a flat table top.

The pulse current was derived from an 8 μ F high-voltage capacitor bank which could withstand voltage reversals up to ± 100 kV. The discharge was initiated by dropping the mechanical switch S. Two parallel current rails F, of the same copper strip of which the pendulum was made, brought the current to the hairpin via two, one-millimeter long, arc gaps in air. The rails were mounted on a rigid frame and two heavy stands, weighed down with lead (not shown in fig.34), to absorb the recoil impulse of the Ampere law with a minimum of deflection. The rails were carefully aligned with the horizontal legs of the hairpin pendulum.

To perform a momentum experiment the capacitor bank

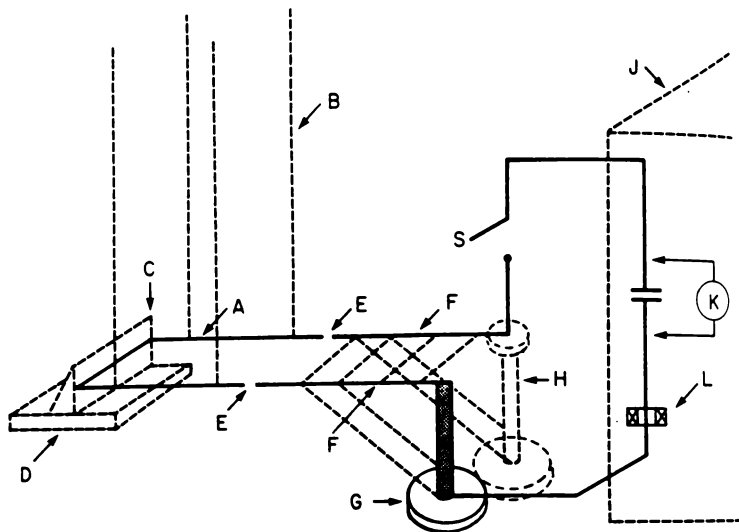


Fig.34 Electrodynamic impulse pendulum used at MIT

- A - hairpin pendulum conductor
- B - cotton suspension threads
- C - cardboard slide
- D - flat table top
- E - 1 mm arc gaps in air
- F - current rails
- G - grounded metal stand
- H - dielectric stand
- J - 100 kV capacitor bank
- K - 200 kV charging set
- L - Rogowski coil
- S - mechanical switch

was charged to a voltage between 30 and 80 kV. The switch was then dropped, causing arcing across the short gaps between current rails and pendulum legs. The damped oscillatory current pulse was recorded with the aid of the Rogowski coil L of fig.34 and an oscilloscope. The current pulse did cause the pendulum to swing away from the current rails and move the cardboard slide through a distance s , subsequently measured with a ruler. The duration of the current pulse was a fraction of a millisecond. Almost all the pendulum displacement occurred after the current had ceased to flow.

The maximum linear momentum $m.u$, imparted to the pendulum by the capacitor discharge, may be calculated from the pendulum length $R=2.56$ m, its mass $m=0.815$ kg, and the measured cardboard slide displacement s . With the aid of fig.35 it

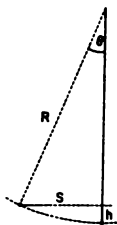


Fig.35 Pendulum parameters

can be seen that

$$m.g.h = (1/2)m.u^2; \text{ or } u = \sqrt{2g.h} \quad (2.27)$$

where g is the acceleration due to gravity, u the maximum horizontal velocity that would be attained in the limit when the impulse duration tends to zero, and h is the maximum vertical lift of the pendulum. The height h may be derived from the two simultaneous equations

$$h = R(1 - \cos\theta) \quad (2.28)$$

$$s = R \sin\theta \quad (2.29)$$

The solution is

$$h = R[1 - \sqrt{1 - (s/R)^2}] = s^2/(2R) \quad (2.30)$$

The approximation is accurate to three significant figures and may be used in equ.(2.27) to calculate u .

The electrodynamic impulse imparted to the pendulum by the Lorentz force $F_L = 10^{-7} k i^2$ may be written

$$P_i = 10^{-7} k \int_0^{\infty} i^2 dt \quad (2.31)$$

where i is the instantaneous current and k (N/A^2) must be determined from the geometry of the circuit. A typical discharge oscillogram is reproduced in fig.36. It shows that the instantaneous current is of the form

$$i = e^{-t/T} I_0 \sin\omega t \quad (2.32)$$

where T is the time constant with which the oscillation decays. The full amplitude I_0 would be reached if the circuit contained negligible resistance. It is possible to integrate (2.32), as required by (2.31), and obtain

$$P_i = 10^{-7} k I_0^2 \{ (T/4) - (1/T) / [(2/T)^2 + (2\omega)^2] \} \quad (2.33)$$

with $\omega = 2\pi f$ being the radian frequency. As far as the pendulum experiments are concerned, the second term of (2.33) is negligible. Hence the electromagnetic impulse may be taken to be

$$P_i = 10^{-7} k I_0^2 (T/4) \quad (2.34)$$

The magnitudes of I_0 and T were measured on the pulse current records.

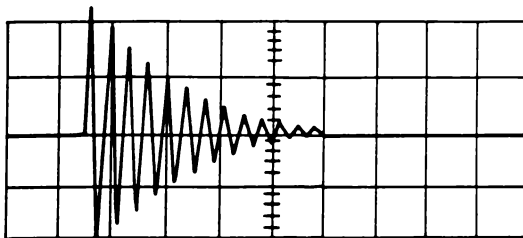


Fig.36 Discharge current oscillogram for 2 μ F and 60 kV;
y=7.5 kA/cm; x=0.1 ms/cm

The electric arcs bridging the 1 mm long gaps between current rails and pendulum legs produced a small amount of molten copper which streamed away from the gaps, in both directions, along the copper strips. The evidence of droplet streaming became unmistakable after the heaviest discharge currents. The arc pressure must have been responsible for generating some of the pendulum momentum over and above the contribution made by the Lorentz force. As the arc pressure must have been symmetrical between rails and pendulum, it would not require to be balanced by a vacuum reaction force.

Approximately 100 discharge shots were carried out at various voltages and capacitance values. A typical set of results is reproduced in table 2. This was obtained with the full 8 μ F capacitance of the bank and therefore involved the largest currents and pendulum displacements. As long as the capacitance and circuit configuration was not changed between shots, the ringing frequency f , the circuit inductance L , the surge impedance $Z = \sqrt{L/C}$, the time constant T , and the effective damping resistance R all remained constant. Their magnitudes were derived from current oscillograms. For the series of discharge pulses to which table 2 refers, these parameters came to

$f = 15.7 \text{ kHz}$; $L = 12.8 \text{ } \mu\text{H}$; $Z_0 = 1.26 \text{ } \Omega$; $T = 0.27 \text{ ms}$;
 $R = 94.8 \text{ m}\Omega$.

Table 2
 Set of results of the MIT experiment

Quantity	Unit	40 kV	50 kV	60 kV	70 kV	80 kV
I_0	A	28 500	35 250	45 000	52 500	60 000
s	cm	1.93	3.50	5.55	7.75	10.95
m.u	kg.m/s	0.0308	0.0558	0.0885	0.1236	0.1742
U_h	J	5 200	7 950	12 960	17 640	23 040
U_c	J	6 400	10 000	14 400	19 600	25 600
$U_c - U_h$	J	1 200	2 050	1 440	1 960	2 560
P_i	N.s	0.0508	0.0778	0.1267	0.1725	0.2253
U_f	MJ	15.24	23.34	38.01	51.75	67.56
U_f/U_c		1 438	1 670	1 840	1 893	2 047
$P_{L,max}$	N	753	1 152	1 877	2 555	3 337
u	cm/s	3.78	6.85	10.86	15.17	21.44

The observed pendulum momenta listed in table 2 varied from just over 0.03 to 0.18 kg.m/s. The kinetic energies ($\frac{1}{2}m.u^2$) associated with these momenta turn out to be less than one Joule while the energy stored in the capacitors, U_c , was as high as 25.6 kJ. Hence very little of the spent energy is being converted to kinetic energy. When the Joule heat generated in the circuit is subtracted from the originally stored energy, only up to 2.5 kJ remain. This immediately suggests that most of the field momentum change must be associated with incoming energy being stopped and converted to Joule heat.

It has to take a certain amount of energy to establish the three arcs at the switch and the two gaps E of fig.34. This energy is sometimes called the latent heat of arc forma-

tion because it eventually appears as heat when the arc ions recombine. The latent heat of arc formation could conceivably account for several kilo-Joule, indicating that little may be available for radiation in the field.

It is instructive to evaluate the Lorentz force on the pendulum bridge and integrate it with respect to time to obtain the impulse which should be balanced by a change in field energy momentum. A finite element method of computing the constant k in equ.(2.34) is available [48]. In reference [48] an identical copper strip was considered which was bent into a rectangular circuit of the same dimensions as the pendulum. The strip was resolved into ten parallel filaments of square cross-section. Each filament was then subdivided into cubic current elements. The computer solution gave $k=9.27 \text{ N/A}^2$. This applied to uniform current distribution over the strip cross-section. At the frequency of 15.7 kHz, to which the results of table 2 refer, the current distribution will have been very non-uniform, with strong concentrations near the strip edges. If it is assumed that all the current flows in the two edge filaments, the constant in (2.34) comes to $k=11.0 \text{ N/A}^2$. Therefore the Lorentz force appears to increase with frequency. A lower limit of this force is obtained by taking the 9.27-figure. Impulse values for this lower limit are listed in table 2.

It will be noted that the calculated electrodynamic impulses P_i are greater than the measured linear momenta. The ratio of the two quantities is approximately 1.4. No field-theoretic explanation of this discrepancy can be offered. In determining the field energy U_f listed in table 2, the measured m.u-momenta were substituted into equ.(2.24). Table 2 also contains the energies U_c stored in the capacitors. The ratio U_f/U_c will be seen to vary between 1400 and 2000. The shortfall in available energy to satisfy field momentum conservation far outweighs all possible experimental errors. It supports the claim by Pappas [46] that the Lorentz

force is not balanced by an equal and opposite reaction force in the vacuum field.

To obtain an idea of the magnitude of the Lorentz force on the pendulum in the direction of its swing, we recognize that it would attain the maximum value of

$$F_{L,max} = 9.27 \times 10^{-7} I_0^2 \quad (2.35)$$

at the peak of the first half-cycle of the current, but for the small exponential decrement due to damping. The force of (2.35) is also listed in table 2. The figures make it clear that, if the Lorentz force is indeed the motive force, the pendulum should feel a very sharp tug at its leading edge. The arc pressure is expected to be small compared to this sudden jerk.

Let us now apply Ampere's force law (1.24) to the impulse pendulum experiment. It predicts a strong repulsion between each current rail and the portion of the pendulum aligned with the rail. This provides the major impetus for the pendulum swing. Equation (1.24) adds to this a small amount for the interaction of the rails with the pendulum bridge, and subtracts a little for the attraction of each rail and the pendulum leg on the other side. On account of the mechanical decoupling by the arc gaps, the total Ampere repulsion between rails and pendulum can be obtained by integration of (1.24). The finite element method with ten parallel filaments of cubic elements will yield virtually the same result. The numerical technique gave the value of $k=9.24 \text{ N/A}^2$. This applies to uniform current distribution over the conductor cross-section. It is remarkably similar to the corresponding $k=9.27 \text{ N/A}^2$ obtained with the Lorentz force formula.

It has been known for many years that the calculated Lorentz and Ampere forces on the sides of a 'rectangular' circuit are almost identical [49]. They differ, however, with regard to how and where they act on the conductor mate-

rial. Lorentz forces are always transverse to the current streamlines and would invariably be in conflict with Newton's third law unless there exist balancing vacuum reaction forces. Ampere forces produce a strong tensile component along current streamlines and have all their reaction forces in the conductor material. For transfer of the electronic Lorentz force to the metal ions one has to rely on the work function at the conductor surface. This mechanism cannot produce tension along the current streamlines.

Since the Ampere force interaction of every pair of material current-elements obeys Newton's third law, the equality of action and reaction between the two parts of the metallic circuit of the impulse pendulum experiment follows automatically. It merely reaffirms that the Ampere electrodynamics ascribes no physical action to empty space.

The Ampere law claims the pendulum is being pushed from the rear rather than being pulled from the front. Hence the hairpin legs may bend and buckle. In this way they must be expected to store some elastic energy which results in vibrations rather than linear mechanical momentum. More elastic energy is likely to be stored in the current rails F of fig.34. In the Ampere electrodynamics it seems plausible that not all of the impulse P_i should be converted to momentum $m.u.$, unless the apparatus is infinitely rigid. In the initial experiments neither the pendulum nor the rails were reinforced with dielectric structures. This resulted in non-reproducible pendulum swings. Although the reinforcement had a considerable stabilizing effect, the equipment was by no means infinitely rigid. This is how the Ampere electrodynamics explains why $m.u$ was smaller than P_i .

In conclusion, therefore, the electrodynamic impulse pendulum invented by Pappas denies the existence of electromagnetic mass in the magnetic field produced by currents flowing in metallic circuits. We seem to have the choice

of believing in reactionless Lorentz forces which openly violate Newton's third law of motion, or we have to fall back on Ampere's force law. However, the discovery in the MIT experiment of the discrepancy between pendulum momentum and calculated Lorentz force impulse removes the Lorentz force alternative and leaves us only with Ampere's law as a viable explanation of the impulse pendulum experiment.

RAILGUN RECOIL

Ampere tension is of practical importance in technological developments concerning exploding wires and fuses. Longitudinal forces of repulsion between pieces of a substantial conductor may be used to generate a multiplicity of electric arcs for limiting current and assisting in the operation of circuit breakers and current interruptors. Prospects are good for employing the latter force mechanism in the design of opening-switches for discharging stores of inductive energy. Pappas' experiment with the electrodynamic impulse pendulum also has technological ramifications. An important one is the recoil mechanism of railgun accelerators.

The railgun is an old concept for the linear acceleration of a metallic projectile bridging the gap between two metallic rails which carry current to and from the projectile. Sliding brush-contacts and electric arcs have been used to transfer the current between the stationary rails and the travelling projectile. However, the most advanced railguns rely on a metal vapor arc between the rails which pushes a dielectric projectile in front of it. This is illustrated by fig.37. The arc exerts an acceleration force F on a plastic (non-conducting) projectile. In the traditional way it would be assumed that the recoil force F is being absorbed in the field and has no effect on the rails.

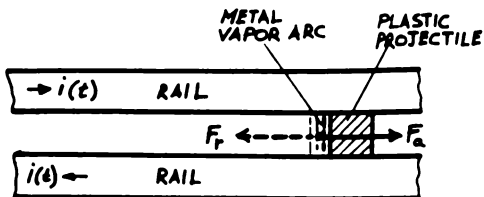


Fig.37 Arc-driven railgun

A variety of different types of railguns are currently under development. Many are directed toward military objectives. Hawke et. al. [50] have described a series of experimental shots in which projectiles ranging from 3 to 165 g mass have been accelerated to velocities as high as 10 km/s. In this particular investigation the greatest momentum imparted to a projectile was of the order of 30 kg.m/s. If that much momentum had had to be produced by electromagnetic energy impinging on the metal vapor arc, it would, according to equation (2.24), have consumed 9000 MJ of stored energy. In fact, as Hawke et. al. state, the total energy stored in their capacitor bank was less than 0.5 MJ. There is no doubt, therefore, that the railgun recoil is not being exerted on the field or vacuum.

In light of Ampere's force law we must expect $0.5 \frac{F}{l}$ to be pushing each rail back to the breach of the gun. The maximum acceleration force--and therefore the total recoil--in the most powerful railguns can be as large as 250,000 N (25 tonweight) and, consequently, the rails have to be very strong in order not to buckle and restrict the progress of the projectile ahead of the seats of the recoil forces in the rails. Rail interference, that is a reduction in the rail-spacing ahead of the projectile, has already been observed by Peterson et. al. [51]. Bedford [52] discovered that his rails had developed a permanent set, bulging outward by as much as 3 cm in a length of 80 cm, consistent with

deformation by buckling. It seems, therefore, that the Ampere recoil has serious consequences with regard to the proper functioning of railguns, unless suitable allowances are made in the design of the accelerators.

The Ampere recoil [53] arises from the current element repulsion across the corners of the railgun circuit, as indicated in fig.38. The current element m of the projectile branch P repels the current element n of rail S because $\cos \epsilon = 0$ and $\cos \beta$ is negative. The transverse component of the repulsion of m is the acceleration force ΔF_a , while the longitudinal component of the repulsion of n is the corresponding recoil force. This holds for any current element combination between projectile and rails. Therefore each rail experiences a distributed recoil force of $\Delta F_a/2$ directed toward the gun breach. It has to be remembered, however, that this prediction of the Ampere electrodynamics is for metallic rails and a metallic projectile branch P .

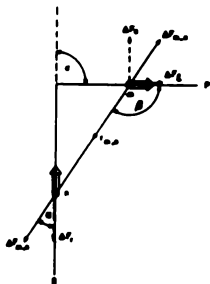


Fig.38 Ampere recoil force between a current element in the projectile branch and another element in the rails.

In an arc-driven railgun the element m of fig.38 would be a plasma element. It is still uncertain whether current elements of arc plasmas behave exactly like metallic ele-

ments. In a later section an experiment will be described in which metallic current elements interact with the elements of an underwater electric arc. In this particular experiment, at any rate, it did appear as if the plasma element obeyed Ampere's force law. It is far too early to consider this an empirically established fact. In the railgun the recoil forces should be felt by metallic elements in the rails. For this reason, and also because no other credible recoil mechanism has been discovered, it is very likely that the Ampere electrodynamics governs the railgun performance.

AMPERE'S HAIRPIN EXPERIMENT

Were it not for the longitudinal forces, the Ampere-Neumann electrodynamics would largely be history. It would add nothing to the development of modern physics and technology that could not be provided by relativistic electromagnetism. Experiments purporting to show the existence of longitudinal Ampere forces have been known for 160 years and fuelled a certain amount of controversy. Many a heated argument could have been avoided had it always been recognized that the validity of the early electrodynamics is confined to metallic conductors. The conduction electron travelling through the metallic lattice appears to be subject to a more complex force system than the free electron travelling through vacuum. More than anything else, it was the discovery of cathode rays (electron beams) which led to the demise of Ampere's law. The predicted longitudinal forces would simply disrupt the flow of convection currents in vacuum tubes. Lorentz really had no choice but to find a law which did not involve longitudinal forces. This requirement was fulfilled by Grassmann's law (1.87).

Long before Lorentz made the change in the 1890's, Ampere himself appears to have been under some pressure to provide an explicit demonstration of longitudinal forces. He had taken the view that his empirical law was the generalization of many experimental results, collected mainly by himself, which all implied the existence of longitudinal forces and no explicit demonstration was necessary. However when Ampere visited the Swiss scientist de La Rive in Geneva in 1822, both men performed a famous test which will be called Ampere's hairpin experiment to distinguish it from his many other demonstrations. The experiment was actually designed by de La Rive. Ampere's sketch of the apparatus in Geneva is reproduced in fig.40.

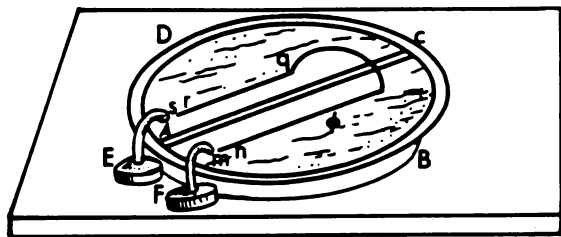


Fig.40 Ampere's sketch of the hairpin experiment

ABCD is a mercury-filled circular dish. The liquid metal is divided in two pools by the insulation barrier AC. Current leads m and s dip into the two mercury pools. A current source has to be connected between the terminals E and F. In Ampere's time this current source would have been a battery of galvanic cells. An insulated copper wire npqr with bare ends r and n, in the shape of a hairpin, floats on the mercury with the two parallel legs np and qr straddling the insulation barrier. The copper wire bridge pq passes over the insulation barrier. When the terminals E and F are connected to the galvanic cells, current will flow from m across a short distance of mercury to n, then mainly along the copper wire from n to p over the bridge to q and back

to r. The current is then returned through another short distance in mercury to the terminal sE.

Ampere and de La Rive observed that a current through the hairpin would make it float away from the terminals toward C. They considered this to be the proof that longitudinal reaction forces existed between the short mercury currents from m to n and from r to s, on the one hand, and copper currents in np and qr, on the other. Ampere no doubt realized that, according to his own law, a small transverse repulsion force should have been exerted by the battery circuit on the hairpin bridge. But this had to be very small compared with the longitudinal repulsion forces. The hairpin legs were made much longer than the bridge to make sure that the transverse Ampere force on the hairpin bridge was negligible. Grassmann proposed his law 23 years later. In 1822 the Geneva experiment was considered to be an unqualified success demonstrating the existence of longitudinal Ampere forces.

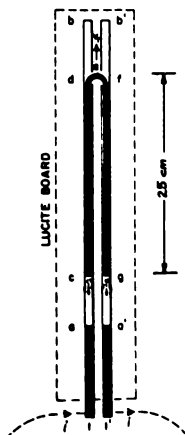


Fig.41 MIT version of Ampere's hairpin experiment

Figure 41 shows a diagram of the circuit with which the author [54] in 1981 performed the hairpin experiment at MIT. The hairpin cdefg is an insulated copper conductor with bare endfaces at c and g floating on two liquid mercury channels ab and a'b'. When more than 200 A of current was passed through this circuit the hairpin moved to the end of the channels b and b'. According to Ampere's law most of the motive force in this experiment is being provided by the repulsion of hairpin leg cd by ct and, equally, the repulsion of gf by gt'.

A new observation was made at MIT which was not reported by Ampere and de La Rive, nor by anyone else who repeated their experiment. When the forward motion of the hairpin was blocked by placing an obstacle in the way of the hairpin bend, strong jets of liquid mercury could be seen to emanate from the hairpin ends c and g. The turbulence in the liquid gave the distinct impression of the hairpin being subject to jet-propulsion. The area of strongest turbulence was quite narrowly defined to the hairpin ends. It did not extend outward to the region where the current streamline pattern in the mercury must have shown the greatest divergence. The jet effect becomes unmistakable at 500 A and so strong at 1000 A that there is danger of liquid mercury splashing out of the troughs. In 1822 Ampere and de La Rive had no way of measuring current and the current was probably too small to show the jets.

It was further noticed at MIT that some turbulence occurred in the liquid mercury at its interfaces with the one-half inch square copper bars at a and a'. This observation became the subject of an independent investigation to be described later. The overall turbulence in the liquid mercury sections ac and a'g could be increased, at constant current, by moving the hairpin closer to the copper bars.

At times the question has been asked: could the hairpin propulsion be due to local heating at the solid¹liquid metal

interfaces? When dry solid conductor surfaces are brought together the electric current is known to flow through a few contact points. The high resistance of the narrow contact necks causes sufficient Joule heating for the contact points to melt and spot-weld together. No evidence has been provided showing the contact point mechanism to be active at a liquid-solid conductor interface. Without it the heat generated at the interface is quite small and incapable of producing relative motion. Any chance of contact point formation was eliminated in an experiment carried out by Tait [55]. He used a 'liquid mercury hairpin' contained in a glass tube and held there by capillary action. It was found to be propelled just the same as a copper hairpin with bimetallic interfaces. Tait's experiment leaves no room for a heat propulsion theory.

Ampere's critics of recent times have held that the motive force on the hairpin is the Lorentz force on the bend *e* of fig.41 passing over the dielectric barrier between the two mercury troughs. The argument of Hillas [56] is typical in this respect. This transverse force is also given by the Ampere formula (1.24), but it is cancelled by longitudinal reaction forces in the hairpin legs and therefore unable to accelerate the hairpin with respect to the mercury on which it floats. The magnetic field at the bend is primarily due to the current in the hairpin legs. One might expect that the reaction force to the Lorentz driving force should reside in the source of this magnetic field. This is not the case, however, because the Lorentz force on the legs is everywhere perpendicular to the direction of relative motion. Instead, the special theory of relativity requires the reaction force to reside in the field and change the momentum of electromagnetic mass, as explained in conjunction with Pappas' electrodynamic impulse pendulum experiment. It will now be recognized that the Pappas experiment is yet another form of Ampere's hairpin experiment. It clearly proves that the relativistic reaction force mechanism does

not exist. This leaves us with the choice of accepting reactionless Lorentz self-forces, which openly violate Newton's third law, or accepting the Ampere electrodynamics. If self-forces could really exist, they would be extremely attractive for space propulsion as they could accelerate matter without burning rocket fuel. The majority of scientists and engineers appear to have no confidence in this prediction of electromagnetic field theory.

This is how Hillas [56] dismisses the jet-propulsion observed in the MIT experiment:

"In the other observation cited, where mercury flowed away from the end of a stationary wire, the current would fan out into the mercury and so exert a force near the point of divergence, directed away from the wire."

In other words, Hillas maintains the motion of the liquid mercury is due to Lorentz forces on the diverging current in the mercury without any reaction in the copper hairpin. This conjures up a second set of self-forces. Besides, the observed flow pattern in the mercury jets is inconsistent with the Hillas explanation.

NEUMANN'S DEMONSTRATION OF LONGITUDINAL FORCES

The existence of longitudinal forces was fully accepted during most of the nineteenth century. Neumann had a classroom experiment with which he demonstrated them routinely to his students. Figure 42 is a diagram of his demonstration as recorded by one of his pupils [57].

A, B, and C are mercury troughs and D and E are copper wire bridges from A to B and from B to C. When current is

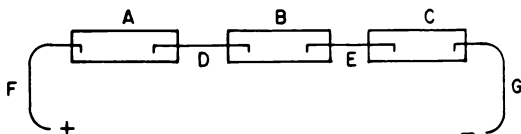


Fig.42 Neumann's longitudinal force demonstration

passed along the troughs the two pieces of wire move away from each other. They must therefore be subject to repulsion. This experiment has at times be criticized because of the small hooks at the ends of the wires which dip into the liquid metal. Transverse forces on these short vertical sections could contribute to, or cause, the longitudinal wire repulsion. To clarify this issue the author analyzed the conductor run ABCDEFGHKL of fig.43 with both the Ampere and Lorentz force formulas. The broken lines AB, EF, and KL of this diagram represent liquid mercury connections while the solid lines are the two wire bridges of Neumann's experiment. For the purpose of the finite element analysis the horizontal portions of the wire bridges were divided into 200 current elements and the vertical dips into four elements. The analysis did not cover the return circuit because this is known to have little influence on the experiment for the fact that both formulas are inverse square laws.

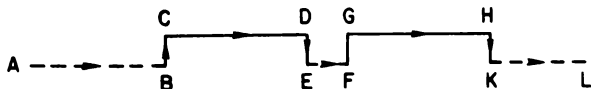


Fig.43 Liquid conductor portions with solid wire bridges.
 Liquid portions: AB - KL - 200 elements. Solid
 portions : BC - DE - FG - HK - 4 elements.
 CD - GH - 200 elements.

Table 3 lists the results of these calculations. Both formulas are seen to predict a horizontal repulsion force

Table 3 Finite element computations for fig.43

GRASSMANN FORMULA

Horizontal force (in dyn for 1 ab.-amp.) on:

	FG	GH	HK	FGHK
Due to AB	$+53.30 \times 10^{-6}$	0	-10.285×10^{-6}	
BC	-255.98×10^{-6}	0	$+79.011 \times 10^{-6}$	
CD	-1531.1×10^{-6}	0	$+44.241 \times 10^{-6}$	
DE	$+6390.4 \times 10^{-6}$	0	-255.98×10^{-6}	
EF	+2.9477	0	-35.991×10^{-6}	
FG	0	0	+b	
GH	-a	0	+a	
HK	-b	0	0	
KL	$+74.986 \times 10^{-6}$	0	-2.9493	
Total				2.95×10^{-3}

AMPERE FORMULA

Due to AB	$+132.71 \times 10^{-6}$	$+219.68 \times 10^{-3}$	-30.855×10^{-6}
BC	-511.87×10^{-6}	$+132.71 \times 10^{-6}$	$+158.02 \times 10^{-6}$
CD	-4.589×10^{-3}	+1.0055	$+132.71 \times 10^{-6}$
DE	$+12.762 \times 10^{-3}$	-4.589×10^{-3}	-511.87×10^{-6}
EF	+3.9795	+1.8594	-107.96×10^{-6}
FG	0	0	0
GH	0	0	0
HK	0	0	0
KL	$+224.93 \times 10^{-6}$	-2.7713	-3.9840
Total			+0.3112

on the bridge FGHK. The Ampere repulsion is more than one hundred times as large as the Lorentz repulsion. Furthermore, the absolute value of the Lorentz force for currents up to 500 A is so small that it would hardly be capable of overcoming the strong adhesion of copper to liquid mercury. In the description [57] of Neumann's experiment no information has been provided of the wire diameter or the current magnitude. It is unlikely that Neumann could have passed more than 500 A around the circuit. For this upper bound the horizontal Lorentz force on FGHK would only be 7.38 dyn. The Ampere formula, on the other hand, predicts as much as 778 dyn. From this evidence alone one would have to conclude that Neumann's experiment favors Ampere's law over the Lorentz force law.

To eliminate the vertical hooks on the wire bridges the author devised a modified version of Neumann's test for longitudinal forces. The apparatus consisted of a straight-through liquid mercury trough of 30.5 cm length and 1.27 by 1.27 cm² square cross-section. The liquid conductor was continued in both directions at the same cross-section with 30.5 cm long copper bars. The circuit was closed by a remote return conductor through a 500 A dc current supply. Two insulated copper rods AB and CD, as shown in fig.44, of 5 cm length and 0.3 cm diameter with bare endfaces were laid end-to-end on the mercury surface in the middle of the trough.

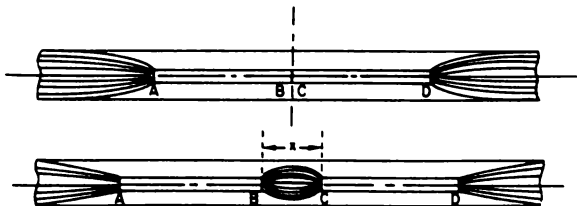


Fig.44 Rod positions before and after passage of current

When a current of 450 A was made to flow along the trough, the rods would submerge and separate axially. As soon as the current was switched off, ten to twenty seconds later, the rods would surface being separated by the distance x shown in fig.44. Because of the 50:1 resistivity ratio of liquid mercury to solid copper, the rods carried a substantial fraction of the total current in their section of the trough. As they carry current in the same direction, the copper and the mercury attract each other under the action of transverse electrodynamic forces. These are the same forces that cause the pinch effect. They urge the copper rod toward the center of the mercury cross-section and thereby cause it to submerge. The distance of separation of the rods was of the order of 2.5 cm. We now consider the longitudinal forces that could have caused the rod separation.

Since the copper rods were coated with magnet wire insulation, but for the endfaces, the current in them must have been directed axially and all Lorentz forces acting directly on the copper rods would have been normal to the direction of relative motion. With no liquid metal at the B-C interface of the two touching rods, the pinch thrust at faces A and D should have pushed the rods together. In the more likely event of liquid metal filling a short gap between B and C, the pinch thrust on these faces should have been equal and opposite to that at A and D. Either way, pinch forces in the mercury could not explain the separation of the rods. The Lorentz forces on the diverging current streamlines in the mercury (see fig.44) could conceivably cause mercury circulation near A and D. No such circulation could take place in the very short B-C gap because there the streamlines are not diverging. Hence the initial separation of the rods, if at all attributable to magnetohydrodynamic actions, would have had to be caused by the circulations at A and D 'pulling' the rods apart. This appears to be a far-fetched explanation.

Over the years there have been suggestions that heat generated at the solid-liquid contact faces could set up propulsion forces. This was investigated by Tait [55] in connection with the hairpin experiment. He obtained a negative result. Even if a thermal propulsion mechanism did exist, it should result in symmetrically disposed opposing forces on all rod ends and therefore be unable to produce relative motion between the rods. Furthermore, if for some unknown reason the thermal propulsion forces were not equal and opposite, the motion of the rods should not stop until they strike the ends of the trough. There appears to exist no plausible explanation why the intensity of the thermal action should relent as the rods separate.

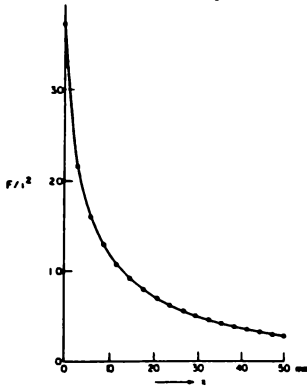


Fig.45 Specific rod separation force as a function of x

Figure 45 is a plot of the specific Ampere repulsion force (F/l^2) acting between the rods as a function of the distance of separation x shown in fig.44. The points on this graph were calculated with finite current element analysis in which the rods were replaced by single filaments of elements, the element length being equal to the rod diameter. According to this graph the rods should strongly repel each other while they are in contact, and the repulsion force should fall off quite sharply with the distance of

separation. For 450 A - 45 ab.-amp., the maximum repulsion comes to 7.5 gram-weight. This decreases to one gram at $x=2.5$ cm which could well be the adhesion drag resisting motion of the rods through the liquid mercury. Hence the Ampere force law provides a natural explanation of the observed phenomenon.

ONE OF HERING'S LONGITUDINAL FORCE EXPERIMENTS

At the turn of the century Carl Hering [58, 59] of Philadelphia designed, built and operated furnaces in which liquid metal was heated by the passage of large currents through molten pools. Electricity was only then becoming abundant and what Hering observed could not have been seen by the 'electricians' of the nineteenth century who forged the Ampere-Neumann electrodynamics and laid the foundations of modern electromagnetic field theory. In the course of his work on liquid metal furnaces Hering discovered the electromagnetic pinch effect which plays an important role in plasma fusion experiments. He also observed what he called 'stretch effects' which were in fact the result of longitudinal Ampere forces. In his widely quoted paper [58] of 1923 he writes as follows about the technological applications of these effects:

"By passing currents, especially at high current densities, through such very mobile conductors as mercury or molten metals in some types of electric furnaces, the writer many years ago noticed the existence of some heretofore unrecognized electromagnetic forces which tended to move the conductors, and being mobile liquids they responded much more readily to such forces than solid conductors do. Some of these new forces were very formidable, for like most of such forces, they presumably increase

with the square of the current. The writer then made use of them in electric furnaces (to pump liquid metal), many of which are in daily use, these new forces being the absolutely essential factor, showing their industrial importance.

Arcs also respond readily to some of these forces."

If the last sentence turns out to be true it will have stunning consequences in the development of fusion power, one of the greatest technological challenges of our time. Several investigators [46, 60, 61] have already claimed the painfully slow progress made to generate at least as much controlled fusion energy as is being expended in producing the plasma (break-even point) may well be due to longitudinal forces disrupting the current-carrying plasma. Here is Aspden's statement:

"What is the most urgent and most important technological problem of our time? Fusion power. Our attempts to emulate the energy generation processes of the sun by triggering fusion in heavy isotopes of hydrogen. Early efforts concentrated on techniques of magnetic confinement by which energy was concentrated to a critical level required for the nuclear reaction. All these efforts have been thwarted by instabilities of the electrical arc discharge which should self-pinch to concentrate the energy and impart this energy to the ions of the fusion process. This whole process is concerned with the transfer of energy from electrons to ions. Interactions between charged particles of different charge/mass ratio are vital to this fusion process. Yet, if we have inadequate understanding of the electrodynamic laws, as suggested in this work, is it surprising that progress has been retarded?"

Returning to liquid metals, in his quotation Hering referred to the invention of the first electromagnetic liquid metal pump. As the metal was driven by longitudinal forces, the Hering pump did not require external magnet coils. Now that longitudinal forces have been forgotten, it is generally believed that only transverse forces can pump liquid metal. Therefore the present generation of electromagnetic liquid metal pumps all rely on external magnets.

In discussing his experiments, Hering made no clear distinction between the Ampere-Neumann electrodynamics and modern field theory. This led to much confusion and, tragically, detracted from what might otherwise have become a revival of the old electrodynamics in the 1920's.

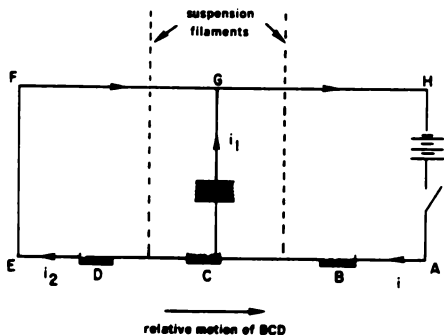


Fig.46 One of Hering's many longitudinal force experiments

The most decisive of Hering's many longitudinal force experiments is illustrated in fig.46. There ABCDEFGH is a rectangular circuit standing in a vertical plane and having a power supply connected in the AH branch. The current i leaving the supply is split at C, with i_1 passing along the vertical branch CG and i_2 completing the journey around

portion BCD contributes a longitudinal force component acting from D toward B. These are the dominant Ampere forces which fully explain the result of Hering's experiment.

Additional longitudinal repulsion forces arise across the two mercury cups B and D. They do not cancel each other because i is greater than i_2 . The net force from these two sources actually opposes the relative motion once the ends of BD have passed the midpoint in the mercury cups B and D. A further set of disturbing forces in cups B and D are the pinch forces which exert opposing thrusts on the ends of the movable conductor. Since $i > i_2$, the net longitudinal force due to pinch is opposing the relative motion and could not be the cause of it.

Finally we must examine the effect of the transverse forces on the short vertical hooks dipping into the liquid mercury at B and D. Because of the inequality of the currents at the two ends of the movable conductor, the combined transverse forces on the hooks should have a resultant in the direction of the observed motion. This type of positive disturbing force has already been investigated in connection with Neumann's longitudinal force experiment and in particular with the help of fig.43. It was then found that the longitudinal Ampere force was more than one hundred times as large as the disturbing Lorentz force. Furthermore, for currents up to 500 A the absolute value of the net force on the hooks was so small that it could not have overcome the strong adhesion of copper to liquid mercury.

The Hering experiment, therefore, furnishes further evidence for the existence of longitudinal Ampere forces. As a matter of interest it may be pointed out that the sum of the transverse components of $\Delta F_{m,o}$ and $\Delta F_{m,n}$ on the element dm is equal to the longitudinal force exerted on elements do and dn . This illustrates how the Ampere forces comply with Newton's third law. On the other hand, the Lorentz force on element dm would have to have its reaction in the field.

CLEVELAND'S EXPERIMENT

It took a surprisingly long time, more than fifty years, before Grassmann's force law (1.85) was seriously criticized for its open violation of Newton's third law which requires that the action of one material particle, or body, on another calls forth an equal and opposite reaction in the other. Not until the end of the nineteenth century, when the energy conservation principle was clearly seen to cross all frontiers between scientific disciplines, was it fully appreciated that the equality of action and reaction is as necessary for electromagnetism as it was for mechanics to substantiate the impossibility of perpetual motion. Yet criticism of Grassmann's law, to this day, is being brushed aside with the argument that isolated current elements of wire do not exist and somehow nature is making sure that the net force on a complete and isolated current circuit is precisely zero.

This line of defense of Grassmann's law really broke down when Lorentz equated the moving electron to a current element because we can easily visualize two electrons, or ions, to move in a vacuum space without being inseparable parts of a closed circuit. The most frequently cited example intended to dramatize the conflict with Newton's third law is sketched in fig.48. Electron e_B moves toward electron e_A while the latter crosses the path of the former. At the instant to which the diagram applies, electron e_B experiences the transverse Lorentz force F_L due to the motion (and magnetic field) of e_A , but the electron e_A senses no reaction force at all. This defies energy conservation because the electron at A can accelerate the electron at B without having to do any work. No one appears to have invented a perpetual motion engine which exploits this curious state of affairs, but it caused quite a few investigators to look more closely at the reaction forces between metallic circuit components.

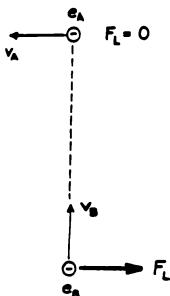


Fig.48 Lorentz forces on two moving electrons

In this category Cleveland's [62] paper published in 1936 seems to have attracted more attention than any other. The abstract of the paper reads :

"The standard force equation (Lorentz's), and Ampere's force equation for the magnetic force between current elements, are applied to determine the forces in a rectangular circuit, one side of which is mechanically separable from the other three. In order to explain the observed forces by the use of the standard equation, it is necessary to make the doubtful assumption that part of the rectangular circuit can lift itself. Ampere's equation gives a reasonably correct value of the forces without the necessity of making this assumption."

The rectangular circuit to which Cleveland referred is shown in fig.49. He mechanically separated side AB from A'DCB' by two mercury cups indicated on the diagram by the liquid links LL. For the measurement of the lift force F_1 on A'DCB' and F_2 on BA, Cleveland suspended, in turn, A'DCB' and BA from a beam balance, making some adjustment to the mercury cup mounting, and weighed F_1 and F_2 for certain

values of the steady current i . Not shown on fig.49 are a pair of closely spaced leads which bring current to the portion of the circuit which is fixed to the laboratory bench.

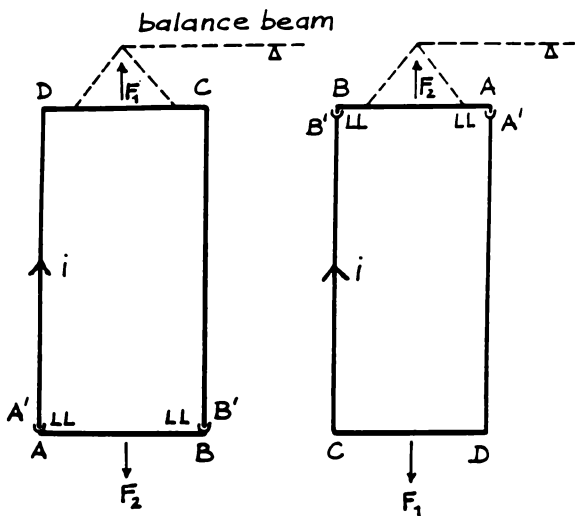


Fig.49 Cleveland's method of weighing lift forces on separable parts of a rectangular circuit

As the currents used in this investigation were quite small, ranging from 15 to 25 A, the measured forces came out to only a fraction of one gram-weight. This made the experiment sensitive to small disturbances, as for example the change in buoyancy in the mercury cups as a result of Joule heating. Despite these problems Cleveland found that $F_1 + F_2 = 0$. No other result would have proved acceptable because, were the two forces unequal and not of opposite sign, the circuit as a whole would have been subject to a finite net force. It could then have been mounted eccentrically

on a horizontal turntable to produce perpetual motion with a persistent supercurrent.

The importance of Cleveland's investigation did not reside in his measurements, but in the clarity with which he explained the self-interaction force dilemma of field theory. Consider first the Lorentz F_1 in the conductor portion DC. The magnetic field in DC is primarily the field of the current i approaching corner D and leaving corner C. Now the Lorentz forces on A'D and B'C are transverse to these sides and therefore perpendicular to F_1 . For this reason Cleveland called F_1 a self-lift. Side AB will make a small contribution to the field in DC, but this can be reduced to a negligible amount by increasing the length of A'D and B'C. Very similar arguments apply to the second case of fig.49 where the side BA is suspended from the beam balance to measure F_2 . This latter force is also a self-force and the equality of F_1 and F_2 appears to be a coincidence, and not the consequence of a mathematical structure which will prevent violations of Newton's third law under all circumstances.

Having outlined the logistic difficulties with Lorentz reaction forces, Cleveland proceeded to calculate F_1 and F_2 with Ampere's formula (1.24). He obtained results which were in fair agreement with his measurements. As they had been derived without "the doubtful assumption that part of a macroscopic circuit can lift itself", he concluded that the possibility of Ampere's equation "being the correct expression for the force between current elements seems worthy of serious consideration".

Cleveland run up against the same integration singularities everyone had met when trying to calculate the reaction forces between parts of the same circuit. To obtain finite results, he adopted the customary procedure of eliminating the corners of the circuit from the integration. This made his calculated forces approximate. Then he makes the curious

statement concerning adjacent corner elements ".... for physical reasons it is known that the elements concerned are not infinitely close together". It seems Cleveland argued a (metallic) current element is of finite size and then the distance between the center points of two adjacent elements can never be zero. This would be true if the metal atom turns out to be the basic current element.

Cleveland either did not know anything about the vacuum reaction forces required by the theory of special relativity or he considered them to be invalid. In view of the Pappas pendulum experiment the answer to this question is mute. He might well have taken the view that Newton's third law applies only to matter interactions and any theory admitting forces on vacuum elements must lead to a non-newtonian mechanics. That is the case with the theory of special relativity.

Cleveland did not make the point that the computed reaction forces obtained with Grassmann's and Ampere's formula lie quite close together, maybe differing by no more than ten percent. Computer-aided finite current element analysis, which was not available to Cleveland in 1936, reveals the same state of affairs. The possibility still exists that any difference is merely a computational error. It is important to know this to understand why the two formulas have survived for so long. Even if the difference was real, it may be difficult to resolve it by experiment.

Although Grassmann's and Ampere's formulas predict almost the same reaction forces between two parts of a rectangular circuit, they decidedly disagree on how these 'reactions' distribute themselves along the wire. In the MIT version of the Pappas pendulum experiment it was finally shown that only Ampere's law predicts correctly where in the conductor portions the reaction forces attach themselves to the metallic lattice.

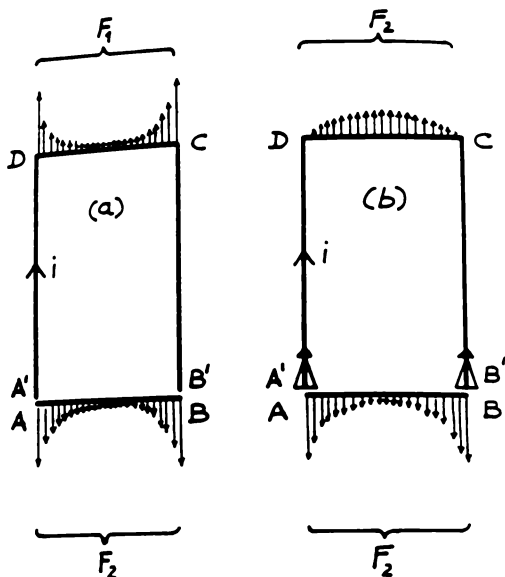


Fig.50 Vertical reaction force distribution in Cleveland's rectangle according to (a) Grassmann's formula and (b) Ampere's formula

Figure 50 has been drawn to show the difference in the two vertical reaction force distributions on an exaggerated scale. According to Grassmann's law all the contributions to F_1 reside in DC and all the contributions to F_2 reside in AB. The Ampere distribution of the F_2 -force differs little from Grassmann's. However there exists a large difference in the F_1 -distributions. The principal upward directed forces in fig.50(b) reside in the vertical legs A'D and B'C, and most of this force must be visualized as being attached

Any contribution to the semicircle tension by the interaction of its elements with the remainder of the circuit will be ignored. This is likely to underestimate the Ampere tension, but the error over the middle portion of the wire will be quite small. The semicircle AXB of fig.51 is divided into z equal elements of arc, each subtending an angle of

$$\Delta\theta = \pi/z \quad (2.36)$$

The elements along XA are labelled 1, 2, ..., m , ..., x ; and those along XB are labelled 1, 2, ..., n , ..., $(z-x)$. The distance between the two general elements m and n is denoted by $r_{m,n}$ and the arc mXn subtends the angle $\theta_{m,n}$. The angles of the Ampere force law (1.24) obey the relationships

$$\alpha = \beta \quad (2.37)$$

$$\epsilon = \theta_{m,n} = 2\alpha = 2\beta \quad (2.38)$$

If R is the radius of the semicircle, then

$$dm = dn = (\pi/z)R \quad (2.39)$$

and

$$r_{m,n}^2 = 2R^2(1 - \cos \theta_{m,n}) \quad (2.40)$$

It can easily be shown that for any element combination on the semicircle the angle function of (1.24) is negative and therefore all the Ampere interactions to be considered are repulsions. With equations (2.36) to (2.40) Ampere's force law may be written

$$\Delta F_{m,n}/l^2 = (\pi/z)^2 [2\cos \epsilon - 3\cos^3(\epsilon/2)] / (2 - 2\cos \epsilon) \quad (2.41)$$

where $\epsilon = (\pi/z)(m+n-1)$.

The tangential component of this repulsion produces tension in a wire which is assumed to behave like an ideal string with no bending strength. The transverse components of (2.41) tend to retain the shape of the semicircle and possibly accelerate the wire away from the center O. Noting that $\cos \alpha = \cos(\epsilon/2)$, the elemental tension contribution may therefore be written

$$\Delta T_{m,n}/i^2 = (\Delta F_{m,n}/i^2) \cos(\epsilon/2) \quad (2.42)$$

Therefore the wire tension across the perpendicular plane containing OX is given by

$$T_x/i^2 = \sum_{m=1}^x \sum_{n=1}^{z-x} (\Delta F_{m,n}/i^2) \cos(\epsilon/2) \quad (2.43)$$

For a semicircle containing 660 elements, computer evaluation of (2.43) gave the results plotted in fig.52.

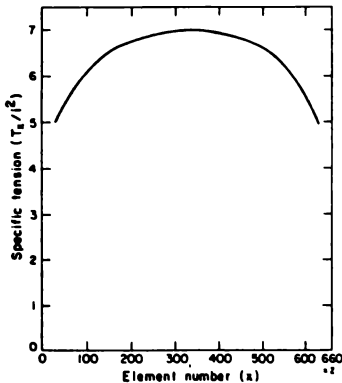


Fig.52 Computed specific Ampere tension in semicircle

The graph shows that the internally generated tension is relatively constant from end to end of the semicircle.

Comparing it with fig.26 we see that the tension in the semicircle is expected to be of a similar magnitude as in the straight wire. Hence a current pulse which fractures a straight wire should also break it after it has been bent in a semicircle. This gave rise to the experiment depicted in fig.53.

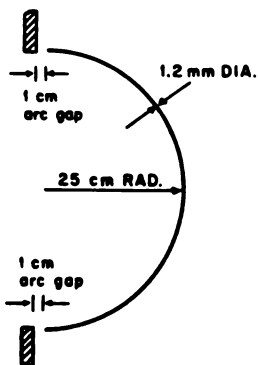


Fig.53 Fragmentation of a wire semicircle

An 8- μ F high-voltage capacitor bank was discharged through a 1000- μ H inductor to produce exponentially decaying oscillatory current pulses up to 10 kA amplitude and ringing down at 2000 Hz over a period of 5 to 10 ms. The discharge currents were passed through a 1.2 mm diameter, 99 percent pure aluminum wire bent into the shape of a semicircle. As shown in fig.53, the wire semicircle of 25 cm radius was suspended in a vertical plane, leaving one centimeter long arc gaps to connect it to the terminals of the discharge circuit. The purpose of the arc gaps was twofold. First they allowed distortion-free thermal expansion. Secondly, assuming that an electric arc in air has no tensile strength, they virtually eliminated the hoop tension which would otherwise have been set up by the transverse Lorentz forces.

The following procedure was adopted. The capacitor bank was charged to 50 kV and then discharged through the inductor and the wire by closing a mechanical switch. This would heat the wire but did not break it. Oscillograms of the discharge current were recorded. They revealed the maximum current amplitude and showed the exponential damping. After the wire had cooled back to room temperature, the experiment was repeated with 52 kV, and subsequently at 2 kV increments. At 62 kV and a peak current of approximately 6000 A the wire would fracture into two or three pieces. A certain amount of melting could always be found on the arc gap ends but none could be seen at the fracture faces.

After the first breaks a new semicircular wire was mounted in place and the discharge experiment was repeated with a further 2 kV voltage increment. This produced a greater number of wire fragments. In this way the fragmentation process could be intensified until, at 68 kV and a peak current of 6600 A, the wire broke into 30 to 50 pieces. A further increase in discharge current would produce visible melting in various places along the wire, thereby destroying the tensile fracture evidence.

The appearance of the wire fragments was similar to those shown in fig.31. The fracture faces were examined with optical and electron scanning microscopes. There was little doubt that tensile fracture had taken place in the solid state.

Alternative tensile fracture causes, other than longitudinal Ampere forces, have been discussed in conjunction with Nasilowski's discovery of wire fragmentation (page 105). An additional consideration, arising from the semicircular shape of the wire, is bending stress created by transverse forces. For bending to assume significant proportions the wire has to deform. This is largely prevented by inertial confinement for the brief period in which the electromagnetic

forces are active. But even if large bending deformations did occur, it would still seem unlikely that the highly ductile, 99 percent pure aluminum wire could be shattered in many pieces. Therefore, on the basis of the present state of knowledge, it seems more than likely that the fragmentation of semicircular wires--and indeed wires bent into any shape--is the result of longitudinal electrodynamic forces. This means Ampere tension must be expected to be present in all electromagnets employing conductors of normal metals. So far no experiments have been carried out to check how superconductors behave.

Ampere tension would play a minor role in solenoids made of many turns because the hoop tension generated by transverse forces on an individual turn, but induced by currents in adjacent turns, would swamp the Ampere tension in the individual turn. In this context a magnet with a winding cross-section dimension comparable with the perimeter of a single turn would be termed a solenoid. The situation is very different in a dipole magnet in which the major dimension of the winding cross-section is very much smaller than the turn perimeter. To obtain an idea of the significance of Ampere tension in dipole magnets let us analyze a specific example.

Consider a thin circular dipole coil of square winding cross-section in which the center turn is 400 times as long as one side of the winding section. This coil may be modelled as a single filament of 400 finite volume elements. For this filament the Lorentz force formula gives a transverse force of $0.096 \text{ i}^2 \text{ dyn}$ on each element of arc, with the current expressed in absolute ampere-turns. The uniform transverse force distribution results in a hoop tension of $6.065 \text{ i}^2 \text{ dyn}$. All this tension may be transferred to a tightly fitting containment ring structure.

If the same calculation is being carried out with the Ampere formula, the transverse force per current element

comes to $0.112 i^2$ dyn which results in a hoop tension of $7.076 i^2$ dyn. Ampere tension calculations on a semicircle of 200 elements furnished a value of $4.504 i^2$ dyn. This has to be added to the hoop tension. Therefore the winding itself, or a totally constraining ring structure, would, according to Ampere's law, be subject to a tension of $11.58 i^2$ dyn. This is nearly twice as much tension as predicted by the Lorentz force theory. Regardless of which formula is chosen, the magnet forces are proportional to the square of the current, or the ampere-turns, and independent of the size of the magnet. The factor by which i^2 has to be multiplied is merely a dimensionless shape constant.

To illustrate how magnet forces increase as a result of the greater number of ampere-turns in larger magnets, we consider three different coil diameters of d of 1, 5, and 10 m. Let the winding cross-section be x times x cm², with $x=100\pi d/400$ cm for a single filament approximation of 400 elements. Large superconducting dipole magnets of 10 m and greater diameter have been studied for magnetic energy storage. Let us further assume that it is possible with superconductors or cryogenically cooled normal conductors to sustain a current density of 20,000 ampere-turns/cm² over the winding cross-section. The maximum tension T predicted by Ampere's law, which a ring structure may have to sustain under these conditions, is listed in table 4.

Table 4 Sum of Ampere and hoop tension in dipole magnet

$d(\text{cm})$	$x(\text{cm})$	$i(\text{amp-turns})$	$T(\text{kg-weight})$
100	0.785	12,325	18
500	3.927	308,427	11,229
1000	7.854	1,233,700	179,663

The results indicate a 10,000-fold increase in tensile force in going from a 1 m to a 10 m diameter dipole magnet. Quite a large error in the force calculation would be of little

practical consequence to the smallest of the three magnets. However to the largest of them the discrepancy between the Lorentz and Ampere predictions of the containment tension amounts to 85 ton-weight.

Before the question of longitudinal magnet forces [63] arose, apparently only one attempt was made to measure the electrodynamically produced tension in a wire circle. This was an experiment by Roper [64] carried out in 1927. He mounted a wire circle of 40.2 cm centerline diameter in a vertical plane. Copper wire of 0.294 cm diameter was used as the conductor. Subdividing the circle horizontally into two semicircles, Roper bridged one of the gaps by the incoming flexible current leads. The other gap he closed with a thin film of liquid mercury. The upper semicircle was fixed to the laboratory frame, while the lower semicircle was hinged with an elastic band around the flexible current leads and hung from a balance beam at the mercury film end. When passing current around the circle, the lower half would be urged downward, deflecting the balance beam. Weights were added to a pan at the other end of the balance to restore equilibrium.

The force F measured in Roper's experiment is approximately half the reaction force between the two semicircles. Using eleven different currents up to 18 ab-amp, the average value of the shape constant by which i^2 (ab-amp)² has to be multiplied to give F came to 5.62. This indicates a total reaction force between the two semicircles of

$$2 F = 11.24 i^2 \text{ dyn}$$

Single-filament finite element calculations provided a value of 14.2 i^2 dyn. Considering that the single-filament approximation usually overestimates forces by 10-20 percent and noting, also, Roper's remark about an uncertainty in the rubber band fulcrum which might have made his measured force 11.94 i^2 dyn, the agreement between Ampere's force law and

experiment is fair.

An important point to recognize is that a reaction force measurement, like Roper's, does not reveal the combined hoop and Ampere tension which a fully constraining magnet structure would experience. His results include most of the Ampere tension but add to it only a fraction of the hoop tension. For example, the interaction between two elements on the same semicircle contributes to the hoop tension in that semicircle but not to the reaction force between the two semicircles. In a fully constraining magnet structure the total tension would be the algebraic sum of hoop and Ampere tension. The two components are of the same order of magnitude. Hence if Ampere tension is ignored, magnets may actually operate at twice the tensile stress for which they were designed.

Rectangular dipole magnets will also be subject to the superposition of two tension components. They are more easily separated than in a circular dipole magnet. Consider the rectangular magnet coil shown in fig.54. Let the force on each of the short sides be F . This will create hoop tension of $F/2$ in each of the long sides. Now if the coil is supported by two end plates, as shown in fig. 54, which are held together by two tie rods, all the hoop tension in the long sides of the rectangle can be transferred to the tie-

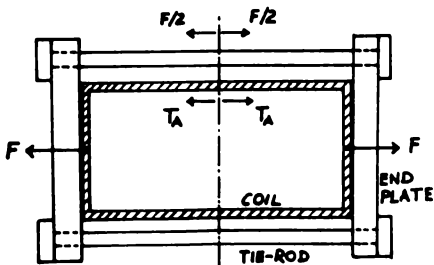


Fig.54 Clamped rectangular dipole magnet

rods. A similar structure may be used for supporting the two long sides and the hoop tension in the short sides could then also be transferred to tie-rods. If only transverse forces were present in the magnet coil, they could in this way be completely taken up by lateral support plates.

The Ampere tension T_A in the long sides of the magnet coil will exist in addition to the hoop tension $F/2$. It will tend to stretch the long sides and if they were welded to the parallel tie-rods, the total tension in these rods would become

$$T = F/2 + T_A \quad (2.44)$$

Finite element computations on rectangular circuits have all indicated the approximation

$$T_A \approx F/2 \quad (2.45)$$

and therefore the Ampere theory predicts approximately twice as much tension in the structure of a totally constrained rectangular dipole magnet than the Lorentz theory.

It will seem surprising that so large a deviation from the Lorentz force law should not have been discovered through force measurements or the operating experience with electromagnets. A few measurements of reaction forces between two parts of a rectangular loop have been published. When interpreted in light of the Ampere electrodynamics, they give only T_A and not the sum of the two terms of equation (2.44). At the time of writing, as far as is known, no measurement technique has been developed that is capable of detecting the sum of the two terms in (2.44). Most electromagnets in use are relatively small and have support structures that are much stronger than they need be for force containment purposes. Only in connection with the largest magnets ever built and particularly in pulse current circuits could Ampere tension have led to mechanical failures.

LIQUID METAL CONDUCTORS

The simple experiment of fig.55 is capable of showing an effect of longitudinal conductor forces in liquid mercury. The conductor dimensions and the current magnitude are not critical for observing the effect. The experiment will work equally well with direct and alternating current.

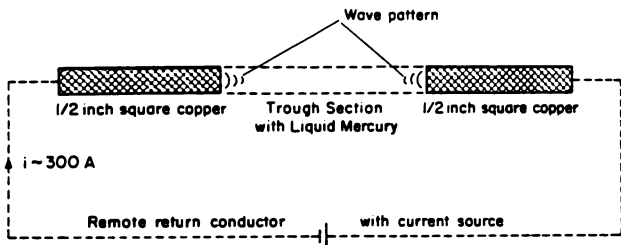


Fig.55 Straight-through liquid mercury channel

The author [43] used 0.5 inch² copper bars set in a rectangular groove in a plastic board, part of the groove forming the liquid mercury trough. The trough was filled with mercury to be level with the top of the horizontal copper bars. In this way the cross-section of the mercury conductor was made the same as that of the copper conductors, except for the meniscus deformation at the top mercury surface caused by the surface tension of the liquid metal. When about 300 A of current were flowing through the copper-mercury-copper conductor, an irregular wave pattern became apparent on the liquid mercury surface close to the interfaces with the copper rods. The waves disappeared almost instantaneously when the current was switched off. The disturbances were strongest right at the solid-liquid interfaces and they died out within a few centimeters of the interfaces.

Transverse forces should have pinched the liquid conductor equally all along its length and not create an irregular

situation at the interfaces. No pinch deformation could be seen anywhere on the mercury surface at the relatively small current of 300 A. This lead to the conclusion that the disturbances responsible for the observable surface wave pattern were caused by longitudinal Ampere forces.

Even after recognizing these facts it remains difficult to see how longitudinal forces can produce relative motion between some liquid metal atoms and others, as demonstrated by the wave pattern. Starting with the assumption that some atoms of the liquid metal are propelled away from the solid interfaces, it follows that others must return to take their places, or the liquid level would continue to fall at the interfaces, which it does not. For some of the atoms to return to the interfaces, not all can experience the same repulsion. In any case we should expect the repulsive (tensile) stress to be strongest at the center of the conductor and weakest along the corners. This will be better understood if the liquid conductor is imagined to be resolved in a number of equal cross-section current filaments. The center filament will have more close-neighbor filaments than any of the corner filaments. The tension, or interface repulsion, in any given filament increases with the number of cooperating close-neighbor filaments. This has been shown in reference [43] and will be proved in a later section of the book. According to the close neighbor argument it is not unreasonable to expect liquid to flow away from the center of the interfaces and return to the periphery of them.

We still have to explain why, in the setup of fig.55, the wave motion and flow is strongest at the interfaces and disappears in the middle section of the liquid mercury trough. It brings us face to face with a new magneto-hydrodynamics resulting from Ampere's force law (1.24). The following qualitative argument barely introduces this new field of science. Each current element (atom?) in the liquid mercury is subject to two sets of forces. One set is generated

by the far-actions of Ampere's force law. The other is due to the hydrodynamic push from neighboring elements caused by contact action taking place throughout the liquid. The vectorial difference between these two sets of forces will set the current element in motion. The motion of the element is then governed by the inertia of the element and the viscous drag on it. Superimposed on this electrodynamic picture are the effects of gravity.

Take the horizontal midplane through the mercury trough and let us consider only those longitudinal Ampere forces on liquid current elements which are due to the solid copper elements. This restricted set of far-action forces is obviously strongest near the interfaces and weakest at the midpoint of the channel. Furthermore, since they act in opposite directions at both ends of the channel, these forces will create hydrostatic pressure (contact action) which is strongest in the middle of the channel and weakest near the ends. If they were the only electrodynamic forces, they would accelerate liquid elements along the trough center-line and away from the interfaces. That motion would stop some distance along the channel because of the opposing pressure gradient. In fact at the outside of the channel the hydrostatic pressure would be greater than the electrodynamic acceleration force, resulting in the return of atoms to the interfaces. How is this picture changed by the interaction of liquid current elements? At first sight it appears the repulsion between liquid current elements will increase the opposing pressure in the center of the trough more than at the interfaces and this should further inhibit the flow of mercury toward the midpoint of the channel and possibly help with the return of liquid to the interfaces. It explains qualitatively why the wave pattern on the surface of the mercury trough of fig.55 dies out toward the center of the trough.

When the current in the mercury was gradually increased, the wave motion would become more violent and extend further

away from the interfaces. A point was reached, in the vicinity of 1000 A, when an arc was struck at one end of the mercury trough or the other, with the arc separating the mercury from the copper bar. This would interrupt the current, allowing the mercury to flow back and close the gap. A little later another arc was struck, and so on. There was no indication of the mercury level being depressed by pinch forces prior to arcing. The arc usually ejected some mercury out of the trough. The only explanation of this phenomena appears to be that longitudinal Ampere forces become so strong that they separate the mercury from the solid copper interface.

The longitudinal separation forces should set up hydrostatic pressure in the middle portion of the trough. This pressure might be expected to increase as the trough section is shortened. In fact it was found that with a very short trough of 0.4 cm length, 1000 A of dc current would suddenly expel all the liquid mercury upward into the air. Prior to this "explosion", the liquid metal was seen to bulge up, as if a bubble was forming underneath, and then collapse again. In order to escape from the trough, the mercury had to pull a vacuum underneath it, and the bulging and retraction appeared to be the result of competing forces due to mercury and atmospheric pressure. Electrodynamic explosions caused by longitudinal Ampere forces have also been observed in conjunction with underwater electric arcs.

ELECTRODYNAMIC EXPLOSIONS IN LIQUIDS

It is generally believed that the shock wave produced by an underwater electric arc is the result of the sudden creation of high pressure steam in the arc column. Transverse electrodynamic forces are either too small to cause the shock or they are containment forces opposing the explosion. Longitudinal Ampere forces, on the other hand, act in directions in which they could promote an explosion [65].

If a short gap between two solid conductor sections is filled with a liquid conductor, the longitudinal repulsion of the liquid current elements by the solid current elements will create hydrostatic pressure in the liquid-filled gap. Provided it is sufficiently large, this pressure, when established by a current pulse, can cause an explosion. To distinguish it from thermodynamic explosions, which rely on the sudden creation of gas, it will be referred to as an electrodynamic explosion. Furthermore, since liquids are normally incompressible, electrodynamic explosions in liquids should be expected to be more rigid, and less forgiving, than thermodynamic explosions.

The existence of longitudinal Ampere forces in solid and liquid metal conductors is by now well established. These forces are certainly not found in convection currents through vacuum. To what extent they play a part in plasma conduction has remained an open question. The experiments described in this section represent the beginning of a search for longitudinal Ampere forces in plasma conductors.

Figure 56 is a diagram of experiments carried out in a saltwater cup. An insulated copper rod, bare at the end-face, projects through the bottom of a dielectric cup filled with a solution of common salt (NaCl) saturated water at room temperature. A bare copper ring electrode is immersed in the upper part of the cup and connected to an energy storage capacitor via an induction coil and switch. The other end of the capacitor is connected to the copper rod. The capacitor C is charged to the voltage V_0 . When the switch S was closed, and depending on the values of C and V_0 , the discharge through the saltwater was either silent and left the water undisturbed or it resulted in a luminous underwater arc in the vicinity of the endface of the copper rod. Visible arcs were always accompanied by a snapping sound and a shock disturbance of the liquid. With the larger discharge currents a column of water was thrown up in the air

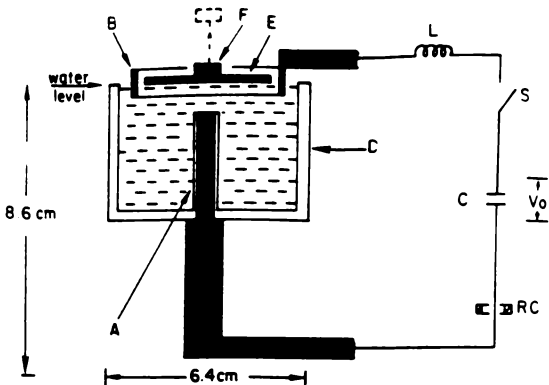


Fig.56 Cross-section of saltwater cup drawn to scale. A: insulated copper rod with bare endface; B: bare copper ring electrode; D: dielectric cup containing saltwater; E: wooden disc float; F: 2.8 g metal weight; L: induction coil; S: switch in air; C: energy storage capacitor; RC: Rogowski coil.

directly above the copper rod. The explosive nature of the arc event could best be demonstrated by placing a wooden float on the water surface with a 2.8 g weight resting on top of it. Then with a silent discharge the float and weight would remain still while an arc would fling the metal weight upward by as much as 20 cm without spilling any water. The float behaved as if the mechanical impulse it was receiving ceased as soon as the arc was extinguished. No followthrough push from expanding steam nor any vapor escape from the cup could be discerned.

The graph of fig.57 shows the combination of C and V_0 values chosen and indicates whether they resulted in arcs or not. The broken line is the approximate boundary of the arcing regime. The number of experimental points is insuffi-

cient to prove that this boundary is actually a straight line. However, the decreasing voltage V_0 with increasing capacitance C along the boundary strongly suggests that arc formation is dependent on the total charge crossing the water. It may be that breakdown and arcing occur only when the number of available sodium and chlorine ions is insufficient to discharge the capacitor.

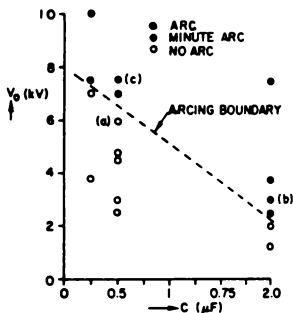
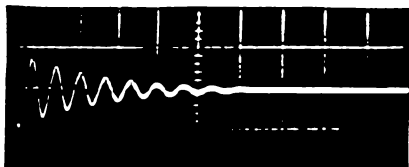


Fig.57 Charging voltages and capacitances chosen for salt-water cup experiment. Points (a) and (b) furnished the data for table 5.

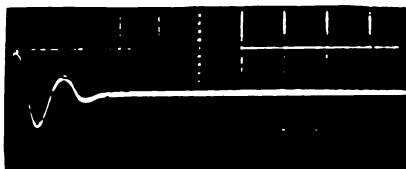
A remarkable feature of the experiment was that combinations of C and V_0 values could be chosen so that, for the same amount of energy stored in the capacitor, the discharge was either silent or produced an arc explosion. Since in those two cases approximately the same amount of energy was being dissipated over roughly the same current path and time, it seemed unlikely that the arc explosion was a thermal event. The energy stored in the capacitor at the arcing boundary of fig.57 shows no particular trend. It is 6.85 J at 0.25 μF , 10.56 J at 0.5 μF , and 4.84 J at 2 μF . Points (a) and (b) on fig.57 were chosen for further analysis in table 5. They are both associated with a stored energy of 9 J, but one resulted in an explosion and the

other did not.

The purpose of the inductance $1.876 \mu\text{H}$ was to prolong the discharge for a more reliable observation of the current pulse decay. The saltwater resistance between the electrodes was small enough to cause an underdamped, oscillatory discharge in both the electrolytic and arc conduction modes, as shown in fig.58.



(a) Electrolytic discharge



(b) Arc discharge

Fig.58 Current oscillograms for points (a) and (b) of fig.57. Scales: $y=75 \text{ A/cm}$; $x=0.2 \text{ ms/cm}$.

Assuming the general form of the discharge current to have been

$$i = I_0 e^{-t/T} \sin(\omega t) \quad 2.46$$

with I_0 being related to the circuit impedance Z by

$$I_0 = V_0/Z \quad 2.47$$

The damping time constant T is given by

$$T = 2L/R_t \quad 2.48$$

where R_t is the total resistance in the discharge circuit. This can be split into a water and an external component as follows

$$R_t = R_w + R_e \quad 2.49$$

By discharging the capacitor first through water and then through a short circuit across the cup, the two respective time constants read off the current oscillograms yielded values for R_t and R_e which, on substitution into equation (2.49), gave the water resistance and therefore a measure of the energy dissipated as heat in the water.

An important quantity in these experiments was the $i^2 dt$ integral, that is

$$\int_0^{\infty} i^2 dt = I_0^2 \{ (T/4) - (1/T) / [(2/T)^2 + (2\omega)^2] \} = I_0^2 T/4 \quad 2.50$$

This integral is proportional to the electrodynamic impulse experienced by any part of the circuit. The integral of (2.50) is known as the action integral. When it is multiplied by R_w it gives the Joule heat dissipated in the water.

Table 5 lists the measured and derived parameters of the experiment to which the oscillograms of fig.58 refer. It will be seen that capacitances and charging voltages were chosen to give the same stored energy of 9.0 J in both cases. Case (b) resulted in an arc explosion and (a) did not. The heat dissipated in the water in either case came to less than one calorie. The measurements, calculations, and visible observations make it unlikely that case (b) involved a thermal explosion while in case (a) there was no hint of it. It is therefore possible and likely that the underwater arc gave rise to electrodynamic forces which were absent in the electrolytic conduction process.

Table 5. Measured and derived quantities for an arc and an arcless discharge.

		(a)	(b)
		NO-ARC	ARC
Capacitance	C	0.5 μF	2.0 μF
Charging voltage	V_0	6.0 kV	3.0 kV
Stored energy	E	9.0 J	9.0 J
Undamped current amplitude	I_0	78.8 A	93.8 A
Discharge time constant	T	0.41 ms	0.28 ms
Total circuit resistance	R_t	4.29 Ω	6.29 Ω
External resistance	R_e	1.61 Ω	0.58 Ω
Water resistance	R_w	2.68 Ω	5.71 Ω
Energy dissipated in water	E_w	1.70 J	3.51 J

Some idea of the magnitude of the forces can be gleaned from the fact that the explosion represented by point (c) on fig.57 hoisted the weight F of fig.56 approximately 1 cm into the air. The potential energy gathered by this weight ($m.g.h$) came to 0.275 mJ. Equating this to the initial kinetic energy ($\frac{1}{2}mv^2$) suggests an initial velocity of the metal weight of $v_0=0.443$ m/s. Since the mechanical impulse $\int F.dt$ received by the weight from the explosion must have been equal to the momentum ($m.v_0$) imparted to the weight, we find that $\int F.dt=1.24$ mN.s. As indicated by approximation (2.50), this impulse may be equated to the product of an average force, proportional to I_0^2 , and one quarter of the decay time constant. The discharge oscillogram of the explosion provided the value of $T=0.23$ ms. With this figure the average force exerted on the metal weight by the explosion comes to 21.6 N. This is a surprisingly large force.

Pinch forces on the current column directly above the copper rod of fig.56 would, according to a formula derived by Northrup [44], exert an endthrust on the copper rod

of $F_{th} = (\mu_0/4\pi)I_0^2/2$ (N). From the oscillogram of the discharge current it is known that $I_0 = 104.7$ A, giving a pinch force thrust of 0.55 mN which is far too small to have thrown the weight 1 cm into the air. If the liquid had the rigidity of the metal lattice, the Ampere electrodynamics would predict an up-thrust, due to repulsion from the copper rod, of about ten times the pinch force thrust. This would still be too small to explain the observed phenomenon. However, in a liquid the Ampere lift forces on individual current elements would be transmitted from molecule to molecule. They could conceivably accumulate up to the free-liquid surface to a value that is consistent with the observed impulse received by the metal weight.

When Lorentz first tried to explain the electrodynamics of convecting charges in vacuum, he found that convection currents did not obey Ampere's force law which had proved infallible in connection with metallic conduction. A similar dilemma has now arisen with the saltwater experiment. The ions in the electrolyte appear to behave like convecting charges in vacuum which almost certainly will experience Lorentz forces but not those predicted by Ampere's law. How Ampere forces may promote an explosion will be better understood from a second experiment.

Figure 59 shows the details of a straight-through channel experiment. A half-inch-wide channel was milled in a transparent plastic board (A). Two copper bars of 0.5×0.5 in. cross-section (B) were glued into the channel, leaving a butt-gap of length g between them. When the gap was 0.4 cm long and filled with liquid mercury, a 1000 A dc current was found to expel the liquid upward into the air. With longer gaps of, say, 10 cm length no liquid expulsion took place, but at about the 1000 A current level the liquid would separate from one or the other copper surface, interrupting the current with an arc. It was easy to expel saltwater from a 1.7 cm long gap with a capacitor discharge that created a diffuse arc over the length of the gap. Yet

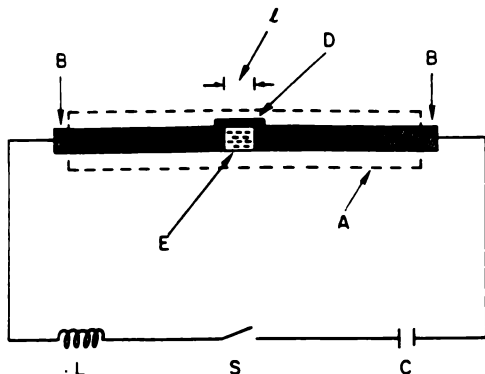


Fig.59 Straight-through channel experiment. A: transparent plastic board; B: 0.5×0.5 in. copper rods; D: dielectric block; E: liquid conductor gap; L: induction coil; S: switch in air; C: energy storage capacitor.

electrolytic, arcless discharges through the saltwater left the liquid still and undisturbed. When a small dielectric block (D) was placed over the water-filled gap, a 15 kV, 2 μ F discharge would produce so strong an explosion that the block was fired at high speed to the laboratory ceiling and rebound to the floor.

In the mercury experiments the current distribution over the conductor cross-section must have been uniform. In none of the experiments was the liquid temperature allowed to exceed 100°C. This was controlled by limiting the period of current flow. The return circuit was situated far enough away from the liquid gap so that it could exert no significant electrodynamic forces on the mercury. In the channel experiments the transverse pinch forces clearly act to contain the explosion rather than produce it. Hence we are left with longitudinal Ampere forces as the only plausible

explanation of liquid mercury expulsion from short gaps. Ampere repulsion between in-line current elements is strong across the solid-liquid interfaces and can separate the two conducting media. The longitudinal repulsion forces also set up pressure in the middle of the gap. In short gaps this apparently becomes strong enough to lift mercury out of the channel. Finite element calculations have shown that the force trying to separate liquid mercury from the copper interfaces at 1000 A is of the order of 0.5 N. This appears sufficient to explain the separation.

Attention is drawn to arc-generated shock waves in toluene photographed by Wong and Forster [66]. A 0.5 cm long cylindrical arc column of 5000 A was found to generate a bulging shock wave with its leading edge traveling radially outward halfway between parallel plate electrodes, just as expected if longitudinal Ampere forces were driving the shock. The shock wave was seen to collapse as soon as the arc was extinguished. Expanding gases generated in the arc column should have given rise to a cylindrical shock wave which persisted after the extinction of the arc.

DO LONGITUDINAL AMPERE FORCES EXIST IN GASEOUS ARCS AND PLASMAS ?

Aspden [60] and Pappas [46] suggested that the instabilities in fusion plasmas may also be the result of longitudinal electrodynamic forces. If correct, this would be of great importance to the halting progress made in one of the most exciting scientific and technological enterprises man has embarked upon.

Nasilowski [67] recently observed that longitudinal, tension-like forces should tend to mechanically disrupt arc columns. He argued, when this occurs the driving voltage

and the energy stored in the magnetic field of the circuit will try and restore the current. This process should be repetitive and cause current fluctuations in what would normally be expected to be a steady arc burning process. In support of his views Nasilowski cites Swiss and Soviet sources.

Bergmann [68] writes that heavy-current arcs are accompanied by continuous acoustic phenomena, that is mechanical disturbances in the arc plasma. Granovsky and Bykhovskaya [69] reported the observation of spontaneous oscillations in low-pressure arc discharges which were driven by dc voltage. The same type of oscillation also occurs in high-pressure arcs. The oscillations fall either in the MHz or GHz band. Granovsky claimed the current fluctuations were caused in the gaseous gap of the circuit and had their seat in the anode zone. The Swiss and Russian authors were not familiar with Ampere's force law and could offer no good explanation of the observed arc instabilities.

CHAPTER 3

THEORETICAL DEVELOPMENTS

FINITE CURRENT ELEMENT ANALYSIS

Maxwell, more than anyone else, was responsible for making the Ampere-Neumann theory obsolete, at least temporarily. At the same time he was also the finest scholar of the old electrodynamics and made a major contribution to it in the form of the geometric-mean-distance method of inductance calculations. This chapter will summarize the various extensions of the Ampere-Neumann electrodynamics made during and since the time of Maxwell. The review will not follow the historical sequence of events but will deal with the most significant milestone first, for it makes it much easier to understand the rest.

This milestone was the digital computer. It makes it possible to explore the predictions of the laws of Ampere and Neumann to a breadth and depth that remained hidden to the founders of newtonian electromagnetism. It is not so much the amount of computing that becomes feasible, rather than the avoidance of integration difficulties which, at any rate in the field of electromechanics, reduced theories to qualitative tools. It is more than a coincidence that, when working with current elements of finite size, the solution process becomes easy and transparent. One quickly gains the impression any mathematical continuum technique, which perforce ignores the indivisibility of electrical charge carriers, is an artifact rather than a mirror of nature. Finite field-element analysis does not concern itself with elements of matter and then looks like an approximation to the truth. Finite current-elements, on the other hand,

are real matter elements. With them approximations arise only from the fact that computers cannot handle the large number of elements when each is shrunk down to its natural atomic size.

There can be no doubt that Ampere himself believed his electrodynamic forces acted directly on the conductor metal, rather than on a subtle electric fluid contained in the metal. The Ampere forces were ponderomotive forces, just like the forces of gravitation. To explain electromagnetic induction, Neumann postulated a second, and totally different, set of forces. He called them electromotive forces (e.m.f.'s). The electromotive forces did not act on the metal, but on the electric fluid contained in the conductor. Since Neumann's law of induction (1.68) follows directly from Ampere's force law (1.24), it seems the same material current elements must be involved with both sets of forces. This fact remains to be reconciled with the modern electron theory of metals.

Finite current element analysis may be used to calculate both ponderomotive and electromotive forces in metallic conductors. In each case it may be assumed the element is a piece of metal containing a certain electric charge structure. The charge configuration must permit current flow under the influence of electromotive forces to coexist with ponderomotive forces on the metal lattice. To start the analysis it is necessary to choose an element shape and size.

Many modern investigators still treat the electric current as being infinitely divisible, as Ampere did. This was quite acceptable in 1820 before the atomicity of matter had become firmly rooted in our understanding of nature. If the current element is an element of matter, it is no longer reasonable to assume it can be infinitely small. The smallest possible current element is the metal atom,

including its conduction electron. In order to sustain ponderomotive forces in the direction of current flow, the amperian current element must involve the atomic nucleus. The size of the atomic current element is then determined by the spacing of atoms in the metal lattice. The shape of the element could be unit cell of the lattice. The number of atoms in metallic conductors is far too large to be handled by even the most powerful computers. Therefore we are compelled to cluster atomic current elements to form macroscopic current elements suitable for finite element analysis.

The infinitely small current elements proposed by Ampere could be marshaled with the integral calculus. This turned out to be very convenient when calculating ponderomotive and electromotive forces between two circuits which did not approach each other very closely. Calculating both types of interactions in the same circuit for just the volume elements--as would be done in specific force calculation--inevitably had to deal with the interaction of neighboring infinitely small volumes. This gave rise to singularities in the determination of the most important contributions to longitudinal forces. Dealing with actual forces, rather than specific forces, would have avoided the problem. For this reason no longitudinal force calculations were published in a century and a half since Ampere's formulated his law.

The integration singularities completely disappear when finite current elements are employed, even if they are as small as unit cell of the metallic lattice. This is the primary reason why the availability of computers has led to renewed interest in the Ampere-Neumann electrodynamics. The difficulties of dealing with elemental interaction forces in an isolated circuit, without computers, no doubt helped to conceal the difference between the Ampere and Lorentz electrodynamics of metals.

In any analysis of two circuits made of wires of a diameter which is small compared to the distance between the circuits, any kind of resolution of the circuits into a reasonable number of elements will give about the same answer for the mutual force or the mutual inductance. However when the circuits nearly touch each other, the choice of current element shape and size greatly influences the computed results. Analytical solutions do not eliminate this difficulty. Take, for example, the mutual inductance of equal coaxial circles as computed by Maxwell with elliptic integrals and later tabulated by Grover [70]. The closest distance for which Grover lists a mutual inductance is four percent of the circle radius. At closer range his formula diverges so rapidly that interpolation becomes meaningless. For extremely close circles Grover recommends a logarithmic formula which could easily arise out of finite element summations.

Element shape and size selection has the greatest effect on the calculation of selfinductances and reaction forces between parts of the same circuit. These calculations require the evaluation of the interaction of adjacent current elements that are 'in contact' with each other. Most investigators shunned the critical issue of element size. Let us look at just one example. Reference [71] by Charles is a useful paper for the computation of Lorentz forces on conductors employed by the electric power industry. This author uses what has become known as the "stick model". He calculates the Lorentz forces between two or more straight conductor sections, or sticks, which do not touch each other. Each stick is treated as a single filament of current elements. Since the stick is straight, the elements within it exert no Lorentz forces on each other. Therefore forces between neighboring elements do not enter the calculations. It will be appreciated that the stick model will not work with Ampere's law because of element interactions within each stick.

Charles devotes a paragraph to the forces at bends and corners of a circuit. This is where two sticks have to meet. In this paragraph he says:

"As x (distance from corner) tends to zero the current in the bend tapers off with a corresponding reduction in the mechanical forces in the vicinity of the corner. The problem is outside the scope of the paper, but an approximate solution may be obtained for a 90 degree bend by assuming that the force starts at the point $x=0.779r$, where r is the radius of the conductor."

Charles' little gap right where two sticks should meet sharply modifies the computed forces acting on either stick. Cleveland [49] too was forced to resort to imaginary conductor gaps at the corners of his circuit to make his force calculations agree with experiment.

Consider a closed circuit made up of a wire of diameter d . For the purpose of calculating the reaction forces between two parts of the circuit, treat the wire as a single filament of elements. How long should the elements be? Neither Ampere nor Neumann, or anyone else, has provided guidelines to answer this question. With computers the author has found that the finite current element method will yield reasonable results only if the element length is approximately equal to the wire diameter. In other words, the length-to-width ratio of the current element should be unity or close to it. If all elements are of this shape and of equal size, then the element length is also equal to the distance between adjacent elements. This implies that the position of an element is given by the geometric center of the element volume.

If a large conductor is thought of as consisting of a bundle of filaments, circular filament cross-sections would not fill the conducting area of the large conductor.

For the subdivision of large conductors into a number of parallel filaments it is more appropriate to choose filaments of square cross-section. The requirement of unity length-to-width ratio then makes the current element a cube. Examples mentioned in this section will therefore be based on cubic current elements. This means both the longitudinal and lateral spacing of adjacent elements will be equal to the element length.

An experiment has been performed to check how computations with cubic current elements compare with measured forces. The apparatus is shown in fig.60. It consists of a 100×30 cm rectangle made of 0.5 inch wide and 0.05 inch thick copper strip. The ABCD plane of the circuit was mounted vertically with the bottom side AB horizontal and hung at 0 from a balance beam. AB was electrically connected to the remaining three sides of the circuit via non-metallic cups A and B filled with liquid mercury. In each cup the current had to cross a depth of about one millimeter of mercury. With the conductivity ratio of copper to liquid mercury being approximately fifty, the current was expected to cross the liquid gap along almost straight and parallel streamlines. Therefore the corners at A and B, as well as those at C and D, were quite sharp, as indicated in fig.60. The current was led in and out of the circuit with closely packed parallel strips between C and D and connected to terminals T-T.

The transverse force F on side AB acts vertically downward. It was measured with a beam balance of a sensitivity of 0.1 gram. Stabilized DC currents up to nearly 500 A were passed around the circuit and gave rise to transverse forces on AB in the range from 10 to 25 gram. The force balance technique is further explained by fig.61. This is a simplified diagram of a commercial beam balance of unequal arms. The weight of side AB with mercury cups and support components will be denoted by W . This weight W , hanging on the

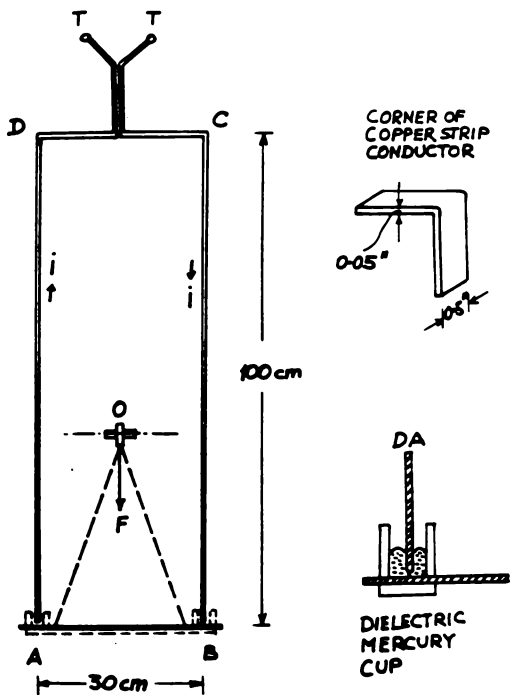


Fig. 60 Reaction force measurement on 100 × 30 cm rectangular circuit

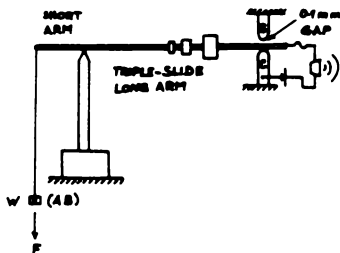


Fig.61 Force balance

short arm, was balanced with the aid of three graded weights on a calibrated triple-slide on the long arm. The balance condition was detected with a battery driven piezoelectric whistle. As shown in fig.61, the whistle circuit was completed through a mechanical contact between the long balance arm and the metallic support C.

Even when no current flows in the circuit, not all of W is dead weight. A small part is due to buoyancy forces in the mercury cups. Copper has a specific gravity of 8.94 while that of liquid mercury is 13.546. Hence the ends of the vertical conductors dipping into the mercury push side AB down. Slight tipping of the balance changes the immersion depth in the cups. When this depth is decreased by one millimeter, W must decrease by 0.15 gram. Therefore the error due to the tipping movement of the balance leads to an underestimate of the electrodynamic force F . To keep this error small, the balance swing was limited to an angle just sufficient to break contact at C. The positioning of the mechanical stop S, of fig.61, restricts immersion level changes to a small fraction of one millimeter.

Another source of error is the thermal expansion of the 100 cm long vertical conductor portions of fig.60. This has been controlled to a certain extent by not allowing the conductor temperature to rise above 70°C. Copper has

a coefficient of linear thermal expansion of 16.42×10^{-6} . The maximum thermal expansion of sides AD and BC therefore was 0.82 mm. The effect of this expansion is to increase the depth of immersion in the mercury cups. It counteracts the error due to beam swinging.

The major measurement error arose from the fact that it seemed to be impossible to obtain a clean break of contact C for a force increment of 0.1 gram, the nominal sensitivity of the balance. The contact resistance at C obviously depends on contact pressure and this, in turn, determines the loudness of the piezoelectric whistle. Besides, vibrations of the laboratory floor actually lead to contact bouncing. The stabilizing effect of buoyancy changes, and possibly also elastic strain in the metal components, hindered clean breaking of contact C. For these various reasons the accuracy of the force measurements was unlikely to be better than ± 0.5 gram.

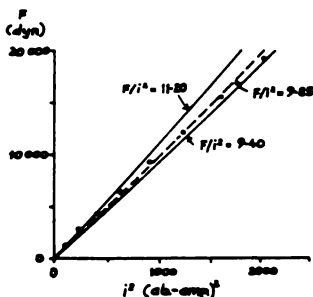


Fig.62 Measured transverse force on AB

Measurement points plotted on fig.62 were obtained by the following procedure.

- (1) With the current switched off, the sliding weights were

adjusted until contact C was just broken, and whistling ceased but for an occasional light bounce, say once per second, caused by floor-born vibrations. A check was made that in this condition the gap at S was clearly open and the piezoelectric whistle would not sound when connected to S.

(2) The weights on the long beam were then adjusted to push the beam firmly down on C, producing a loud whistle sound. The value of the weight adjustment w (referred to the short-arm side) was noted. This operation pre-loaded the balance negatively by w .

(3) Next a preset dc current through the rectangular circuit was switched on for 30 seconds. If this did not interrupt the whistle sound, a higher current level was pre-selected and the experiment was repeated. A note was made of the current I which just broke contact C according to the definition given in (1). In order to arrive at this condition the circuit was allowed to cool down between repeated current applications.

(4) The balance was then preloaded to a different value of w and the corresponding value of I was determined by the method of (3). The weights w were taken to represent the transverse electrodynamic force F on circuit side AB.

The measurement points plotted on fig.62 show quite reasonable--but not perfect--proportionality of the force to the square of current. The slope of the broken line which is meant to represent the measurements, or the specific downward force on AB of the rectangular circuit of fig.60, was found to be 9.85.

The finite current element analysis was carried out for two separate cases. In one of them the circuit was modelled as a single filament, carrying the full current i , made up of 1 cm long current elements. Each element then

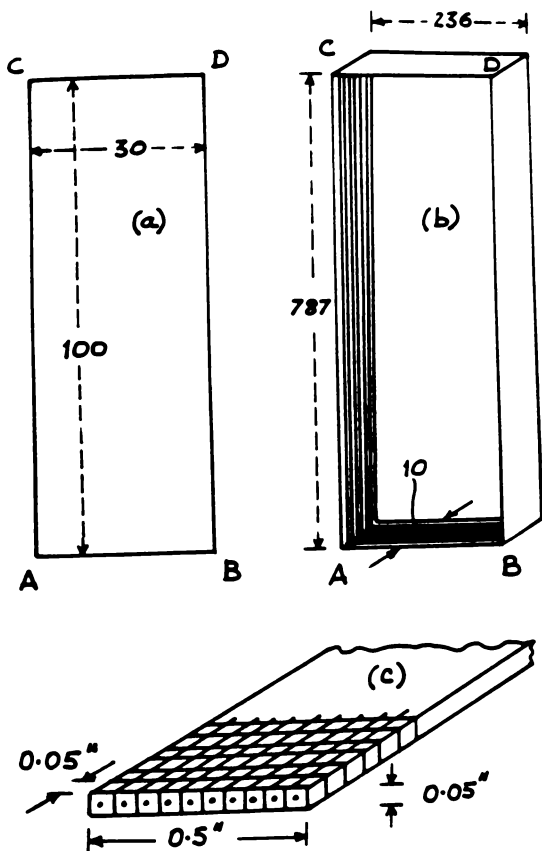


Fig. 63 Current element representation
 (a) single filament model
 (b) 10-filament model
 (c) strip of 10 filaments

took the shape of a 0.05 inch thick, 1 cm \times 0.5 inch plate. This made the ratio of the greatest width to element length approximately equal to one. The other representation is sketched on fig.63. It involves the subdivision of the rectangular conductor strip into ten square-section filaments, each carrying $(i/10)$ ab-amp of current. Individual filaments are then further divided into 0.05 inch long cubic current elements. This resolved the circuit into 20,460 cubic elements compared with 260 plate elements of the single filament model. The finer resolution of the conductor is of course expected to give more accurate results.

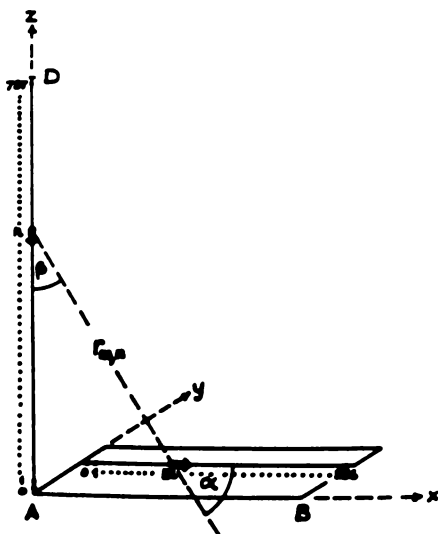


Fig.64 Three-dimensional element interaction

The vertical downward force on AB is mainly due to the interaction of this side with AD and BC. The single-filament model results in a two-dimensional problem, while the 10-filament model is more complex, involving all three dimensions of space. We will immediately analyze the more difficult three-dimensional case as this also explains how to handle a two-dimensional circuit. With respect to the 10-filament model, let the corner A be placed at the origin of a rectangular coordinate system, as indicated in fig.64. The y-coordinate labels the ten parallel filaments from $y=0$ to $y=9$. Once the interaction of an end-filament in AD and all filaments of AB has been calculated, the total interaction between the two sides of the rectangular circuit may be determined from a 10×10 filament interaction matrix.

Now consider the general element m (fig.64) in AB which has coordinates $m(x_m, y_m, 0)$ and the general element n in the first filament of AD which lies on the z -axis and has coordinates $n(0, 0, z_n)$. The distance between those two elements is given by

$$\begin{aligned} r_{m,n}^2 &= (x_m - x_n)^2 + (y_m - y_n)^2 + (z_m - z_n)^2 \\ &= x_m^2 + y_m^2 + z_n^2 \end{aligned} \quad (3.1)$$

The required direction cosines of $r_{m,n}$ are

$$\cos \alpha = x_m / r_{m,n} \quad (3.2)$$

$$\cos \beta = z_n / r_{m,n} \quad (3.3)$$

It should be noted that for interactions between sides AB and AD the angle of inclination of the current elements is $\epsilon = 90^\circ$ and therefore $\cos \epsilon = 0$. Then from (1.24), the downward component of the elemental Ampere force $\Delta F_{m,n}$ is

$$\begin{aligned} (\Delta F_{m,n})_v &= -(i/10)^2 (dm \cdot dn / r_{m,n}^2) (-3 \cos \alpha \cos \beta) \cos \beta \\ &= 3(i/10)^2 (dm \cdot dn / r_{m,n}^2) \cos \alpha \cos^2 \beta \end{aligned} \quad (3.4)$$

which can be solved by substitution of (3.1) to (3.3). Equation (3.4) has to be summed for all combinations of m and n indicated by fig.64. This task can only be accomplished with a computer.

It will be realized that, if all the current would flow in just one filament--say the filament coinciding with the coordinate axes of fig.64--the force between AD and AB would be significantly greater than for the case where the current is distributed over ten parallel filaments. For lack of a better term, the reduction in force with increasing conductor cross-section will be called "force dilution".

One of the advantages of writing the equations of the Ampere-Neumann electrodynamics in fundamental electromagnetic units (e.m.u.) is that the force is seen to be dimensionally equivalent to the square of a current. This is obvious from Ampere's force law (1.24) and also equation (3.4). It means the force equations are independent of the unit of length. Length may be measured in meters, feet, or any other unit, without changing the equations. Finite current element analysis can be greatly simplified by making the chosen length of current elements also the unit of length. We therefore set

$$dm = dn = 1 \text{ unit of length} \quad (3.5)$$

Of course, in any given problem, all elements must then be of the same length. With (3.5) the distance between two current elements has to be expressed by a number of current element lengths. The recurring ratio $(dm \cdot dn / r_{m,n}^2)$ is in any case a dimensionless number. Hence in fundamental electromagnetic units we may divide the force by the square of the current (i^2) and obtain another dimensionless number which will be referred to as the "specific force".

The downward force on the y th filament in AB (see fig.64) due to the corner filament in AD is

$$F_{0,y} = 3(1/10)^2 \sum_{m=1}^{236} \sum_{n=1}^{787} (\cos \alpha \cos^2 \beta) / r_{m,n}^2 \quad (3.6)$$

This shows that AB-30 cm has been resolved into 236 elements and AD-100 cm into 787 elements. Furthermore, $r_{m,n}$ of (3.6) is equal to the number of elements that can be fitted into the distance between the general element m and the general element n .

The interactions of all ten filaments in AD with the ten filaments in AB can be compiled in a 10×10 square, symmetrical matrix of the form

$$\begin{array}{cccccc} F_{0,0} & F_{1,0} & F_{2,0} & \dots\dots\dots & F_{9,0} \\ F_{0,1} & F_{1,1} & F_{2,1} & \dots\dots\dots & F_{9,1} \\ F_{0,2} & F_{1,2} & F_{2,2} & \dots\dots\dots & F_{9,2} \\ . & . & . & . & . \\ . & . & . & . & . \\ . & . & . & . & . \\ . & . & . & . & . \\ . & . & . & . & . \\ F_{0,9} & F_{1,9} & F_{2,9} & \dots\dots\dots & F_{9,9} \end{array}$$

The total vertical force on AB due to AD is the sum of the elements of this matrix. Since it is symmetrical, and the elements along any diagonal are all equal to each other, we find the force in question to be

$$F_v = 10F_{0,0} + 18F_{0,1} + 16F_{0,2} + 14F_{0,3} + 12F_{0,4} + 10F_{0,5} + 8F_{0,6} + 6F_{0,7} + 4F_{0,8} + 2F_{0,9} \quad (3.7)$$

It is convenient to solve (3.6) in terms of the specific force $F_{0,y}/l^2$ and then (3.7) may be written

$$\begin{aligned} F_v/l^2 = & 0.10F_{0,0}/l^2 + 0.18F_{0,1}/l^2 + 0.16F_{0,2}/l^2 \\ & + 0.14F_{0,3}/l^2 + 0.12F_{0,4}/l^2 + 0.10F_{0,5}/l^2 \\ & + 0.08F_{0,6}/l^2 + 0.06F_{0,7}/l^2 + 0.04F_{0,8}/l^2 \\ & + 0.02F_{0,9}/l^2 \end{aligned} \quad (3.8)$$

Equation (3.8) is a force dilution formula. It will be appreciated that it also gives the force exerted by side BD, of fig.63, on side AB in the downward direction. This is a result of the symmetry of the rectangular circuit.

Finally we have to compute the downward force exerted by CD on AB. For the wide separation between these two sides the shape and size of current elements chosen has little influence on the result. CD contributes less than two percent to the downward force on AB and force dilution due to the parallel filaments will be negligible. Hence a single-filament representation may be used for this side pair in which each side is resolved in 30 1-cm-long plate elements. Using this approximation, the specific downward force on AB due to CD came to 0.1724. The total downward force on AB due to all three remaining sides of the rectangle was found to be

$$F_V/l^2 = 9.40$$

which has been plotted on the graph of fig.62.

Pinch forces in the mercury cups should exert a downward thrust on AB in each cup of 0.51^2 . The pinch force theory supporting this claim was carried out by Northrup [44]. With pinch thrust added to the finite element calculations, using cubic elements, the total specific downward force on AB comes to 10.40 compared to the experimental value of 9.85. Taking experimental uncertainties into account, this is considered to be sufficient justification for basing the finite element analysis on macroscopic, cubic current elements.

With the rectangular circuit of fig.63 being represented by just a single filament of 1 cm long elements in the shape of little plates, the calculated specific downward force on AB came to

$$F_{\sqrt{i^2}} = 11.20.$$

This has also been plotted on fig.62. It clearly is an overestimate of the specific force even when the pinch thrust is ignored. However, in view of the greatly reduced amount of computation, the single filament model provides a worthwhile approximation.

The example of the rectangular circuit illustrates that the force on part of a circuit due to the remainder of the circuit is primarily determined by the interaction of the circuit portion considered with elements in its neighborhood. Remote parts of the circuit make only a small contribution, and in many practical situations they may be safely ignored. The strong local interactions are the result of the inverse square law contained in Ampere's formula (1.24). The same would be true for Lorentz force calculations, which may also be handled by the finite current element method, because the inverse-square-of-distance relationship is also contained in Grassmann's law (1.85).

Five principal rules of finite current element analysis were laid out on page 98. They were then applied to the single filament model of a square circuit to explain what is meant by Ampere tension. We will now delve deeper into the subject of Ampere tension by studying a section of a straight conductor subdivided into a number of parallel filaments. First we ask the question: what will be the tension in two adjacent, straight filaments which share the current of one absolute ampere? To obtain an answer consider the two square-section filaments of fig.65. They have been subdivided into four portions a, b, c, and d. Each portion consists of $z/2$ cubic current elements with their vectors all pointing in the same direction. Let us now determine the specific tension $T_{\sqrt{i^2}}$ across the midplane of the filament combination when each filament carries half the total current, or $i/2$. The tensile force due to the interaction of portions a and b can be derived directly from (2.6) or

or (2.18). An equal component will arise from the interaction of portions c and d. Let these two components be $T_{a,b}$ and $T_{c,d}$, then from (2.18)

$$T_{a,b} = T_{c,d} = (4)(0.19 \cdot \ln z) i^2 \quad (3.9)$$

For the calculation of $T_{a,d}$ and $T_{c,b}$ which, because of symmetry, are equal to each other, we find from fig.65 that

$$r_{m,n}^2 = (m+n-1)^2 + 1 \quad (3.10)$$

$$\cos \epsilon = 1 \quad (3.11)$$

$$\cos \alpha = \cos \beta = (m+n-1)/r_{m,n} \quad (3.12)$$

Applying Ampere's force law (1.24) to portions a and d of the filament pair of fig.65 and resolving the elemental interaction force in the direction of the current, we obtain

$$\begin{aligned} T_{a,d} = T_{c,b} &= (4) i^2 \int_{-z/2}^{z/2} \int_{-z/2}^{z/2} (1/r_{m,n}^2) \times \\ &\times (2 \cos \epsilon - 3 \cos \alpha \cos \beta) \cos \alpha \quad (3.13) \end{aligned}$$

Solving the simultaneous equations (3.10) to (3.13) by computer for a range of z -values, and applying regression analysis to the results revealed the logarithmic relationship

$$\begin{aligned} T_{a,d}/i^2 = T_{c,b}/i^2 &= (4)(-1.64 \cdot \ln z) \quad (3.14) \end{aligned}$$

Fig.65 Tension across midplane of filament pair

Hence the total tension T_t across the midplane of the filament combination is

$$T_t = 2T_{a,b} + 2T_{a,d} = (0.73 \cdot \ln z) i^2 \quad (3.15)$$

which is smaller than the force given by (2.18). This result demonstrates that the amperian tension will be reduced if the current divides between two adjacent filaments, and represents what has been called force dilution.

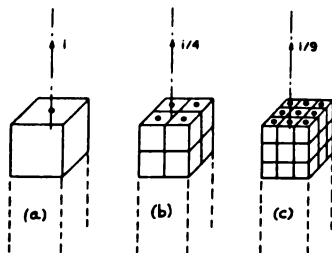


Fig.6.66 Cubic element subdivision of a straight conductor

The single filament representation of a straight conductor is the crudest model one can use. Finer subdivision of the conducting matter into smaller cubes should result in better approximations to the specific tension. How far must this process be driven to obtain meaningful results? To investigate this question let every element of fig.66(a) be subdivided into eight smaller cubes, as shown in (b) of the diagram. This simple subdivision multiplies the computational work by a factor of at least 64. Hence too fine a subdivision of the conductor can be costly in computing time. For fig.66(b) angles α and β are no longer zero for all relevant current element combinations and equation (3.13) has to be used in addition to (2.6).

To obtain a quantitative indication of the magnitude of force dilution for successively thinner filaments, let us analyze a relatively short conductor of 2 m length and 1 cm^2 cross-section. The return circuit would make a significant contribution to the maximum tension in this short conductor, but we will not compute this. Using finite current element analysis, the midplane tension due only to the two

meter long straight conductor portion was found to be

Number of filaments:	1	4	9	16	25
T_c/i^2 :	5.49	4.71	4.55	4.49	4.46

This example indicates that the computed specific Ampere tension converges quite rapidly as the number of parallel filaments increases. Hence a modest degree of subdivision should give good approximations.

As a final illustration of the finite current element technique we will calculate force distributions in a railgun circuit. The railgun is actually a rectangular circuit with one of the short sides being mobile. While practical railguns are relatively long and use closely spaced rails, the wider and shorter circuit of fig.63 will be employed for calculating force distributions. Side AB will be treated as the projectile branch p and side AC as the rail s, as shown in fig.67. The acceleration force of this oddly shaped railgun has already been calculated and compared with measurements in fig.62. The recoil force in rail s is entirely due to interactions of elements of s with elements in the projectile branch p. All ten filaments of s have to be considered. Their y-coordinates vary from 0 to 9. The lengths of p and s are 236 and 787 units, respectively. In this example let i stand for the filament current, so that the total circuit current is 10i. The specific elemental interaction force between the general element m on the yth filament in s and the general element n in the corner filament of p on the x-axis is

$$\Delta F_{m,n}/i^2 = -(1/r_{m,n}^2)(2\cos\epsilon - 3\cos\alpha\cos\beta) \quad (3.16)$$

where $r_{m,n}$ is the number of elements that can be fitted in the distance between m and n. Let us denote the recoil component of the elemental force of (3.16) by $F_{y,0}$. Since

$\cos \epsilon = 0$, this is given by

$$\Delta F_{y,0}/i^2 = (3\cos^2 \alpha \cos \epsilon)/r_{m,n}^2 \quad (3.17)$$

In the coordinate system of fig.67 the two general elements are situated at

$$m(0, y_m, z_m); \quad n(x_n, 0, 0)$$

and therefore

$$r_{m,n}^2 = x_n^2 + y_m^2 + z_m^2 \quad (3.18)$$

Making use of the definition of direction cosines we find that

$$\cos \alpha = z_m/r_{m,n} \quad (3.19)$$

$$\cos \beta = x_n/r_{m,n} \quad (3.20)$$

Coordinates x and z vary between 1 and 236 and 787, respectively. This is sufficient information to solve (3.17) for every element m .

Let $\Delta F_{r,z}$ be the sum of the recoil forces on all ten elements across rail s , having the same coordinate z_m , and caused by the ten elements across the p -branch which include n and have the same coordinate x_n . $\Delta F_{r,z}$ arises from a 10×10 symmetrical interaction matrix and is numerically equal to the 100 matrix elements. Specific forces may be substituted for actual forces to make the result more general. The symmetry of the interaction matrix derives from

$$\Delta F_{y,0} = \Delta F_{0,y},$$

that is the y and x Coordinates may be interchanged without affecting the elemental forces.

It can further be shown that the elements along any diagonal of the matrix are equal to each other. Since the rail current $i_R = 10$ i, the specific force dilution formula may then be written

$$\begin{aligned} \Delta F_{r,z}/i_R^2 = & 0.10 \Delta F_{0,0}/i_R^2 + 0.18 \Delta F_{1,0}/i_R^2 + 0.16 \Delta F_{2,0}/i_R^2 \\ & + 0.14 \Delta F_{3,0}/i_R^2 + 0.12 \Delta F_{4,0}/i_R^2 + 0.10 \Delta F_{5,0}/i_R^2 \\ & + 0.08 \Delta F_{6,0}/i_R^2 + 0.06 \Delta F_{7,0}/i_R^2 \\ & + 0.04 \Delta F_{8,0}/i_R^2 + 0.02 \Delta F_{9,0}/i_R^2 \end{aligned} \quad (3.21)$$

Hence the recoil force distribution is given by

$$F_{r,z}/i_R^2 = \sum_{x=1}^{236} \Delta F_{r,z}/i_R^2 \quad (3.22)$$

Computer evaluation of (3.22) provided the results listed in table 6.

Table 6. Recoil force distribution in rail s

m	$F_{r,z}/i_R^2$	m	$F_{r,z}/i_R^2$
1	0.26794	20	0.04830
2	0.18224	30	0.03293
3	0.15934	50	0.01983
4	0.14353	100	0.00944
5	0.13032	150	0.00566
6	0.11893	200	0.00366
7	0.10903	300	0.00172
8	0.10037	394	0.00094
9	0.09277	500	0.00052
10	0.08608	650	0.00026
15	0.06235	787	0.00015

Sum for 787 elements = 4.69358

A little over 71 percent of the recoil force in one rail has its seat in the first 10 cm of the rail behind the projectile. Nevertheless, a not negligible fraction of the recoil is distributed over the remaining 90 cm. The recoil force distribution is of course the same in both rails.

An equally important issue in railgun design is the distribution of the acceleration force over the p-branch. This distribution tends to peak at the ends of the projectile branch. The specific transverse force distribution was computed over the p-branch of the 10-filament model. As this distribution is symmetrical about the center line of the railgun, only half the elements (236/2-118) have been listed in result table 7. This table also shows the Lorentz force distribution for comparison. It will be noted that the two distributions are very similar and the total transverse forces differ by less than 1.5 percent. The major distinguishing feature is the contribution of the corner element. The measure of agreement between the two distributions is quite remarkable.

Table 7. Transverse force distribution over p-branch

n	Ampere	Lorentz
1	0.37538	0.26962
2	0.23261	0.23242
3	0.19884	0.19913
4	0.17360	0.17389
5	0.15363	0.15393
6	0.13744	0.13774
7	0.12409	0.12438
8	0.11293	0.11322
9	0.10349	0.10379
10	0.09544	0.09574
40	0.02967	0.03000
118	0.01637	0.01674
Total	4.70148	4.63420

A more uniform transverse force distribution over the p-branch may be brought about by moving the rails closer together. Military railguns seem to employ rail spacings that are equal to the rail height. It results in what is known as a square bore gun. The more uniform distribution of the acceleration force is being bought at a high price. For the same current, closely spaced rails furnish a much smaller acceleration force than widely spaced rails. For example, the specific acceleration force of a square bore gun may only be two as compared to 9.4 in the circuit to which table 7 refers.

The finite current element analysis is best suited to electrodynamic interactions inside and between straight conductor portions. In bends and at corners of metallic circuits the current distribution is generally non-uniform and unknown. In addition, it does not seem possible to fill circuit corners with equal-size cubic current elements without producing some overlap of current elements. Experiment indicates that the error caused by the imperfect modelling of circuit corners can be small in a circuit like that of fig.63. The strip geometry ensures relatively even current distribution and element overlap is small. However, it may be this overlap which is responsible for the difference between the transverse Ampere and Lorentz force on the corner element indicated in table 7. Errors caused by imperfect corner modelling are expected to be greater when the conductor is a round rod or of square cross-section. It is hoped that a more widespread use of the finite current element analysis will lead to improved methods of conductor modelling.

Microscopic current elements in the form of metal atoms do not overlap. There is plenty of space between atoms to allow for the bending of conductors. Hence the element overlap problem arises from the necessity of having to employ macroscopic current elements.

REACTION FORCES FROM THE SELFINDUCTANCE GRADIENT

The most frequently used formula for calculating the reaction forces between two parts of a current-carrying circuit, consisting of metallic conductors, is not the Ampere nor the Lorentz force law, but

$$F_x = \pm \frac{1}{2} i^2 (\partial L / \partial x) \quad (3.23)$$

where ∂x is a virtual displacement between the two parts of the circuit in the direction x in which F_x is required. The complete circuit of selfinductance L carries a current i . Equation (3.23) is written in e.m.u. in which inductance has the dimension of length. The positive x -direction is the direction in which the circuit portions separate from each other by the virtual displacement. The \pm sign signifies that (3.23) is sometimes written with the negative sign. Whether the force represents attraction or repulsion appears to be left to the judgement of the reader. In fundamental electromagnetic units, the magnetic energy stored by the circuit to which (3.23) refers is

$$E = \frac{1}{2} i^2 L \quad (3.24)$$

For two closed circuits m and n , Neumann's electrodynamic potential (= stored magnetic energy) is given by equation (1.25). It involves the mutual inductance (1.26) of the two circuits which may be viewed as a measure of the capability of the two circuits of storing mutual magnetic energy. By using the concept of virtual work, Neumann related the mutual force of attraction or repulsion of the two circuits by (1.27). This force may be expressed as

$$(F_{m,n})_x = -(\partial / \partial x)(i_m i_n M_{m,n}) \quad (3.25)$$

where $M_{m,n}$ is the mutual inductance of the circuits.

The capability of complete circuits to store mutual

magnetic energy must derive from their electrodynamic interactions which are governed by Ampere's law (1.24). This argument suggests that each pair of current elements stores mutual magnetic energy in accordance with the elemental mutual inductance of

$$\Delta M_{m,n} = -[(2\cos\epsilon - 3\cos\alpha \cos\beta)/r_{m,n}]dm.dn \quad (3.26)$$

If it is known that (3.26) will be integrated around at least one closed circuit, the angle function in (3.26) may be replaced by $\cos\epsilon$. This was proved by Neumann (see pages 29 to 33). Hence (3.26) is compatible with the negative form of (1.26).

It follows logically that the selfinductance $L_{o,o}$ of an isolated, closed circuit o is also composed of elemental contributions defined by equation (3.26). In the case of selfinductances we must not simplify the angle function of (3.26) to $\cos\epsilon$, because the sum of the interactions of one element dm with all 'other' elements of the circuit o does not involve a closed curve integration. The selfinductance of the closed circuit o will then be given by

$$L_{o,o} = -\frac{1}{2} \sum_m \sum_n [(2\cos\epsilon - 3\cos\alpha \cos\beta)/r_{m,n}]dm.dn \quad (3.27)$$

where m and n are sequentially numbered labels on the conductor elements of o . The angles of (3.27) are the angles of Ampere's law as drawn in fig.3 on page 11. The factor $\frac{1}{2}$ is required because the double sum of (3.27) counts every element pair interaction twice.

Equation (3.27) is actually a single-filament formula of selfinductance which can be solved by finite element analysis. Let us evaluate it for a circle of radius R , as shown in fig.68. The circle has been divided into $z+1$ elements of equal length which are labelled $0, 1, 2, \dots, n, \dots, z$. Let dm be the 0 -th and dn be the n -th element. With the

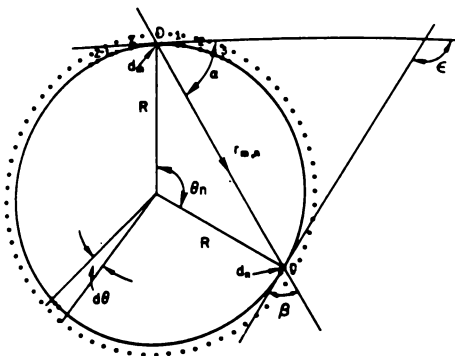


Fig.68 Construction for selfinductance of a circle

symbols defined in fig.68 we let

$$dm = dn = R \cdot d\theta = [2\pi/(z+1)]R \quad (3.28)$$

$$\theta_n = n \cdot d\theta \quad (3.29)$$

$$r_{m,n}^2 = 2R^2(1 - \cos\theta_n) \quad (3.30)$$

The double sum of equation (3.27) can be reduced to the single sum

$$L_{0,0} = -\frac{1}{2}(z+1)dm \cdot dn \sum_{n=1}^z (2\cos\epsilon - 3\cos\alpha \cos\beta) / r_{m,n} \quad (3.31)$$

because the symmetry of the circle ensures that the inductive interaction of dm with all other elements dn is the same wherever dm is situated. In (3.31) each element pair interacts twice when it should interact only once. This is being corrected by the factor $\frac{1}{2}$.

The relation between the angles of fig.68 is as follows:

$$a = a, \quad \varepsilon = a \cdot 8 = 2^1 + 2^2, \quad \varepsilon = a_n \quad (3.32)$$

Finally, the symmetry of the circle permits us to sum only half-way around it and multiply the result by two. After making the necessary substitutions in (3.31), the following formula was evaluated by computer for z ranging from 300 to 20 000

$$L_{0,0}/R = \sqrt{2} \cdot z / (z+1) \int_{n=1}^{z/2} [3 - \cos(n \cdot d\theta)] / \sqrt{1 - \cos(n \cdot d\theta)} \quad (3.33)$$

In fundamental electromagnetic units this is a dimensionless shape constant. The computer results are listed in table 8. Regression analysis revealed that the figures closely obey the logarithmic formula

$$L_{0,0}/R = 13.56 + 12.63 \ln(z+1) \quad (3.34)$$

Table 8 $L_{0,0}/R$ of a circular filament

z	$L_{0,0}/R$	
	from equ. (3.33); from equ. (3.34)	
300	42.800	42.820
400	44.635	44.632
500	46.054	46.038
600	47.211	47.187
1000	50.442	50.409
2000	54.814	54.783
3000	57.365	57.342
5000	60.581	60.567
10 000	64.939	64.944
15 000	67.489	67.504
20 000	69.299	69.321
10^6		94.025
10^{12}		181.270

This leads to the conclusion that z must not approach infinity as the Ampere-Neumann electrodynamics would then become absurd. In any case, since the forces are exerted on matter which is not infinitely divisible, it is only reasonable that the current element size should have a finite lower limit. In the absence of any better information, assume that the lower limit is the atomic spacing, or approximately 10^{-10} m. For practicle circles ranging in radius from 1 mm to 1000 m, this implies 10^6 to 10^{12} elements per circle. For these two extremes the respective $L_{0,0}/R$ ratios listed in table 8 were obtained. They are not unreasonably large.

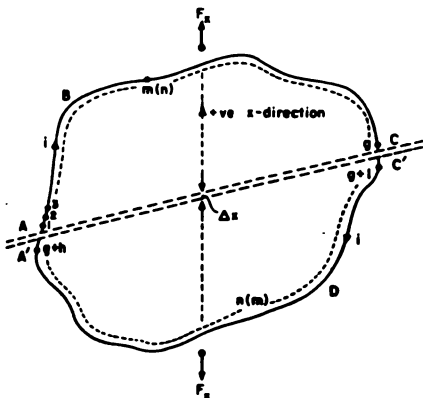


Fig.69 Virtual displacement between parts of a filament

Now that we have a method of calculating the selfinductance of a closed filament--and this need not be a circle--we return to the evaluation of the reaction force between two parts of an arbitrarily shaped circuit or by the virtual work equation (3.23). To do this it is necessary to determine the selfinductance gradient along some specified direction x . Consider the particular example of fig.69. The current elements are labelled from 1 to g along circuit portion

ABC and from $g+1$ to $g+h$ along the remaining circuit portion C'DA'. The sums in the selfinductance equation (3.27) have to proceed from $m=1$ to $m=g+h$ and from $n=1$ to $n=g+h$.

In a newtonian theory we expect only those elemental interactions to contribute to the reciprocal reaction forces in which one element lies in one portion of the closed circuit o and the other in the remaining portion. It helps to sort the summations of the selfinductance of the circuit of fig.69 as follows

$$\begin{aligned}
 L_{o,o} = & \frac{1}{2} \left\{ \left[\sum_{m=1}^g dm + \sum_{m=g+1}^{g+h} dm \right] \left[\sum_{n=1}^g ((2\cos\epsilon - 3\cos\alpha \cos\beta)/r_{m,n}) dn + \right. \right. \\
 & \left. \left. + \sum_{n=g+1}^{g+h} ((2\cos\epsilon - 3\cos\alpha \cos\beta)/r_{m,n}) dn \right] \right\} - \\
 & - \frac{1}{2} \left\{ \sum_{m=1}^g dm \sum_{n=g+1}^{g+h} [(2\cos\epsilon - 3\cos\alpha \cos\beta)/r_{m,n}] dn + \right. \\
 & + \sum_{m=g+1}^{g+h} dm \sum_{n=1}^g [(2\cos\epsilon - 3\cos\alpha \cos\beta)/r_{m,n}] dn + \\
 & + \sum_{m=1}^g dm \sum_{n=1}^g [(2\cos\epsilon - 3\cos\alpha \cos\beta)/r_{m,n}] dn + \\
 & \left. + \sum_{m=g+1}^{g+h} dm \sum_{n=g+1}^{g+h} [(2\cos\epsilon - 3\cos\alpha \cos\beta)/r_{m,n}] dn \right\} \quad (3.35)
 \end{aligned}$$

How much will the selfinductance change when the two circuit portions of fig.69 are separated by the small virtual displacement ∂x ? Let this change be

$$\Delta L = L_2 - L_1 \quad (3.36)$$

The third and fourth terms of (3.35) are not affected by the virtual displacement. They remain constant and, therefore, drop out of the difference equation (3.36). It should also be noted that the first term of (3.35) is equal to the second term and the two terms may conveniently be combined into one by dropping the factor $\frac{1}{2}$.

Potential energy and mutual inductance are scalar quantities. The energy storage capacitance (inductance) does not

of the constant sum of the two angles, we may also express them as

$$\alpha_2 = \alpha_1 - \Delta\alpha, \quad \beta_2 = \beta_1 + \Delta\alpha$$

Then

$$\begin{aligned} \cos \alpha_1 \cos \beta_1 - \cos \alpha_2 \cos \beta_2 &= \frac{1}{2} [\cos(\alpha_1 - \beta_1) - \cos(\alpha_2 - \beta_2)] = \\ &= \frac{1}{2} [\cos(\alpha_1 - \beta_1) - \cos(\alpha_1 - \beta_1) \cos(2\Delta\alpha) - \sin(\alpha_1 - \beta_1) \sin(2\Delta\alpha)] \end{aligned}$$

Therefore, in the limit in which $\Delta x \rightarrow x$ and $\Delta\alpha \rightarrow 0$, the second term becomes equal to the first and the last term vanishes. Hence the change in the angle function $2\cos\epsilon - 3\cos\alpha \cos\beta$ tends to zero as the virtual displacement tends to zero. The change is, in fact, a first-order infinitely small quantity, but this is sufficient for it to be negligible compared with the other quantities of equation (3.37), that is $dm \cdot dn$ and $r_{m,n}$, which are all of finite size. It would, of course, be insufficient in an integration over infinitely small current elements.

To a first approximation (3.37) may, therefore, be written as

$$(\Delta L)_x = \sum_{m=1}^g \sum_{n=g+1}^{g+h} dm \, dn (2\cos\epsilon - 3\cos\alpha \cos\beta) [(r_2 - r_1)/r_1 r_2] \quad (3.38)$$

As will be seen from fig.70, for a very small virtual displacement ∂x ,

$$r_1 r_2 = r_{m,n}^2 \quad (3.39)$$

$$r_2 - r_1 = \partial r = \partial x \cos\theta \quad (3.40)$$

where θ is the angle of inclination of the x -direction to the $r_{m,n}$ -direction. Substituting equations (3.39) and (3.40) into (3.38) and dividing by ∂x gives

$$\partial L / \partial x = \lim_{\Delta x \rightarrow 0} (\Delta L / \Delta x) = - \sum_{m=1}^g \sum_{n=g+1}^{g+h} [(2 \cos \epsilon - 3 \cos \alpha \cos \beta) / r_{m,n}^2] \cos \theta \, dn \quad (3.41)$$

Now consider the reaction force between the two circuit portions in the x -direction according to Ampere's law (1.24). It comes to

$$(F_{m,n})_x = -i^2 \sum_{m=1}^g \sum_{n=g+1}^{g+h} [(2 \cos \epsilon - 3 \cos \alpha \cos \beta) / r_{m,n}^2] \cos \theta \, dn \quad (3.42)$$

By comparing this last equation with (3.41) we conclude that the reaction force may be written

$$(F_{m,n})_x = -i^2 (\partial L / \partial x) \quad (3.43)$$

This agrees with equation (3.23) but for the factor $\frac{1}{2}$ which is a mathematical technicality of no physical consequence. This factor could be brought into (3.42) by extending the sums from $m=1$ to $g+h$ and from $n=1$ to $g+h$. Equation (3.43) removes the uncertainty about the sign of (3.23). To be consistent, the negative sign has to be chosen for the virtual work formula.

The foregoing analysis indicates that, in general, a pair of interacting current elements are associated with a potential energy of

$$\Delta P_{m,n} = -i^2 \sum_{m,n} [(2 \cos \epsilon - 3 \cos \alpha \cos \beta) / r_{m,n}] dm \, dn \quad (3.44)$$

When the angle function $2 \cos \epsilon - 3 \cos \alpha \cos \beta$ is positive, the mutual potential energy of the two elements is of the negative variety (see pages 23 to 25). $\Delta P_{m,n} / \Delta r_{m,n}$ will then be positive and the elemental reaction force becomes

$$\begin{aligned} \Delta F_{m,n} &= -(\partial P_{m,n} / \partial r_{m,n}) \\ &= -i^2 \sum_{m,n} [(2 \cos \epsilon - 3 \cos \alpha \cos \beta) / r_{m,n}^2] dm \, dn \end{aligned} \quad (3.45)$$

which is Ampere's force law (1.24).

Applying (3.44) to the circuit portions ABC and A'DC' of the circuit of fig.69 defines the mutually stored energy as

$$P_{m,n} = -i^2 \int_{m=1}^g dm \int_{n=g+1}^{g+h} [(2\cos\epsilon - 3\cos\alpha \cos\beta)/r_{m,n}] dn \quad (3.46)$$

This should be the quantity E of equation (3.24). If this is positive energy, then the gradient $\partial P_{m,n}/\partial x$ must be negative because the stored energy decreases with increasing $r_{m,n}$ and the distance between each relevant pair of current elements will be lengthened by the virtual displacement. Alternatively, if the stored energy turns out to be of the negative variety, $\partial P_{m,n}/\partial x$ must be positive. But

$$\partial P_{m,n}/\partial x = (\partial P_{m,n}/\partial r_{m,n})(\partial r_{m,n}/\partial x) \quad (3.47)$$

and from fig.70 $\partial r_{m,n}/\partial x = \cos\theta$, so that

$$\partial P_{m,n}/\partial x = -i^2 \int_{m=1}^g dm \int_{n=g+1}^{g+h} [(2\cos\epsilon - 3\cos\alpha \cos\beta)/r_{m,n}^2] \cos\theta dn \quad (3.48)$$

Comparing this with (3.41) proves that

$$\partial P_{m,n}/\partial x = i^2 (\partial L/\partial x) \quad (3.49)$$

Then, using Neumann's sign convention of the force being given by the negative gradient of the electrodynamic potential, we arrive once more at equation (3.43) which proves that equation (3.23) with the negative sign is compatible and in full agreement with results that would be obtained with Ampere's force law.

Whereas the reaction force between two parts of the same circuit is related to the selfinductance gradient, as shown in (3.49), the reaction force between two complete circuits m and n is a function of the mutual inductance

gradient contained in (3.25). This leads directly to Neumann's force law (1.50). As explained on pages 46 to 48, both the Grassmann and Ampere laws reduce to the Neumann formula (1.50) when computing the reaction force and its distribution over two complete circuits.

The virtual work formulas (3.25) and (3.43) are not as useful as the fundamental force laws, because they do not give the distribution of the reaction forces. As fig.50 on page 154 demonstrates, this distribution can be very different, depending on whether it has been calculated with Grassmann's or Ampere's force law.

INDUCTANCE CALCULATIONS

The Relationship between Self and Mutual Inductance

Selfinduction is generally interpreted as a special case of mutual induction with primary and secondary circuit merged into one conductor. This view is supported by the fact that both quantities have the same dimension which in e.m.u. is length. It is the natural dimension of mutual inductance because this parameter appears to depend solely on the length and disposition of lines in space. In contrast to this, conventional selfinductance formulas apply to three-dimensional conductors. Measurements show selfinductance to be function of such non-geometrical quantities as resistivity, material homogeneity, and energizing frequency.

The concepts of self and mutual inductance arose in the explanation of Faraday's discovery of electromagnetic induction. Ampere did not take part in this effort. It was Neumann who derived the fundamental mutual inductance formula (1.26), but he barely referred to selfinductance. In the closing remarks of his book [57] there is mention of the "extracurrent". By this he meant the induced current arising

from switching currents on and off in an isolated circuit. The term selfinductance was probably coined by Kelvin [76] in order to define the total inductively stored energy. Maxwell [14] greatly illuminated the meaning of the two inductance parameters, but his efforts in this direction reveal a dichotomy.

On the one hand Maxwell believed the magnetic manifestations of the electric current to be kinetic effects, and on the other he developed the mean-geometric-distance method of computing inductances which is firmly rooted in Neumann's non-kinetic theory. To underpin his kinetic current model, Maxwell [14] built a machine in which two flywheels, representing primary and secondary currents, are connected through a differential gear to a third rotating member which makes "mutual inductance" possible. This machine is being preserved in the Cavendish laboratory. As a result many scientists now treat selfinductance as a kind of electrical inertia and mutual inductance as the gearing together of selfinductances. Maxwell's GMD method is embodied in the following treatment of selfinductance.

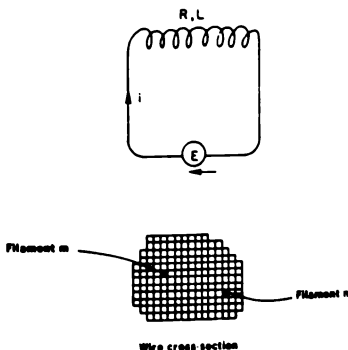


Fig.71 Wire loop in series with external e.m.f.

Consider a wire loop as shown in fig.63, part of which may take the form of a coil or solenoid. The loop current i is assumed to be driven by an externally generated e.m.f. E . At this stage no restrictions need be placed upon the shape or size of the loop, nor the conductor cross-section and homogeneity, or on the rate of change of the applied e.m.f., so long as no charge accumulation takes place anywhere along the conductor.

If R is the resistance of the loop and L its selfinductance, then the loop current i is determined by the well-known equation

$$iR = E - (d/dt)(Li) \quad (3.50)$$

Let us now look at two general filaments, m and n , of the wire cross-section. All filaments must be thin tubes of flow filled with conducting matter. In fig.71 the filaments have square cross-sections, but any other shape could have been chosen provided this left no empty space between filaments. According to the classical definition of a tube of flow, its cross-sectional area may vary along its length, but each cross-section must carry the same current. The current i flowing in filament m may be calculated from

$$i_m R_m = E - \sum_n (d/dt)(M_{m,n} i_n) \quad (3.51)$$

where R_m is the resistance of the m -th filament and i_n is the current in the n -th filament, while $M_{m,n}$ is the mutual inductance between the two general filaments. The summation in (3.51) covers all possible positions n in the wire cross-section, including that position in which n coincides with m . This coincidence defines the selfinductance of an individual filament as

$$L_m = M_{m,m} \quad (3.52)$$

Bearing in mind that

$$1/R = \sum_m (1/R_m) \quad (3.53)$$

$$i = \sum_m i_m = \sum_n i_n \quad (3.54)$$

Equation (3.51) can be solved for i_m , and summing this solution for all filament currents in accordance with (3.54) gives

$$i = E \sum_m (1/R_m) - (d/dt) \sum_m (1/R_m) \sum_n M_{m,n} i_n \quad (3.55)$$

Substitution of (3.53) into (3.55) and multiplication by R results in

$$iR = E - (d/dt) \left[\sum_m (R/R_m) \sum_n M_{m,n} i_n \right] \quad (3.56)$$

A comparison of (3.56) with (3.50) defines the selfinductance of the wire loop as

$$L = \sum_m (R/R_m) \sum_n M_{m,n} (i_m/i) \quad (3.57)$$

This is the most general and exact expression of selfinductance in terms of the filament self and mutual inductances of which the closed circuit is composed.

The expression for L takes on a more simple form when dealing with a wire of constant cross-section and uniform conductivity; a wire that is also very long compared to its cross-sectional dimension. All filaments are then substantially of the same length and they may all be made to have the same cross-section. The resistance and current ratios of (3.57) depend then merely on the total number of filaments. If this number is g , we have

$$R/R_m = i_m/i = 1/g \quad (3.58)$$

Equation (3.58) holds only so long as the rate of change of the applied voltage is sufficiently small for the current distribution over the conductor cross-section to remain substantially constant.

With (3.58) the expression for the loop selfinductance reduces to

$$L = (1/g^2) \sum_{m,n} M_{m,n} \quad (3.59)$$

In this form L is seen to be the mean of all possible mutual inductance permutations of the g filaments, including a total of g combinations in which the positions m and n coincide.

Maxwell [14] recognized that the mutual inductance of a pair of parallel straight lines is largely a function of the logarithm of the distance of separation d . For the purpose of mutual inductance calculations he further assumed that each conductor filament of finite thickness could be represented by a line coinciding with the filament axis. Then the average value of all the mutual inductances making up a long, straight conductor is determined by the average value of $\ln d$. Since there are g filaments involved, we have to deal with $g(g-1)/2$ different mutual inductances. A geometric mean distance (GMD) d' for all the filament combinations may now be defined by

$$\ln d' = 2/[g(g-1)] \sum_{g(g-1)/2} \ln d \quad (3.60)$$

Once the GMD of the conductor cross-section has been found, it becomes possible to equate the selfinductance of this conductor--in accordance with (3.59)--to the mutual inductance of a single pair of lines separated by d' . Maxwell has shown how to compute the GMD of a variety of conductor cross-sections. Furthermore, his GMD technique may equally well be applied to derive the mutual inductance of a pair

of straight and parallel conductors, each of them being subdivided into filaments. This latter computation requires the GMD of one conductor cross-section from the other, while the selfinductance calculations with (3.59) depend on the geometric mean distance of an area from itself.

Maxwell [14] found the GMD's for the most useful conductor configurations by analytical means. For example, the GMD of a circular area of radius r came to $0.7788r$, and that of a square area of side ' a ' to $0.44705a$. The GMD of a two-wire line is equal to the axial spacing between the conductors. The conductors have to be round wires, rods or tubes, but they need not be of the same diameter. In the case of a coaxial cable in which the outer conductor tube has an inner radius of r_i and an outer radius of r_o , the GMD, d' , is given by

$$\ln d' = (r_o^2 \ln r_o - r_i^2 \ln r_i) / (r_o^2 - r_i^2) - \frac{1}{2} \quad (3.61)$$

The shape and size of the inner conductor does not influence d' . Today it is possible to calculate the GMD for any conductor shape by computer assisted finite element analysis, using equation (3.60).

Maxwell's GMD method continues to be indispensable for practical inductance calculations. It is now often forgotten that, strictly speaking, it is valid only for very long, straight conductors. Even in this restricted domain it involves Sommerfeld's approximation. Sommerfeld [77] was the first to solve Neumann's mutual inductance formula (1.26) for a pair of parallel, straight filaments of finite length L and spacing d . His result was

$$M_{m,n} = 2 \{ L \ln[(L + \sqrt{L^2 + d^2})/d] - \sqrt{L^2 + d^2} + d \} \quad (3.62)$$

When L is very much greater than d , (3.62) simplifies to Sommerfeld's approximation

$$M_{m,n}/(2L) = -1 + \ln(2L) - \ln d \quad (3.63)$$

Only in this last approximation is the mutual inductance per unit length proportional to $\ln d$, as assumed by Maxwell.

Maxwell's GMD method, inter alia, ignores the selfinductance of the individual filaments. Applying Neumann's formula (1.26) to two coinciding filaments gives an infinite result, which must be meaningless. This is of fundamental importance because it shows the elements of filaments used in inductance calculations must be of finite size. It makes eminent sense only if they are elements of matter. There is no reason to believe that the elements of inductance calculations are not the very same elements which have been used in the computation of ponderomotive forces. In other words, we are dealing once again with metal atoms. Therefore, in the Ampere-Neumann electrodynamics, inductance is a property of matter and subject to the graininess of matter. It must be the metal atom which experiences both ponderomotive and electromotive forces, and there should be a difference between the two forces.

It has already been shown, in conjunction with equation (3.26), that every pair of conductor elements should be associated with an elemental mutual inductance $\Delta M_{m,n}$. This is true regardless of whether the elements belong to two different filaments or to the same filament. The selfinductance of a closed filament is then simply the sum of all the elemental mutual inductances of its element combinations. This disposes of the last vestige of selfinductance being something other than mutual inductance.

There exist formulas for the calculation of the selfinductance of thin wire circuits. They all suggest that the selfinductance of an infinitely thin wire should be infinite [78]. This cannot be true because it would prevent the start-up of any current flow in metals. The concept of the finite-size conductor element and equation (3.26) remove this difficulty from electromagnetic theory.

Inductance of Single-Filament Circuits

A filamentary circuit is taken to be a circuit in which the conductor cross-section is so small that forces and inductances may be calculated to adequate accuracy without further subdivision of the conducting area. Knowledge of the filament selfinductance is required for computing self and mutual inductances of relatively thick conductors. Take for example equation (3.59). The selfinductance defined by this equation depends on the sum of the elements of a $g \times g$ mutual inductance matrix which contains the filament selfinductances along the principal diagonal. In fact the diagonal elements will be greater than any other element in the matrix, which makes them particularly important when g is small.

The selfinductance of a closed filamentary circuit has been computed on page 205 and is given by equation (3.27). This formula was applied to a filament circle and gave its selfinductance, per unit radius, by a logarithmic law involving the number of elements of which the filament was composed, that is (3.34). The individual conductor (filament) element should be approximately as long as it is wide. This rule determines z , the number of elements in the filamentary circuit.

Self and mutual inductances, based on the elemental mutual inductance (3.26), may be assigned to portions of circuits without loss of physical meaning. Particularly useful are straight-line filaments of finite length, which can later be combined to make up complete circuits.

Let a straight filament section of length l be subdivided into z equal-length conductor elements. Then all inductive interaction within this section can be listed by a symmetrical, square matrix of order $z \times z$ with zeros along the principal diagonal. The selfinductance of the filament section is the sum of all matrix elements on one side of the princi-

pal diagonal. According to (3.26), two similarly directed conductor elements lying on the same straight line have a mutual inductance of

$$\Delta M_{m,n} = dm \cdot dn / r_{m,n} \quad (3.64)$$

The interactions of all neighbor-element combinations spaced dn apart will be found in the second diagonal, adjacent to the principal diagonal. The neighbor-pairs all have the same mutual inductance of $dm \cdot dn / dn - dm$ and there exist $(z-1)$ of them. The third diagonal contains the mutual inductances of pairs spaced two element-length apart. Their magnitudes are $dm/2$ and there are $(z-2)$ of them. Continuing in this way from diagonal to diagonal, the selfinductance of the straight filament may be written

$$\begin{aligned} L(\text{straight}) &= dm \cdot dn [(z-1)/dn + (z-2)/2dn + (z-3)/3dn + \dots] \\ &= dm \sum_{x=1}^{z-1} (z-x)/x \end{aligned} \quad (3.65)$$

Now the length l of the filament is

$$l = z \cdot dm = z \cdot dn \quad (3.66)$$

so that

$$L(\text{straight})/l = (1/z) \sum_{x=1}^{z-1} (z-x)/x \quad (3.67)$$

This summing operation has been performed for eight values of z from 100 to 40 000. The results are reproduced in table 9 and fig.72. As expected, they obey a logarithmic relationship. Regression analysis has shown this to be

$$L(\text{straight})/l = -0.42 + \ln z \quad (3.68)$$

Extrapolations of (3.68) to $z \cdot 10^6$ and 10^{12} are also noted on table 9. For a fundamental element length of 10 Angstrom, the two large z -values correspond to conductor filaments of

1 mm and 1 km length, respectively, which comprises most practical applications.

Table 9 Selfinductance per unit length of a straight filament

z	L(straight)/l	
	from (3.67)	from (3.68)
100	4.187	4.185
500	5.793	5.794
1000	6.485	6.487
2000	7.178	7.179
5000	8.095	8.095
10 000	8.788	8.788
20 000	9.481	9.480
40 000	10.174	10.173
10^6		13.390
10^{12}		27.196

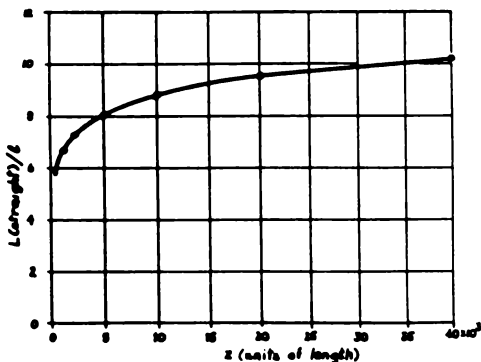


Fig.72 Selfinductance per unit length of straight filament. Curve from (3.68); points from (3.67).

If we treat a wire as a single filament, then for a fixed length of the filament, an increase in z implies a reduction in wire diameter. Figure 72 may therefore be used to determine the relationship between the selfinductance of a straight wire and its diameter. Alternatively, if the wire diameter is held constant, the increase in z represents a proportional increase in wire length. The selfinductance per unit length of a given wire is seen to increase logarithmically with length and never tends to a limit, however long the wire may be.

Knowledge of the selfinductance of rings, circular turns, and helically wound, circular solenoids is of the greatest importance in many areas of electromagnetic engineering. Maxwell addressed this subject with his GMD technique which has endured to this day. It is by no means perfect, nor easy, but it was the best one could do until computers became available. As Maxwell himself pointed out, the GMD method is rigorous only in the case of straight conductors, but it will furnish good approximate results when the cross-sectional dimension of the conductor, or the winding of a number of turns, is small compared to the diameter of the ring or the solenoid. Just how large the dimensional ratio must be for the approximation to hold, Maxwell did not specify.

To examine this last point we compare the mutual inductance of a pair of straight, parallel filaments with that of a pair of coaxial, circular filaments, the two pairs having the same length and spacing, as indicated in fig.73. The mutual inductance of the straight filament pair, M_s , is given by Sommerfeld's equation (3.62) and approximation (3.63). It was Maxwell who solved Neumann's mutual inductance formula (1.26) for two coaxial circles of radius r_1 and r_2 and a separation d between the planes of the circles. The solution takes the form

$$M_c = 4\pi\sqrt{r_1 r_2} \{[(2/k)-k]K - (2/k)E\} \quad (3.69)$$

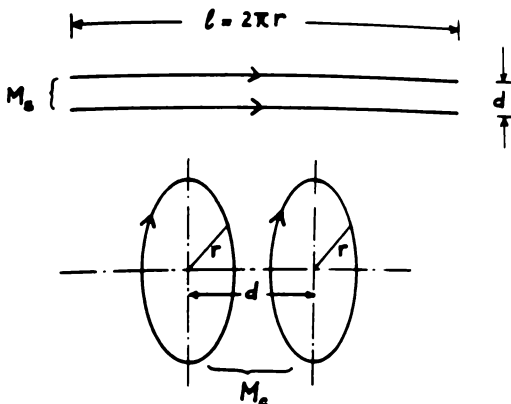


Fig.73 Comparison of the mutual inductance of a pair of straight with a pair of circular filaments of the same length and spacing

where K and E are complete elliptic integrals of the first and second kind, of modulus k . The modulus of the elliptic integrals is

$$k = 4r_1r_2/[(r_1+r_2)^2 + d^2] \quad (3.70)$$

Tables of elliptic integrals are readily available but interpolation between tabulated values is frequently inadequate. Grover [70] reports that no less than 100 series expansions and other formulas have been published to overcome this interpolation difficulty. For circles very close together Grover cites a logarithmic relationship corresponding to

$$M_c/(2\pi r) = \ln[4(r/d)^2 + 1] - 1.2275 \quad (3.71)$$

Figure 7.4 has been constructed for the computation of

the mutual inductance of two equal, coaxial filament circles by the finite element method. Each circle is divided into z equal arc-elements numbered from 0 to $z-1$. The element dm is held fixed in position $m=0$, while dn is taken around the circle n . Any individual position of dn is described in terms of the angle ϵ , which is related to n by

$$\epsilon = 360 n/z \quad (\text{degrees}) \quad (3.72)$$

The conductor element length is best written in terms of the radius r

$$dm = dn = 2\pi r/z \quad (3.73)$$

The distance between dm and dn can then be shown to be

$$r_{m,n} = r \sqrt{(d/r)^2 + 2[1 - \cos(360n/z)]} \quad (3.74)$$

Therefore, with (3.26), the mutual inductance between dm and the whole of the circle is

$$dm \int_{n=0}^{z-1} (\cos \epsilon / r_{m,n}) dn \quad (3.75)$$

This quantity would be same regardless where dm is situated on the circle m . Hence the mutual inductance between the two filament circles is simply z times (3.75). Substituting appropriately for the various parameters, this result is expressed by

$$M_c = 4\pi^2 (r/z) \int_{n=0}^{z-1} \cos(360n/z) / \sqrt{(d/r)^2 + 2[1 - \cos(360n/z)]} \quad (3.76)$$

Equation (3.76) tends to a finite limit as z is increased and fortunately it reaches this limit quite quickly unless the circles are extremely close together. Table 10 shows this convergence for two d/r ratios.

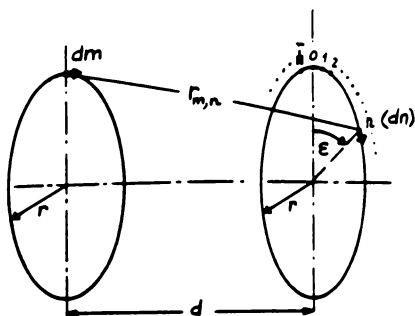


Fig.74 Construction for the solution of (3.76)

Table 10 Convergence of the mutual inductance of coaxial filament circles ($r=1$ cm)

$d/r=1$		$d/r=1/20$	
z	M_c (cm)	z	M_c (cm)
2	10.9116	20	53.4477
4	5.4558	50	40.3413
6	4.9999	100	38.7651
8	4.9482	200	38.6721
10	4.9417	300	38.6717
20	4.9408	400	38.6717
30	4.9408	500	38.6717
40	4.9408		
50	4.9408		

The data plotted on fig.75 compares the mutual inductance per unit length of a pair of parallel, straight filaments

(curve 1) with the mutual inductance per unit length of a pair of filament circles of the same length as the straight filaments. Curve 2 for the filament circles indicates excellent agreement of the finite element formula (3.76) with Grover's logarithmic formula (3.71).

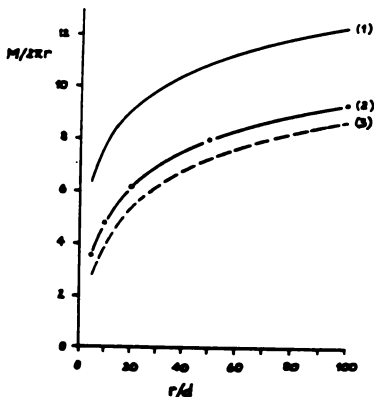


Fig.75 Mutual inductance per unit length of (1) parallel, straight filaments by (3.62); (2) coaxial filament circles by (3.71), points from (3.76); (3) coaxial filament circles by (3.69), k given to three significant figures.

Interpolation from tables of elliptic integrals for Maxwell's solution (3.69) predicts lower inductance values for the filament circles. Nevertheless, as curve 3 of fig.75 indicates, the Maxwell solution is a reasonable approximation to (3.71) and (3.76). A regression analysis of the computer data obtained with (3.76) for the interval $10 \leq r/d \leq 100$ produced the following logarithmic formula of the finite element analysis

$$M_c/(2\pi r) = 0.18 + 1.99 \ln(r/d) \quad (3.77)$$

When substituting numerical values into (3.71) and (3.77) it will be found that these two logarithmic formulas are almost identical.

Let us return to the question of the value of r/d at which the GMD method applied to filament circles becomes unreliable? First of all it should be noted on fig.75 that up to $r/d=100$ the mutual inductance per unit length of two circles differs appreciably from that of straight filaments. The percentage gap between the two quantities decreases as r/d becomes larger. For $d=10^{-7}$ cm (i.e. atomic spacing) and $2\pi r=100$ cm it is down to eight percent. In view of this finding, it seems unrealistic to assume, as Maxwell did, that the two quantities can be equated to each other. Here it must be remembered that Maxwell did not have the benefit of knowing Sommerfeld's formula (3.62). For very large r/d ratios both the elliptic integral and the finite element solutions agree with (3.77), and then the GMD method may be applied to circular conductors. Therefore the selfinductance of a circular ring made, for example, of a round wire of radius 'a' may be computed with (3.77) so long as the GMD of the wire cross-section ($-0.7788a$) is substituted for d .

How large must r/GMD be for this approximation to hold? It certainly would not hold when $r/\text{GMD}=1$ cm, for (3.77) would then give a mutual inductance of 1.13 cm while the finite element method (table 10) indicates a value of 4.94 cm. But as fig.75 indicates, for $r/d=10$ agreement becomes more reasonable. It is therefore suggested that the GMD method applied to circular conductors cannot be relied upon unless the r/GMD ratio is at least ten.

The finite element method of computing the selfinductance of an isolated conductor filament may be applied to any circuit geometry. Computation times strongly depend on cir-

cuit symmetry. To show some of the complexity that may arise, the filament square of fig.76 will be taken as the final example. The sides of the square have been labelled (1) to (4) and each is divided into z equal-length conductor elements, so that the length of one side is given by

$$a = z \cdot dm = z \cdot dn \quad (3.78)$$

Element dm successively occupies positions 1 to $z/2$ along side (1). The inductance contributions from the remaining positions of dm may be deduced from the symmetry of the square. In fact the elemental inductance matrix will be of the order of $4z \times 4z$. The mutual inductance of each element pair is listed twice on this matrix but makes only one contribution to the filament selfinductance. Hence just the $8z^2 - z/2$ matrix elements to one side of the principal diagonal need be summed. Now if dm moves from 1 to $(z/2)$ on side (1) while dn travels around the whole square, $4z \cdot z/2 - 2z^2$ positions in the inductance matrix will be filled. A similar area of the matrix will be covered if dm moves from $(z/2)+1$ to z , and the sum of the respective elements will be identical to that obtained in the first operation. By repeating the process for dm on the remaining three sides, the whole of the inductance matrix may be filled. Therefore symmetry permits us to write

$$\begin{aligned} L(\text{square}) = (8/2) \sum_{m=1}^{z/2} \sum_{n=1}^z \{ & [F(\alpha, \beta, \epsilon) dn/r_{m,n}]_{S1} + \\ & + [F(\alpha, \beta, \epsilon) dn/r_{m,n}]_{S2} + \\ & + [F(\alpha, \beta, \epsilon) dn/r_{m,n}]_{S3} + \\ & + [F(\alpha, \beta, \epsilon) dn/r_{m,n}]_{S4} \} \quad (3.79) \end{aligned}$$

where $S1$ stands for side (1) and so on. With the construction of fig.76 the individual terms of the n -sum of (3.79) are seen to be

$$L(\text{square})/(4a) =$$

$$= (1/z) \sum_{m=1}^{z/2} \sum_{n=1}^z \{ 1/|m-n| + 3(z+k-m)(n-k) / [(z+k-m)^2 + (n-k)^2]^{1.5} \\ + 1/[(m-n)^2 + z^2]^{0.5} - 3(m-n)^2 / [(m-n)^2 + z^2]^{1.5} \\ + 3(m-k)(n-k) / [(m-k)^2 + (n-k)^2]^{1.5} \} \quad (3.84)$$

Equation (3.84) has been solved by computer for five values of z from 6 to 80. The results are listed in table 11. As in previous examples, the filament selfinductance per unit length again obeyed a logarithmic relationship. For the square this was found to be

$$L(\text{square})/(4a) = 2.38 + \ln z \quad (3.85)$$

The extent of the agreement between (3.84) and (3.85) is also indicated in table 11.

Table 11 Selfinductance per unit length of a filament square

z	L(square)/(4a)	
	by (3.84)	by (3.85)
6	4.0711	4.0643
20	5.1572	5.1960
40	5.8247	5.8475
60	6.2049	6.2287
80	6.5050	6.4991
10^6		15.3666
10^{12}		28.3532

Inductance of Straight Conductors and Cables

Circuit self and mutual inductances are useful only if the current distribution over the conducting cross-section is uniform, or approximately so. Approximate uniform current distribution always applies to circuits of so small a cross-section that they may be safely treated as single filaments. It has been the major reason for developing and employing single-filament formulas.

One cause of the non-uniform current distribution in a homogeneous conductor are differences in filament length that arise, for example, in solenoids and all curved conductor sections. The second cause of current concentrations in certain parts of the conductor cross-section are skin effect phenomena due to the flow of alternating or pulse currents. As the inductance of an ac or pulse current circuit is responsible for the induced back e.m.f. generated by the time-varying current, it turns out that no adequate inductance formulas are available for precisely the cases where inductance is of greatest importance.

However there is some interest in the inductance of straight conductors which are too large to be treated as single filaments and carry dc or low-frequency ac currents that do not significantly disturb the uniformity of current distribution. This applies to many power conductors used for the transmission and distribution of electricity. In these cases the computed circuit inductance may be required for reactance calculations, or the determination of magnetically stored energy and electrodynamic forces derived from the energy via the virtual work concept.

Although a straight conductor of finite length does not form a closed circuit, in the Ampere-Neumann electrodynamics it is permissible and expedient to associate it with force, inductance, and stored energy. The selfinductance of a homogeneous, finite-length, straight conductor is given

by equation (3.59). This last expression implies that each place in the square matrix of the filament mutual inductances contains a number, and therefore each mutual inductance appears twice in the double summation, once on either side of the principal diagonal. Hence the selfinductance of a homogeneous, straight conductor is simply the average of the mutual inductances of the filament pairs and the selfinductances of individual filaments.

It is convenient to work with filament self and mutual inductances per unit length. Equation (3.68) is the appropriate formula for the selfinductance. To comply with the rules of finite element analysis, the number of elements in each filament must be

$$z = l/dm = l/dn \quad (3.86)$$

Sommerfeld's solution (3.62) should be used for the filament mutual inductances. Per unit length, this takes the form

$$M_{m,n}/l = 2\{\ln[(l/d) + \sqrt{1 + (l/d)^2}] - \sqrt{1 + (d/l)^2} + d/l\} \quad (3.87)$$

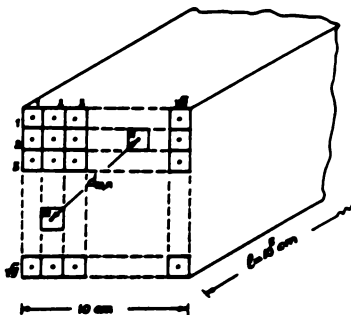


Fig. 77 Square-section conductor resolved into filaments

The amount of computation involved in determining the selfinductance of a straight conductor by (3.59) depends, of course, on the total number of filaments g into which the conductor is resolved. Surprisingly, a relatively small number of filaments gives a quite accurate result. This will be illustrated with the 10 x 10 cm square-section conductor of fig.77 which is 1 km long and has been subdivided into g square-section filaments. Computer results for this arrangement are listed in table 12 for g varying between 100 and 10,000. It will be seen that multiplication of the number of filaments by a factor of 100 adjusts the L/l value by only 1.5 percent. Hence, at least in this particular example, 100 filaments give a fairly accurate result.

Table 12 Selfinductance per unit length of a 1 km long straight conductor of 10 x 10 cm square cross-section

g	L/l
100	19.7215
400	19.4899
900	19.4486
2500	19.4281
10 000	19.4198

It should be observed that the selfinductance per unit length of a 1 km long, straight filament ($z=10^{12}$) is 27.196. The selfinductance per unit length of the 10 x 10 cm conductor is significantly smaller. Even though the length-to-width ratio of this conductor is 10,000, it cannot be adequately represented by a single filament. It should also be noted that resolution into too small a number of filaments will overestimate the selfinductance. The data of table 12 does not obey a logarithmic law. Therefore L/l for the smallest possible filament cross-section cannot be computed. However the trend of the data of table 12 suggests that it would not differ much from 19.4.

The geometric mean distance (GMD) of a square area of side 'a' is 0.44705a. Equating this to d in equation (3.87) makes the selfinductance per unit length of the 10 x 10 cm square conductor of 1 km length equal to 19.4172. This is remarkably close to the value listed in table 12 for g-10,000. It is likely to be the limiting value when the filament subdivision is driven to the atomic limit. The GMD method represents by far the easiest way of calculating the selfinductance of a straight conductor when the GMD of the conductor cross-section is known. For any other conductor shape the finite element analysis illustrated by fig.77 may be used with confidence.

The equivalence of the GMD and finite element techniques may also be shown as follows. When $d/l \ll 1$, the non-logarithmic part of (3.87) is very nearly equal to -1 and constant, that is independent of the actual length of the conductor. Sommerfeld's solution (3.87) for this case reduces to the approximation

$$M_{m,n}/l = 2[-1 + \ln 2 + \ln l - \ln d] \quad (3.88)$$

Since the selfinductance is equal to the average mutual inductance of the filament combinations, we may write

$$L/l = (M_{m,n}/l)_{av} = -2 + 2\ln 2 + 2\ln l + 2(\ln d)_{av} \quad (3.89)$$

where $(\ln d)_{av}$ is the average value of $\ln d$. This may be equated to

$$(\ln d)_{av} = \ln(\text{GMD}) \quad (3.90)$$

The Sommerfeld approximation (3.88) is not valid when d/l cannot be ignored compared to 1. In such cases the average mutual inductance has to be determined by the much longer finite element process. To obtain an idea over what range of d/l approximation (3.88) may not be adequate, the logarithmic part (A) and the remainder (B) of (3.87) have

have been computed with d/l ranging from 1 to 10^{-5} .

In this particular case, it seems, Sommerfeld's approximation becomes unreliable when $d/l > 10^{-2}$. As a rule of thumb, therefore, the GMD method should not be used unless the conductor is more than 100 times as long as it is wide.

A straight conductor arrangement of great practical import is the parallel go-and-return circuit. When the distance between the conductors is less than one percent of their length, the end connections closing the circuit have little effect on the total inductance and they may be ignored. While studying the selfinductance of a single conductor, the direction of current flow was of no consequence, so long as it was the same in each conductor element. This is not the case in the go-and-return circuit. It has to be remembered that Sommerfeld's solution (3.62) or (3.87) of Neumann's mutual inductance formula (1.26) assumes that dm and dn point in the same direction. If one of them is reversed, $\cos\epsilon$ of every element combination changes from +1 to -1 and (3.62) and (3.87) change sign.

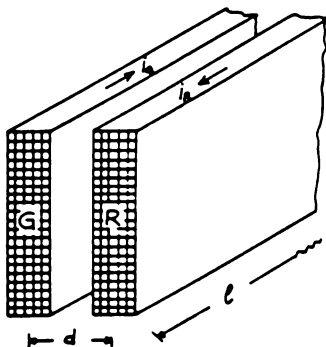


Fig.78 Filament model of a symmetrical, straight go-and-return circuit

Consider the go-and-return circuit of fig.78. Each of the two conductors is of the same uniform cross-section and made of the same homogeneous conductor material. In this symmetrical situation it is convenient to subdivide each conductor into the same number of equal-area filaments. Figure 79 is the concomitant $2g \times 2g$ mutual inductance matrix with each filament selfinductance doubled. In this particular form of the matrix, each real inductance appears twice and the sum of all real inductances is half the sum of the elements in the matrix.

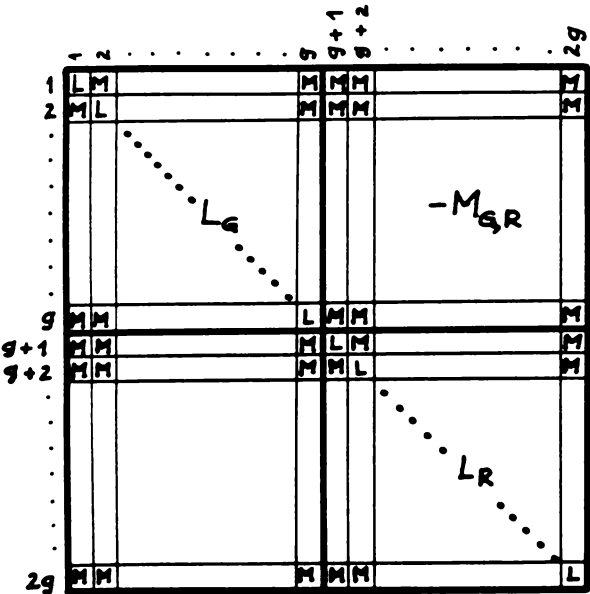


Fig.79 Mutual inductance matrix of symmetrical, straight go-and-return circuit

The energy stored by any pair of filaments m and n is

$$\Delta P_{m,n} = M_{m,n} i_f^2 \quad (3.91)$$

where the filament current is defined by

$$i_f = i_G/g = i_R/g \quad (3.92)$$

If the subscript G-R stands for the complete go-and-return circuit, the total stored energy may be written

$$P_{G-R} = \frac{1}{2} L_{G-R} i_G^2 = \frac{1}{2} i_f^2 \sum_m \sum_n M_{m,n} \quad (3.93)$$

The double summation of (3.93) must comprise all the elements of the matrix of fig.79. According to (3.92) and (3.93) the selfinductance of the go-and-return circuit is

$$L_{G-R} = (1/g^2) \sum_m \sum_n M_{m,n} \quad (3.94)$$

The matrix of fig.79 may be partitioned into four quarters, and with these partial matrixes equation (3.94) may be split into

$$L_{G-R} = (1/g^2) \left(\sum_{m=1}^g \sum_{n=1}^g M_{m,n} - \sum_{m=1}^g \sum_{n=g+1}^{2g} M_{m,n} - \sum_{m=g+1}^{2g} \sum_{n=1}^g M_{m,n} + \sum_{m=g+1}^{2g} \sum_{n=g+1}^{2g} M_{m,n} \right) \quad (3.95)$$

It will be recognized that the first term of (3.95) is the selfinductance L_G of the conductor G and the last term is L_R . The middle terms are equal to each other and represent the mutual inductance between G and R. Hence (3.95) is equivalent to

$$L_{G-R} = L_G + L_R - 2M_{R,G} \quad (3.96)$$

An equation like (3.96) applies to any go-and-return circuit, regardless of symmetry. If each conductor is resolved into

a different number of filaments, then the mutual inductance matrix corresponding to that of fig.79 has to be partitioned into two squares of different size and two rectangles. The same method may be applied to the three conductors of a three-phase power transmission circuit [79]. Equation (3.96) is particularly useful when the circuit is long compared with the distance between the conductors so that the GMD method may be used for determining L_G , L_R , and $M_{G,R}$.

By way of an example, take two round conductors of radius r and separated from each other by the axial spacing d . The GMD of the circular area is $0.7788r$ and the GMD between two circular areas is equal to the axial spacing d . Then with Sommerfeld's approximation and (3.96) we obtain

$$L_{G-R}/l = 4[-1 \cdot \ln 2 + \ln l - \ln(0.7788r)] - 4[-1 \cdot \ln 2 + \ln l - \ln d] \\ - 4 \ln[d/(0.7788r)] \quad (3.97)$$

The selfinductance formula normally quoted for parallel wire lines agrees with (3.97) except that sometimes the logarithm is approximated to $\ln(d/r)$. In the development of (3.97) it becomes clear why the selfinductance per unit length of a go-and-return circuit does not depend logarithmically on circuit length. The $\ln l$ terms cancel. The selfinductance per unit length of an isolated, straight conductor is length-dependent, as can be seen from equation (3.89).

Maxwell [14] derived a useful theorem relating to the GMD between two areas A and X , when X can be split up in subareas $X_1, X_2, X_3, \dots, X_n$, in such a way that the GMD's between A and the subareas are known to be $x_1, x_2, x_3, \dots, x_n$. The theorem states that the GMD between A and X is

$$\ln(\text{GMD}) = (X_1 \ln x_1 + X_2 \ln x_2 + X_3 \ln x_3 + \dots + X_n \ln x_n) / X \quad (3.98)$$

$$\text{where } X = X_1 + X_2 + X_3 + \dots + X_n \quad (3.99)$$

TRANSIENT AND ALTERNATING CURRENTS IN LINEAR CONDUCTORS

The term linear conductor is meant to imply that the current streamlines, and therefore the conductor filaments, are straight and parallel. The mutual inductance between filaments is then given by Sommerfeld's solution (3.62) and the selfinductance of individual filaments may be calculated with (3.68). The current distribution over the cross-section of linear conductors is of interest in pulse and ac power technology.

Maxwell [14] was first to address the question of the distribution of time-varying currents over the area of linear conductors. He spoke of cylindrical conductors and the difference in current intensity in the various cylindrical strata. This was the beginning of the skin effect theory which was further developed by Raleigh [80] and others. Skin effect equations derived from field theory have been solved only for circular section conductors. In the case of non-circular conductors the analytical approach fails because of a lack of knowledge of the appropriate boundary conditions. This deficiency in the quantitative evaluation of skin effect phenomena--and its impact on Joule heating, magnetic energy storage, and force distribution--was first overcome by Silvester [81] with a computer-assisted finite element method.

We start by considering the irregularly shaped conductor cross-section of fig.80. This has been subdivided into a total of g equal-area square filaments. The two general filaments, m and n , are separated by the distance $d_{m,n}$. For the sake of simplicity we make the conductor of a homogeneous material such that each filament of length l has the same resistance R_f . If a time-varying current is driven along this conductor by an electromotive force e , which will be the same for every filament, then the current in the general filament m is governed by

$$e = i_m R_m + e_{b,m} \quad (3.100)$$

where $e_{b,m}$ is the back e.m.f. induced in the filament m . The task facing us is to find this back e.m.f. which depends on all the other filament currents. The latter, in turn, are also controlled by an equation like (3.100). Unless the number of filaments is very small, the solution process is complex and time consuming. Not until computers became available was it possible to make any headway in this endeavor.

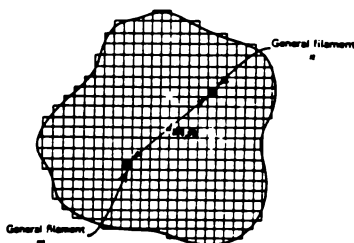


Fig.80 Conductor subdivision into square filaments

If we denote the mutual inductance between two general filaments by $M_{m,n}$ and the selfinductance of the general filament m by L_m a set of simultaneous equations corresponding to (3.100) may be structured as follows

$$\begin{aligned}
 e &= (R_f i_1 + L_1 i_1') + M_{1,2} i_2' + \dots + M_{1,g} i_g' \\
 e &= M_{2,1} i_1' + (R_f i_2 + L_2 i_2') + \dots + M_{2,g} i_g' \\
 &\vdots \\
 e &= M_{g,1} i_1' + M_{g,2} i_2' + \dots + (R_f i_g + L_g i_g')
 \end{aligned}
 \tag{3.101}$$

where i_m' stands for the time derivative of i_m . When all currents are constant, (3.101) reduces to the dc case in

which the current distribution is determined only by resistances. As all filament resistances are the same, the current distribution would then be uniform.

Let us immediately concentrate on the most important practical example in which the driving e.m.f., and therefore all filament currents, are sinusoidal of radian frequency ω , so that

$$M_{m,n} i'_n = j\omega M_{m,n} i_n = Z_{m,n} i_n \quad (3.102)$$

$$R_f i_m + L_m i'_m = (R_f + j\omega L_m) i_m = Z_{m,m} i_m \quad (3.103)$$

where $j = \sqrt{-1}$. $Z_{m,n}$ and $Z_{m,m}$ are now mutual and self impedances replacing the back e.m.f.'s of (3.100).

The array of simultaneous equations (3.101) may be abbreviated in matrix notation to

$$e = [Z]\{i\} \quad (3.104)$$

where $\{i\}$ is a vector or column matrix. The impedance matrix is square, symmetrical and of order g , the number of filaments in the conductor.

$$[Z] = \begin{bmatrix} Z_{1,1} & Z_{1,2} & \dots & Z_{1,g} \\ Z_{2,1} & Z_{2,2} & \dots & Z_{2,g} \\ \vdots & \vdots & \ddots & \vdots \\ Z_{g,1} & Z_{g,2} & \dots & Z_{g,g} \end{bmatrix} \quad (3.105)$$

One of the solutions of (3.104) may be written

$$\{i\} = [Z]^{-1} e \quad (3.106)$$

In full the solution (3.106) should be written

$$\begin{Bmatrix} i \\ i \\ \cdot \\ \cdot \\ \cdot \\ i \end{Bmatrix} = (1/|Z|) \begin{bmatrix} |Z_{1,1}| & |Z_{1,2}| & \dots\dots\dots & |Z_{1,g}| \\ |Z_{2,1}| & |Z_{2,2}| & \dots\dots\dots & |Z_{2,g}| \\ \cdot & & & \\ \cdot & & & \\ \cdot & & & \\ |Z_{g,1}| & |Z_{g,2}| & \dots\dots\dots & |Z_{g,g}| \end{bmatrix} \quad (3.107)$$

Many sophisticated mathematical techniques have been described which marshal and, to a certain extent, diminish the monumental amount of arithmetic involved in solving (3.106) when g is greater than, say, ten. Sylvester [81] was first to point out that the problem could be handled with what he called modal network theory. It turns out to be an exercise in eigenvector and eigenvalue calculus. Not only does this method reduce the computational work, but its main advantage is the ready availability of computer programs which have been devised to determine the eigenvectors of any square and symmetrical matrix such as (3.107).

For a small number of filaments, the direct solution process involving the determinant of the impedance matrix (3.107) may be employed. To illustrate this we take the simple example of the strip conductor of fig.81. The strip has been subdivided into three square-section ($a \times a$) filaments. The length of the straight conductor is l . If the strip is made of copper and $a=1$ cm, $l=1000$ cm, the room temperature resistance of each filament is $R_f=1.76$ m Ω .

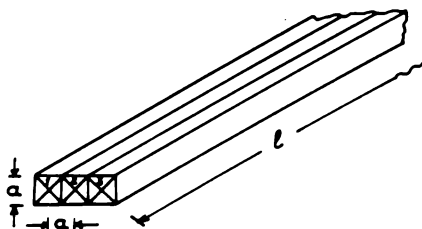


Fig.81 Three-filament rectangular strip conductor

Since the GMD of the square filament section is 0.44705a, the self and mutual inductances resulting from (3.62) are, this time in MKS-A units

$$L_1 = L_2 = L_3 = 14.813 \mu\text{H}$$

$$M_{12} = M_{23} = 13.204 \mu\text{H}$$

$$M_{13} = 11.820 \mu\text{H}$$

Let us write the simultaneous equations for the three-filament conductor as follows

$$Z_{11}i_1 + Z_{12}i_2 + Z_{13}i_3 = e$$

$$Z_{21}i_1 + Z_{22}i_2 + Z_{23}i_3 = e \quad (3.108)$$

$$Z_{31}i_1 + Z_{32}i_2 + Z_{33}i_3 = e$$

where i_1 , i_2 , and i_3 are the three sinusoidal filament currents, e is the driving e.m.f. and the Z impedances are complex. As the selfinductances of the filaments are all the same we have

$$Z_{11} = Z_{22} = Z_{33} = R_f + j\omega L_1 \quad (3.109)$$

Also because $M_{12} = M_{23}$

$$Z_{12} = Z_{21} = Z_{23} = Z_{32} = j\omega M_{12} \quad (3.110)$$

$$Z_{13} = Z_{31} = j\omega M_{13} \quad (3.111)$$

The determinant D of the impedance matrix may be evaluated in terms of its cofactors. Then because of the equality of the selfinductances and certain mutual inductances, the determinant reduces to

$$D = Z_{11}^3 - 2Z_{12}^2(Z_{11} - Z_{13}) - Z_{11}Z_{13}^2 \quad (3.112)$$

The numerical value of this determinant depends on the frequency of e . Let this be the power frequency $f=60$ Hz. Therefore $\omega = 2\pi f = 377$ rad/s. Then

$$Z_{11} = R_f + j\omega L_1 = (1.76 + 5.58j) \times 10^{-3} \quad \Omega$$

$$Z_{12} = j\omega M_{12} = 4.98 \times 10^{-3} j \quad \Omega$$

$$Z_{13} = j\omega M_{13} = 4.46 \times 10^{-3} j \quad \Omega$$

and the determinant is found to be

$$D = -36.64 + 44.66j$$

The three solutions of (3.108) are given by

$$i_1 = C_1/D; \quad i_2 = C_2/D; \quad i_3 = C_3/D \quad (3.113)$$

C_1 , C_2 , and C_3 are modified impedance determinants in which, for C_k , the k -th column is replaced by the constants of (3.108). From the symmetry of the conductor we know that $i_1 = i_3$ and therefore $C_1 = C_3$. Only C_1 and C_2 need be computed.

$$C_1 = \begin{vmatrix} e & Z_{12} & Z_{13} \\ e & Z_{22} & Z_{23} \\ e & Z_{32} & Z_{33} \end{vmatrix} = e(Z_{11}Z_{22}Z_{33} - Z_{11}Z_{23}Z_{32} - Z_{12}Z_{21}Z_{33} - Z_{13}Z_{23}Z_{31}) \quad (3.114)$$

$$C_1 = e(2.43 + 3.03j) \times 10^3$$

$$C_2 = \begin{vmatrix} Z_{11} & e & Z_{13} \\ Z_{21} & e & Z_{23} \\ Z_{31} & e & Z_{33} \end{vmatrix} = e(Z_{11}(Z_{22}Z_{33} - Z_{23}Z_{32}) - Z_{12}(Z_{21}Z_{33} - Z_{23}Z_{31}) + Z_{13}(Z_{21}Z_{32} - Z_{22}Z_{31})) \quad (3.115)$$

$$C_2 = e(3.01 + 2.12j) \times 10^3$$

From this it follows that

$$i_1 = i_3 = C_1/D = (13.87-65.79j)e$$

$$i_2 = C_2/D = (-4.68-63.56j)e$$

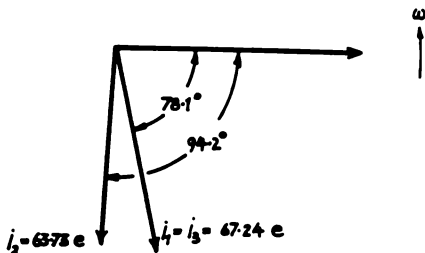


Fig.82 Phasor diagram of strip currents

The amplitudes and phase relationships of the filament currents with respect to the driving e.m.f. are shown in fig.82. As expected, the current amplitudes in the two outer filaments are larger than in the center filament. This is a manifestation of the skin effect. It would be more pronounced at higher frequencies. Figure 82 also shows the phase differences between the filament currents. The total current I flowing in the conductor is the phasor sum of the filament currents, or

$$I = 2(13.87-65.79j)e + (-4.68-63.56j)e$$

$$= (23.06-195.14j)e$$

$$|I| = 196.5 e \text{ (lagging by } 83.3^\circ)$$

This example also demonstrates that isolated linear conductors made of copper or aluminum are highly inductive with the ac current through them lagging the driving e.m.f. by

nearly 90 degrees. However, when two closely spaced conductors form a go-and-return circuit, their combined inductance is greatly reduced.

One of the primary reasons for computing the ac current distribution is to determine what is known as the ac resistance of the conductor. In the present example this would be given by

$$R_{ac} = (2|i|^2 R_f + |i|^2 R_f) / |I|^2 = 0.3394 R_f$$

The dc resistance of the strip conductor is $0.3333 R$. Hence by passing 60 Hz current instead of dc through the conductor the Joule heating is increased by just under two percent. At higher frequencies this increase would of course be greater. Finally we note that the ac current distribution is a steady-state distribution in which the current in the center is permanently smaller than at the perimeter. This will not be the case for pulse currents. At the pulse-front the current distribution is similar to the ac case, but on the decaying side of the pulse the current is more concentrated in the core of the conductor than on the outside. This is a little known phenomenon which may be called the 'core effect' [82].

A qualitative explanation of the core effect may be obtained from the back e.m.f. equation (3.100). On the rising side of the pulse, where de/dt and all di/dt are positive, the back e.m.f. will oppose current flow. The back e.m.f. is greatest where the inductance is greatest, that is where a filament has the most close neighbors. Hence on the pulse front the back e.m.f. will reduce current flow in the center of the conductor. At the peak of the pulse, when de/dt and all di/dt are zero, the current distribution will be governed by the filament resistances. Now on the decaying side of the pulse the time derivatives of e and i are everywhere negative, and the back e.m.f.'s reverse sign and assist continued current flow most in the center of the conductor

and least at the perimeter.

A quantitative proof of the core effect is best provided with the help of Laplace transformations. This requires the conversion of a function of time $f(t)$ into a function $f(s)$ of the Laplace operator s by

$$f(s) = \int_0^{\infty} f(t) e^{-st} dt \quad (3.116)$$

Algebraic operations are then performed on $f(s)$ until it is in a convenient form for re-conversion to the desired solution $f(t)$. Even for the simple three-filament conductor of fig.81 the procedures are quite lengthy and only an outline will be given here, omitting much of the detail. An excellent account of the handling of transient currents with Laplace transforms has been published by Greenwood [83].

The starting point is to set up the array of three simultaneous equations for the conductor of fig.81. The format of this array has been provided by (3.101). Instead of applying a voltage pulse we will consider the switch-on transient e -constant for $t > 0$, $e=0$ for $t < 0$, and later the corresponding switch-off transient. A combination of the two is equivalent to a square voltage pulse. In the case of the switch-on transient the initial current in each filament is zero and the Laplace transforms of the filament current i and its time derivative are simply I and $I.s$, respectively. Furthermore, the Laplace transform of the voltage step e is e/s . With this notation, and remembering that all three filaments have the same resistance R and selfinductance L , and $M_{12} = M_{23}$, the three simultaneous equations may be written

$$\begin{aligned} s(R+Ls)I_1 + M_{12}s^2I_2 + M_{13}s^2I_3 &= e \\ M_{12}s^2I_1 + s(R+Ls)I_2 + M_{12}s^2I_3 &= e \\ M_{13}s^2I_1 + M_{12}s^2I_2 + s(R+Ls)I_3 &= e \end{aligned} \quad (3.117)$$

The impedance determinant of (3.117) is

$$D = \begin{vmatrix} s(R+Ls) & M_{12}s^2 & M_{13}s^2 \\ M_{12}s^2 & s(R+Ls) & M_{12}s^2 \\ M_{13}s^2 & M_{12}s^2 & s(R+Ls) \end{vmatrix} - s^3 \begin{vmatrix} (R+Ls) & M_{12}s & M_{13}s \\ M_{12}s & (R+Ls) & M_{12}s \\ M_{13}s & M_{12}s & (R+Ls) \end{vmatrix} \quad (3.118)$$

With the resistance and inductance values which have already been specified for the ac example, the derterminant can be shown to be equal to

$$D = 1.918 \times 10^{-16} s^3 (s+44.19)(s+588.09)(s+1093.7) \quad (3.119)$$

The two modified impedance determinants corresponding to (3.114) and (3.115) are

$$C_1 = \begin{vmatrix} e & M_{12}s^2 & M_{13}s^2 \\ e & s(R+Ls) & M_{12}s^2 \\ e & M_{12}s^2 & s(R+Ls) \end{vmatrix} \quad (3.120)$$

$$C_2 = \begin{vmatrix} s(R+Ls) & e & M_{13}s^2 \\ M_{12}s^2 & e & M_{12}s^2 \\ M_{13}s^2 & e & s(R+Ls) \end{vmatrix} \quad (3.121)$$

Having made the appropriate numerical substitutions, the last two determinants were found to be equal to

$$C_1 = 4.816 \times 10^{-12} s^2 (s^2 + 1682s + 6.432 \times 10^5) e \quad (3.122)$$

$$C_2 = 6.734 \times 10^{-13} s^2 (s^2 + 8410s + 4.6 \times 10^6) e \quad (3.123)$$

Hence the Laplace transform of the currents in filaments 1 and 3 is

$$I_1 - I_3 = C_1 / D$$

$$= 25,109 e (s^2 + 1682s + 6.432 \times 10^5) / [s(s+44.19)(s+588.09)(s+1093.7)] \quad (3.124)$$

Similarly, I_2 , the current in the center filament is

$$I_2 = C_2 / D$$

$$= 2.043 \times 10^6 e (s^2 + 8410s + 4.6 \times 10^6) / [s(s+44.19)(s+588.09)(s+1093.7)] \quad (3.125)$$

The s-functions of (3.124) and (3.125) have to be split into partial fractions for which the inverse Laplace transforms are known. This can be achieved with

$$(s^2 + us + v) / [s(s-a)(s-b)(s-c)] = A_1 / [s(s-a)] + B_1 / [(s-a)(s-b)]$$

$$+ C_1 / [(s-b)(s-c)] \quad (3.126)$$

and the identity

$$s^2 + us + v \equiv A_1 (s-b)(s-c) + B_1 s(s-c) + C_1 s(s-a) \quad (3.127)$$

The three partial fraction numerators come to

$$A_1 = v / (bc) \quad (3.128)$$

$$B_1 = (a + u + v/a) / (a-c) - A_1 (a-b)/a \quad (3.129)$$

$$C_1 = (c + u + v/c) / (c-a) \quad (3.130)$$

It follows from (3.124) and (3.126) that the inverse transform of the currents in filaments 1 and 3 may now be written

$$i_1 = i_3$$

$$-25.109e[A_1(1 - \epsilon^{at})/(-a) + B_1(\epsilon^{at} - \epsilon^{bt})/(a-b) + C_1(\epsilon^{bt} - \epsilon^{ct})/(b-c)]$$

(3.131)

where ϵ is the base of natural logarithms. Using (3.127) another set of partial-fraction numerators A_2 , B_2 , and C_2 may be found for the current in the middle filament (3.125). The time dependence of this current may then be expressed by

$$i_2 = 2.043 \times 10^6 e[A_2(1 - \epsilon^{at})/(-a) + B_2(\epsilon^{at} - \epsilon^{bt})/(a-b) + C_2(\epsilon^{bt} - \epsilon^{ct})/(b-c)]$$

(3.132)

It should be noted that the roots a , b , and c are the same for i_1 and i_2 and they are all negative. Substituting the previously specified filament resistance and self and mutual inductances for obtaining the A , B , C , coefficients, evaluation of the filament currents resulted in the figures listed in table 13 which apply to the conductor of fig. 81.

One second after applying the electromotive force to the conductor, the currents have attained their steady state values of 568.2 A. This is equal to e/R when $e=1$ volt. It will be seen that during the switch-on transient the current in the center filament is smaller than the current in the two outer filaments. In this case the difference between i_1 and i_2 is quite small. The true current distribution would be less uniform because the small number of three filaments gives too crude an approximation. The small number of filaments hides the fact that the current density will be a maximum right at the corners of the conductor where a thin filament has fewer near-neighbors than anywhere else

in the conductor cross-section. It is the multiplicity of near-neighbor filaments and their associated strong inductive interactions which delay current growth in the center of the conductor. Computer solutions for 100 filaments are feasible and they would show quite accurately how the transient current distributes itself within the conductor.

The current distribution for the switch-off transient has been calculated by the same finite filament method and the results are also shown in table 13. It will be noticed that the current distribution in the strip conductor is reversed. The induced e.m.f.'s, due to near neighbor interactions, now reinforce the center current more than the outside currents. This has been called the "core effect" [82] to distinguish it from the skin effect.

Field theory relies on the idea of magnetic field diffusion into the conductor metal for explaining the skin effect. The diffusion model cannot deal with the core effect. Presumably this is the reason why switch-off current distributions have never been analysed in the literature. The finite filament model solves this problem for the first time. Skin effect calculations also benefit from the finite filament method. A rigorous solution of magnetic field diffusion exists only for infinite half-space. The resulting formula is inadequate for many practical situations involving wires and cables. Maxwell [14] himself fell back on the Ampere-Neumann filament concept and developed the elliptic integral technique for calculating skin effects in round conductors. Until the finite filament method became available it was not possible to calculate the skin effect in rectangular conductors.

We may consider the two switching transients to be the front and tail of a square voltage pulse. At the front the e.m.f. applied to each filament is the same. This applies a certain constraint to the current distribution which is absent in the tail of the pulse. When the external e.m.f. is removed, the induced e.m.f.'s in the filaments may differ,

Table 13 Current distributions in the strip conductor

SWITCH-ON TRANSIENT			SWITCH-OFF TRANSIENT		
t	i_1/e	i_2/e	t	i_1-i_3	i_2
sec	A/V	A/V	sec	A	A
0	0	0	0.001	493	859.3
0.001	24.6	17.9	0.002	507.3	720.2
0.005	112.7	97.6	0.003	495.3	623.7
0.006	132.3	117.4	0.004	479.8	557.4
0.007	151.2	136.5	0.005	460.4	510.5
0.008	169.2	155.0	0.006	440.9	475.5
0.009	186.5	172.8	0.007	422.0	447.6
0.010	203.0	189.8	0.008	403.8	424.2
0.020	333.4	324.9	0.009	386.4	403.5
0.030	417.3	411.8	0.010	369.7	384.8
0.040	471.2	467.7	0.015	296.4	307.2
0.050	505.8	503.6	0.020	237.7	246.3
0.060	528.1	526.7	0.025	190.6	197.4
0.070	542.4	541.5	0.030	152.8	158.3
0.080	551.6	551.1	0.035	122.5	127.0
0.090	557.6	557.2	0.040	98.2	101.8
0.100	561.4	561.2	0.045	78.8	81.6
0.110	563.8	563.7	0.050	63.1	65.4
0.120	565.4	565.3	0.055	50.6	52.4
0.130	566.4	566.4	0.060	40.6	42.0
0.140	567.0	567.0	0.065	32.6	33.7
0.150	567.5	567.5	0.070	26.1	27.0
1.000	568.2	568.2	0.075	20.9	21.6
			0.080	16.8	17.4
			0.085	13.5	13.9
			0.090	10.8	11.2
			0.095	8.6	9.0
			0.100	6.9	7.2

causing a lateral current exchange. This is the reason why during the switch-off transient i_2 is initially greater

than the steady state current of 568.2 A. After about four milliseconds the lateral exchange of current appears to have died out. The results show the core effect, that is during the switch-off transient the current in the center filament is greater than the currents in the outer filaments.

When the number of filaments is greater than ten it is advisable to abandon the foregoing solution process. Kelly [84] has outlined the bestknown alternative techniques suitable for computer handling. As previously mentioned, Silvester [81] found that modal network analysis provides additional tools for solving the set of simultaneous linear equations. This involves eigenvectors (mode vectors) and eigenvalues (mode frequencies). The particular eigenvector approach that will now be outlined is due to Parker [85].

We start with the set of equations (3.101) and assume sinusoidal excitation so that the time derivatives of the currents are defined by (3.102) and (3.103). This leads to

$$\begin{aligned}
 (R + j\omega L_{1,1})i_1 + j\omega M_{1,2}i_2 + \dots + j\omega M_{1,g}i_g &= e \\
 j\omega M_{2,1}i_1 + (R + j\omega L_{2,2})i_2 + \dots + j\omega M_{2,g}i_g &= e \\
 \cdot & \\
 \cdot & \\
 \cdot & \\
 j\omega M_{g,1}i_1 + j\omega M_{g,2}i_2 + \dots + (R + j\omega L_{g,g})i_g &= e
 \end{aligned}
 \tag{3.133}$$

where the filament resistance $R = R_f$ is related to the electrical conductivity σ , conductor cross-sectional area A , and the conductor length l by

$$R = R_f = (1/\sigma)(l/A) \tag{3.134}$$

If U is the unit matrix of order $g \times g$ and $M_{m,n}$ is the square $g \times g$ inductance matrix, then the matrix form of (3.133) is

$$[RU + j\omega M_{m,n}]\{i_n\} = \{e\} \quad (3.135)$$

Dividing throughout by R and substituting (3.134) into the $M_{m,n}$ -term results in

$$[U + j\Omega(M_{m,n}/l)]\{i_n\} = \{e\}/R \quad (3.136)$$

Now Ω will be called the generalized frequency related to the actual frequency ω by

$$\Omega = \omega \sigma A/g \quad (3.137)$$

This will be useful for establishing the scaling laws for current distributions. It should also be appreciated that the mutual inductance per unit length ($M_{m,n}/l$) is--in electromagnetic units--a dimensionless number. So is the unit vector U . Furthermore, since in e.m.u.'s resistance has the dimension of velocity, it will be found that the generalized frequency Ω is also a dimensionless number. Therefore the square matrix of (3.135) may be treated as a matrix of pure numbers.

This matrix is associated with a set of g eigenvectors, each being a column of g elements. The eigenvectors may be placed side-by-side in a $g \times g$ square matrix of the form

$$I_{m,n} = \begin{bmatrix} I_{1,1} & I_{1,2} & \dots & I_{1,g} \\ I_{2,1} & I_{2,2} & \dots & I_{2,g} \\ \vdots & \vdots & \ddots & \vdots \\ I_{g,1} & I_{g,2} & \dots & I_{g,g} \end{bmatrix} \quad (3.138)$$

Eigenvector theory then asserts that

$$[U + j\Omega(M_{m,n}/l)]\{I_{m,n}\} = \{I_{m,n}\}\{\Lambda_n\} \quad (3.139)$$

where $[\Lambda_n]$ is the diagonal matrix of the eigenvalues of $[U + j\Omega(M_{m,n}/l)]$. Both $[I_{m,n}]$ and $[\Lambda_n]$ can be determined with available computer algorithms. The number of filaments g , which fixes the order of the matrixes, may be as large as 500. Once the relevant eigenvectors and eigenvalues are known, they may be used for calculating the ac current distribution over the conductor cross-section. The unit matrix U arose from the filament resistances which are all equal and therefore do not influence the current distribution (1). Hence the eigenvectors and eigenvalues needed to derive the current distribution are actually those of the mutual inductance matrix $[M_{m,n}/l]$. The eigenvector elements of this matrix will be denoted by $I_{m,n}$ and the eigenvalues by λ_n .

Parker's method relies on the fact--here stated without proof--that the solution vector $\{i_n\}$ of (3.135) can be expressed in the form

$$\{i_n\} = \sum_{n=1}^g a_n \{I_n\} \quad (3.140)$$

I_n is the n -th eigenvector column of the $I_{m,n}$ eigenvector matrix and a_n is a coefficient, different for each eigenvector, which is not an eigenvalue of the $[U + j\Omega(M_{m,n}/l)]$ matrix, but takes the place of some eigenvalue. Equation (3.140) implies that the current in the general filament n is related to the row-sum of the eigenvector matrix.

Now if the left side of (3.136) can be transformed to an eigenvector expression, so can the right side. Therefore

$$\{e\} = \sum_{n=1}^g b_n \{I_n\} \quad (3.141)$$

where b_n is some eigenvalue which may be found with the following consideration. The eigenvectors are orthogonal and if $\{I_n\}^T$ is the transpose of $\{I_n\}$, orthogonality implies

$$\{I_m\}^T \cdot \{I_n\} = \delta_{m,n} \quad (3.142)$$

where the Kronecker- δ signifies that the product vanishes unless $m=n$. Hence by multiplying (3.141) by the transpose of the eigenvector we obtain

$$b_n = \{I_n\}^T \cdot \{e\} \quad (3.143)$$

Substitute (3.140) and (3.141) into (3.136)

$$[U + j\Omega(M_{m,n}/l)] \sum_{n=1}^g a_n \{I_n\} = (1/R) \sum_{n=1}^g b_n \{I_n\} \quad (3.144)$$

Now since

$$[M_{m,n}/l] \{I_n\} = \lambda_n \{I_n\} \quad (3.145)$$

by the definition of eigenvectors and eigenvalues, (3.144) may be expanded to

$$\sum_{n=1}^g a_n \{I_n\} + j\Omega \sum_{n=1}^g a_n \lambda_n \{I_n\} = (1/R) \sum_{n=1}^g \{I_n\}^T \cdot \{e\} \cdot \{I_n\} \quad (3.146)$$

This last equation also involves a substitution for b_n from (3.143). The equation may be shortened to

$$\sum_{n=1}^g (1 + j\Omega \lambda_n) a_n \{I_n\} = (1/R) \sum_{n=1}^g \{I_n\}^T \cdot \{e\} \cdot \{I_n\} \quad (3.147)$$

Multiplying both sides of (3.147) by $\{I_n\}^T$ and using the orthogonality property of (3.142) results in

$$(1 + j\Omega \lambda_n) a_n = (1/R) \{I_n\}^T \cdot \{e\} \quad (3.148)$$

This gives the a_n coefficient as

$$a_n = \{I_n\}^T \cdot \{e\} / [R(1 + j\Omega \lambda_n)] \quad (3.149)$$

which can now be substituted into (3.140), thereby providing the solution of the current distribution problem, that is

$$\{i_n\} = (1/R) \sum_{n=1}^g \{I_n\}^T \cdot \{e\} \cdot \{I_n\} / (1 + j\Omega \lambda_n) \quad (3.150)$$

THE INDUCTION OF EDDY CURRENTS

The term "eddy currents" is a misnomer. It suggests flow irregularities when, in fact, electromagnetic induction is very precise and regular. Nevertheless, the subject is complex and continues to spore publications in what is already a vast literature. In several instances the Ampere-Neumann electrodynamics has proved to be a more powerful tool than field theory for solving eddy current problems. However, there is no room in this short book for the voluminous analysis of induced currents in three-dimensional conductors. Instead the reader will be referred to some of the relevant publications.

Eddy currents are of practical importance in induction heating, non-destructive electromagnetic testing, shielding and electromagnetic compatibility engineering, and in a variety of ac power problems. Thirty years ago the author became involved in what was then known as eddy current testing of travelling wires and metallic pipes. The superposition of relative motion between a stationary, high-frequency induction coil and a moving test object led to dynamic induction which was difficult to visualize in field theory, but became more transparent in the Ampere-Neumann electrodynamics. The interested reader is directed to references [86], [87], and [88].

Two significant facts emerged from these early investigations which, ultimately, were responsible for this book. The first was that a newtonian theory, based on galilean relativity, could explain precisely the same fact, involving relative motion, as electromagnetic field theory which rests on Einstein's special relativity. This being possible, neither of the two relativities can be as fundamental as they are thought to be. The second fact concerned the time delay occurring between the cause of induction and the induced effect itself. It could be explained with equal precision by the energy transmission lag of field theory and the simul-

taneous matter interaction processes of the Ampere-Neumann electrodynamics. The second fact suggest that a time may come when the eight minutes it takes sunlight to reach the earth can be accounted for by a 'simultaneous' action-at-a-distance theory. Again, with two explanations at hand, neither should be treated as "the final truth".

In this early research a model of successive filament interactions was developed. It resulted in infinite power-series solutions of the eddy current distributions. Looked at it from the mathematical point of view, each term of the series represented an iteration to the final answer. In terms of physics the model suggested that when nature is faced with multiple interactions (the many-body problem), it adjusts to the final state by a series of steps, which could be infinitely small and infinite in number. Each step takes the result of the previous step in account and than applies it to a greater number of reciprocal interactions. This could be the way analogue computers work. Self-consistent field theory must achieve the same result. Then it appears nature is a digital supercomputer which looks at all the interaction matrixes and finds eigenvalues 'before' anything happens.

The model of successive filament interactions has a severe defect. All the infinite power series diverge when the generalized frequency of equation (3.137) becomes greater than one. Up to the limiting value of one, the series give perfectly, though slowly, convergent results which agree with experiment and any other method of calculating induced current distributions. The possibility exists that the relevant power series may be analytically continued to higher frequencies which would breathe new life into the successive interaction model.

CHAPTER 4

ATOMIC CURRENT ELEMENTS

THE CURRENTS ELEMENTS OF AMPERE, WEBER AND LORENTZ

How can one reconcile the continued experimental success of the Ampere-Neumann electrodynamics with its archaic physical foundation which predates any quantitative understanding of the atomic and electronic structure of metals? This question can only be answered by studying the nature of the metallic current element and particularly its microscopic makeup. Current elements are the 'particles' of electrodynamics. Like all so-called fundamental particles, they grow in complexity the closer they are observed. Moreover, since it is now obvious that different force laws apply to convecting charges in vacuum and conduction currents in metals, we most likely have to deal with two distinct types of current element.

Ampere wrote the beginning of the current element story. To him one of these elements was simply an infinitely small piece of the conductor material containing an infinitely small amount of electric fluid in motion. In this he adhered closely to the principles of remote matter interactions first suggested by Newton. There was no doubt in the mind of Ampere and his followers that the forces defined by Ampere's law (1.24) acted directly on the substance of the conductor and not on the electric fluid which was free to slide through the metal without drag or any other mechanical manifestation. Ampere also knew current elements did not have to be infinitely small, so long as the separation between them was large compared to their size. Therefore, referring to the remote element interaction, Weber would

later speak of Ampere's ponderable wire-elements. Precisely these wire elements have been resurrected in computer-assisted finite current element analysis. By not defining the mechanical linkage between the electric fluid and the conductor material, Ampere's electrodynamics has been able to survive such scientific innovations as atomism, crystallinity, electron structure, and quantum mechanics.

A postulated property of the newtonian matter element is that it does not interact with itself. This is almost certainly true for any particle which can be described as fundamental and indivisible. As we have seen, the postulate also holds approximately for quite large macroscopic current elements. In the absence of selfinteractions, Ampere's current elements are invariably studied in pair combinations. All actions of the Ampere-Neumann electrodynamics are mutual actions between the members of a pair of elements. For mutual mechanical forces to exist, both elements must carry currents. In the case of electromagnetic induction, only one of the two elements need carry a current, the other can be a neutral element of matter.

Although he lived through the second half of the nineteenth century, Neumann was as vague as Ampere about the inevitable atomic nature of the current element. To this day, this vagueness can be found in many modern texts on electromagnetism which, by their silence on the makeup of the metallic current element, perpetuate the antiquated notion of the infinitely divisible, subtle fluid of electricity. Neumann's extension of the Ampere theory dealt with electromotive forces on the imponderable electric fluid. The parallel existence of ponderable and imponderable (electromotive) forces have become a hallmark of the Ampere-Neumann electrodynamics. Modern electromagnetism has done away with the difference between mechanical and electromotive forces. All forces on charges are now considered to be of the same nature, that is they are mechanical forces. Later in this chapter it will be shown how, on the assumption of a specific

mechanical linkage between electrons and the metal lattice, we can do away with the imponderables of the old electrodynamics.

The first step toward atomic current elements was taken by Weber [13]. His elements are depicted in fig.19 on page 59. He thought of positively and negatively charged particles moving through the metal at equal velocity in opposite directions. His force law (1.90), which agrees with (1.24), involved these equal and opposite charge velocities with respect to the conductor metal in terms of the dr/dt derivatives. Weber pointed out that in his current element model the charge velocity v could never become greater than c , which we now know as the velocity of light. This suggests that Weber's theory contained the germ of Einstein's special relativity. Furthermore, this state of affairs arose from attributing magnetic actions to the finite velocity of particles endowed with electric charge. With no current flowing in the metal, that is when in fig.19 $v=0$, the charges in the Weber current element are still subject to electrostatic attraction. Weber did not assert the two charges of his element would then combine and form a neutral particle. His hesitation on this point probably derived from the fact that electromotive forces could never start a current if all particles in the metal were electrically neutral. Nevertheless, the invention of a current element which could respond, at the same time, to electrostatic and electrodynamic forces was truly remarkable.

In Wesley's [61] view, Weber came close to the quantization of charge. In any case he assumed the positive and negative charge in the individual current element to be equal to each other. They could be the conduction electron and its associated lattice ion, but for the immobility of the ion. When he formulated his current element, in the 1840's, Weber had no knowledge of electrons and the atomic lattice. With neither of his charges being coupled to the substance of the conductor metal, he painted a confused

picture of how forces on charges were transferred to the body of the metal. At the same time the mobile charges could respond well to electromotive forces. This he considered to be an advantage of his current element over that of Ampere.

Ampere clearly attributed all magnetic actions to the motion of the electric fluid. Weber went one step further by claiming this fluid to consist of discrete charged particles. Electromagnetism then became a manifestation of the motion of charges relative to the host metal. This concept has survived to our time, but it will be challenged by a new type of metallic current element. A weakness of Weber's current element was its inability to establish mechanical interactions between the charges and the substance of the metallic conductor.

The essential modification which Lorentz made to the metallic current element was the dropping of the positive charge. What survived is the drifting conduction electron. The Lorentz force as written in equation (1.133) still combines electrostatic with electrodynamic forces but it then no longer refers to the mutual interaction of two elements of matter. Lorentz retained Weber's idea of the current element strength being given by the product of charge and relative velocity with respect to the host metal. Hence all magnetic effects of currents in metallic conductors are still being attributed to the charge velocity.

Lorentz's drifting electron element recognizes only one type of force which acts on the mass of the electron. This easily takes care of what were electromotive forces, but it has its problems with mechanical forces on the body of the metal. Whilst the concentration of electrons transverse to the direction of current flow can push against the surface, and therefore the body, of a metallic conductor, there seems to be no way in which the drifting electron can produce anything resembling Ampere tension. It is sur-

prising, however, that the shortcoming of the Lorentzian current element model was not noticed in the 1920's, when Hering [58, 59] published his experiments, or in the 1930's when Cleveland's [62] experiment stirred considerable interest, or in the 1960's when Nasilowski [39] fragmented the first wires with current pulses.

MUTUAL TORQUES BETWEEN AMPERIAN CURRENT ELEMENTS

At this point of the development of the Ampere-Neumann electrodynamics we know that each pair of current elements must be associated with an amount of mutually stored magnetic energy $\Delta P_{m,n}$ given by equation (3.44). Turning the elements about certain axes relative to each other will change the stored energy. The principle of virtual work then requires the existence of mutual torques between the amperian current elements. We will now determine these mutual torques.

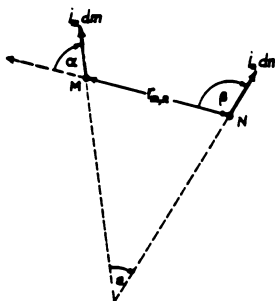


Fig.83 Angle convention for torque calculations

Consider the two coplanar current elements of fig.83. Equation (3.44) contains three angles, one of them being dependent on the other two. This fact may be expressed by

$$\beta = \alpha + \epsilon \quad (4.1)$$

The positive direction of angular displacements and torques is taken to be a clockwise rotation about the positive direction of the axis. In fig.83 the positive direction of the axis of rotation is into the plane of the paper. With (4.1) the angle function of (3.44) may be equated to

$$2\cos\epsilon - 3\cos\alpha \cos\beta = 0.5\cos\epsilon - 1.5\cos(2\alpha + \epsilon) \quad (4.2)$$

Using the symbol T for torque, the principle of virtual work then defines two independent, elemental, mutual torques with respect to the two angles of (4.2).

$$\begin{aligned} (\Delta T_m)_\epsilon &= -(\partial/\partial\epsilon)\Delta P_{m,n} \\ &= 2i_m i_n (dm \cdot dn / r_{m,n}) [1.5\sin(2\alpha + \epsilon) - 0.5\sin\epsilon] \end{aligned} \quad (4.3)$$

$$\begin{aligned} (\Delta T_{m,n})_\alpha &= -(\partial/\partial\alpha)\Delta P_{m,n} \\ &= 3i_m i_n (dm \cdot dn / r_{m,n}) \sin(2\alpha + \epsilon) \end{aligned} \quad (4.4)$$

If the two elements do not lie in the same plane, they have to be resolved into coplanar components. The resolved components will obey (4.3) and (4.4).

With (4.2) the magnetic energy equation (3.44) becomes

$$\Delta P_{m,n} = -i_m i_n (dm \cdot dn / r_{m,n}) [0.5\cos\epsilon - 1.5\cos(2\alpha + \epsilon)] \quad (4.5)$$

This not only controls the torques but also the mechanical interaction.

$$\begin{aligned} \Delta F_{m,n} &= -(\partial/\partial r_{m,n})\Delta P_{m,n} \\ &= -i_m i_n (dm \cdot dn / r_{m,n}^2) [0.5\cos\epsilon - 1.5\cos(2\alpha + \epsilon)] \end{aligned} \quad (4.6)$$

This last equation is of course merely an alternative form

of Ampere's force law (1.24).

It is instructive to examine the angle functions of (4.3) and (4.4). An underlying assumption of the derivation of the torque equations is that when α suffers a virtual displacement, the angle ϵ is kept constant, and vice versa. This means the action of the alpha-torque must be such that it leaves the angle of inclination between the elements unchanged. Therefore the alpha-torque (4.4) will try and swing one element around the other in a circle of radius $r_{m,n}$, while the elements remain parallel to themselves. The alpha-torque clearly tends to displace atoms and it is therefore a mechanical or ponderomotive torque. Not in solid conductors, but in plasma and liquid metal conductors, the atomic displacements can actually take place.

Next we examine the epsilon-torque of (4.3). With reference to fig.83, a virtual angular displacement $\Delta\epsilon$ must mean a small rotation of one or both elements about their pivots M and N. The torques at the two pivots are in opposite directions which is indicated by the \pm sign of (4.3). The mutual angular displacement should not change the locations of M and N. Is it possible for the elements to turn about these pivots?

Our object remains to show that the fundamental current element is the conductor atom. A neutral atom is likely to be spherical symmetric with no feature which could represent current direction. To remedy this situation we have to think of the atomic current element to be some form of dipole, possibly a diamagnetic dipole, which, like all other magnetic dipoles, can turn on the lattice site. The epsilon-torque, which turns this diamagnetic dipole, would then be an electromotive rather than a ponderomotive torque. It remains to be seen what the relation of the conduction electron to the element dipole is. It must be the absence of the electron which creates the dipole.

The epsilon-torque should have a certain ordering effect in a collection of current elements. The sign of (4.3) depends on whether the torque is evaluated at M or at N of fig.83. In both cases it will be zero when

$$1.5\sin(2\alpha+\epsilon) = 0.5\sin\epsilon. \quad (4.7)$$

Solving (4.7) for ϵ gives

$$\epsilon = \tan^{-1}[1.5\sin 2\alpha/(0.5-1.5\cos 2\alpha)]. \quad (4.8)$$

When the zero epsilon-torque angles have been determined for a series of alpha values, stability may be explored with small angular displacements $\pm\Delta\epsilon$ from the zero torque positions. In this way it will be found that co-linear elements always tend to counter-align each other while side-by-side elements will tend to co-align each other. Both stable arrangements result in attraction between the elements.

This is an interesting result. It suggests that a dense plasma sphere, in which positive ions represents dipole current elements, should contract under the action of Ampere forces. The electrodynamic forces are far stronger than gravitational forces. Therefore the plasma collapse should be a noticeable phenomenon. The contraction will be counter-acted by the thermal agitation of the plasma ions. The collapsing sphere might, therefore, not form at all or it may stabilize at some finite radius. This leads to the suspicion that ball lightning may ultimately be explained with the epsilon-torque.

Whereas the ordinary Ampere forces obey an inverse square law, the mutual torque interactions are of longer range and proportional to the inverse of distance. The effect of elemental torques should consequently be quite large unless the two independent torques somehow cancel.

GENERALIZATION OF NEUMANN'S LAW OF INDUCTION

Neumann's elemental law of induction (1.68) applies to current elements of fixed orientation, constant current, and variable distance. We expect that suitable formulas for the elemental induced e.m.f.'s can be established when the angular orientation and the inducing current change. To derive these formulas it will, first of all, be shown that any interaction between two amperian current elements reduces to a two-dimensional problem. It is then sufficient to derive elemental induction formulas for coplanar element pairs.

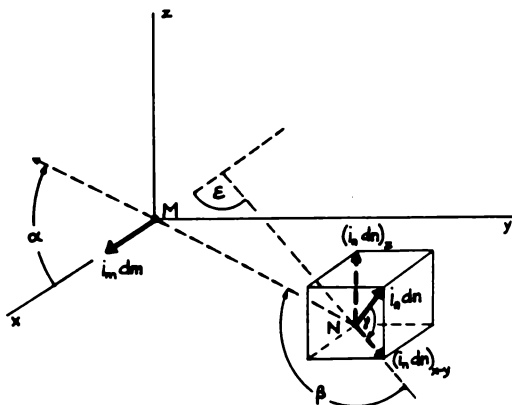


Fig.84 Two-dimensional element interactions

It is always possible to put the locations M and N of two current elements in a common plane with the direction of one of the elements, say $i_m dm$. In fig.84 x-y is the common plane and M the origin of a cartesian coordinate system with $i_m dm$ pointing in the positive x-direction. If $i_n dn$, making the angle γ with the common plane, is resolved in

parallel and perpendicular components $(i_n dn)_{x-y}$ and $(i_n dn)_z$ to this plane, the angles β and ϵ and equation (4.1) apply to the coplanar elements $i_m dm$ and $(i_n dn)_{x-y}$. No magnetic energy is stored between $i_m dm$ and $(i_n dn)_z$ and no mutual forces nor torques exist between these orthogonal elements, whatever the orientation of $i_n dn$. This is in agreement with Ampere's theorem stated at the top of page 13. For the orthogonal pair $i_m dm$ and $(i_n dn)_z$, $\cos \epsilon$ and $\cos \beta$ are zero and therefore $\Delta P_{m,n}$ is zero regardless of any virtual displacement given to $i_n dn$. Here it should be realized that in the three-dimensional case all three angles are independent of each other and equation (4.1) does not hold. We can ignore the orthogonal element combination. This means all current element interactions reduce to a two-dimensional problem for which (4.1) holds.

A pair of coplanar, amperian current elements has five degrees of freedom. They are the two element strengths, the angle of inclination between the elements, the distance of separation, and the inclination of one element to the distance vector (see fig.83). It will now be shown that a time-variation of any of these five quantities generates induced e.m.f.'s in the elements. The process requires four energy source-sink units. One is the store of magnetic energy which will be denoted by S . The elements communicate with their own electrical supplies E_m and E_n . Finally, there must exist a mechanical agency which controls the distance of separation between the elements, which will be denoted by M .

Variable $r_{m,n}$.

For attracting elements and increasing distance, M must supply energy to the elements. At the same time S loses energy. These two streams of energy have to flow into E_m and E_n which sustain the currents i_m and i_n . Joule heating plays no part in the conservative energy exchanges between M , S , E_m and E_n . It will be left out of the analysis. If

the induced electromotive force in a complete circuit is the sum of the elemental contributions, then each pair of current elements should furnish

$$\Delta e_m = -(d/dt)(\Delta M_{m,n} i_n) \quad (4.9)$$

For increasing distance and constant currents and angles this becomes

$$\Delta e_m = -[(\partial/\partial r_{m,n})\Delta M_{m,n}](dr_{m,n}/dt)i_n \quad (4.10)$$

Let $v_r = dr_{m,n}/dt$ stand for the relative velocity of one element with respect to the other along the distance vector. From the definition of the mutual force in terms of the gradient of the stored energy (3.45) it follows that

$$(\partial/\partial r_{m,n})\Delta M_{m,n} = \Delta F_{m,n}/(i_m i_n) \quad (4.11)$$

and the induced electromotive force becomes

$$\Delta e_m = -(\Delta F_{m,n}/i_m)v_r \quad (4.12)$$

This agrees with Neumann's law of induction (1.68). The instantaneous power exchange between the mechanical source M and the electrical source E_m therefore is

$$\Delta e_m i_m = -\Delta F_{m,n} v_r \quad (4.13)$$

This is a forward e.m.f. in the sense that it supplies energy to E_m , while the negative sign on the other side of (4.13) indicates that M is supplying energy. Since the induced e.m.f. of (4.13) is the result of relative motion it must cause the same energy exchange in both elements, such that

$$\Delta e_n i_n = -\Delta F_{m,n} v_r \quad (4.14)$$

For this to be possible S must give up just as much power as M. The power flow from S is

$$(d/dt)\Delta P_{m,n} = (\partial/\partial r_{m,n})\Delta P_{m,n}(dr_{m,n}/dt) = -\Delta F_{m,n}v_r \quad (4.15)$$

which proves that energy is being conserved and

$$\Delta e_{m,i_m} + \Delta e_{n,i_n} = -2\Delta F_{m,n}v_r \quad (4.16)$$

The same kind of analysis can be performed for a reversal of relative velocity, that is decreasing distance, and also for the two corresponding cases of repelling elements. The energy exchanges for the four different circumstances are summarized in fig.85. Let us briefly look at repelling elements and increasing distance. It requires S to supply energy to M. Calculations prove that all the energy subtracted from the magnetic store is being absorbed by the mechanical source. There will still be e.m.f.'s induced in the elements in accordance with (4.12), but they must now facilitate an energy exchange between E_m and E_n . This is possible because one of the e.m.f.'s turns out to be a forward-e.m.f. and the other a back-e.m.f. In performing these calculations care must be taken with the sign of the mutual inductance between the elements. This sign reverses whenever a current element is reversed.

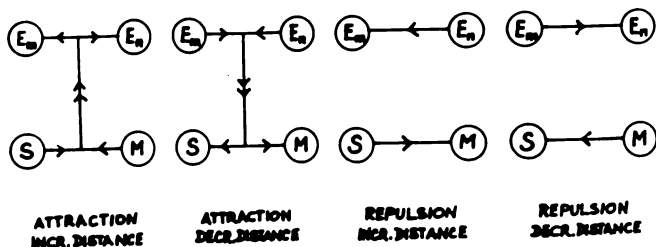


Fig.85 Power exchanges for variable distance

Variable ϵ .

Instead of attracting and repelling forces we now have to deal with the mutual torque of equation (4.3). For any value of α there exists a 180° interval of ϵ over which the torque tries to increase ϵ , and the remaining 180° over which the torque tends to decrease ϵ . At the change-over points the torque will be zero, but only one of these angular positions is stable. Two stable arrangements have been discussed in conjunction with equations (4.7) and (4.8).

The e.m.f. equation applicable to the variable ϵ case has to be derived from (4.9). It is found to be

$$\begin{aligned}\Delta e_m &= -i_n[(\partial/\partial\epsilon)\Delta M_{m,n}](d\epsilon/dt) \\ &= -[(\Delta T_{m,n})_\epsilon/i_m]\omega_\epsilon\end{aligned}\quad (4.17)$$

where ω_ϵ is the angular velocity with which the elements rotate with respect to each other. The electrical power flow in relation to the mechanical power is given by

$$-\Delta e_m i_m = (\Delta T_{m,n})_\epsilon \omega_\epsilon = +\Delta e_n i_n \quad (4.18)$$

Variable α .

The mutual torque for this case is given by (4.4). When the elements are parallel, the stable angular positions are $\alpha = \pm \pi/2$. Other element inclinations result in other stable angular positions. Parallel to (4.17), the e.m.f. equation is found to be

$$\Delta e_m = -[(\Delta T_{m,n})_\alpha/i_m]\omega_\alpha \quad (4.19)$$

Variable current.

Finally we examine the most common case of electromagnetic induction, that due to variable current intensity.

$$\Delta e_m = -\Delta M_{m,n}(di_n/dt) \quad (4.20)$$

This formula involves i_n but not i_m . The other three e.m.f. equations--(4.12), (4.17), and (4.19)--involve both currents, because they depend on mutual forces or torques. The value of the induced e.m.f. of (4.20) appears not to depend on the strength nor the direction of the current in the element that experiences the induction. In fact that latter current may be set to zero and the e.m.f. would still exist. This is the major difference between statically and motionally induced e.m.f.'s. How can the sign of the mutual inductance be fixed if the direction of one of the current elements is left undefined? To find an answer we have to fall back on experimental evidence.

The line of action of the induced e.m.f. will generally be determined by the circuit (wire) layout, but we are uncertain in which direction along this line the induced e.m.f. will tend to transport current. If we take two parallel wires and increase the current in one of them, then we know from experience that the induced e.m.f. in the other will point in the direction opposite to that in which the inducing current flows. This follows from Lenz's law and accounts for the negative sign in (4.20). We may generalize the empirical finding and Lenz's law by saying that the direction of i_{dm} in (4.20) must be chosen such that $\Delta M_{m,n}$ is positive. No other rule appears to satisfy the law of induction.

The four induced e.m.f. equations--(4.12), (4.17), (4.19) and (4.20)--represent the generalization of Neumann's law of electromagnetic induction at the current element level. The electromotive forces are given in e.m.u. of potential difference. The conversion factor from e.m.u. (cgs) to practical MKS units is 1 volt = 10^8 e.m.u. As far as dimensions are concerned it should be remembered that velocity is the e.m.u. of resistance. Therefore all the velocities in the e.m.f. equations could be converted to resistances by 1 ohm = 10^9 cm/s. It would conceal the fact that induced elec-

tromotive forces are the result of relative velocities between current elements.

How does the induced e.m.f. produce charge transport? Two possibilities exist. First, the swinging of elemental dipoles through 180° represents charge transport and current flow. Alternating currents may be partly or entirely due to swinging dipole elements. The second possibility is that the e.m.f. acting on an elemental dipole, once the dipole has been aligned with the e.m.f., tends to increase or decrease the distance between the conduction electron and the ion. Forward e.m.f.'s would cause increases, and back-e.m.f.'s decreases, in this distance which may be related to the element strength, say $i_m dm$. For a sufficiently large e.m.f. the bond holding the atomic current element together may break, allowing the electron to jump to the next ion. A back-e.m.f. might achieve the same result as a forward e.m.f., but with reversed current flow. Both e.m.f.'s could be assisted or opposed by externally applied e.m.f.'s.

DIAMAGNETISM AND THE MEISSNER EFFECT

Briefly recapitulating, it became clear amperian current elements had to be of finite size and involve the lattice ion in order to explain Ampere tension in wires. The conductor atom is of a suitable size and would be the smallest possible current element. Inductance calculations made it necessary to associate each atomic conductor element pair with a finite amount of mutual inductance. This automatically assigned a certain quantity of stored magnetic energy to interacting current element pairs. The principle of virtual work then required every element pair to be subject, not only to a mutual ponderomotive force, but also to a mutual torque. The α -torque turned out to be ponderomotive, but the ϵ -torque could be treated as being electromotive, provided the atomic element formed a dipole with the conduction

electron swinging freely around the lattice site. This made it possible to derive all induced electromotive forces from the pivoted atomic current element model.

The primary purpose of this chapter is to outline a consistent theory in which the ponderomotive and electromotive forces of the Ampere-Neumann electrodynamics are clearly associated with the same atomic current element model. However, other electrodynamic effects in metals may also conform with the pivoted current element model. An interesting phenomenon, in this respect, is diamagnetism and the related flow of persistent currents in superconductors. Persistent supercurrents are strong and lend themselves to an experimental test of the pivoted current element model.

The phenomenological London [89] theory of superconductivity indicates that inside a singly-connected superconducting body the magnetic vector potential \underline{A} obeys the diffusion equation

$$\nabla^2 \underline{A} = \lambda^2 \underline{A} \quad (4.21)$$

where λ is a material constant determining the depth in which the persistent surface supercurrents flow, which are a feature of the Meissner effect. Equation (4.21) is associated with a similar diffusion equation for the magnetic field vector \underline{B} . These equations require that the magnetic field and the magnetic vector potential be expelled from the interior of the superconductor but persist in a thin surface layer. The expulsion of magnetic flux is taken to be the physical manifestation of the Meissner effect. But the vector potential explains the induction of persistent surface currents equally well and it is not possible to strip it of all its physical relevance. The Aharanov-Bohm [90] experiment, and quantum mechanics in general, have delegated a more physical role to the vector potential than has been customary in field theory. The magnetic vector potential exists in field theory and the Ampere-Neumann

electrodynamics and is, therefore, of particular interest. Equation (4.21) is under all circumstances in accord with the Ampere-Neumann electrodynamics, even when the superconducting body is not singly-connected, as a ring would be. This suggests the Meissner effect should be observable in a superconducting ring encircling a very long solenoid or a toroidal coil. In both these situations the ring would be located in a region where there exists practically no magnetic field, but the vector potential is strong. Hence if persistent supercurrents were induced in the ring, they would be due to the vector potential and not the magnetic field. It would indicate that the flow of persistent currents in superconductors is controlled by the Ampere-Neumann electrodynamics.

To probe how pivoted current elements could interact to cause the Meissner effect, we examine what kind of order can be established in a set of these current elements under the influence of an external current. For this purpose we calculate the torque exerted on a pivoted element $i_m dm$, lying on a conductor circle of radius R , by all elements of a current circle of radius r , coaxial and coplanar with the larger R -circle, and carrying the current i_n .

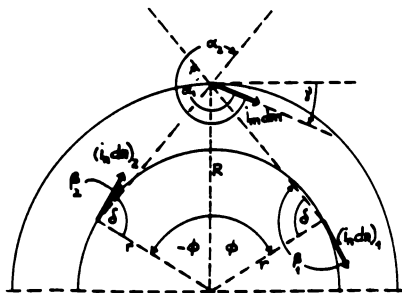


Fig.87 Construction for coplanar current circles

As fig.87 shows, we direct our attention initially on two symmetrically disposed elements, $(i_n dn)_1$ and $(i_n dn)_2$. The deflection of $i_m dm$ from the tangential position has been denoted by the angle γ . Figure 87 also depicts how the position of the two $i_n dn$ elements is given by the angles $\pm\phi$. From this it can be seen that

$$\epsilon_1 = \phi - \gamma; \quad \epsilon_2 = -\phi - \gamma$$

The torque to be calculated is

$$(\Delta T_{m,n})_\gamma = -(\partial/\partial\gamma)\Delta P_{m,n} \quad (4.22)$$

The currents and dm and dn are obviously not functions of γ . Furthermore, if the conductor circles are rigid and fixed, $r_{m,n}$ cannot vary with γ . For the same reason the angle β is also independent of γ . The angles which are functions of γ and must therefore be involved in the differentiation of (4.22) and (3.44) are ϵ and α . Therefore

$$(\Delta T_{m,n})_\gamma = i_m i_n (dm \cdot dn / r_{m,n}) [-2 \sin \epsilon (\partial \epsilon / \partial \gamma) + 3 \cos \beta \sin \alpha (\partial \alpha / \partial \gamma)] \quad (4.23)$$

$$\text{But } \alpha = \epsilon + \beta = \phi - \gamma + \beta; \quad (\partial \alpha / \partial \gamma) = -1; \quad (\partial \epsilon / \partial \gamma) = 1$$

Substitution into equation (4.23) then gives

$$(\Delta T_{m,n})_\gamma = i_m i_n (dm \cdot dn / r_{m,n}) [2 \sin(\phi - \gamma) - 3 \sin(\phi - \gamma + \beta) \cos \beta] \quad (4.24)$$

Now for the two positions of $i_n dn$ indicated in fig.87 the angle β is

$$\beta_1 = 90^\circ + \delta; \quad \beta_2 = 90^\circ - \delta$$

Therefore the torque exerted by either of these two elements on $i_m dm$ becomes

$$(\Delta T_{m,n})_{\gamma} = i_m i_n (dm \cdot dn / r_{m,n}) [2 \sin(\phi - \gamma) - 3 \cos(\phi - \gamma \pm \delta) \sin(\pm \delta)] \quad (4.25)$$

where $+\delta$ goes with $(i_n dn)_1$ and $-\delta$ with $(i_n dn)_2$.

The angle function of (4.25) for $(i_n dn)_1$ is

$$2 \sin(\phi - \gamma) - 3 \cos(\phi - \gamma + \delta) \sin \delta$$

and that for $(i_n dn)_2$ is

$$2 \sin(-\phi - \gamma) - 3 \cos(-\phi - \gamma - \delta) \sin(-\delta)$$

When the sum of these two functions is zero, no torque will be exerted on $i_m dm$ by the two symmetrically disposed elements on the r -circle. This will be the case when $\gamma = 0$ or 180° , and it is true for any value of ϕ and δ . Therefore there will be no torque exerted on $i_m dm$ by the whole of the r -circle when $\gamma = 0$ or 180° . To determine which of the two values of γ represents the stable equilibrium we have to compute the sum

$$2 \sin(\phi - \gamma) - 3 \sin(\phi - \gamma + \delta) \sin \delta + 2 \sin(-\phi - \gamma) - 3 \sin(-\phi - \gamma - \delta) \sin(-\delta)$$

for a range of ϕ and γ values.

The results of this computation are listed on table 14. They show that the only stable angular position of $i_m dm$ is $\gamma = 180^\circ$. Maximum torques in opposite directions are being exerted on the test element when $\gamma = 90^\circ$ and 270° . From this analysis we may conclude that the i_n -circle as a whole tends to counteralign $i_m dm$ with i_n . Because of symmetry this will be true for all atomic current elements on the larger of the two conductor circles. It means the steady (dc) current i_n should be able to induce a steady diamagnetic current (dc) i_m flowing in the opposite sense of i_n . By a diamagnetic current we mean a current which does not involve

Table 14 Results of stability calculations

γ°	ϕ°	$(\Delta T_{m,n})_\gamma / [i_m i_n (dm \cdot dn / r_{m,n})]$	Remarks
0	30	0	UNSTABLE
10	30	0.339	
30	30	0.975	
60	30	1.689	
90	30	1.950	
120	30	1.689	POS. MAX.
150	30	0.975	
170	30	0.339	
180	30	0	
190	30	-0.339	
210	30	-0.975	NEG. MAX.
240	30	-1.689	
270	30	-1.950	
300	30	-1.689	
330	30	-0.975	
350	30	-0.339	
0	135	0	UNSTABLE
10	135	0.643	
170	135	0.643	STABLE
180	135	0	
190	135	-0.643	
350	135	-0.643	
0	70	0	
180	70	0	
0	90	0	
180	90	0	
0	165	0	
180	165	0	
0	180	0	
180	180	0	

charge transport but nevertheless produces the magnetic effect of an electric current. Neugebauer [91] called this absolute diamagnetism. It should be remembered that induced diamagnetism in a normal conductor metal will produce an external magnetic field which is indistinguishable from the field that would be produced by currents in the conduc-

tor. In normal metals this effect is extremely weak but in superconductors it becomes large. It is impossible to decide by experiment whether the persistent supercurrents are electron transport currents, as commonly believed, or diamagnetic currents. To prove charge transport, the metallic circuit of the superconductor would have to be interrupted and this would destroy the magnetic order associated with a diamagnetic current.

On the assumption that diamagnetic currents account for the persistent currents, we can also gain an understanding of supercurrent skin formation and screening as required by equation (4.21). Adding a third and more conductor circles on the outside of the two circles shown in fig.87, we expect i_n will also induce diamagnetic currents in the additional circles. But their strength in the successive circles will be reduced, not only because of the greater distance from i_n , but also because the various diamagnetic currents tend to counteralign each other. In this way i_m performs a screening function and every subsequent circle helps to screen those that lie beyond it. This tendency of diamagnetic currents to counteralign each other becomes dominant when thermal disordering ceases in the superconducting state. The ordering effect of the external current is then suppressed within just a short distance inside the superconducting body.

Since the number of atomic current elements in the superconducting body is finite, there must come a time, with increasing external current intensity, when all elements of the skin are aligned. It would represent some kind of diamagnetic saturation and should impair the screening function of the persistent currents. When this happens the persistent current skin should grow thicker until it pervades all of the superconductor and thereby eliminates the Meissner effect. The pivoted dipole model of the current element therefore provides a new explanation of the quenching of superconductivity by what could be called a critical magnetic

field. It is expected that any kind of diamagnetic order in normal metals is continuously being upset by thermal agitation. This agitation must be capable of turning dipole elements. Normal metals would then experience an extremely weak Meissner effect, probably too small to be detectable. This argument is consistent with the experimental fact that superconductivity occurs only at very low temperatures.

Unlike paramagnetism and ferromagnetism, diamagnetism does not occur spontaneously. It is an induced effect which depends on the proximity of an electric current (an applied magnetic field). The pivoted dipoles of the metal are likely to exist at all times, even when the metal is not in the vicinity of an electric current, because otherwise an induced e.m.f. could not start a current in the metal. It should therefore be possible to show the dipole elements cannot spontaneously--without assistance from the outside--establish magnetic order in the metal. To investigate this point we will return to the α -torque equation (4.4) and the question of the stable inclination of the dipole elements for variable α .

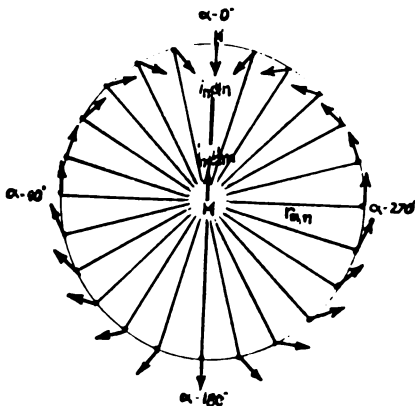


Fig. 88 Stable angular positions of pivoted elements

Figure 88 illustrates the results of stability calculations for the general pair of co-planar dipole current elements $i_{m dm}$ and $i_{n dn}$ with α varying in steps of 15 degrees. The radius of the circle is the distance $r_{m,n}$ and $i_{m dm}$ is held fixed at the center. From these results it follows that in a spherical shell only the dipole elements lying in the equatorial plane will align themselves spontaneously. All the others will be disordered. In addition to this general disorder, thermal agitation of the atomic elements will interfere with any possible cooperative alignment. Hence it may be concluded that any collection of atomic dipole elements of the metal lattice, when left to themselves, will be completely disordered. This excludes spontaneous diamagnetism.

It still remains to be shown that the diamagnetic counteralignment of dipole elements in co-planar circles also holds for coaxial circles which do not lie in the same plane. If this turns out to be the case, then a very long solenoid, consisting of many parallel current circles, should induce diamagnetic currents in a superconducting ring surrounding the center portion of the solenoid. Furthermore, the diamagnetic currents in the ring should give rise to screening and the formation of a persistent current skin. It would provide the theoretical demonstration of how the Ampere-Neumann electrodynamics requires the occurrence of the Meissner effect in a region of curl-free vector potential. Even more important, the solenoid and superconducting ring experiment would be a test of the validity of the pivoted dipole model, for--on the basis of conventional field theory--the Meissner effect should not arise in a region where the magnetic field is zero.

The solenoid will be modeled by one layer of closely packed conductor circles, each carrying a current i_n . In the center plane of the solenoid, and closely coupled to it, lies another coaxial conductor turn which models the

superconducting ring. Figure 89 shows the parameters of the surrounding turn and one turn of the solenoid which will be used in the analysis. The circle of radius R , which experiences the diamagnetic induction, has its center O located at the origin of a cartesian coordinate system and lies in the y - z plane. The solenoid turn is of radius r with its center at O' separated from O by the distance d along the x -axis.

We consider one atomic current element $i_m dm$ situated at the top of the R -circle. Its coordinates are $m(0, 0, R)$. Let this interact with the two elements $(i_n dn)_1$ and $(i_n dn)_2$ on the r -circle. These two elements are disposed symmetrically about the z -axis as indicated in fig.89 by the $\pm\phi$ angles. Their coordinates are $n_1(d, r.\sin\phi, r.\cos\phi)$ and $n_2(d, -r.\sin\phi, r.\cos\phi)$. The element $i_m dm$ will be turned through the test angle γ in the y - z plane. If $(r_{m,n})_1$ and $(r_{m,n})_2$ are the distance vectors pointing from the n -elements to the m -element, their direction cosines are, respectively

$$\cos\theta_x = -(d/r_{m,n}); \cos\theta_y = -(r/r_{m,n})\sin\phi; \cos\theta_z = (R-r.\cos\phi)/r_{m,n} \quad (4.26)$$

with the appropriate distances inserted in (4.26). The direction cosines of the three current elements $i_m dm$, $(i_n dn)_1$, $(i_n dn)_2$, in this order, are

$$\cos\theta_x = 0; \cos\theta_y = \cos\gamma; \cos\theta_z = \sin\gamma \quad (4.27)$$

$$\cos\theta_x = 0; \cos\theta_y = \cos\phi; \cos\theta_z = \sin\phi \quad (4.28)$$

$$\cos\theta_x = 0; \cos\theta_y = \cos\phi; \cos\theta_z = \sin\phi \quad (4.29)$$

Noting that $r_{m,n}$ is the same in both cases, this gives the cosines of α and β of the electrodynamic potential for the two distance vectors as

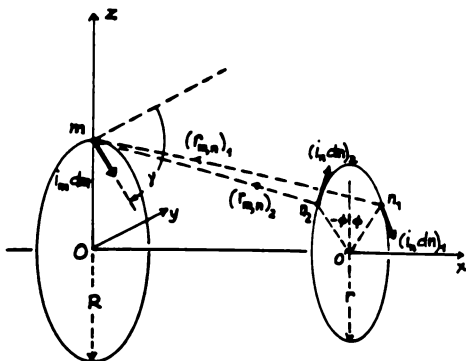


Fig.89 Diagram for solenoid calculations

$$(\cos \alpha)_1 = -(r/r_{m,n}) \sin \phi \cos \gamma - [(R-r \cos \phi)/r_{m,n}] \sin \gamma \quad (4.30)$$

$$(\cos \beta)_1 = -(r/r_{m,n}) \sin \phi \cos \phi - [(R-r \cos \phi)/r_{m,n}] \sin \phi \quad (4.31)$$

$$(\cos \alpha)_2 = (r/r_{m,n}) \sin \phi \cos \gamma - [(R-r \cos \phi)/r_{m,n}] \sin \gamma \quad (4.32)$$

$$(\cos \beta)_2 = (r/r_{m,n}) \sin \phi \cos \phi + [(R-r \cos \phi)/r_{m,n}] \sin \phi \quad (4.33)$$

Now the torque experienced by $i_m dm$ in the plane of the R-circle and due to an element on the r-circle is

$$\begin{aligned} (\Delta T_{m,n})_\gamma &= -(\partial/\partial \gamma) \Delta P_{m,n} \\ &= -i_m i_n (dm \cdot dn / r_{m,n}) (\partial/\partial \gamma) (2 \cos \epsilon - 3 \cos \alpha \cos \beta) \end{aligned} \quad (4.34)$$

The angle β is not a function of γ , and ϵ is the difference

$$\epsilon = \phi - \gamma \quad (4.35)$$

Therefore

$$(\Delta T_{m,n})_{\gamma} = i_m i_n (dm \cdot dn / r_{m,n}) [2 \sin(\phi - \gamma) - 3 \cos \phi \partial(\cos \alpha) / \partial \gamma] \quad (4.36)$$

But

$$(\partial / \partial \gamma)(\cos \alpha)_1 = (r / r_{m,n}) \sin \phi \sin \gamma - [(R - r \cdot \cos \phi) / r_{m,n}] \cos \gamma \quad (4.37)$$

$$(\partial / \partial \gamma)(\cos \alpha)_2 = -(\partial / \partial \gamma)(\cos \alpha)_1 \quad (4.38)$$

It is the sum of the products $\cos \phi [\partial(\cos \alpha) / \partial \gamma]$ for $(i_n dn)_1$ and $(i_n dn)_2$ which determines whether the combined effect of the two elements on $i_m dm$ cancels for certain values of γ . Hence we have to evaluate

$$\begin{aligned} & \{-(r / r_{m,n}) \sin \phi \cos \phi - [(R - r \cdot \cos \phi) / r_{m,n}] \sin \phi\} \times \\ & \quad \times \{(r / r_{m,n}) \sin \phi \sin \gamma - [(R - r \cdot \cos \phi) / r_{m,n}] \cos \gamma\} \\ & + \{(r / r_{m,n}) \sin \phi \cos \phi + [(R - r \cdot \cos \phi) / r_{m,n}] \sin \phi\} \times \\ & \quad \times \{-(r / r_{m,n}) \sin \phi \sin \gamma - [(R - r \cdot \cos \phi) / r_{m,n}] \cos \gamma\} \\ & -- \{(2r^2 / r_{m,n}^2) \cos \phi + [2(R - r \cdot \cos \phi) / r_{m,n}^2] \sin^2 \phi \sin \gamma \} \end{aligned} \quad (4.39)$$

Hence the torque on $i_m dm$ due to the two symmetrical elements on the r -circle is

$$\begin{aligned} (\Delta T_{m,n})_{\gamma} = i_m i_n (dm \cdot dn / r_{m,n}) \{ & 2 \sin(\phi - \gamma) + 2 \sin(-\phi - \gamma) + \\ & + 3[(2r^2 / r_{m,n}^2) \cos \phi + 2(R - r \cdot \cos \phi) r / r_{m,n}^2] \sin^2 \phi \sin \gamma \} \end{aligned} \quad (4.40)$$

It is obvious that this torque will be zero when $\gamma = 0$ and 180° . As this is true for all pairs of symmetrical element combinations on the r -circle, regardless of ϕ , it is also true for the circle as a whole.

Since $\cos\theta_x = 0$ for all three elements and d appears only in $\cos\theta_x$ of the direction cosines of the distance vector $r_{m,n}$, neither ϵ nor α and β depend on d . Therefore all solenoid turns to the right of the R-circle produce zero torque on i_{mdm} when $\gamma = 0$ or 180° . For turns of the solenoid lying to the left of the R-circle on fig.89, only the x-coordinate of $(i_{ndn})_1$ and $(i_{ndn})_2$ changes from $+d$ to $-d$. This has no effect on $\cos\alpha$, $\cos\beta$, and $r_{m,n}$ so long as the magnitude of d is the same. Therefore for all values of d the solenoid turn at $-d$ will produce a torque on i_{mdm} in the same direction and of the same magnitude as the turn at $+d$.

It remains to be shown that, as in the case of coplanar circles, the element i_{mdm} is in stable equilibrium when $\gamma = 180^\circ$. This has been proved by computing $(\Delta T_{m,n})_\gamma / (i_m i_{ndm} \cdot dn)$ for a range of γ and d values. Table 15 lists the results which confirm that $\gamma = 180^\circ$ is the stable equilibrium position of i_{mdm} .

Table 15 Stability calculation results

γ°	$(\Delta T_{m,n})_\gamma / (i_m i_{ndm} \cdot dn)$			Remarks
	$d=0$	$d=30$	$d=300$	
0	0	0	0	UNSTABLE
10	0.8074	0.0467	0.888×10^{-4}	
30	2.3249	0.1343	2.56×10^{-4}	POS. MAX.
60	4.0268	0.2327	4.43×10^{-4}	
90	4.6498	0.2687	5.11×10^{-4}	
120	4.0268	0.2327	4.43×10^{-4}	
150	2.3249	0.1343	2.56×10^{-4}	
170	0.8074	0.0467	0.888×10^{-4}	STABLE
180	0	0	0	
190	-0.8074	-0.0467	-0.888×10^{-4}	NEG. MAX
210	-2.3249	-0.1343	-2.56×10^{-4}	
240	-4.0268	-0.2327	-4.43×10^{-4}	
270	-4.6498	-0.2687	-5.11×10^{-4}	
300	-4.0268	-0.2327	-4.43×10^{-4}	
330	-2.3249	-0.1343	-2.56×10^{-4}	
350	-0.8074	-0.0467	-0.888×10^{-4}	

We conclude, therefore, that the solenoid as a whole tends to counteralign all dipole elements of the R-circle to the current i_n . In other words if i_n flows anti-clockwise about the positive x-direction, as in fig.89, the diamagnetic current i_m is directed clockwise. This analysis predicts the induction of diamagnetic currents in a region of curl-free magnetic vector potential, but it does not specify the magnitude of these currents.

A quantitative assessment of the diamagnetic currents is possible. As only closed currents are involved in the relevant interactions, the vector potential component parallel to dm at the position of the element dm , which is being generated by the second element $i_n dn$, may from (1.76) be written

$$\Delta A_{m,n} = i_n (\cos \epsilon / r_{m,n}) dn \quad (4.41)$$

The complete circuit n gives

$$\int_n \Delta A_{m,n} dn = i_n \int_n (\cos \epsilon / r_{m,n}) dn \quad (4.42)$$

The long solenoid may be treated as consisting of z circular turns (r-circles) each carrying the current i_n .

One of London's [89] equations of the superconducting state is

$$j = -kA \quad (4.43)$$

where j is the persistent current density at a location where the magnetic vector potential is A . We now investigate whether the Ampere-Neumann electrodynamics will yield a value for the constant k . The single filament representation of the R-circle implies that $i_m = ja$, where 'a' is the filament cross-sectional area. The constant k must be a function of this area. Combining (4.42) and (4.43) we write for z solenoid turns

$$i_m = -i_n \sum_z \int_n (\cos \epsilon / r_{m,n}) dn \quad (4.44)$$

Integrating (4.44) around the R-circle results in

$$i_m \int dm = -i_n \sum_z \int_m \int_n (\cos \epsilon / r_{m,n}) dn \cdot dm \quad (4.45)$$

The double integral will be recognized as Neumann's mutual inductance formula (1.26) for two closed curves m and n. The sum over z of the circle mutual inductances is the mutual inductance between the solenoid and the surrounding R-circle. If this is denoted by M, equation (4.45) reduces to

$$i_m / i_n = -M / (2\pi R) \quad (4.46)$$

There are techniques available for measuring and computing M. Hence (4.46) may be used for determining the constant k in (4.43). The negative sign of (4.46) indicates that the two currents flow in opposite directions. This complies with the observed Meissner effect. Equation (4.46) is likely to fail when diamagnetic saturation is reached and superconductivity is being destroyed by the inducing current.

Take the practical example in which the solenoid radius is $r=1$ cm and $R=1.1$ cm. Furthermore, let the solenoid be wound as one layer of 600 closely packed turns of 0.063 cm diameter wire. Using the single filament approximation for all 601 wire circles, M has been computed to come to 5.99 cm. Hence according to (4.46), the current ratio in this practical example should be $i_m/i_n = -0.867$.

An experimental test of this theory may be performed by cooling the superconducting ring through the transition temperature while the solenoid carries a steady current. A coaxial detector coil of copper wire should be placed next to the superconducting ring and cooled with it. If the Meissner effect is due to the expulsion of the magnetic field, as commonly believed, no voltage pulse should be induced in the copper coil at the transition temperature

when the ring becomes superconducting. On the other hand, if a voltage pulse is being detected, it would establish that the Meissner effect is the result of the expulsion of the magnetic vector potential from the bulk of the superconductor. It would lend strong support to the concept of pivoted, atomic current elements.

UNIFICATION NOTWITHSTANDING

These last few pages are devoted to speculation. Mathematical reasoning and restraint are put aside to reveal motivation and aspiration. In the physics of the 1980's the Ampere-Neumann electrodynamics is, at best, a foreign body of knowledge. How can it be reconciled with all we have been taught or may be teaching ourselves? How does it fit in with current research to unravel more secrets of nature? It is not only that the old electrodynamics has a strange appearance; it is outright disliked and unpopular. It might forever remain a curiosity in the annals of science, were it not for some undeniable experimental facts. Science is not the black-and-white, right-or-wrong, cold, logical activity young idealists choose as a career to insulate them from the prejudices and questionable judgements of other pursuits. It embodies all the passions, fashions and irrationalities of human enterprises. In the long run, however, physics has to comply with the facts of experience. For a while some of these facts can be concealed, talked away, or glossed over for the sake of retaining some unity in the presentation and teaching of the subject.

Relativistic electromagnetism has been a closed topic for eighty years, neatly packaged in a great variety of textbooks which all preach the same sermon. Moreover, starting with Einstein's endeavors, late in his life, the fashionable thing to do in physics has become to work on the unification of electromagnetic with nuclear and gravitational

forces. It is not at all clear what can be gained from unification. Are we to believe the Creator had some incentive to use only one kind of force, or law of nature, to make the miraculous universe tick? Was his purpose to make it easy for man to understand Nature? Unification brings unquestionable advantages to the teaching of physics. What could sound more convincing to the unexperienced than telling them that all knowledge flows from a single abstract concept? Most of all, unification would add immensely to the aesthetics of science. None of these noble ends make unification necessary or inevitable.

There is another side to unification. The discovery of the rules of action prevailing in the physical world have ultimately enabled us to create the civilization in which we live. Man's separation from the animals has come about through his power of invention which culminated in the technology of the twentieth century. The inventor has to be able to predict and visualize when certain things are put together in a certain way and supplied with energy. To do this he calls on a vast amount of scientific information, some experimental and some theoretical. The more varied this information is, the better are the inventor's chances to find solutions to new challenges. If unification means the combination of different scientific fields into one subject, then the condensation of knowledge will in fact reduce the armory of inventors.

Considering the huge success of Newton's gravitation and mechanics, how could the action-at-a-distance concept become so unpopular? No compelling reason seems to exist for the dislike of it. Contact-action is a more graphic experience in everyday life. Yet in the sophisticated fabric of physics, it would seem too simplistic to think that everything that moves has to be pushed around by something leaning on it. I believe the philosophers of science, men like Faraday, Maxwell, Lorentz and Einstein have been drawn to theories of the ether and the field by their limitless imagina-

tion which these intangible ideas set free to roam. Matter interaction theories do not dwell on that part of physics which is totally unobservable. They are a form of mental straight-jacket subduing the evolution of abstract models and mechanisms.

While Faraday and Maxwell assembled most of electromagnetic field theory, with elastic lines of flux, flywheels of self and mutual inductance, ether stresses, and so on, the final stamp of approval was placed upon it by Einstein. His ideas were accepted eagerly, even by those who knew little about physics and mathematics. He disagreed with action-at-a-distance but said very little about it. When discussing the foundations of theoretical physics [92] he once wrote: "From Newton's time on, the theory of action-at-a-distance was constantly found artificial." Following this remark he quoted just one example, that of iron filings tracing out a field pattern on a sheet of paper. "How was each single iron filing among a lot scattered on a piece of paper to know of the single electric particles running round in a nearby conductor?" Ampere provided the answer to this question 130 years before Einstein asked it. When Einstein's book was published, Ampere was long forgotten and never mentioned.

Mechanics as developed by Newton and his followers is not a perfect simultaneous matter interaction theory. It contains the concept of inertia which Newton did not base on the interaction of pairs of matter elements. Inertia is apparently experienced by an isolated particle without the participation of other matter. It caused Newton to invoke absolute space as a participant in the physical action spectacle. This facet of inertia is out of step with the remainder of newtonian mechanics. It suggests relative positions, velocities and accelerations between particles of matter are not sufficient to state the laws of nature. Nevertheless, Newton's physics remained true to galilean relativity, just as Weber's electrodynamics did, inspite of the latter's

involvement with the velocity of light.

In my opinion Mach [93] proposed the best, and possibly a sufficient, resolution of the riddle of inertia. He said it looks as if the inertia of a body is its gravitational interaction with the distant matter of the universe residing outside the solar system. It would then be a gravitational pull in all directions and not just toward one body which dominates gravitation because of its proximity. This long-range, distributed gravitational interaction is likely to influence the translatory and rotational motion of the body. Apparently we can take care of the immensely complex, simultaneous interaction manifold by assigning inertia to a body in proportion to its gravitational mass. It rather looks as if linear and rotational momentum are conserved in the universe as a whole. To insure momentum conservation at all times there must be instant communication between bodies and particles on earth and the matter of distant galaxies. Newton's law of gravitation provides this simultaneity of interaction over any distance. What we observe, however, is not force but the results it produces in terms of the relative motion of bodies. Cause (force) and effect (velocity) do involve time derivatives leading to time delays.

So far no mathematical system of equations has been found which adequately describes the interaction complex of bodies and particles in the solar system and the huge amount of mass in the remainder of the universe, while complying with Newton's law of gravitation and Mach's principle. A number of attempts have been made, but in the end they resulted in models that could not be described as being truly newtonian. One of these attempts is Einstein's general theory of relativity. In another Moon and Spencer [94] modified Newton's law of gravitation so that the distant matter in the universe would be repelled from the solar system. A most interesting treatment of the subject was provided by Sciama [95] who showed that "... matter has inertia only in the presence of other matter". In Sciama's

theory inertia turns out to be an induced effect depending on the rate of change of a vector potential, very much like the generation of distant e.m.f.'s with Neumann's law. But Sciama then retards the vector potential which gives rise to a special relativity which is alien to newtonian physics.

The real shortcoming of simultaneous matter interaction theories has been that they were not developed to embrace radiation phenomena. At first sight it seems plausible that the simultaneous interactions of the Ampere-Neumann electrodynamics are not compatible with the experimentally observed delays between the emission and reception of light. Precisely this argument led to the introduction of retarded potentials to save the action-at-a-distance concept. Burniston Brown [28], Moon and Spencer [21], and very recently Wesley [96], have all made laudable efforts in combining retarded potentials with action-at-a-distance to formulate complete electromagnetic theories.

I will argue that simultaneous matter interactions can be retained and made compatible with the time delays of radiation phenomena, although the mathematics for such a scheme are still wanting. It would be a newtonian theory invariant under galilean transformations. Consider the classical example of infinite half-space filled with a metal and subjected to an alternating magnetic field parallel to its surface. Field theory teaches us that alternating currents will be induced in the metal, the current amplitude decreasing exponentially with depth in the metal. Furthermore, the phase shift of the induced currents, relative to the surface field, also varies with depth. This phase shift may be interpreted as the delay caused by the transport of energy from the surface to a given depth in the metal. It will be remembered that the velocity of electromagnetic energy propagation in metals is very much smaller than the velocity of light in free space. Field theory and the Ampere-Neumann electrodynamics actually predict exactly the same

amplitude decrement and phase shift of the induced currents as a function of depth in the metal. Therefore, in the half-space example, the Ampere-Neumann electrodynamics predicts the same induced phenomena and time delays as a theory that is based on energy transport at finite velocity. This curious state of affairs could be demonstrated more directly with a field pulse. Both theories would then indicate the same time-lag with which the pulse arrives at a certain depth in the metal. For this reason I believe I am justified to express some hope that the much longer time delays of electromagnetic induction over astronomical distances may some day also be explained by a simultaneous matter interaction theory.

In connection with Mach's principle it was argued that, if simultaneous ponderomotive forces between two bodies are the cause, and the attainment of a certain relative velocity between the bodies is the effect, then we will observe time delays between cause and effect. A similar case can be made for electromagnetic induction. The cause would then be a time-varying inducing current, and the effect the attainment of a certain induced current. This clearly involves a time delay between cause and effect, even though the electromotive force interaction of (4.20) is simultaneous.

The rediscovery of Ampere tension and other associated experimental results force us to take a second look at the electromagnetic theory which held good for eighty years. This may be disturbing to teachers, but it should not surprise us, unless we believe that we already know the absolute truth. The beginning of physics could be coupled with the beginning of quantitative, experimental science. Galilei deserves much credit for starting this line of investigation. Therefore quantitative physics is about 400 years old. Compared to the time of evolution of the human intellect, which set us apart from the animal world, the last four centuries are but a brief instant. We should not expect to have dis-

covered all the secrets of nature in so short a time. Much remains concealed to us, and the journey of discovery is as exciting now as it has ever been. I do not agree with Hawking [97] that the end of theoretical physics may be in sight and could come with a grand unified theory by the end of this century. He speculated that after grand unification, theoretical physics could possibly be left to computers. Hawking mirrors the arrogance of some mathematical thinkers who underestimate the power of experiment as a tool of discovery for charting unexplored territory.

Hesse [98] has written a beautiful account of action-at-a-distance in the history of science. It brings out the point that we human beings have been unable to think up more than two action principles. Far-actions, as they are called in the German literature, and the contact-actions of the aether and the field. The contact-action philosophy has been far more popular than that of far-actions. Yet for the most important single advance made in science, that by Newton, it was necessary to drop contact-actions in favor of far-actions. One gains the impression that far-actions lead to greater rigor. This was insufficient, however, to terminate the love affair of the human mind with something spiritual pervading all space. The unchallenged reign of newtonian physics lasted hardly more than two hundred years, which is half the age of quantitative physics. By the end of the twentieth century we are as totally immersed in 'the field' as Descartes was just before the rise of Newton.

One of the cherished philosophical notions of modern physics is the flight of the photon through space. This 'particle' belongs to philosophy because there exists no experimental proof of its existence. The separation of energy from matter is essential when one wishes to do away with the other philosophical notion, that of far-actions. In Newton's cosmos we had only one substance, which was matter. Now we have two substances, matter and energy, unification

notwithstanding. They can co-exist in the same location or part company. Not always is energy a separate substance. A moving particle, for example, which possesses kinetic energy is only matter.

What would happen to physics if we were to do away with free energy? Well, to begin with, we would no longer have to quantize energy. This quantization was the perplexing aspect of Planck's discovery. The wave-particle duality would disappear, for we then would have to explain the wave-like behavior of the particle by far actions without a wave of energy. This has already been done quite successfully by Burniston Brown [28]. It would also mean, as mentioned before, that energy transmission time lags would have to be explained by simultaneous matter interactions depending on time derivatives. Abolishing free energy would spell the end of special and general relativity. So much hinges on choosing one of the only two available philosophical principles of far and contact action.

The Ampere-Neumann electrodynamics is utterly dependent on the quantization of matter and electric charge. It associates bound energy with the arrangement of material current elements and charges. It is compatible with the quantization underlying newtonian mechanics. It gave rise to the magnetic vector potential which has become so important in quantum mechanics. There is every indication that the Ampere-Neumann electrodynamics makes an ideal partner of quantum theory, albeit a causal quantum theory.

REFERENCES

1. Bern Dibner, Oersted and the discovery of electromagnetism, Blaisdell Publishing, New York, 1962.
2. H.C. Oersted, "Experiments on the effect of a current on the magnetic needle", *Annals of Philosophy*, Vol.16, 1820.
3. P. Hammond, "Andre-Marie Ampere: the Newton of electricity", *Journal IEE*, May 1961, pp.274-277.
4. R.A.R. Tricker, "Ampere as a contemporary physicist", *Contemporary Physics*, Vol.3, pp.453-468, 1962.
5. R.A.R. Tricker, Early electrodynamics, Pergamon Press, London, 1965.
6. E. Whittaker, A history of the theories of aether and electricity, Thomas Nelson, London, 1951.
7. A.M. Ampere, "La determination de la formule qui represente l'action mutuelle de deux portions infiniment petites de conducteur voltaïques", *L'Academie Royale des Sciences*, Paris, June 10, 1822.
8. F.E. Neumann, "Die mathematischen Gesetze der inducirten elektrischen Stroeme", *Akademie der Wissenschaften*, Berlin, 1845.
9. F.E. Neumann, "Ueber ein allgemeines Prinzip der mathematischen Theorie inducirter elektrischer Stroeme", *Akademie der Wissenschaften*, Berlin, 1847.
10. O.D. Kellog, Foundations of potential theory, Dover, New York, 1929, p.53.
11. H.G. Grassmann, "A new theory of electrodynamics", *Poggendorf's Annalen der Physik und Chemie*, Vol.64, pp.1-18, 1845.
12. G.T. Fechner, "About the link between Faraday's induction phenomena and Ampere's electrodynamic phenomena", *Poggendorf's Annalen der Physik und Chemie*, Vol.64, pp.337-345, 1845.
13. W. Weber, Elektrodynamische Maasbestimmungen ueber ein allgemeines Grundgesetz der elektrischen Wirkung,

Wilhelm Weber's Werke, Springer, Berlin, 1893.

14. J.C. Maxwell, A treatise on electricity and magnetism, Oxford University Press, Oxford, 1873.
15. W. Weber, R. Kohlrausch, "Ueber die Elektricitaetsmenge welche bei galvanischen Stroemen durch den Querschnitt der Kette fliesst", Annalen der Physik und Chemie, Vol.99, pp.10-25, 1856.
16. G. Kirchhoff, Annalen der Physik und Chemie, 1857, p.193 and p.251.
17. L.V. Lorenz, "On the identity of the vibrations of light with electrical currents", Philosophical Magazine, Vol.34, pp.287-301, 1867.
18. B. Riemann, Riemann's Werke, (H. Weber, Editor), Leipzig, 1892.
19. C.G. Neumann, "Ueber die elektrodynamischen Elementarwirkungen", Leipziger Berichte, 1896, pp.221-290.
20. A. Einstein, "Zur Elektrodynamik bewegter Koerper", Annalen der Physik, Vol.17, 1905. English translation in: The principle of relativity, Dover, New York, 1923.
21. P. Moon, D.E. Spencer, "On the Ampere force", Journal of the Franklin Institute, October 1955, pp.295-311.
22. A. O'Rahilly, Electromagnetic theory, Vols.1 and 2, Dover, New York, 1965.
23. E. Mach, History and root of the principle of the conservation of energy, Open Court Publishing, London, 1911.
24. A. Einstein, "Die Grundlagen der allgemeinen Relativitaetstheorie", Annalen der Physik, Vol.49, 1916.
25. A. Einstein, The meaning of relativity, Methuen, New York, 1946.
26. D.W. Sciama, "On the origin of inertia", Royal Astronomical Society, Monthly Notices, Vol.113, pp.34-42, 1953.
27. P. Moon, D.E. Spencer, "Mach's principle", Philosophy of Science, Vol.26, pp.125-133, 1959.
28. G. Burniston Brown, Retarded action-at-a-distance, Cortney Publications, Luton, 1982.

29. H.A. Lorentz, The theory of electrons, Teubner, Leipzig, 1909.
30. H. von Helmholtz, Wissenschaftliche Abhandlungen, Vols. 1 to 3, Leipzig, 1882, 1883, 1895.
31. G. Helm, Die Theorien der Elektrodynamik, Veit, Leipzig, 1904.
32. J.G. Munker, Die Grundgesetze der Elektrodynamik synthetisch hergeleitet und experimentell geprüft, Herman Ballhorn, Nuernberg, 1883. (Claims experimental proof of Ampere's longitudinal force does not exist.)
33. H. Hertz, Electric waves, London, 1893.
34. P. Silvester, Modern electromagnetic fields, Prentice-Hall, Englewood Cliffs, 1968.
35. H.A. Rowland, C. Hutchinson, Philosophical Magazine, Vol.27, p.445, 1889.
36. A.M. Ampere, Theorie mathematique des phenomenes electrodynamiques uniquement deduite de l'experience, Blanchard, Paris, 1958.
37. C. Blondel, Ampere et la creation de l'electrodynamique, Bibliotheque Nationale, Paris, 1982.
38. J. Nasilowski, "Phenomena connected with the disintegration of conductors overloaded by short-circuit currents" Przeglad Electrotechniczny (Poland), Vol.37, No.10, p.397, 1961.
39. J. Nasilowski, "Unduloids and striated disintegration of wires", Exploding wires, (W.G. Chase, H.K. Moore, Editors), Vol.3, Plenum, New York, 1964, p.295.
40. J. Nasilowski, "Ampere tension in electric conductors", IEEE Transactions on Magnetics, Vol.MAG-20, p.2158, 1984.
41. H.W. Baxter, Electric fuses, Arnold, London, 1950.
42. P. Graneau, "First indication of Ampere tension in solid electric conductors", Physics Letters, Vol.97A, p.253, 1983.
43. P. Graneau, "Ampere tension in electric conductors", IEEE Transactions on Magnetics, Vol.MAG-20, p.444, 1984.

44. E.F. Northrup, "Some newly observed manifestations of forces in the interior of an electric conductor", *Physical Review*, Vol.24, p.474, 1907.
45. L.J. Ruscak, R.N. Bruce, "Multiarc generator", *IEEE Transactions on Plasma Science*, Vol.PS-15, p.51, 1987.
46. P.T. Pappas, "The original Ampere force and Biot-Savart and Lorentz forces", *Nuovo Cimento*, Vol.76B, p.189, 1983.
47. W.H.K. Panofsky, M. Phillips, Classical electricity and magnetism, Addison-Wesley, Reading MA, 1962.
48. P. Graneau, "Application of Ampere's force law to rail-gun accelerators", *Journal of Applied Physics*, Vol.53, p.6648, 1982.
49. F.F. Cleveland, "Magnetic forces in a rectangular circuit", *Philosophical Magazine*, Vol.21, p.416, 1936.
50. R.S. Hawke, A.L. Brooks, F.J. Deadrick, J.K. Scudder, C.M. Fowler, R.S. Caird, D.R. Peterson, "Results of railgun experiments powered by magnetic flux compression generators", *IEEE Transactions on Magnetics*, Vol.MAG-18, p.82, 1982.
51. D.R. Peterson, C.M. Fowler, C.E. Cummings, J.F. Kerrisk, J.V. Parker, S.P. Marsh, D.F. Adams, "Design and testing of high-pressure railguns and projectiles", *IEEE Transactions on Magnetics*, Vol.MAG-20, p.252, 1984.
52. A.J. Bedford, "Rail damage in a small caliber rail-gun", *IEEE Transactions on Magnetics*, Vol.MAG-20, p.348, 1984.
53. See [48].
54. P. Graneau, "Electromagnetic jet propulsion in the direction of current flow", *Nature*, Vol.295, p.311, 1982.
55. P.G. Tait, "Note on a modification of the apparatus employed for one of Ampere's fundamental experiments in electrodynamics", *Philosophical Magazine*, Vol.21, p.319, 1861.
56. A.M. Hillas, "Electromagnetic jet propulsion: Nonlorentzian forces on currents?", *Nature*, Vol.302, p.271, 1983.

57. F.E. Neumann, Vorlesungen ueber elektrische Stroeme, Teubner, Leipzig, 1884.
58. C. Hering, "Electromagnetic forces: a search for more rational fundamentals; a proposed revision of the laws", Journal AIEE, Vol.42, p.139, 1923.
59. C. Hering, "Revision of some of the electromagnetic laws", Journal of the Franklin Institute, Vol.194, p.599, 1921.
60. H. Aspden, Physics unified, Sabberton Publications, Southampton, 1980.
61. J.P. Wesley, Causal quantum theory, Benjamin Wesley, Blumberg, 1983.
62. See [49].
63. P. Graneau, "Longitudinal magnet forces", Journal of Applied Physics, Vol.55, p.2598, 1984.
64. J.W. Roper, "Experimental measurements of mechanical forces in electric circuits", Journal AIEE, Vol.46, p.913, 1927.
65. P. Graneau, P.N. Graneau, "Electrodynamic explosions in liquids", Applied Physics Letters, Vol.46, p.468, 1985.
66. F.P. Wong, E.O. Foster, "The dynamics of electrical breakdown in liquid hydrocarbons", Journal of Electrostatics, Vol.5, p.157, 1978.
67. J. Nasilowski, "A note on longitudinal Ampere forces in gaseous conductors", Physics Letters, Vol.111A, p.315, 1985.
68. L. Bergmann, Der Ultraschall und seine Anwendung, Zurich, 1956.
69. B. Granovsky, L. Bykhovskaya, "Spontaneous electrical oscillations in low-pressure arc discharges", Journal of Physics (Moscow), Vol.10, p.351, 1946.
70. F.W. Grover, Inductance calculations, Dover, New York, 1945.
71. E.D. Charles, "Mechanical forces on current-carrying conductors", Proceedings IEE, Vol.110, p.1671, 1963.
72. H. Kolm, P. Mongeau, "An alternative launching medium", IEEE Spectrum, April 1982, p.30.

73. S. Rashleigh, R. Marshall, "Electromagnetic acceleration of macroparticles to high velocities", *Journal of Applied Physics*, Vol.49, p.2540, 1978.
74. R.S. Hawke, "Railgun accelerators for gram-sized projectiles", *IEEE Transactions*, Vol.NS-28, p.1542, 1981.
75. R. Hoffeld, "Demonstration of rail recoil", Internal Report, Center for Electromagnetics Research, Northeastern University, Boston.
76. W. Thompson (Lord Kelvin), Mathematical and physical papers, Vol.1, p.521, 1853.
77. A. Sommerfeld, Electrodynamics, Academic Press, New York, 1952.
78. P. Graneau, "A re-examination of the relationship between self- and mutual inductance", *Journal of Electronics and Control*, Vol.12, p.125, 1962.
79. P. Graneau, Underground power transmission, Wiley-Interscience, New York, 1979.
80. Lord Raleigh, "On the selfinduction and resistance of straight conductors", *Philosophical Magazine*, Vol.21, p.381, 1886.
81. P. Silvester, "Modal network theory of skin effect in flat conductors", *Proceedings IEE*, Vol.54, p.1147, 1966.
82. P. Graneau, "Alternating and transient conduction currents in straight conductors of any cross-section", *International Journal of Electronics*, Vol.19, p.41, 1965.
83. A. Greenwood, Electrical transients in power systems, Wiley-Interscience, New York, 1971.
84. L.G. Kelly, Handbook of numerical methods and applications, Addison-Wesley, Reading, 1967.
85. R.R. Parker, "Normal modes in RLC networks", *Proceedings IEEE*, Vol.57, p.39, 1969.
86. P. Graneau, "Coupled circuit theory for electromagnetic testing", Progress in non-destructive testing, Vol.3, p.163 (E.G. Stanford, Editor), Heywood, London, 1961.
87. P. Graneau, "Coupled circuit theory for electromagnetic testing", Ph.D. Thesis, University of Nottingham, 1962.

- 88 P. Graneau, "Steady-state electrodynamics of a cylindrical body in axial motion", Journal of Electronics and Control, Vol.14, p.459, 1963.
- 89. F. London, Superfluids, Vol.1, Dover, New York, 1961.
- 90. Y. Aharonov, D. Bohm, "Significance of electromagnetic potentials in quantum theory", Physical Review, Vol.115, p.485, 1959.
- 91. T. Neugebauer, "Zu dem Problem des absoluten Diamagnetismus und der Supraleitung", Acta Physica Hungaria, Vol.17, p.203, 1964.
- 92. A. Einstein, Out of my later years, Thames and Hudson, London, 1950.
- 93. E. Mach, Die Mechanik in ihrer Entwicklung, Brockhaus, Leipzig, 1897.
- 94. See [27].
- 95. See [26].
- 96. J.P. Wesley, Advanced fundamental physics, Benjamin Wesley Publishers, 7712 Blumberg, Germany, 1991, p.217.
- 97. S.W. Hawking, "Is the end in sight for theoretical physics?", Physics Bulletin, Vol.32, p.15, 1981.
- 98. M.B. Hesse, Forces and fields, Greenwood Press, Westport CT, 1962.
- 99. A.K.T. Assis, "On Mach's principle", Foundation of Physics Letters, Vol.2, p.301, 1989.

INDEX

- Absolute ampere, 19
- Absolute diamagnetism, 280
- Absolute space, 82, 292
- Absolute truth, 295
- AC current, 97, 178, 233, 241-260
- AC resistance, 248
- Acceleration force, 202-203
- Action-at-a-distance, 2-3, 55, 57, 72, 78, 260, 290-297
- Action integral, 173
- Aepinus, 6
- Aether, 2, 45, 72, 83, 89, 116, 296
 - stress, 72
- Aharanov, Y., 276, 304
- Aharanov-Bohm, experiment, 276
 - effect, 283
- Ampere, A.M., 3, 44-45, 80, 84, 105, 133-136, 261-262, 292, 298, 300
- Ampere's force law, 7-22, 38, 44, 92, 95, 104, 129, 137, 149-155, 192, 195, 205, 213, 266
- Ampere's rule, 12-14, 47, 270
- Ampere tension, 95-105, 195-198, 264, 295
 - across corners, 114, 149-155
 - in curved wires, 155-158
 - in dipole magnets, 155-164
 - stress of, 114, 163
- Angle current, 52
- Angle function, 8, 10-19, 43, 65, 95, 156, 266
- Angles in Ampere's law, 11, 156
- Aspden, H., 145, 177, 302
- Atomic current element, 104, 261-265
- Atomic metal lattice, 263
- Atomicity of electricity, 56, 85, 180, 262
- Athens experiment, 118
- Attraction,
 - of currents, 25
 - of current elements, 19
- Arc, high pressure, 178
 - low pressure, 178
 - plasma, 132, 145
 - pressure, 125
 - propulsion, 130-131
 - underwater, 133, 168-177
- Back e.m.f., 242-248, 272-275
- Baxter, H.W., 108, 300
- Bedford, A.J., 131, 301
- Beginning of electromagnetism, 1
- Bending stress, 159
- Bends of circuits, 203
- Bent-wire experiment, 20-21
- Bergmann, L., 178, 302
- Biot, J.B., 3
- Biot-Savart law, 4-5, 48, 54
- Blondel, C., 105, 300
- Body force: see ponderomotive force
- Bohm, D., 272, 304
- Bruce, R., 115, 301
- Bruce's experiment, 115
- Burniston Brown, 82, 294, 297, 299
- Cathode rays, 86
- Cardinal formula, 80
- Causal time delays, 40, 78, 82, 294-295
- Capacitor discharges, 97, 121, 158, 169
- Charge,
 - neutralization, 74
 - splitting, 74
 - transport, 275, 281
- Charles, E.D., 182-183, 302
- Circuit breakers, 130
- Circular filament, 205-207, 221
- Colinear current elements, 268
- Cleveland, F.F., 128, 149, 183, 265, 301
- Cleveland's experiment, 149-155
- Commutating interruptors, 97
- Conduction currents, 261
- Conductor modelling, 203
- Convection currents, 92-94, 133, 171, 175, 261

- Copenhagen experiment, 3
- Coplanar current,
 - circles, 277
 - elements, 265-275, 283
- Contact action, 3, 72, 167, 296
- Contact points, 137
- Corners of circuits, 203
- Core effect, 248-254
- Coulomb interactions, 59-70, 89
- Coulomb's law, 6-7, 60, 93
- Critical magnetic field, 282
- Cubic current elements, 95, 184-198
- Current, 68
 - circle, 205-207
 - continuum, 19, 179, 262
 - distribution, 241-260
- Current elements, 5, 7, 261-265
 - amperian, 93, 98, 261-265,
 - charge velocity, 51, 59
 - components of, 12
 - direction cosines of, 14
- divisibility of, 19
 - finite size, 104, 153, 208
 - forces between, 79
 - Grassmann's, 49-53
 - length-to-width ratio, 103, 183
 - Lorentz's, 88, 149, 264
 - microscopic, 56, 203, 267
 - partial differentials, 15
 - selfinteraction, 19
 - shape and size, 182-184
 - substance of, 37
 - Weber's, 56-64, 87, 263
- Current interruptors, 138
- Current limiting, 109
- DC current, 223
- Degrees of element freedom, 270
- De LaRive, A., 105, 134
- Descartes, R., 296
- Diamagnetic,
 - counteralignment, 281
 - current, 279-290
 - saturation, 281, 289
- Diamagnetism, 275-290
- Dibner, B., 1, 298
- Diffusion,
 - equation, 276
 - of heat and sound, 76
 - of potentials, 77
- Direction of current flow, 62
- Discharge of inductive energy, 97, 130
- Displacement current, 77
- Distribution of electricity, 97
- Divergences, 96
- Eddy currents, 259-260
- Eigenvector matrix, 256
- Einstein, A., 76, 79, 82, 89, 259, 292, 299, 304
- Elastic energy, 129, 155
- Electric,
 - conflict, 1
 - effluvia, 6
 - fluid, 55, 69, 261
 - field strength, 6, 44
 - source/sink, 270-275
- Electrodynamics
 - explosions in liquids, 168
 - impulse, 124, 173
 - pendulum, 116-130
 - unit of current, 19
- Electrodynamics of metals, 45, 144-148
- Electrodynamic potential, 23-33, 42, 85
 - angular gradient, 36
 - pair of current elements 42, 212, 265-268,
 - rate of change, 40
 - single circuit, 213
 - two circuits, 204
 - Weber's, 56-70
- Electrolytic discharge, 172
- Electromagnetic
 - accelerators, 97
 - field, 72, 77, 79, 89, 116, 144
 - induction, 23, 28, 214
 - mass, 70, 81, 85, 117-119, 137
 - pulse (EMP), 97
 - units, (e.m.u.), 57, 192, 204-207, 214, 256, 274
 - testing, 259
- Electromotive force (e.m.f.), 38-45, 55, 60, 81, 180, 241, 269-275
- Electrostatic units (e.s.u.) 57
- Electrostatics, 5-7
- Electron, 84-87, 133
 - beams, 133
 - charge, 86

- current element, 149-151
- theory of metals, 86-89
- structure, 262
- Elements of metal, 220
- Element strength, 270
- Elliptic integrals, 224
- Empirical laws,
 - Ampere, 22, 44
 - Coulomb, 44
 - Grassmann-Lorentz, 51, 91
 - Newton, 44
- Energy conservation, 22, 83, 149, 268
- Exploding wires, 97, 130
- Extracurrent, 214
- Far-actions, 167, 261, 296
- Faraday, M., 40, 49, 55, 58, 72, 78, 105, 214, 292
- Faraday's law, 41
- Fault currents, 97
- Fechner, G.T., 55, 67, 298
- Fechner's hypothesis, 67
- Field
 - energy, 47, 116-130
 - momentum, 116-130
 - theory, 276, 283, 294
- Final truth, 260
- Filament circle, 205-207, 221
- Filament cross-section, 184
- Filament model, 215-220, 235, 237-240
- Filament selfinductance, 216
- Filament square, 230-232
- Finite element analysis, 179
- Finite current elements, 153
- Finite-size filaments, 220
- Fizeau and Foucault, 70
- Flight of energy, 81
- Force
 - balance, 186
 - dilution, 192, 194, 201
 - distribution, 241
 - of attraction, 7, 50, 63, 65
 - of repulsion, 7, 50, 63, 65
 - law, 44
 - on liquid elements, 166, 175
 - reversal, 50
 - transmission, 60
- Forward e.m.f., 271-275
- Franklin, B., 5-7
- Franklin's law, 5
- Free energy, 80-84, 116-130, 297
- Fundamental electromagnetic units, 192
- Fuses, 97, 108, 130
- Galilean
 - transformations, 56, 294
 - relativity, 75, 78, 259, 292
- Galileo, G., 84, 295
- Galvanometer, 4
- Gas expansion, 177
- Gay-Lussac, 3
- General relativity, 293, 297
- Generalized frequency, 256-260
- Geneva experiment, 105, 134
- Geometric-mean-distance method (GMD), 179, 215, 218-220, 236, 240
- Go-and-return circuit, 237-240, 248
- Granovsky and Bykhovskaya, 178, 302
- Grassmann, H.G., 45-55, 91, 135, 298
- Grassmann's law, 44-55, 79, 92, 133, 149-155, 195, 214
- Gravitation, 2, 167, 291
- Gravitational forces, 290
- Greenwood, A., 249, 303
- Grover, F.W., 182, 225, 302
- Hairpin experiment, 105, 116, 118, 133-138
- Hammond, P., 3, 298
- Hawke, R.S., 131, 301, 303
- Hawking, S.W., 296, 304
- Helm, G., 300
- Helmholtz, H. von, 83, 300
- Hering, C., 144-148, 265, 302
- Hertz, H., 85, 300
- Hesse, M.B., 296, 304
- Hillas, A.M., 137-138, 301
- Hoffeld, R., 303
- Homogeneity of conductors, 216-218, 233, 238
- Hoop tension, 158, 160-164
- Hutchinson, C., 300
- Hydrostatic pressure, 167-171
- Imagination, 291
- Impact failures, 114
- Impedance matrix, 243
- Imponderable electric fluid, 262
- Imponderable forces, 262
- Impulse pendulum experiment, 116-130, 137
- Induced currents, 60, 91
- Induced e.m.f., 269-275
- Inducing current, 39-41
- Inductance matrix, 221, 230
- Inductance, 209

- Inductance calculation, 24, 214-240
 - by GMD, 179, 218-240
 - of cables, 233-240
 - of single filaments, 221-232
- Induction heating, 259
- Inductive action, 39
 - in metallic circuits, 44
 - in open circuits, 43
- Inductively stored energy, 215
- Inertia, 82, 293
 - of current elements, 167
- Infinite power series solution, 260
- Infinitely long filaments, 52, 98
- Inertial confinement, 115, 159
- Ion current element, 149-151
- Ion dynamics, 89
- Interaction
 - matrix, 191, 193, 200
 - of liquid elements, 167
- Integration difficulties, 179
- Inverse-distance-law, 268
- Inverse-square-law, 6, 53, 268
- Jet propulsion, 136-138
- Joule heat, 24-28, 83, 118, 137, 151, 173, 241, 270
- Kellogg, O.D., 25, 298
- Kelly, L.G., 255
- Kelvin, Lord, 72, 83, 215, 303
- Kinetic energy, 24, 70, 81, 82, 85
- Kinetic interpretation of magnetism, 264
- Kirchhoff, G., 70, 299
- Kohlrausch, R., 69, 299
- Kolm, H., 302
- Lagrange force, 71
- LaPlace, 5
 - transformation, 249
- Laser drives, 97
- Latent heat of arc formation, 126
- Lattice
 - force, 153
 - ion, 263
- Law of induction, 38
- Length unit, 100, 192
- Lenz's law, 39, 274
- Lightning, 1, 6, 97
- Liquid metal
 - furnaces, 144
 - conductors, 165-168
 - pumps, 145
- Liquid mercury
 - channel experiment, 165-168
 - explosion, 168, 175
- London, F., 276, 288, 304
- London's theory, 276, 288
- Longitudinal Ampere forces, 95-178
 - in plasmas, 169-178
- Longitudinal force dilution, 104, 195-198
- Lorentz, H.A., 49, 83, 86, 89, 264 300
- Lorentz force, 38, 44, 47, 49, 79, 89-94, 104, 116, 127-130, 137, 149-154, 158, 195, 202
- Lorentz hypothesis, 93
- Lorenz, L.V., 72, 299
- Mach, E., 82, 293, 299, 304
- Mach's principle, 295
- Macroscopic current elements, 179-184
- Magnetic
 - energy, 37, 81, 204, 239
 - field strength, 4
 - flux, 276
 - flux linkage, 24, 41, 44
 - pressure, 116
 - shell, 45
- Magnetism, 45
- Magneto-hydro-dynamics (MHD), 105, 166
- Magnetic field, 152, 276
 - diffusion, 253
 - energy, 178, 241, 266
- Many-body problem, 260
- Mass-energy relationship, 71, 117
- Matter-bound energy, 80-84
- Matter interaction,
 - of mutual inductance, 41
 - simultaneous, 40, 56, 84, 294
- Maxwell, J.C., 3, 44-45, 65-68, 71-73, 78-85, 179, 215, 218, 224, 240-241, 253, 292, 299
- Maxwell's
 - equations, 44, 49, 73, 77
 - stress tensor, 117, 120

- Mechanical source/sink, 270-275
- Mechanics, 2
- Mega-ampere circuits, 96
- Meissner effect, 275-290
- Marshall, R., 303
- Metal ions, 55, 86
 - force transfer to, 129
- Metallic current element, 56, 88, 261-264
- Michelson-Morley experiment, 47
- Modal analysis, 244, 255
- Momentum conservation, 47, 116-129, 137
- Momentum of energy, 47, 81, 116-131, 137
- Mongeau, P., 302
- Moon and Spencer, 82, 293, 294, 299
- Mutual electrodynamic potential 27-33, 40, 56
- Mutual actions, 262
- Mutual energy, 82
- Mutual elemental force, 271
- Mutual inductance, 41, 214
 - dimension of, 214
 - formula, 23, 38, 41, 237, 289
 - gradient, 213
 - matrix, 234
 - measurement of, 38
 - of coaxial cable, 219
 - of current elements, 205, 222
 - of two-wire line, 219
 - of parallel circles, 224
 - of straight filaments, 224
 - per unit length, 220
- Mutual simultaneous interaction 2
- Mutual torque
 - between circuits, 33-37
 - between current elements, 265-268
- Mutual potentials, 74, 85
- Mutual repulsion and attraction 47
- Munker, J.G., 300
- Nasilowski, J., 105-109, 159, 177, 265, 300, 302
- Nature of force, 26
- Near neighbor interactions, 95-102, 166, 181
- Neugebauer, T., 280, 304
- Neumann, C.G., 299
- Neumann, F.E., 71, 84, 138-143, 237, 298, 302
- Neumann's
 - electrodynamic potential, 23
 - force law, 28-33, 47, 53, 214
 - law of induction, 38-44, 269-274
 - proof, 28-33
 - sign convention, 24, 213
- Newton, Sir I., 2, 44, 72, 261, 296
- Newtonian force term, 47
- Newton's
 - first law, 82
 - third law, 47, 53, 91, 129, 138, 148
- Normal metals, 281
- Northrup, E.F., 194, 301
- Nuclear forces, 290
- Oersted, H.C., 1-3, 298
- Opening switches, 97, 130
- O'Rahilly, A., 77, 299
- Order of current elements, 277
- Orthogonal elements, 270
- Panofsky, W.H.K., 301
- Pappas, P.T., 116-129, 137, 145, 153, 177, 301
- Paramagnetism, 282
- Parker, R.R., 255, 303
- Parker's eigenvector method, 255-258
- Pendulum parameters, 123
- Perpendicular forces, 46
- Perpetual motion, 84, 149, 152
- Persistent supercurrents, 276, 288
- Peterson, D.R., 131, 301
- Philosophy
 - field energy, 37
 - Maxwell-Faraday, 79
 - newtonian, 2
- Photon, 84, 296
- Planck, M., 297
- Plasma
 - conduction, 169
 - fusion experiments, 97, 144-145, 177
- Pinch
 - effect, 144, 165-166
 - force, 174-176
 - force thrust, 194
- Ponderable matter, 77

- Ponderomotive force, 55, 60, 81, 88, 105, 180, 264, 276
- Ponderomotive torque, 275
- Potential
 - energy, 24-26, 81
 - spherical wave of, 72-76
 - theory, 25-37
- Power conductors, 97
- Power flow, 40, 272
- Priestley's law, 5-6
- Poynting's
 - law, 83
 - vector, 116, 119
- Projectile of railguns, 130
- Pulse
 - current, 248
 - magnets, 97
 - power circuits, 97
- Quanta, 84
- Quantization
 - of charge, 263
 - of energy, 297
- Quantum mechanics, 262, 276
- Quenching of superconductivity 281
- Railgun, 97, 130-133, 198-203
- Rail interference, 131
- Raleigh, Lord, 241, 303
- Rashleigh, S., 303
- Reaction forces
 - between parts of circuit, 38, 149-155
 - from selfinductance gradient, 204-214
 - in the field, 116
 - in railguns, 130-133
 - measurement of, 184-188
- Recoil forces, 121-126, 130-133, 198-203
- Rectangular circuits, 128, 132, 146, 150-154, 163, 184-190
- Region of curl-free vector potential, 288
- Relationship between self and mutual inductance, 214-220
- Relative acceleration of charges, 64
- Relative motion
 - between current elements, 38-41
 - between charges, 60, 62
- Relative velocities, 48, 82
- Relativistic
 - electrodynamics, 55
 - force, 47
- Repulsion of
 - current elements, 18, 95-143
 - currents, 27
 - liquid current elements, 166-175
- Rest mass, 71
- Retarded potentials, 72-79, 294
 - cancellation of, 74
 - positive and negative, 75
- Riemann, B., 72, 299
- Romagnosi, 1
- Roper, J.W., 162, 302
- Rowland, H.A., 300
- Saltwater
 - cup experiment, 169-174
 - gap experiment, 175-177
 - resistance, 172
- Savart, F., 4
- Sciama, D.W., 82, 293, 299
- Self-energy of electron, 92
- Self-force, 138, 150-153, 262
- Selfinductance equation, 219, 224, 229, 234-241
- Selfinductance of
 - infinitely thin wire, 220
 - current elements, 205
 - circle, 205-207
 - filament square, 232
 - single filament circuits, 221-223
 - single filament approximation, 205, 216
 - straight conductor, 234
 - two-wire line, 239
- Selfinductance gradient, 38, 204-206
- Selfinductance per unit length 223
- Self-potential, 37
- Selfinductance of
 - straight filament, 222
 - wire loop, 216-218
- Scaling laws, 256
- Screening current, 281
- Shape constant, 161, 207
- Shock waves, 177
- Short-circuit currents, 97
- Sign of mutual inductance, 274

- Simultaneous matter interaction, 40, 77, 259, 293
 Singularities, 181
 Sinks of energy, 270-274
 Single filament approximation, 99, 143, 160, 183, 187, 205, 221, 235
 Skin depth in superconductors, 281
 Skin effect, 241-254
 Silvester, P., 241, 244, 255, 300, 303
 Solenoid, 216, 224, 233, 283
 Solid-liquid interface, 165
 arc separation of, 168, 177
 Sommerfeld, A., 219, 229, 303
 Sommerfeld's
 equation, 219, 224, 229, 234, 236, 241
 approximation, 220, 224, 236
 Special relativity, 71, 76, 78, 86, 89, 94, 116, 137, 153, 259, 263, 294, 297
 Specific Ampere tension, 100-105, 195-198
 Specific force, 192
 Specific transverse force, 188
 Square circuit, 98-104
 Square-section filaments, 195-198
 Store of magnetic energy, 270-275
 Sources of energy, 270-275
 Stable torques on elements, 268, 273, 282, 287
 Straight conductor, 195-198
 Straight filament, 221
 Straight-through channel, 176
 Stress reflections, 113
 Stress tensor, 117
 Stretch effect, 144
 Strip conductor, 244
 Subtle electric fluid, 19, 180, 262
 Successive filament interactions, 260
 Superconducting ring, 277, 283
 Superconductors, 276, 281
 Tait, P.G., 137, 143, 301
 Tensile stress, 163
 Thermal disorder, 281
 Thermal expansion, 187
 Thermal shock, 113
 Thermodynamic explosion, 168, 173
 Thompson, W., 72, 215, 303
 Three-circle experiment, 9
 Three-phase circuit, 240
 Time delays, 293-296
 Torque
 between circuits, 33-37, 265-268
 on pivoted element, 277-287
 Transient currents, 241-255
 Transmission lag, 78, 259, 294
 Transmission of electricity, 97
 Transport of energy, 294
 Transverse forces, 46, 164
 Tricker, R.A.R., 5, 298
 Two-dimensional element interaction, 269
 Unification of electrostatics and electrodynamics, 56
 Unification theories, 290-297
 Unit lattice cell, 181
 Vacuum reaction forces, 116-129, 130-133, 153
 Vector analysis, 42, 49
 Vector potential, 42-45, 276
 Velocity of electricity, 40
 Velocity of light, 57, 69-72, 263, 293
 Virtual displacement, 204-213
 Virtual work, 23, 27-30, 38, 204-213, 265-268
 Wave-particle duality, 297
 Weber, W., 55, 84, 86, 261, 263, 298, 299
 Weber's
 electrodynamics, 55-71, 89, 292
 facts, 58, 86
 force law, 55-71, 69, 92, 263
 rule, 61-65
 Wesley, J.P., 145, 263, 294, 302, 304
 Whittaker, Sir E., 5, 47, 77, 298
 Wire-arc experiment, 17, 43, 52
 Wire fragmentation, 105-115, 158-164
 arcs of, 106
 current pause of, 108
 Wire loop, 215
 Wong and Forster, 177, 302

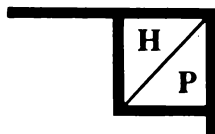
About the Book

This book outlines the Newtonian electrodynamics of A. M. Ampere and F. A. Neumann which was further developed by Maxwell and Graneau. This topic is not covered in standard textbooks. The volume reviews a 170-year series of experiments which demonstrate the existence of longitudinal Ampere forces. Tension and compression predicted by Ampere force law is shown to be present in wire explosions, railgun recoil action, electromagnetic jets in liquid metals, and electric arc phenomena. The conventional Lorentz force law denies the existence of longitudinal forces acting along current streamlines. Experiments with an electrodynamic impulse pendulum have provided striking evidence of a failure of the relativistic energy law ($E = mc^2$). The second edition of the book is highly recommended to physicists and engineers.

About the Author

Dr. Peter Graneau was attracted to the Ampere-Neumann electrodynamics while a graduate student at the University of Nottingham, England, in the 1950s. Since then he has published approximately fifty papers, in prestigious physics and electrical engineering journals, which confirm the validity of the old Newtonian electrodynamics and extend it to computer assisted finite element analysis. Most of his experimental work was performed in an electrodynamics laboratory at the Massachusetts Institute of Technology. In 1972 Dr. Graneau set up this laboratory with assistance from the U. S. National Science Foundation. NSF has commended him on his work on Ampere forces. Since 1987 the author has been associated with the Center for Electromagnetics Research of Northeastern University, Boston. During that period he co-authored with his son Dr. Neal Graneau of Oxford University a book and various articles on the subject.

I S B N 0 - 9 1 1 7 6 7 - 7 5 - 4



HADRONIC PRESS, INC.

35246 US 19 North # 115, Palm Harbor, FL 34684, USA